

MATHEMATICAL MODELLING OF A TUBULAR  
REACTOR FOR CONTINUOUS PRODUCTION OF  
SYNTHETIC RESINS

by

AMIR SOLOMON MESKIN

Thesis submitted to the Senate of the  
University of Aston in Birmingham in  
partial fulfillment of the requirements  
for the degree of Doctor of Philosophy.

Department of Chemical Engineering  
Birmingham, May 1977.

TO

BABA JOHN, KHALIL AND LYDA

MANOUCHEHR AND KYAN

SHAHRAM AND SHOHREH

MATHEMATICAL MODELLING OF A TUBULAR REACTOR  
FOR CONTINUOUS PRODUCTION OF SYNTHETIC RESINS

A.S. MESKIN

Ph.D., 1977

SUMMARY

Synthetic resins have, so far, been universally produced by batch processes. A continuous process however is shown to have some general advantages which make it desirable in commercial production.

The physical properties of the resin systems have resulted in the choice of a tubular reactor for continuous operation and the urea-formaldehyde resin system is selected for detailed examination.

To account theoretically for the performance of the tubular reactor two mathematical models are developed. The first model, which ignores all but the bulk transports, is a plug-flow model catering for good radial mixing in the reactor. The second model, involving a parabolic velocity profile with inclusion of radial and axial diffusion is a complex model and caters for laminar flow in the reactor tubes. The physical data necessary for the solution of the models are estimated using standard procedures. The chemical kinetic data available are shown to be inadequate for use at the elevated temperatures employed in the reactor. A novel technique is therefore developed for evaluation of the high temperature urea-formaldehyde reaction data. The data are then described mathematically with postulation of chemical reaction mechanisms, followed by optimisation of the rate constants for the proposed reaction schemes to give good mathematical fits.

To test the models, an available rig is modified. The problems of sampling under reactor conditions are overcome by the introduction of a novel design of a sampling valve and sample collection technique which avoids physio-chemical change to the resin. The experimental results are discussed with regard to the performance of the reactor as affected by various parameters. The best conditions for production of the addition products of the urea-formaldehyde reaction with a minimum formation of the condensation products are shown to be high formaldehyde to urea molar ratios, high temperatures, low concentrations and low residence times.

The plug-flow and complex models are solved using both a Honeywell 316 and an ICL 1904S computer. A novel numerical solution technique, in conjunction with the use of computers, is introduced for the solution of the complex models.

The simulation results show excellent predictions by the plug-flow models, and poor accuracy of prediction by the complex models. The reason for the good plug-flow predictions, at comparatively low Reynolds numbers, is attributed to the shape of the reactor which also explains the shortcomings of the complex models.

Key Words : Mathematical Modelling  
Tubular Reactors

## ACKNOWLEDGMENTS

In recognition to the help and advice received, the author wishes to extend his gratitude to:

Mr. A.F. Price for his encouragement, optimism, moral support and valuable supervision during the various stages of the project and his patient review of the manuscript.

Mr. A.R. Cooper for his direction and critical review of the work through its development and the review of the manuscript.

Professor G.V. Jeffreys, Head of Department, for providing the research facilities, particularly in terms of workshop expertise and computation.

Dr. G. Inverarity for his support of the project and Mr. R.W. Yates for his cooperation in making the time and equipment available.

Mrs. S.G. Williams for her valuable assistance with the analytical work.

Mr. J. Ferriday and BIP Ltd., Chemicals Division, for their flexibility in the research time schedules, some financial support of the computer costs, supplying the raw materials, making available the equipment for modification and experimentation and permitting the analytical work.

Miss S. Mehrali for her diligent typing of this thesis.

## TABLE OF CONTENTS

	<u>PAGE</u>
LIST OF TABLES .....	xii
LIST OF FIGURES .....	xiv
NOMENCLATURE .....	xvii
CHAPTER ONE - INTRODUCTION .....	1
1.1. Historical Background .....	1
1.2. The Traditional Batch Production .....	3
1.3. Disadvantages of the Batch Production Route .....	5
1.4. Desirability of a Continuous Process ....	6
1.5. Choice of a Continuous Process .....	7
1.6. Statement of the Objectives of the Research .....	8
1.7. Choice of the Chemical System .....	9
1.8. Areas of Research .....	9
CHAPTER TWO - THE MATHEMATICAL MODELS .....	11
2.1. Mathematical Modelling .....	11
2.1.1. Deterministic Modelling .....	12
2.2. Literature Survey .....	15
2.2.1. Continuous Polymerisation Reactors	16
2.2.2. Continuous Reactors for 'Ordinary Reactions' .....	20
2.2.3. Summary of the Literature Survey .	23
2.3. Mathematical Models .....	25
2.3.1. Plug-Flow Models .....	26
Mass Model .....	27

	<u>PAGE</u>
Energy Model .....	28
Auxiliary Mass Models .....	29
2.3.2. Dispersed Laminar Flow (Complex)	
Models .....	29
Energy Model .....	31
Mass Model .....	33
Auxiliary Mass Models .....	34
Momentum Model .....	35
2.3.3. Dimensionless Complex Models .....	38
Dimensionless Energy Model .....	39
Dimensionless Mass Models .....	40
Dimensionless Momentum Model .....	41
2.3.4. Summary of Mathematical Models ...	41
 CHAPTER THREE - THE CHEMISTRY OF UREA-FORMALDEHYDE	
(UF) REACTIONS .....	44
3.1. Introduction .....	45
3.2. The Kinetics and Mechanisms of the Inter-	
action of Urea with Formaldehyde .....	45
3.2.1. Addition Reactions of UF .....	47
Chemical Mechanism of Methylolurea	
Formation .....	52
3.2.2. Condensation Reactions of UF .....	55
Condensation Reactions in Alkaline	
Solutions .....	56
Condensation Reactions in Acid	
Solutions .....	57
3.2.3. The UF Resins .....	61

	<u>PAGE</u>
Theories of UF Resin Formation ...	62
The Chain Growth Theory .....	64
The Trimerisation Theory .....	65
The Azomethine Theory .....	65
3.2.4. Summary of UF Reactions .....	66
3.3. Evaluation of Rate of Reaction at Low Temperatures.....	68
3.3.1. Development of Concentration-Time Curves .....	70
3.3.2. Mathematical Representation of Concentration-Time Curves .....	73
3.3.3. Results and Discussion of Results .	80
3.4. Investigation of High Temperature UF Kinetics .....	84
3.4.1. The Experimental Technique .....	85
3.4.2. Results and Discussion of Results	87
3.5. Representation of Kinetic Data over the entire Temperature Range .....	93
3.5.1. Non-Linear Regression Analysis ...	95
The Optimisation Routine .....	98
3.5.2. Results and Discussion of Results .	103
Discussion of Results .....	111
CHAPTER FOUR - SOLUTION OF MATHEMATICAL MODELS ..	112
4.1. Solution of Plug Flow Models .....	112
Effect of Choice of Step Length on Accuracy of Results .....	117
4.2. Solution of Complex Models .....	117

	<u>PAGE</u>
CHAPTER FIVE - EXPERIMENTAL .....	126
5.1. Description and Operating Procedure for the Original Plant .....	126
5.2. Necessity of Modifications .....	129
5.2.1. Investigation of Feed to the Reactor .....	130
5.2.2. Sampling from the Reactor .....	134
5.3. The Modified Plant Description .....	138
5.4. Plant Operation and Experimental Procedure .....	148
5.4.1. The Sampling Technique .....	151
5.5. The Analytical Technique .....	153
5.5.1. The Quantitative Analytical Method .....	155
5.5.2. Free Formaldehyde Analysis .....	158
5.6. Scope and Range of Experimental Investigation .....	160
5.7. Experimental Error .....	163
5.7.1. Analytical Techniques .....	163
5.7.2. Measurement .....	164
5.7.3. Calculations .....	166
5.8. Experimental Results .....	166
CHAPTER SIX - DISCUSSION AND COMPARISON OF RESULTS	176
6.1. Discussion of Experimental Results .....	176
6.1.1. Reproducibility of Results .....	177
6.1.2. Effect of Variation in Steam Temperature .....	179

	<u>PAGE</u>
6.1.3. Effect of Variation in Molar Ratio .....	185
6.1.4. Effect of Variation in Concentration .....	190
6.1.5. Effect of Variation in Residence Time .....	194
6.1.6. Some Conclusions of Examination of Experimental Results .....	194
6.2. Comparison of Experimental Results with Plug-Flow Model Predictions .....	196
6.3. Comparison of Experimental Results with Complex Model Predictions .....	205
6.3.1. Calculation of Average Reactor Concentrations .....	206
6.4. Discussion of Model Predictions .....	222
6.4.1. Plug-Flow Model Predictions .....	222
6.4.2. Complex Model Predictions .....	229
6.5. Possible Improvement of models .....	233
CHAPTER SEVEN - CONCLUSIONS AND RECOMMENDATIONS .	234
7.1. Conclusions .....	234
7.1.1. Conclusions relating to the Chemical Investigation .....	234
7.1.2. Conclusions relating to the Experimental Performance of the Reactor .....	235
7.1.3. Conclusions relating to the Mathematical Model Predictions ...	237

	<u>PAGE</u>
7.2. Recommendations .....	238
7.2.1. Recommendations with regard to the Improvement of the Chemical Kinetic Investigation .....	238
7.2.2. Recommendations with regard to the Extension of the Experimentation Program .....	239
7.2.3. Recommendations with regard to Improvement of Mathematical Models .....	240

#### APPENDICES

Appendix 1 - Validity of Basic Assumptions .....	241
Appendix 2 - Evaluation of Heat Transfer Coefficient .....	248
Appendix 3 - Physical Data and Evaluation of Diffusion Effects .....	250
Appendix 4 - Evaluation of Boundary Conditions for Complex Energy Model .....	257
Appendix 5 - Estimation of Equilibrium Con- centrations of Urea-Formaldehyde . Reaction Mixture .....	263
Appendix 6 - Specification of Raw Materials and Chemicals .....	269
Appendix 7 - Listing of Computer Programs .....	274

	<u>PAGE</u>
Appendix 8 - Calculations and Calibration	
Charts .....	313
Appendix 9 - Quantitative Analysis .....	322
 BIBLIOGRAPHY .....	 331

LIST OF TABLES

<u>TABLE</u>		<u>PAGE</u>
2.1.	Stratum of detail of physio-chemical principles .....	13
3.1.	Formation and decomposition of MMU ....	48
3.2.	Equilibrium and rate constants in UF addition reactions .....	52
3.3.	Rate constant values for possible condensation reactions .....	59
3.4.	Concentration-time data for formaldehyde .....	71
3.5.-3.8.	Concentration-time data for UF mixtures .....	89-92
3.9.	Chemical mechanisms for description of UF reactions .....	97
3.10.-3.21.	Comparison of experimental and predicted results .....	105-110
5.1.	Adequacy of mixing for the modified feed system .....	134
5.2.-5.9.	Experimental results .....	168-175
6.1.	Reproducibility of results .....	177
6.2.	Effect of variation in steam temperature .....	180
6.3.	Effect of variation in molar ratio ....	186
6.4.	Effect of variation in concentration ..	191
6.5.-6.11.	Plug-flow model predictions .....	198-204
6.12.-6.18.	Complex model predictions .....	215-221

TABLEPAGE

A.1.1.	Time required to reach steady state ..	243
A.3.1.	Densities of feeds to reactor .....	250
A.5.1.	Equilibrium concentrations .....	267
A.6.1.	Formalin specifications .....	271

## LIST OF FIGURES

<u>FIGURE</u>		<u>PAGE</u>
2.1.	Plug-flow incremental element .....	27
2.2.	Co-ordinates of the reactor tube .....	30
2.3.	Complex model incremental element ....	30
3.1.	Urea .....	53
3.2.	Tautomeric imidol form .....	53
3.3.	Definition of rate of reaction .....	69
3.4.	Concentration-time curve for formaldehyde .....	72
3.5.	Logic diagram for solution of kinetics	79
3.6.-3.7.	Prediction of low temperature UF Kinetics .....	82-83
3.8.	Reaction vessel for investigation of high temperature UF Kinetics .....	86
3.9.	Nelder and Mead Logic diagram .....	99
3.10.	Logic diagram for subroutine to define objective function for minimisation .....	102
4.1.	Logic diagram for solution of plug-flow models .....	116
4.2.	Classification of grid points used for solution of complex models .....	119
4.3.	Logic diagram for solution of complex models .....	125
5.1.	Original plant layout .....	127
5.2.	Concentration and temperature history curves for the feed to the reactor ...	131
5.3.	Reactor sampling valve .....	136

<u>FIGURE</u>	<u>PAGE</u>
5.4.	Experimental plant flow and instrumentation diagram ..... 139
5.5.	Tube reactor arrangement ..... 142
5.6.	Sample valve arrangement ..... 146
5.7.	Thermocouple arrangement ..... 147
5.8.	Sample collection arrangement ..... 152
6.1.	Reproducibility of results ..... 178
6.2.	Effect of variation in steam temperature ..... 181
6.3.	Effect of variation in molar ratio ... 188
6.4.	Effect of variation in concentration . 192
6.5.-6.11.	Comparison of experimental and predicted results ..... 208-214
6.12.	Best plug-flow concentration prediction ..... 223
6.13.	Worst plug-flow concentration prediction ..... 224
6.14.	Best plug-flow temperature prediction ..... 226
6.15.	Worst plug-flow temperature prediction ..... 227
6.16.	Worst complex model temperature prediction ..... 230
6.17.	Best complex model temperature prediction ..... 231
A.4.1.	Shell-tube heat transfer ..... 258
A.8.1.	Urea pump calibration chart ..... 318
A.8.2.	Urea pump calibration chart ..... 319

FIGURE

PAGE

A.8.3.	Formalin pump calibration chart .....	320
A.8.4.	Formalin pump calibration chart .....	321

## NOMENCLATURE

A	Cross sectional area of reactor tube, $\text{cm}^2$
$d_o$	Outside tube diameter, cm
$d_i$	Inside tube diameter, cm
$D_M$	Molecular diffusion coefficient, $\text{cm}^2\text{s}^{-1}$
$D_{TH}$	Thermal diffusivity coefficient, $\text{cm}^2\text{s}^{-1}$
F	Formaldehyde in stoichiometric equations and text (Chapter 3)
F	Formaldehyde concentration in Mathematical equations, $\text{g cm}^{-3}$
G	Mass flow rate, $\text{g s}^{-1}$
h	Heat transfer coefficient (Chapter 2), $\text{cal cm}^{-2}\text{s}^{-1}\text{K}^{-1}$
$h_{cs}$	Convective heat transfer coefficient, $\text{cal cm}^{-2}\text{s}^{-1}\text{K}^{-1}$
$h_f$	Film heat transfer coefficient, $\text{cal cm}^{-2}\text{s}^{-1}\text{K}^{-1}$
k	Reaction rate constant (first and second order) time units, $\text{s}^{-1}$ , concentration units, $\text{mol cm}^{-3}$
K	Reaction equilibrium constant
$K_M$	Thermal conductivity of mixture, $\text{cal cm}^{-1}\text{s}^{-1}\text{K}^{-1}$
L	Reactor length, cm
M	Radial position on complex model solution grid (Fig.4.2.)
N	Axial position on complex model solution grid (Fig.4.2.)
r	Variable reactor radius, cm
R	Internal tube radius, cm
RP	Rate of reaction, $\text{g cm}^{-3}\text{s}^{-1}$
S	Specific heat, $\text{cal g}^{-1}\text{K}^{-1}$
T	Variable reactor temperature, K

T4	Reactor temperature on grid point closest to wall (Appendix 4), K
TW	Reactor wall temperature, K
TS	Reactor steam temperature, K
U	Urea in stoichiometric equations and text (Chapter 3)
U	Urea concentration in mathematical equations, $\text{g cm}^{-3}$
UF1	Monomethylolurea concentration, $\text{g cm}^{-3}$
UF2	Dimethylolurea concentration, $\text{g cm}^{-3}$
UF3	Trimethylolurea concentration, $\text{g cm}^{-3}$
V	Incremental element volume, $\text{cm}^3$
$V_o$	Average inlet velocity, $\text{cm s}^{-1}$
$V_{\text{max}}$	Maximum velocity at tube centre, $\text{cm s}^{-1}$
$V_{x(r)}$	Variable velocity as function of radius, $\text{cm s}^{-1}$
x	Variable distance in the direction of flow, cm

#### DIMENSIONLESS GROUPS

$Da_I$	Damköhler number group I
$Da_{III}$	Damköhler number group III
Nu	Nusselt number
Re	Reynolds number
Pe	Peclet number
$Pe_t$	Peclet number for heat transfer
Pr	Prandtl number
Sc	Schmit number

## GREEK LETTERS

$\Delta E$	Activation energy, cal mol <sup>-1</sup>
$\Delta E_r$	Error
$\Delta H_R$	Heat of reaction, cal g <sup>-1</sup>
$\Delta r$	Radial grid dimension for solution of complex models (Fig.4.2.), cm
$\Delta x$	Axial grid dimension for solution of complex models (Fig.4.2.), cm
$\mu$	Viscosity, g cm <sup>-1</sup> s <sup>-1</sup>
$\rho$	Density, g cm <sup>-3</sup>
$\zeta$	Shear stress, dyne cm <sup>-2</sup>
$\zeta_w$	Shear stress at the tube wall, dyne cm <sup>-2</sup>
$\zeta_{rx}$	Variable shear stress, dyne cm <sup>-2</sup>
$\phi$	Ratio of external to internal diameter

## SUBSCRIPTS

EQ	At equilibrium
EXP	Experimental value
f	At fluid property
f <sub>av</sub>	At average fluid properties
F	Formaldehyde
M	Mixture
Max	Maximum
o	Inlet
PRE	Predicted value
(r)	In radial direction
U	Urea

UF1      Monomethylolurea  
(x)      In axial direction

SUPERSCRIPT

'          Dimensionless quantity of variable

Some of the symbols having localised meaning are defined in the text at the appropriate places.

# C H A P T E R 1

## INTRODUCTION

Chapter one describes the background from which the need for this research has arisen. The conventional batch manufacture of synthetic resins is described with emphasis on the shortcomings of this method of operation. Hence the potential advantages of a continuous operation are identified and the research for this change of operation specified. The chapter is terminated with a section on the choice of the reaction media for detailed examination. Although the work is described with particular emphasis on the chemical system chosen, it is considered that the principles established have wider application to other resins as well as to reaction media with similar physical properties.

### 1.1. HISTORICAL BACKGROUND

There are a number of commercial processes in existence which still rely on the traditional batchwise methods of production. The majority of synthetic resins fall into this category with the typical example of Amino resins (1). In those cases where volumetric production rates are small or where a large number of different end products originate from a common intermediate, the use of continuous methods may not be attractive. In other

cases, the process chemistry may preclude the continuous production of a required product. Lack of knowledge of the chemistry or a detailed engineering background may also prevent serious consideration of employing continuous means of production.

However, in the case of products with high volumetric output, modern industry favours continuous operation where possible. All such continuous processes in existence today have, at some time, been operated in a batch mode, either on a commercial scale or a research laboratory scale prior to the design of a continuous facility. Examples of successful conversion from traditional batch to continuous production of synthetic resins are polyesters of both thermoplastic(2) and thermosetting(3) types.

Since the commercial introduction of such resins in the 1920's, in the majority of cases the basic batch manufacturing technique has changed very little from that developed by its originators (4,5,6,7,8); these references are by no means exhaustive. Efforts since then have been, essentially, concentrated on the establishment of a better understanding of the reaction schemes and to the application of the product resins to a more diverse market. Some fundamental understanding of the system behaviour in the early stages of the reaction schemes has been established but the nature of the more complex later stages remains speculative in most cases.

## 1.2. THE TRADITIONAL BATCH PRODUCTION

In general the batch procedure for the manufacture of synthetic resins consists of three major stages. The mixing stage is followed by the reaction stage which yields the product. The product is then further processed into a suitable form for the end-user.

The first stage entails the mixing in correct proportions of raw materials. Due to the diverse nature and chemical properties of the raw materials, various means have to be employed to complete this step in the process.

Examples of these are:

(i) The batch manufacture of phenol-formaldehyde resins, where solid paraform is added to a high viscosity phenol-cashew-oil mixture. In this case adequate agitation is of prime importance.

(ii) In the case of melamine-formaldehyde resins, temperatures of between 90-100 degrees Celsius must be provided for the dissolution of melamine in aqueous formaldehyde (Formalin) to produce the reaction mixture which yields the desired product at these temperatures.

(iii) With urea as the coreactant, dissolution of urea in Formalin can be endothermic or exothermic, depending on the molar ratios employed. Hence heat has to be provided or removed as required to produce the reaction mixture at approximately 60°C for manufacture of this type of resin.

On completion of mixing the chemical properties of

the mixture are adjusted before passage to the next stage. As an example in the case of phenol-formaldehyde resins the pH of the mix is adjusted with sodium hydroxide.

In the second stage the reaction mixture is allowed to react under the required conditions of temperature, pressure and residence time. For the case of the thermosetting resins of the types described above, temperatures are of the orders given above and atmospheric pressure is invariably employed. Residence times vary according to each process, but are designed to allow the preliminary stages of the reaction only. This usually entails the methylation of the various raw materials with formaldehyde, known as 'Addition reactions'. However the methylols so formed are believed to condense to a slight extent in this stage of the operation.

The reaction is in general terminated by a combination of temperature and pH manipulation.

The products so formed could then take a variety of routes before despatch to the end-user. The phenol-formaldehyde resins, for instance, possess a very high viscosity at the end of the reaction stage and are therefore diluted with a suitable solvent. Conversely, urea-formaldehydes are vacuum concentrated to remove excess water, which is present in the system as a result of using aqueous formaldehyde.

### 1.3. DISADVANTAGES OF THE BATCH PRODUCTION ROUTE

2  
The relative merits of batch and continuous methods of production are well established. Those disadvantages of the batch route of processing which have a particularly detrimental effect on the cases under consideration are listed below(9).

- (i) The raw materials for manufacture of the majority of synthetic resins are comparatively cheap and abundant. However the process is highly labour intensive with high unit labour costs.
- (ii) The labour has direct involvement in making judgments to anticipate and implement various adjustments in the process. This results in a non-uniform product between batches due to variations in the operators' judgment especially when production extends over two or in some cases three shifts.
- (iii) As a result of quality variation from this method of manufacture, a quality control team is required to ensure that specification limits are maintained. Additional personnel with higher unit cost are required for this function.
- (iv) Economical production necessitates high volumetric outputs. As a result, the use of massive 'batch kettles' and equally large supporting platforms becomes unavoidable.

This consequently restricts the most economic use of floor area for further expansion to meet market demand.

- (v) To use the reactors for 'reaction time' only and therefore more efficient production, massive auxiliary equipment has to be provided for the intermediate hold-up of the resins as well as pre-dispatch processing. Even more floor area has to be used for this purpose, which makes the process highly disadvantageous.

#### 1.4. DESIRABILITY OF A CONTINUOUS PROCESS

One of the major facets of continuous production is its suitability for automation. Automatic operation reduces the use of labour, avoids its involvement in the process and significantly reduces the necessity for a quality control team. Hence the disadvantages of the batch route described in parts (i), (ii) and (iii) of Section 1.3 are remedied to some extent if not altogether. Furthermore, continuous operation will not require the use of auxiliary hold-up equipment referred to in Section 1.3 part (v), relieving the disadvantages associated with the use of large floor areas considerably. A comprehensive study of the relative merits of continuous and batch processing can be found elsewhere(9).

### 1.5. CHOICE OF A CONTINUOUS PROCESS

Of the three stages involved in the production of synthetic resins, described in Section 1.2, that of the reaction is the most important. Hence the choice of a continuous reactor becomes the prime task. Obviously there are a number of ways of achieving continuous operation. The criteria for the choice, however, should be based on the chemical features of the materials processed, together with maximum versatility for production of as many different resins as possible. Furthermore, any other improvements to be gained on the batch process, as a result of this conversion, should reinforce the choice. These improvements could be in the form of savings in space or reaction time. The reaction time can be reduced in most cases by elevation in temperature,

The reactions producing synthetic resins generally take place in a 'carrier' material. Should this material be water, such as in urea-formaldehydes and melamine-formaldehydes, the resins are termed 'Aqueous synthetic resins'. The presence of water gives rise to vapour pressure problems at higher temperatures. Non-aqueous resins usually exhibit higher boiling points than water, at atmospheric pressure. Hence exploitation of elevation in reaction temperature for a reduction in reaction time necessitates the introduction of pressure,

The choice of a continuous tubular reactor will accommodate the above improvements while providing the versatility required for the production of the majority

of synthetic resins. The problems of vapourisation associated with aqueous as well as some non-aqueous resins can be overcome with the provision of the required pressure. This can be done by the choice of a feed pump and a controlled orifice outlet.

The choice is made in preference to the possible use of a continuous stirred tank reactor (CSTR) as an alternative. The main reason for this is the extremely low residence times which satisfy the extent of reaction required under conditions of high pressure and temperature. This infers large throughputs in conjunction with low process volume which further precludes the use of CSTR. Furthermore tubular reactors are less costly for operation under pressure, occupying less space which are further advantages.

#### 1.6. STATEMENT OF THE OBJECTIVE OF THE RESEARCH

The object of the research is to develop mathematical models for a tubular reactor producing synthetic resins with the specific task of testing the models on one particular chemical system.

Although the work is presented in connection with this chemical system, the models are developed in the most general manner and it is considered that they will have a much wider application to all resins and chemical media with similar physical properties. Furthermore, such models as well as predicting the performance of the reactor would also be beneficial in design, optimisation

and control of a continuous facility.

### 1.7. CHOICE OF THE CHEMICAL SYSTEM

3  
The criteria governing the choice of the chemical media for detailed investigation were industrially orientated.

In the first instance it was essential to choose an industrially established synthetic resin. This would have the benefit of permitting comparison with the normal batch product, both in terms of ease of production and economic evaluation. Furthermore, the resin so produced could be tested in established markets for viability assessments.

The resources available to satisfy the above criteria restricted the choice to that of urea-formaldehyde systems. The disadvantages of such a choice may not be apparant at this point. However, two important disadvantages are:

(i) That almost invariably products of industrial significance are of highly complex natures.

(ii) Lack of data, due to commercially restricted publication.

The choice of urea-formaldehyde suffers from both of these disadvantages, but not as extensively as some other systems since there is some kinetic data published.

### 1.8. AREAS OF RESEARCH

Having specified the type of reactor, the objects of

the research and the chemical system to be investigated, the work was divided into the following five areas:-

- (i) Mathematical modelling of the reactor.
- (ii) Evaluation of data and specification of operating conditions for solution of models.
- (iii) Mathematical solution of models.
- (iv) Modification of available equipment for practical testing of the models.
- (v) Analysis and comparison of experimental and theoretical data for verification of the models.

Areas (i), (iii), (iv) and (v) are self-explanatory. Area (ii) of the research includes the chemical investigation of the urea-formaldehyde system which is presented in detail in Chapter 3.

## C H A P T E R 2

### THE MATHEMATICAL MODELS

In Chapter Two, a short introduction into various concepts of mathematical modelling is followed by a critical review of the available literature. The procedures for setting up mass, momentum and energy balances are then presented with particular emphasis on underlying theories. This gives rise to the generation of plug-flow and complex field equations which describe the two extreme possibilities for the general performance of a flow system through a tubular reactor involving chemical reaction. The assumptions applicable to the case under consideration are highlighted and used to adapt the models for this particular investigation. The chapter concludes with sections summarising the mathematical models.

#### 2.1. MATHEMATICAL MODELLING

A mathematical model can be defined as a unified explanation of a physio-chemical phenomenon by means of mathematical equations.

The various techniques employed to describe any physio-chemical process mathematically fall into the following three categories (10,11,12,13):

(4)

I : Deterministic

II : Probabilistic

III : Empirical

Deterministic mathematical modelling, although not always possible or adequate, is the most desirable modelling approach to a given problem. This is because deterministic models use for their description the basic laws of transport of mass, momentum and energy.

The equations of change describing the conservation of mass, momentum and energy are examples of deterministic modelling(10).

Probabilistic mathematical modelling is generally applied to those cases where deterministic models are only capable of describing a local region in the process and not the whole system. A classical application of probabilistic modelling can be found in the "kinetic theory of gases"(12). The general chemical engineering use of such models is associated with batch and continuous stirred tank reactors.

The application of empirical mathematical models is confined, to a large extent, to representation of experimental data. Examples of typical empirical models are the polynomials used to fit empirical data by the method of "least squares" (Chapter 3).

### 2.1.1. DETERMINISTIC MODELLING

The scope of deterministic mathematical modelling is presented in Table 2.1. which is adapted from

Stratum of physio-chemical description	Extent of use	Topical Designations
Molecular & atomic	Fundamental Background	Treats discrete entities Quantum mechanics Statistical mechanics
Microscopic	Applicable only to special cases	Laminar transport phenomena. Statistical theories of turbulence
Multiple gradient	Applicable only to special cases	Laminar & turbulent transport phenomena; transport in porous media
Maximum gradient	Used for continuous flow systems "plug flow"	Laminar & turbulent transport phenomena; reactor design
Macroscopic	Very widely used	Process engineering, unit operations. Classical kinetics and thermodynamics

TABLE 2.1

STRATUM OF DETAIL OF PHYSIO-CHEMICAL PRINCIPLES

As can be deduced from table 2.1. a tubular reactor can be described deterministically by microscopic, multiple and maximum gradient models.

The use of microscopic models is hindered by their extreme complexity, rendering them practically incapable of mathematical analysis.

The multiple gradient models are the next most complex, yet managable descriptive forms which can be used for analysis of a tubular reactor. The modelling

is based on the velocity profile of the fluids flowing through the tubes with the inclusion of dispersion effects for both mass and heat transport. On this basis the multiple gradient models can vary in complexity from those which include an assumed velocity profile together with radial and axial dispersion to those which assume a flat velocity profile ignoring all dispersion effects (plug flow models). This simplest form of a multiple gradient model can also be classified as a maximum gradient model.

The velocity profile in the multiple gradient models is generally represented by the Ostwald-de Waele equation or the 'power law model' which is capable of accommodating 'non-Newtonian' and 'Newtonian' fluids. Assuming a power index of unity the equation will represent a laminar velocity profile through the reactor tubes. However different dispersion mechanisms are possible with the same laminar flow profile depending on its velocity. These can be described as follows:-

(i) Under high velocities in the laminar flow region, dispersion occurs solely as a result of bulk flow since molecular diffusion is negligible. Such a flow is called a 'segregated' flow.

(ii) Under moderate velocities in the laminar flow region, dispersion is by way of convective and molecular diffusion. The flow is therefore 'partially segregated'.

(iii) Under very low velocities in the laminar flow regions, convective diffusion resulting from the velocity

profile is much smaller than molecular diffusion. Therefore dispersion is controlled by molecular diffusion alone.

Particular attention is drawn to the terms in inverted commas. This is for the purpose of clarifying definitions used in the review of the published literature which follows.

## 2.2. LITERATURE SURVEY

Published literature on the analysis of the performance of continuous reactors appears to naturally fall into two main subject areas, namely "ordinary" and "polymerisation" chemical reactions. This is confirmed in the case of tubular reactors where there is a definite tendency to differentiate between 'continuous polymerisation reactors' and 'continuous reactors for ordinary chemical reactions'.

The reason for this differentiation seems to lie in the chemical reaction mechanisms which take place in the reactor. In polymer chemistry, reactions result in chain growth, chain branching and cross-linking. Furthermore, steps such as initiation, propagation and termination have to be considered. As a result, techniques for analysis of polymerisation kinetics differ widely from those of ordinary chemical reactions. In this context, ordinary chemical reactions are exemplified by those of general order forward, reversible, simultaneous and consecutive reactions.

Since the applications of the mathematical models, derived in this chapter are general and inclusive of both polymerisation and ordinary chemical reactions in a tubular reactor, both areas have been surveyed in detail. However for purposes of clarity each review will be presented separately.

### 2.2.1. CONTINUOUS POLYMERISATION REACTORS

A review of the literature describing the process models of polymerisation reactors is now presented.

The broader field of chemical reactor engineering is itself relatively new, with the pioneer modern texts appearing in the late 1950's (14,15).

Of the literature published since, only a recent few deal with polymerisation reactors, hardly sufficient recognition of their commercial importance.

The new surge of interest seems to have been triggered by the availability of more general reactor theory, advances in mathematical modelling techniques and the advent of computers which permit the highly complex problems of polymerisation reactors to be treated quantitatively.

Chappelear and Simon(16) carried out a survey on the general work connected with the analysis of polymerisation systems and found that the greatest effort has been put into batch or Continuous Stirred Tank Reactors (CSTR) for mass/solution polymerisation. As they confirm, this is undoubtedly due to the relatively simple mathematical

(5)

formulations as well as the commercial importance of the above systems.

Of the recent moderate interest in the modelling of polymerisation reactors much has been channelled into the analysis of batch (17,18,19) or CSTR's (20,21,22,23,24, 25,26), these references by no means being exhaustive.

Chappelear and Simon refer to, in all, seven references published in connection with mass/solution polymerisation in a tubular reactor. However, only a few of these references deal with mathematical modelling of such reactors.

It can be concluded that there is little development in the modelling of polymerisation in tubular reactors. The following discussion of relevant literature cited will confirm the above conclusion.

Lynn and Huff(27) developed models for anionic polymerisation in a laminar flow tubular reactor. Assuming constant density and neglecting radial velocities and the axial diffusion of mass and heat, their models predicted axial and radial variations in composition, temperature and velocity. Profiles highly distorted relative to the predictions were obtained experimentally. The distortion in the velocity profile suggested deviation from the parabolic mode and the distortions in the temperature and concentration profiles were as serious. It is interesting to note that they confirmed the reason for reluctance in use of tubular reactors for solution polymerisation processes, namely, large radial temperature gradients. However, their conclusion seems

to be more governed by their choice of geometry than the actual polymerisation process.

The large tube diameter (2.9 inches) used in combination with their choice of relatively high wall temperature caused runaway polymerisation at the reactor wall. The material at the centre of the tube had not yet increased in temperature, so the polymerisation rate was much slower and consequently the solution far less viscous. The lower viscosity caused a large increase in velocity along the centre line of the reactor. When the heat finally reached the centre of the tube, thereby increasing the polymerisation rate and hence the viscosity, the velocity profile in the tube returned to parabolic shape even though the temperature gradients were still relatively large. This indicates that concentration has a large influence on viscous properties. The above authors, however, did not extend their analysis to include the effects on conversion or the molecular weight of the product.

The above work suggests that a good choice of tube geometry and wall temperature is therefore imperative to the successful operation of a tubular reactor for polymerisation reactions.

An investigation by Merrill and Hamrin(28) reports the numerical solution to a set of similar but simpler partial differential equations which are comparable to the complex models developed later in this work. Their main relevant conclusion was that radial diffusion had little effect on conversion.

Wallis(29) discussed the bulk polymerisation of Styrene by Azobisisobutyronitrile in a tubular reactor. His models for constant and variable density situations predicted molecular weights and conversions which compared favourably with the experimental results, but were between two to six per cent higher depending on whether a complex diffusion model or a plug flow model was used. From his studies he concluded that:

(i) Radial diffusion of the monomer and initiator had little effect on the model predictions of conversion and molecular weight.

(ii) Increased wall temperature, initiator concentration and reactor radius caused broad molecular weight distributions.

(iii) For a minimal molecular weight dispersion the reactor should be operated at a wall temperature five to ten degrees centigrade below that required for optimal conversion.

His results(29) seem to confirm deductions made from Lynn and Huff's paper(27), but it should be noted that the assumption that radial diffusion of both monomer and initiator can be neglected may well only apply to Styrene polymerisation.

Cintron-Cordero and co-workers(30) used for simulation a hypothetical free radical polymerisation process with zero order initiation and chain termination by radical disproportionation into two polymer molecules.

Besides assuming negligible radial diffusion and constant wall temperature, they further assumed that the

velocity profile conformed to a fluid of a consistency which could be approximated by a power law. From their results they concluded that the pseudo-plastic flow behaviour as characterised by the power-law flow index had an indirect influence on the product. This assumption in fact provided an explanation for the distorted velocity profile or in other words deviation from parabolic flow.

Biesenberger and co-workers(31) carried out simulation studies on homogenous free radical polymerisation of styrene initiated by azobisisobutyronitrile. Assuming constant density, no axial diffusion, no radial diffusion and a plug flow velocity profile their models presented molecular weights and conversions in the form of dimensionless plots. No experimental data were presented. Their use of higher initiator concentrations resulted in low molecular weight polystyrene which they note is of no industrial value.

They also listed a set of partial differential equations, but no results, for a more rigorous model(31). This more elaborate model included radial gradients but neglected axial mass and heat diffusion.

### 2.2.2. CONTINUOUS REACTORS FOR ORDINARY REACTIONS

When diffusion is neglected, the amount of reaction taking place inside a tube of a tubular reactor is determined solely by the velocity profile. A fluid element moving down one of the annular spaces can be considered

as behaving exactly like a batch system. The average composition of the fluid at the reactor outlet can be obtained by a process of averaging over the residence times corresponding to the infinite set of annuli. This segregation effect in laminar flow tubular reactors is on the molecular level, so that residence time distribution and the kinetic rate information are adequate to determine the reactor conversion for any reaction order.

Edwards and Salettan(32) reviewed the studies on segregation effects in pseudo-laminar or truly-laminar-flow reactors. They presented results which show the separate effects of reaction order, degree of radial transport, velocity profile and extent of conversion upon conversion loss attributable to segregation effects.

Bosworth(33) derived the residence time distribution function for a Poiseuille velocity profile. He deduced approximate limits for which diffusional effects on the residence time distribution may be neglected.

Johnson(34) collected the results for n-th order single and first order consecutive reactions. The effect of flattened velocity profiles caused by non-Newtonian flow has been investigated by Novosad and Ulbrecht(35) for various reaction orders and complete radial segregation, using a power-law model.

Ulrichson and Schmitz(36) studied numerically first order reactions in the entrance length of a viscous-flow-tubular reactor. They concluded that the entrance effect is negligible for most practical purposes.

Cleland and Wilhelm(37) solved numerically the

equations describing first-order chemical reaction coupled with radial diffusion and radial distribution of residence times in tubular reactors accommodating viscous flow. Experimental results for the hydrolysis of acetic anhydride were found to be described by their models for tubes less than 0.5 inch in diameter.

Hsu(38) and Lauwerier(39) formulated analytical solutions for the Cleland and Wilhelm equations. Weisler and Schechter(40) also presented the above analytical solutions and extended it further to include first-order consecutive chemical reaction cases.

Vignes and Trambouse(41) and Hovorka and Kendal(42) independantly investigated numerically and experimentally the single second-order chemical reaction in the laminar flow region. They (42) concluded that the effect of reducing the baffle spacing in a reactor on the conversion level is to increase the efficiency of the reactor until a limit of conversion equal to that obtainable in an equivalent plug flow reactor.

Wan and Ziegler(43,44) in two papers investigated the effects of rate constants and mixing parameters on yield loss, for distributed laminar flow. Using Taylor's expression for a dispersive Peclet number, they developed solutions and criteria for simulating laminar flow in the case of irreversible and consecutive reactions. Their results were presented in dimensionless form and physical explanations were offered in support of their conclusions as to the validity of their results and criteria.

They report (44) solutions for both first-and second-order sequential reactions in segregated laminar flow by Gianetto and Berbetto(45,46,47).

When the diffusion effect is taken into account, the residence time distribution functions will be modified by the diffusional transport of molecules between different annuli. Farrel and Leonard(48) developed a general solution for the residence time distribution function with regard to laminar diffusion-convection models. For these cases the residence time distribution function can no longer be used directly to predict the reactor performance for reactions other than those of first-order.

Felder and Hill(49) found that when radial mixing in a tubular reactor has an effect, it is to enhance fractional conversion, regardless of the nature of the residence time and local reaction rate distribution. This can be compared to a batch system where mixing either increases or does not have any effect on the overall conversion at a given time.

### 2.2.3. SUMMARY OF THE LITERATURE SURVEY

Among all the simulation studies discussed with regard to those concerned with polymerisation reactions, the following general deductions of prime importance are evident:

(i) Only in two instances is the theoretical work compared with experimental data.

(ii) There seems to be little emphasis on the effect of various operating conditions on the physical properties of the products or conversions in the reactors.

(iii) The work carried out by Lynn and Huff(27) and Wallis(29) suggests that there exists an optimum tube radius-wall temperature combination for each particular case. Increases in the radius coupled with high temperatures result in runaway reactions.

(iv) The work of Wallis(29) confirms that the radial diffusion of monomer has little effect on the model predictions of conversion.

(v) The Cintron-Cordero studies(30) suggest that it is justifiable to assume that moderately distorted velocity profiles have little effect on average polymer properties and consequently make use of a parabolic velocity profile for model simplification.

With regard to the literature reviewed in connection with continuous tubular reactors for ordinary reactions, the following important deductions are listed:-

(i) The predominant approach has been that of probabilistic modelling with emphasis on analysis of residence time distributions. This is due to the fact that convection effects have been considered of more importance in comparison with molecular diffusion by most authors.

The convective mechanism causes broad profiles and therefore residence time distributions have to be considered. This necessitates probabilistic modelling.

(ii) Much work has been channelled into the

analytical solution of the simpler cases which are of little industrial use.

(iii) Studies by Ulrichson and Schmitz(36) suggest that entrance effects are negligible for viscous flow tubular reactors.

### 2.3. THE MATHEMATICAL MODELS

Two types of deterministic mathematical models are developed to describe the performance of the tubular reactor.

Maximum gradient models describe one limiting case of the reactor behaviour. These models assume a plug-flow situation where all reactants spend exactly the same time in the reactor. In physical terms this system behaves in the same manner as a batch reactor. Therefore the performance of the reactor approaches the limiting condition where all reactants have the same opportunity for reaction under exactly the same conditions, irrespective of their radial position in the tubes and with the reactor being devoid of any mixing effects.

Multiple gradient models describe the other limiting case of the reactor behaviour. For this case an assumed velocity profile, based on the Reynold's number, represents the more realistic flow of the fluid in the reactor. The suitable velocity profile is then modified to account for the mixing mechanisms which exhibit themselves in such a system. These include the convection and diffusion of the reactants both axially and radially.

Therefore the performance of the reactor approaches the limiting condition where the state of each particular element is a function of its axial and radial position in the reactor tube and the prevailing conditions in that particular position. This limiting condition also accounts for all probable mixing mechanisms.

It has been emphasised that the models developed are for general use. The technique of modelling described above is aimed to serve this purpose. The plug flow and complex models in their final form can cover a wide range of operating conditions. In fact the models are universal if it can be assumed that the flow is not turbulent and that there are no natural convection effects in the reactor tubes.

If the above two assumptions can be justified, then the proximity of experimental results to either model prediction will indicate the more appropriate model and therefore the more likely physio-chemical mechanism taking place, for a particular system operating under a given set of conditions, in a tubular reactor.

### 2.3.1. PLUG-FLOW MODELS

The mass and energy balances can be developed from basic principles by considering an incremental element in the tube (Fig.2.1.), with the following assumptions:

- (i) Steady-state conditions prevail so that all time derivatives are zero.
- (ii) Flow takes place only in the axial direction.

(iii) The fluid is incompressible and therefore has a constant density.

(iv) Dissipation of energy through viscous flow of fluid is negligible.

(v) Heat effects caused by radiation are negligible.

The justifications for the above assumptions are presented in Appendix 1.

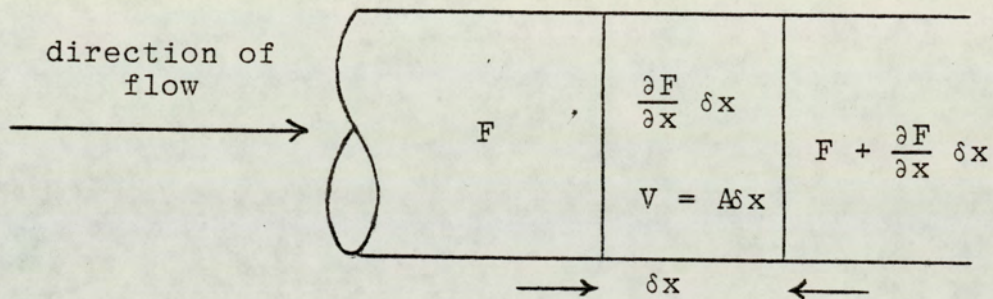


FIG 2.1.

PLUG FLOW INCREMENTAL ELEMENT

MASS MODEL

With reference to Fig. 2.1. and using the law of conservation of mass which states, at steady state:

$$\text{Mass input} = \text{Mass output} - \text{Mass generation}$$

The Mass Model for the component F can be written as:

$$AV_0 F - AV_0 \left( F + \frac{\partial F}{\partial x} \delta x \right) = RP_F A \delta x \quad 2.1.$$

On simplification equation 2.1. reduces to:

$$V_0 \frac{\partial F}{\partial x} = -RP_F$$

with the boundary condition:

$$F = F_0 \text{ at } x = 0$$

### ENERGY MODEL

Considering the same element and with the aid of the concept of heat transfer coefficient between the tube wall and the reacting fluid, the energy model can be set up as follows:

$$\begin{array}{l} \text{Energy into element} \\ \text{by bulk flow} \end{array} = \rho_M V_0 S \Pi R^2 T$$

$$\begin{array}{l} \text{Energy out of element} \\ \text{by bulk flow} \end{array} = \rho_M V_0 S \Pi R^2 T + \frac{\partial}{\partial x} (\rho_M V_0 S \Pi R^2 T) \delta x$$

$$\begin{array}{l} \text{Energy into element} \\ \text{by convection} \end{array} = 2 \Pi R h (T_W - T) \delta x$$

$$\text{Energy generation} = \Delta H_{R_F} R P_F \Pi R^2 \delta x$$

Balancing the inputs with the outputs according to the law of conservation of energy and simplifying:

$$\rho_M S V_0 \frac{\partial T}{\partial x} = \frac{2h}{R} (T_W - T) - \Delta H_{R_F} R P_F \quad 2.2.$$

with the boundary condition

$$T = T_0 \text{ at } x = 0$$

The analysis can be taken a stage further by evaluating the film heat transfer coefficient from the following equation (Appendix 2),

$$h = \frac{4.364 K_M}{2R} \quad 2.3.$$

Incorporating equation 2.3. in equation 2.2. results in:

$$\rho_M SV_O \frac{\partial T}{\partial x} = \frac{4.364 K_M}{R^2} (T_W - T) - \Delta H R_F R_P R_F \quad 2.4.$$

### AUXILIARY MASS MODELS

The kinetics of urea-formaldehyde reactions necessitates the inclusion of two more mass models for urea and monomethylolurea in order that the equations become numerically soluble (Chapter 4).

These are:

$$V_O \frac{\partial U}{\partial x} = -R_P U \quad 2.5.$$

$$V_O \frac{\partial UF1}{\partial x} = -R_P UF1 \quad 2.6.$$

with boundary conditions

$$U = U_O \quad \text{at} \quad x = 0$$

$$UF1 = 0 \quad \text{at} \quad x = 0$$

### 2.3.2. COMPLEX MODELS

The complex field equations can be developed from first principles(10) with the following assumptions:

(i) Steady-state conditions prevail so that all time derivatives are zero.

(ii) Bulk flow is taking place in the axial direction only so that all velocity terms except  $V_{x(r)}$  are zero.

(iii) Dissipation of energy through viscous flow of fluid is negligible.

(iv) The fluid is incompressible.

(v) Heat effects caused by radiation are negligible.

(vi) Natural convection has no effect on the models and does not cause distortion in the velocity profile.

The above assumptions have been justified in Appendix 1. With reference to figures 2.2 and 2.3, considering the incremental element in the tube, the models can be set up as follows:

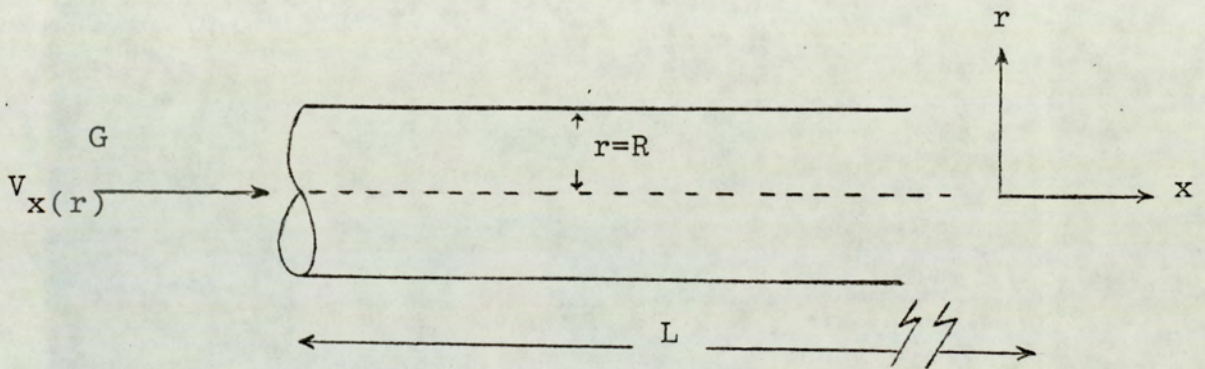


FIG. 2.2.

CO-ORDINATES OF THE REACTOR TUBE

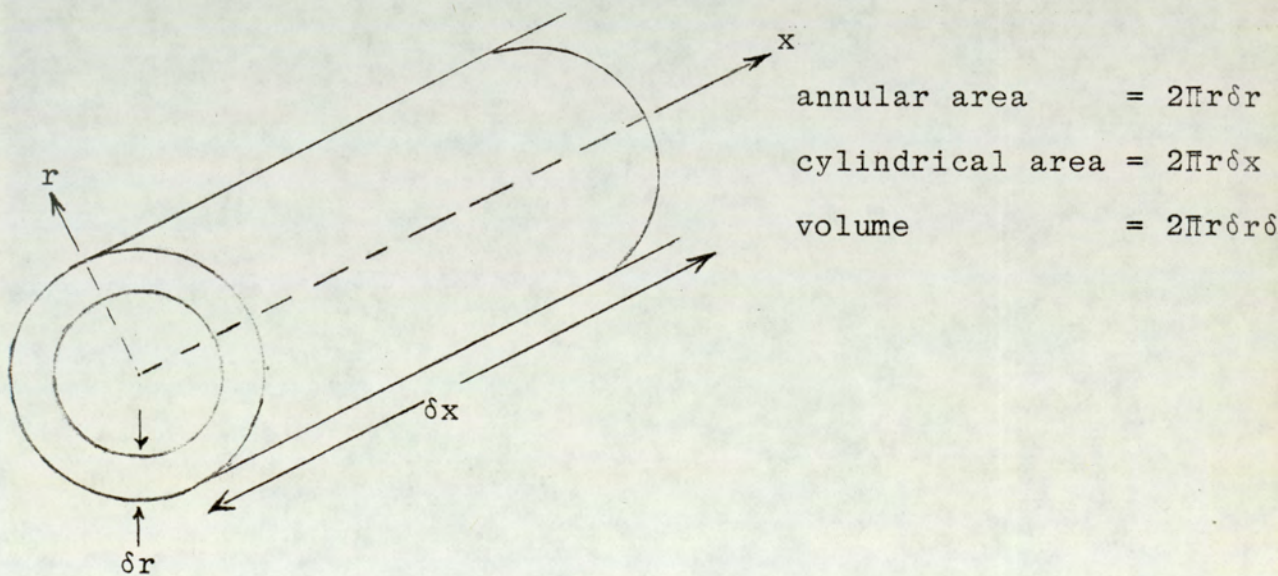


FIG. 2.3.

COMPLEX MODEL INCREMENTAL ELEMENT

## ENERGY MODEL

The energy input, output and generation terms on the element can be listed as:

Energy input

$$\text{by radial conduction} = -2\pi r \delta x K_{M(r)} \left( \frac{\partial T}{\partial r} \right)_r$$

$$\text{by axial conduction} = -2\pi r \delta r K_{M(x)} \left( \frac{\partial T}{\partial x} \right)_x$$

$$\text{by axial enthalpy transport} = 2\pi r \delta r \rho_M S V_{x(r)} T$$

Energy output

$$\begin{aligned} \text{by radial conduction} &= -2\pi r \delta x K_{M(r)} \left( \frac{\partial T}{\partial r} \right)_r + \\ &\quad \frac{\partial}{\partial r} \left\{ -2\pi r \delta x K_{M(r)} \left( \frac{\partial T}{\partial r} \right)_r \right\} \delta r \end{aligned}$$

$$\begin{aligned} \text{by axial conduction} &= -2\pi r \delta r K_{M(x)} \left( \frac{\partial T}{\partial x} \right)_x + \\ &\quad \frac{\partial}{\partial x} \left\{ -2\pi r \delta r K_{M(x)} \left( \frac{\partial T}{\partial x} \right)_x \right\} \delta x \end{aligned}$$

$$\begin{aligned} \text{by axial enthalpy transport} &= 2\pi r \delta r \rho_M S V_{x(r)} T + \\ &\quad \frac{\partial}{\partial x} \left\{ 2\pi r \delta r \rho_M S V_{x(r)} T \right\} \delta x \end{aligned}$$

$$\text{Energy generation} = 2\pi r \delta r \delta x R P_F (\Delta H R_F)$$

The law of conservation of energy can be written as, at steady state:

$$\text{Energy Output} - \text{Energy Input} = \text{Energy Generation}$$

Substitution of the terms according to the above law

results in:

$$V_{x(r)} \frac{\partial T}{\partial x} = \frac{K_{M(x)}}{S \rho_M} - \frac{\partial^2 T}{\partial x^2} + \frac{K_{M(r)}}{S \rho_M} \left\{ \frac{\partial^2 T}{\partial r^2} + \frac{1}{r} \frac{\partial T}{\partial r} \right\} - \frac{R P_F \Delta H R_F}{S \rho_M}$$

2.6.

$$\text{Now } \frac{K_M(x)}{S\rho_M} = D_{TH(x)}$$

$$\frac{K_M(r)}{S\rho_M} = D_{TH(r)}$$

where  $D_{TH(x)}$  is the thermal diffusivity coefficient axially and  $D_{TH(r)}$  is the thermal diffusivity coefficient radially.

Hence equation 2.6 becomes

$$V_{x(r)} \frac{\partial T}{\partial x} = D_{TH(x)} \cdot \frac{\partial^2 T}{\partial x^2} + D_{TH(r)} \left\{ \frac{\partial^2 T}{\partial r^2} + \frac{1}{r} \frac{\partial T}{\partial r} \right\} - \frac{RP_F \Delta HR_F}{S\rho_M}$$

2.7.

Equation 2.7. is the most complex field equation describing the energy effects on the system. This equation makes provision for all variable parameters except those considered to have a negligible effect in the original assumptions.

However the energy model can be further simplified as follows:

(i) The thermal diffusivity coefficients are not functions of radius and axial length so that  $D_{TH(r)} = D_{TH}$  and  $D_{TH(x)} = D_{TH}$ . This assumption is justified by the order of magnitude of these coefficients, which is in the region of  $10^{-5}$  (Appendix 3) and any variations will not affect their magnitude significantly.

(ii) Axial diffusion of heat is negligible compared with the sensible heat arising from the bulk flow, whereas radial heat diffusion has to be included (Appendix 3).

This reduces the equation to:

$$V_{x(r)} \frac{\partial T}{\partial x} = D_{TH} \left\{ \frac{\partial^2 T}{\partial r^2} + \frac{1}{r} \frac{\partial T}{\partial r} \right\} - \frac{RP_F \Delta HR_F}{\rho_M S} \quad 2.8.$$

Equation 2.7. is first-order with respect to 'x' and second-order with respect to 'r'. Hence three boundary conditions are necessary for its solution. These can be arrived at from considerations at the entry to the tube, tube centre and tube wall,

thus:

$$T = T_o \text{ at } x = 0 \text{ for all } r$$

$$\frac{\partial T}{\partial r} = 0 \text{ at } r = 0 \text{ for all } x$$

$$TW = TS \text{ at } r = R$$

$$TW = \frac{hfT4 + \phi hcs TS}{hf + \phi hcs} \text{ at } r = R \quad 2.9.$$

where

TS Temperature of steam in shell

TW Tube wall temperature

hf Tube side film coefficient

hcs Outside film coefficient

$\phi$  Ratio of external to internal diameter

T4 Temperature closest to the wall on the Mesh grid used for solution of model (see Chapter 4)

The reason for the necessity of specifying two boundary conditions at the reactor tube wall is presented in Appendix 4. Appendix 4 also includes the derivation of equation 2.9. and the numerical evaluation of all the necessary variables.

#### MASS MODEL

The concentration model can be developed by analogy

to the energy model. These will be identical except for the fact that concentration replaces temperature, molecular diffusivity replaces thermal diffusivity and terms for generation of heat are replaced by terms for the rate of reactions.

Hence the mass model predicting the behaviour of formaldehyde becomes:

$$V_{x(r)} \frac{\partial F}{\partial x} = D_{M(x)} \left( \frac{\partial^2 F}{\partial x^2} \right) + D_{M(r)} \left\{ \frac{\partial^2 F}{\partial r^2} + \frac{1}{r} \frac{\partial F}{\partial r} \right\} - RP_F \quad 2.10.$$

The assumption of  $D_{M(x)} = D_{M(r)} = D_M$  and negligible axial diffusion of mass (Appendix 3) can be made in a similar manner to those for the energy model.

Hence the final equation is:

$$V_{x(r)} \frac{\partial F}{\partial x} = D_{MF} \left\{ \frac{\partial^2 F}{\partial r^2} + \frac{1}{r} \frac{\partial F}{\partial r} \right\} - RP_F \quad 2.11.$$

with the boundary conditions:

$$F = F_0 \quad \text{at} \quad x = 0 \quad \text{for all } r$$

$$\frac{\partial F}{\partial r} = 0 \quad \text{at} \quad r = 0 \quad \text{for all } x$$

$$F = F_{EQ} \quad \text{at} \quad r = R \quad \text{for all } x \quad 2.12.$$

Appendix 5 presents a technique for evaluating the equilibrium concentration of formaldehyde which has been used in boundary condition 2.12.

#### AUXILIARY MASS MODELS

The kinetics of urea-formaldehyde reactions necessitate the inclusion of two more mass models for

urea and monomethylolurea in order that the equations become numerically solvable (Chapter 4).

These are:

$$V_{x(r)} \frac{\partial U}{\partial x} = D_{MU} \left\{ \frac{\partial^2 U}{\partial r^2} + \frac{1}{r} \frac{\partial U}{\partial r} \right\} - R P_U \quad 2.13.$$

$$V_{x(r)} \frac{\partial UF1}{\partial x} = D_{MUF1} \left\{ \frac{\partial^2 UF1}{\partial r^2} + \frac{1}{r} \frac{\partial UF1}{\partial r} \right\} - R P_{UF1} \quad 2.14.$$

with the boundary conditions:

$$U = U_0, \quad UF1 = 0 \quad \text{at } x = 0 \quad \text{for all } r$$

$$\frac{\partial U}{\partial r} = \frac{\partial UF1}{\partial r} = 0 \quad \text{at } r = 0 \quad \text{for all } x$$

$$U = U_{EQ}, \quad UF1 = UF1_{EQ} \quad \text{at } r = R \quad \text{for all } x \quad 2.15.$$

The equilibrium values of urea and monomethylolurea are evaluated in Appendix 5.

### MOMENTUM MODEL

The momentum model is primarily developed to express a relationship for the velocity profile as a function of viscosity and radius. In the light of findings by Cintron-Cordero (30), which are discussed in the literature survey, it can be assumed that moderately distorted velocity profiles have little effect on average product properties and hence use can be made of the parabolic velocity profile associated with laminar flow (Appendix 1), so that,

$$V_{x(r)} = V_{Max} \left( 1 - \left( \frac{r}{R} \right)^2 \right)$$

and since  $V_{Max} = 2 V_0$

$$\text{Then } V_{x(r)} = 2 V_0 \left( 1 - \left( \frac{r}{R} \right)^2 \right) \quad 2.16.$$

This model will provide adequate description although non-Newtonian Viscous effects have been neglected. However a more elaborate model is developed in the following pages and can be used in cases where equation 2.16 proves to be inadequate.

Assuming that the fluid behaviour corresponds to a Newtonian model whose viscosity is a function of temperature, pressure, polymer concentration, time and molecular weight, then one can write:

$$\zeta_{rx} = -\mu \left( \frac{\partial V_x(r)}{\partial r} + \frac{\partial V_r}{\partial x} \right) \quad 2.17.$$

where  $\mu = f(T, P, P_c, t, MW)$

The term  $\frac{\partial V_r}{\partial x}$  can be neglected due to its small magnitude compared with the term  $\frac{\partial V_x(r)}{\partial r}$ , so that,

$$\zeta_{rx} \approx -\mu \frac{\partial V_x(r)}{\partial r} \quad 2.18.$$

Equation 2.18 gives the variation of shear stress with velocity and suggests that shear stress is zero at the centre of the tube where  $r = 0$  and varies linearly with  $r$ , assuming a value  $\zeta_W$  at the wall i.e.

$$\zeta_{rx} = \zeta_W \frac{r}{R} \quad 2.19.$$

Equating equations 2.18 and 2.19 gives

$$dV_{x(r)} = \frac{-\zeta_W}{R} \cdot \frac{r}{\mu} dr$$

which on integration of the L.H.S. yields

$$V_{x(r)} = \frac{-\zeta_W}{R} \int_{r=R}^{r=r} \frac{r}{\mu} dr \quad 2.20.$$

Considering the incremental element in the tube, Fig.2.3., the mass flow rate for the element is given by

$$2\pi r \rho_M V_{x(r)} dr$$

The total mass flow rate is then

$$G = \int_{r=0}^{r=R} 2\pi r \rho_M V_x(r) dr$$

Since the total mass flow rate is constant at any cross-section, then,

$$G = 2\pi R^2 \rho_M V_o = \int_{r=0}^{r=R} 2\pi r \rho_M V_x(r) dr \quad 2.21.$$

rewriting equation 2.21,

$$V_o = \frac{2}{R^2} \int_{r=0}^{r=R} V_x(r) r dr \quad 2.22.$$

and substituting for  $V_x(r)$  from equation 2.20. into 2.22.

$$V_o = \frac{2}{R^2} \left( \frac{-\zeta W}{R} \right) \int_{r=0}^{r=R} r \int_{r=R}^{r=r} \frac{r}{\mu} dr dr \quad 2.23$$

Hence finally the relationship between velocities can be established by dividing 2.20. by 2.23. and simplifying, so that,

$$V_x(r) = V_o \frac{R^2}{2} \frac{\int_{r=R}^{r=r} \frac{r}{\mu} dr}{\int_{r=0}^{r=R} r \int_{r=R}^{r=r} \frac{r}{\mu} dr dr} \quad 2.24.$$

The momentum model given in equation 2.24. is capable of predicting the velocity profile once the viscosity is known as a function of position in the tube. If viscosity is treated as a constant, 2.24. reduces to 2.16. on integration. It is interesting to note that even for non-Newtonian behaviour the equation will hold, once the dependance of viscosity on shear stress has been allowed for in 2.17.

### 2.3.3. DIMENSIONLESS COMPLEX MODELS

In this section dimensionless and normalised complex models are developed. This exercise serves two important purposes. Normalisation of the models will bound the range of all variable parameters, except temperature, between the numerical values of zero and one. This results in reduction of round off error on the computer when numerical solutions are attempted. In cases where the numerical value of numbers used are very high or very low, round off error could effect the accuracy of results significantly. Making the models dimensionless introduces the use of accepted groups which can be valuable in generalising the results.

With the above in mind the dimensionless variables can be introduced as follows:

Reactor Radius

$$r' = \frac{r}{R} \quad \text{where } 1 \geq r' \geq 0 \quad 2.25.$$

Reactor Length

$$x' = \frac{x}{L} \quad \text{where } 1 \geq x' \geq 0 \quad 2.26.$$

Formaldehyde Concentration

$$F' = \frac{F}{F_0} \quad \text{where } 1 \geq F' \geq 0 \quad 2.27.$$

Urea Concentration

$$U' = \frac{U}{U_0} \quad \text{where } 1 \geq U' \geq 0 \quad 2.28.$$

Momethylolurea Concentration

$$UF1' = \frac{UF1}{UF1_{EQ}} \quad \text{where } 1 \geq UF1' \geq 0 \quad 2.29.$$

Velocity

$$V'_{x(r)} = \frac{V_x(r)}{V_{\max}} = \frac{V_x(r)}{2V_0} \quad \text{where } 1 \geq V' \geq 0 \quad 2.30.$$

Reactor Temperature

$$T' = \frac{T}{T_0} \quad \text{where } N \geq T' \geq 1 \quad 2.31.$$

where N is a value of the ratio greater than one.

### DIMENSIONLESS ENERGY MODEL

Substituting the appropriate dimensionless variables for the dimensional variables in equations 2.8, results in:

$$V'_{x(r)} \frac{\partial T'}{\partial x'} = \frac{D_{THL}}{2R^2 V_0} \left( \frac{\partial^2 T'}{\partial r'^2} + \frac{1}{r'} \frac{\partial T'}{\partial r'} \right) - \frac{\Delta H R_F R_P F}{\rho_M S} \cdot \frac{L}{2V_0 T_0} \quad 2.32.$$

$$\text{Now } \frac{D_{THL}}{2R^2 V_0} = \frac{1}{Pe_t} = \frac{1}{Re Pr} \quad 2.33$$

where

$Pe_t$  is Peclet number for heat transfer

Re is Reynolds number =  $\frac{2\rho_M R^2 V_0}{L \mu}$

Pr is Prandtl number =  $\frac{S \mu}{K_M}$

$$\text{and } \frac{\Delta H R_F R_P F L}{2\rho_M S V_0 T_0} = Da_{III} \quad 2.34.$$

where  $Da_{III}$  = Damkohler number group III (50)

So that the dimensionless energy model becomes,

$$V'_{x(r)} \frac{\partial T'}{\partial r'} = \frac{1}{Pe_t} \left( \frac{\partial^2 T'}{\partial r'^2} + \frac{1}{r'} \frac{\partial T'}{\partial r'} \right) - Da_{III} \quad 2.35$$

with dimensionless boundary conditions:

$$T' = 1 \quad \text{at } x' = 0$$

$$\frac{\partial T'}{\partial r'} = 0 \quad \text{at } r' = 0$$

$$TW' = \frac{TS}{T_0} \quad \text{at } r' = 1$$

$$TW' = \frac{hfT_4' + \phi hcs \, TS/T_0}{hf + \phi hcs} \quad \text{at } r' = 1$$

where  $TW' = \frac{TW}{T_0}$  and  $T_4' = \frac{T_4}{T_0}$

### DIMENSIONLESS MASS MODELS

Similarly the dimensionless forms of equations 2.11., 2.13. and 2.14. become:

$$V'_{x(r)} \frac{\partial F'}{\partial x'} = \frac{1}{Pe_F} \cdot \frac{L}{R} \left( \frac{\partial^2 F'}{\partial r'^2} + \frac{1}{r'} \frac{\partial F'}{\partial r'} \right) - Da_{IF} \quad 2.36$$

$$V'_{x(r)} \frac{\partial U'}{\partial x'} = \frac{1}{Pe_U} \cdot \frac{L}{R} \left( \frac{\partial^2 U'}{\partial r'^2} + \frac{1}{r'} \frac{\partial U'}{\partial r'} \right) - Da_{IU} \quad 2.37.$$

$$V'_{x(r)} \frac{\partial UF1'}{\partial x'} = \frac{1}{Pe_{UF1}} \cdot \frac{L}{R} \left( \frac{\partial^2 UF1'}{\partial r'^2} + \frac{1}{r'} \frac{\partial UF1'}{\partial r'} \right) - Da_{IUF1} \quad 2.38.$$

where

$$Pe \text{ is Peclet number for mass transfer} = \frac{2V_0R}{DM_G}$$

$$Da_I \text{ is Damkohler number group I (50)} = \frac{RP_G L}{2V_0 C_{0G}}$$

$C_0$  is the initial concentration of F, U and UF1 depending on the equation used. Subscripts F, U and UF1 refer to formaldehyde, urea and monomethylolurea respectively. Subscript G denotes the fact that the values of parameters change according to each equation to account for the particular reactant.

The boundary conditions for the above models become:

$$F' = U' = 1 \text{ at } x' = 0$$

$$UF1' = 0 \text{ at } x' = 0$$

$$F' = \frac{F_{EQ}}{F_0} \text{ at } r' = 1$$

$$U' = \frac{U_{EQ}}{U_0} \text{ at } r' = 1$$

$$UF1' = 1 \text{ at } r' = 1$$

$$\frac{\partial F'}{\partial r'} = \frac{\partial u'}{\partial r'} = \frac{\partial UF1'}{\partial r'} = 0 \text{ at } r' = 0$$

### DIMENSIONLESS MOMENTUM MODEL

Substitution of 2,25. and 2,30. into 2,16. gives the dimensionless momentum model as:

$$v' = 1 - (r')^2$$

### 2.3.4. SUMMARY OF MATHEMATICAL MODELS

#### 1. PLUG FLOW MODELS

$$V_0 \frac{\partial F}{\partial x} = -RP_F \quad 2.40.$$

$$V_0 \frac{\partial u}{\partial x} = -RP_U \quad 2.41.$$

$$V_0 \frac{\partial UF1}{\partial x} = -RP_{UF1} \quad 2.42$$

$$\rho_M S V_0 \frac{\partial T}{\partial x} = \frac{4.364 K_M}{R^2} (TW-T) - \Delta HR_F PR_F \quad 2.43.$$

with boundary conditions:

$$T = T_0, F = F_0, U = U_0, UF1 = 0 \text{ at } x = 0 \text{ For all } r$$

## 2. COMPLEX MODELS

$$V_{x(r)} \frac{\partial T}{\partial x} = D_{TH} \left\{ \frac{\partial^2 T}{\partial r^2} + \frac{1}{r} \frac{\partial T}{\partial r} \right\} - \frac{RP_F \Delta HR_F}{\rho_M S} \quad 2.44.$$

$$V_{x(r)} \frac{\partial F}{\partial x} = D_{MF} \left\{ \frac{\partial^2 F}{\partial r^2} + \frac{1}{r} \frac{\partial F}{\partial r} \right\} - RP_F \quad 2.45$$

$$V_{x(r)} \frac{\partial U}{\partial x} = D_{MU} \left\{ \frac{\partial^2 U}{\partial r^2} + \frac{1}{r} \frac{\partial U}{\partial r} \right\} - RP_U \quad 2.46.$$

$$V_{x(r)} \frac{\partial UF1}{\partial x} = D_{MUFI} \left\{ \frac{\partial^2 UF1}{\partial r^2} + \frac{1}{r} \frac{\partial UF1}{\partial r} \right\} - RP_{UF1} \quad 2.47$$

$$V_{x(r)} = 2V_0 (1 - (r/R)^2) \quad 2.48$$

with boundary conditions

$$T = T_0, \quad F = F_0, \quad U = U_0, \quad UF1 = 0 \quad \text{at } x = 0$$

$$\frac{\partial T}{\partial r} = \frac{\partial F}{\partial r} = \frac{\partial U}{\partial r} = \frac{\partial UF1}{\partial r} = 0 \quad \text{at } r = 0$$

$$\left. \begin{aligned} F &= F_{EQ} \\ U &= U_{EQ} \\ UF1 &= UF1_{EQ} \\ TW &= \frac{hfT4 + \phi hcsTS}{hf + hcs} \\ TW &= TS \end{aligned} \right\} \text{ at } r=R$$

## 3. DIMENSIONLESS AND NORMALISED COMPLEX MODELS

$$V'_{x(r)} \frac{\partial T'}{\partial x'} = \frac{1}{Pe_t} \left( \frac{\partial^2 T'}{\partial r'^2} + \frac{1}{r'} \frac{\partial T'}{\partial r'} \right) - Da_{III} \quad 2.49$$

$$V'_{x(r)} \frac{\partial F'}{\partial x'} = \frac{1}{Pe_{FR}} \left( \frac{\partial^2 F'}{\partial r'^2} + \frac{1}{r'} \frac{\partial F'}{\partial r'} \right) - Da_{IF} \quad 2.50$$

$$V'_{x(r)} \frac{\partial u'}{\partial x'} = \frac{1}{Pe_{UR}} \left( \frac{\partial^2 U'}{\partial r'^2} + \frac{1}{r'} \frac{\partial U'}{\partial r'} \right) - Da_{IU} \quad 2.51$$

$$V'_{x(r)} \frac{\partial UF1'}{\partial x'} = \frac{1}{Pe_{UF1R}} \left( \frac{\partial^2 UF1'}{\partial r'^2} + \frac{1}{r'} \frac{\partial UF1'}{\partial r'} \right) - Da_{IUF1} \quad 2.52$$

$$V' = 1 - (r')^2 \quad 2.53$$

With boundary conditions:

$$T' = F' = U' = 1, \quad UF1' = 0 \quad \text{at } x' = 0$$

$$\frac{\partial T'}{\partial r'} = \frac{\partial F'}{\partial r'} = \frac{\partial U'}{\partial r'} = \frac{\partial UF1'}{\partial r'} = 0 \quad \text{at } r' = 0$$

$$F' = \frac{F_{EQ}}{F_0}$$

$$U' = \frac{U_{EQ}}{U_0}$$

$$UF1' = 1$$

$$TW' = \frac{hfT_4' + \phi hcs \, TS/T_0}{hf + \phi hcs}$$

$$TW' = TS/T_0$$

} at  $r'=1$

## C H A P T E R 3

### THE CHEMISTRY OF UREA-FORMALDEHYDE (UF) REACTIONS

In Chapter Two, mathematical models describing the limiting conditions of the reactor behaviour are developed. The values of the physical data, required for solution of the models are reported in Appendix 3. In this Chapter the kinetics of the reactions between urea (U) and formaldehyde (F) are examined to complete the information required in order to apply the models. A survey of published research into UF reactions is followed by the postulation of a tentative reaction mechanism taking place under the reactor operating conditions. The representation of experimental data over the investigated temperature range is attempted on this basis and the discrepancies highlighted. The need for research into high temperature reaction between urea and formaldehyde is subsequently emphasised and a novel technique developed to carry out the investigation required.

Finally, non-linear regression analysis is applied to the results to provide a mathematical description of the rate of reaction over the temperature range. Incorporation of the kinetic data, in this final form, into the reactor models completes the reactor description.

### 3.1. INTRODUCTION

Perhaps the first research on the reaction of formaldehyde (F) with urea (U) was reported by Tollens(61) in 1884, where he isolated monomethylolurea (MMU), the first addition product of the UF reaction. Dimethylolurea (DMU) was isolated by Einhorn and Hamberger(62) who conducted further pioneering research in this field. John(63) achieved practical application of UF resins about 1920, causing much interest in the commercial exploitations of these products. This was followed by more vigorous research which includes the work of Pollak(64), Walter(65), Ellis(66), Henkel and Cie(67), Dixon(68) and others.

Although many papers have been published in this field, the contributions on kinetics and mechanisms have been rather limited, probably due to the complexity of the reactions involved and the lack of advanced analytical techniques for the chemical analysis of the various components. However, as new analytical tools have been developed, research on kinetics and mechanisms has progressed.

### 3.2. THE KINETICS AND MECHANISMS OF THE INTERACTION OF UREA WITH FORMALDEHYDE

Of the research reported on the reaction of U and F, much has been confined to the early stages of the reaction.

De Jong and de Jonge(75-82) made extensive research into UF reaction mixtures in the early stages of the reaction. Landquist(83-87) substantially confirmed the work by de Jong and de Jonge(75-82) and further contributed to the literature by developing a spectrophotometric method of following the reactions (88-91). His latter work confirmed the findings of de Jong and de Jonge over a wide range of conditions.

In 1961, Ito(92) introduced a paper chromatographic technique for isolating and measuring the rate of development of the condensation products of a UF reaction mixture, thereby contributing to a better understanding of the mechanisms and kinetics.

The more general findings reported in the above literature can be summarised as follows:-

(i) The initial interaction of U with F is by addition reactions which can lead to condensation reactions under the correct conditions.

(ii) The rates of reactions are pH dependant.

(iii) The rates of reactions are temperature dependant.

(iv) The extent of reaction is dependant on F to U molar ratio.

(v) Concentration has little effect on the rate constants over a wide range of conditions.

(vi) The reactions are reversible and are generally second order forward and first order reverse.

(vii) While the addition reactions are both acid and base catalysed the condensation reactions are subject

to specific hydrogen-ion catalysis.

The literature is therefore presented with particular reference to the above and under the individual sections of addition reactions, condensation reactions and UF resins formation.

### 3.2.1. ADDITION REACTIONS OF UF

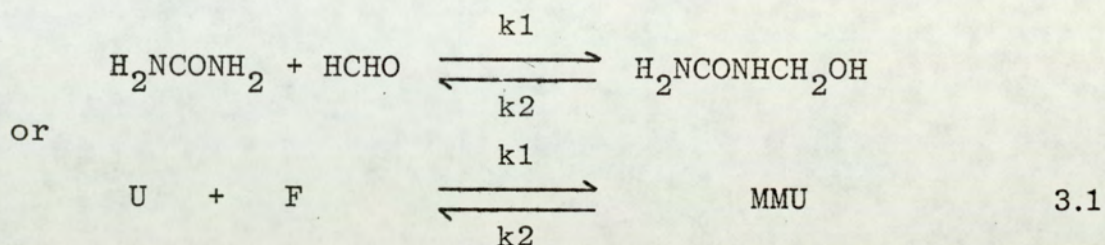
The rate of reaction between urea and formaldehyde was investigated extensively by de Jong and de Jonge (75) who followed the reaction by determining the consumption of F. In neutral, acidic and basic solutions the forward reaction for formation of MMU was found to be bimolecular. The reverse reaction causing dissociation of MMU proved to be monomolecular. Data were obtained over a pH range of 2-11 in 0.045 to 0.2M solutions at 25-59°C.

Reaction conditions were so chosen to minimise condensation reactions. The total F content (unreacted F + Methylolated F) was determined using the alkaline Iodine method. The free F was detected using the acidimetric sulphite method and the extent of methylation was thus obtained by difference. The use of this technique served to confirm that condensation remained small.

They(75) evaluated the equilibrium level of F at 59°C by sustaining a 0.045M phosphate buffer solution at pH 7.0 for twenty hours.

The reversibility of the reaction was studied by using pure MMU (M.P. 109° - 110°C, 99.7% theoretical

methylol content) which was placed in aqueous solution. F was formed and the equilibrium reaction 3.1 was demonstrated.



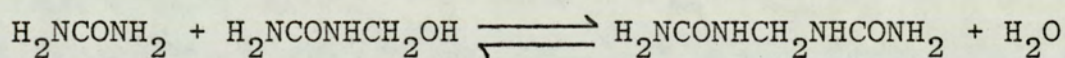
Second order characteristics were established for the forward reaction and first order kinetics shown for the reverse reaction. The rate and equilibrium constants evaluated over a range of conditions are presented in Table 3.1.

Temp. °C	pH	Forward Rate k1 exp (lit/mol s)	Reverse Rate k2 exp (s <sup>-1</sup> )	Equilib. Const. K = k2/k1 Exp. (mol/lit)
25	7	0.6 x 10 <sup>-4</sup>	1.2 x 10 <sup>-6</sup>	2.0 x 10 <sup>-2</sup>
35	11	1.6 x 10 <sup>-4</sup>	5.5 x 10 <sup>-5</sup>	3.7 x 10 <sup>-2</sup>
35	7	1.1 x 10 <sup>-4</sup>	3.2 x 10 <sup>-6</sup>	3.7 x 10 <sup>-2</sup>
35	2	1.5 x 10 <sup>-4</sup>	4.2 x 10 <sup>-5</sup>	
42	7	1.9 x 10 <sup>-4</sup>	6.8 x 10 <sup>-6</sup>	4.1 x 10 <sup>-2</sup>
59	7	5.7 x 10 <sup>-4</sup>	3.1 x 10 <sup>-5</sup>	5.6 x 10 <sup>-2</sup>

TABLE 3.1.

FORMATION AND DECOMPOSITION OF MMU(75)

Good agreement between experimental equilibrium constants and theoretical equilibrium constants evaluated from  $k_1$  and  $k_2$ , obtained from the isolated forward and reverse reactions, was noted over a wide range of conditions. The rate of reaction was shown to be independent of pH over the range of 4-9, while the equilibrium constant demonstrated no dependence on pH over the range of 2-11. In more acid solutions the equilibrium was affected by the condensation reaction between U and MMU according to equation 3.2,



3.2.

Corrections for this effect were applied to kinetic data obtained at  $\text{pH} \approx 2.0$  for calculation of equilibrium constants. According to de Jong and de Jonge(75) the rate constants had also to be corrected to account for further addition of F to MMU to produce DMU,

Both the forward and reverse reaction rates were shown to be catalysed by hydronium ions and hydroxyl ions and affected by ionised salts acting as buffers. Neutral salts had very little effect on reaction rates.

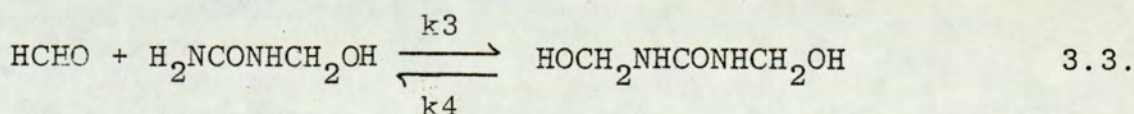
The activation energy for the forward reaction was estimated at 13 Kcal/mol and in the case of the reverse reaction a value of 19 Kcal/mol was obtained. The heat of reaction is thus -6 Kcal/mol. The activation energies were calculated from Arrhenius plots and it was further shown that the equilibrium shifts

to the left in equation 3.1. with increasing temperature, therefore confirming conclusions which could be reached by the application of Le Chatelier's rule.

De Jong and de Jonge(77) later repeated the above investigations in more concentrated solutions, 4M. The small differences they observed were explained by the influence of formation of hemiformals and the effects of the influence of the dielectric constant of the reaction media. Otherwise the effect of concentration on rate of reaction was concluded to be negligible.

Since U is a tetra-functional compound and possesses four reactive points, F can add from one to four molecules to U to give mono., di., tri., and tetra-methylolurea. The extent to which the addition reactions can proceed depends on the molar ratio of F to U. While conflicting results regarding isolation of tetra-methylolurea (TEMU) have been reported, there is general agreement(92,93) that DMU and trimethylolurea (TMU) formation occurs quite readily under the correct conditions.

De Jong and de Jonge(76) followed the formation and dissociation of DMU in depth and elucidated the kinetics of the reaction as:



The conditions were again chosen to minimise condensation. The reaction scheme in 3.3. was investigated using the same techniques as for 3.1. and the results seemed to follow the same pattern.

The forward reaction was second order while the reverse reaction showed first order characteristics. The reaction was both acid and base catalysed and its rate did not depend on pH within the same limits as found for MMU. Their results for equilibrium and rate constants over a range of temperature were presented in the form of Arrhenius plots(76). The heat of reaction for this case was estimated at -5 Kcal/mol.

(Forward 14 Kcal/mol - Reverse 19 Kcal/mol)

The reaction of F with DMU to produce TMU was investigated in a similar manner and reported by de Jong and de Jongein (78). In order to ensure the formation of TMU, molar ratios of F to U of 4:1 were employed. The equilibrium constants for this reaction, were estimated algebraically and the data is given in Table 3.2. The calculations assumed no formation of TeMU.

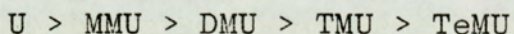
It would appear that TeMU is extremely unlikely to be formed even at U:F ratios of up to 1:20. The only account of TeMU formation has been reported by Ito(92), who used paper chromatographic techniques to detect this compound from a solution of U and F reacted at 60°C and under highly alkaline conditions.

Constant at 35°C and pH 7.0.	$U+F \rightleftharpoons MMU$	$MMU+F \rightleftharpoons DMU$	$DMU+F \rightleftharpoons TMU$
Forward, $k_1$ (lit/mol s)	$0.9 \times 10^{-4}$	$0.38 \times 10^{-4}$	$0.1 \times 10^{-4}$
Reverse, $k_2$ ( $s^{-1}$ )	$2.5 \times 10^{-6}$	$0.69 \times 10^{-5}$	
Equilibrium Experimental, $K_{exp} = \frac{k_2}{k_1}$ (mol/lit)	0.036	0.22	1.2

TABLE 3.2.

EQUILIBRIUM AND RATE CONSTANTS IN  
UF ADDITION REACTIONS(76)

From the above studies it can be concluded that the reaction proceeds step-wise with increasing difficulty. Thus the ease of formation of nitrogen methylol derivatives is in the order

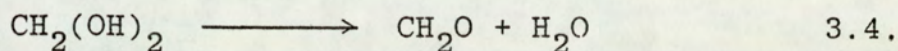


Landquist, in a series of papers(83-91) confirmed the findings of de Jong and de Jonge at 20°C, using both quantitative chemical analysis and a spectrophotometric technique. He further investigated the effect of the presence of methanol in commercial formalin (Appendix 6). This was found to retard the rate of reaction considerably (90).

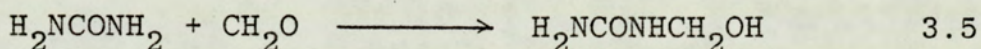
CHEMICAL MECHANISM OF METHYLOLUREA FORMATION

In aqueous solution F is present largely as the

monohydrate, methylene glycol (Appendix 6). As it is unlikely that the hydrated form of F can react directly with U, then the dehydration of methylene glycol must precede the UF reaction according to Equation 3.4.



It is generally believed that the addition reaction then takes place by U contributing an electron pair which provides the carbon-nitrogen link with F. This suggests that F has an electrophilic tendency for reaction with U as shown in Equation 3.5.



The detailed reaction mechanism of Equation 3.5. is different in alkaline and acid solutions. Two theories by Smythe(69,70) and de Jong and de Jonge(75) have been suggested for the formation of methylolureas in alkaline solutions.

Smythe(69,70) has suggested that in alkaline solutions U may change its form from Fig.3.1. to Fig.3.2.

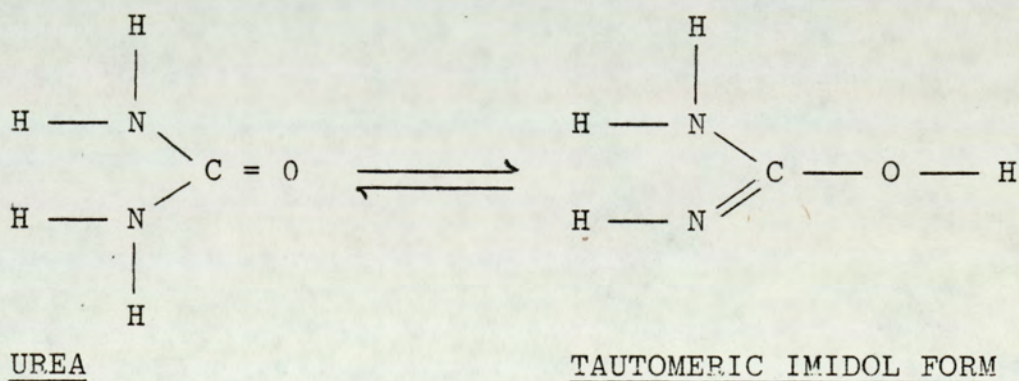
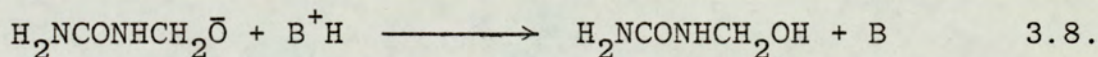
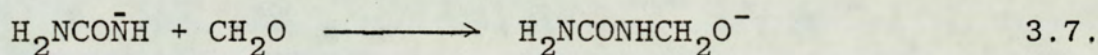
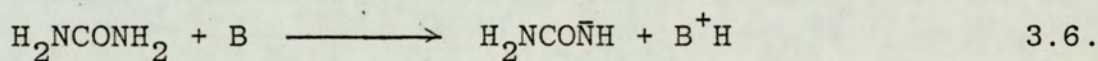


FIG. 3.1.

FIG. 3.2.

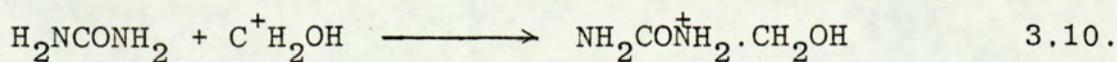
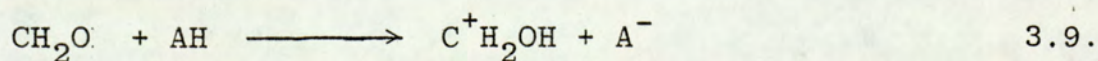
The latter known as the Tautomeric Imidol form of U possesses a U anion (Imidol urea anion) which Smythe suggests is the active specie in the UF reaction.

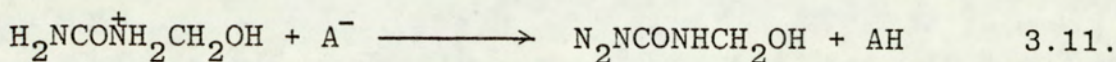
De Jong and de Jonge on the other hand theorise that the base itself is involved in the reaction mechanism. According to their theory the base takes up a proton from U, leaving it in the anionic form. In this form U then has the opportunity of becoming activated for electrophilic attack by F. The mechanism then proceeds as in Equations 3.6. to 3.8., where 'B' represents the base which is usually either sodium hydroxide or hexamine.



The de Jong and de Jonge theory for methylolurea formation in alkaline solutions can be extended to describe the mechanism in acid solutions. By a comparative mechanism the F becomes activated by addition of a proton in acid solutions, F in this state should attack U more readily than the un-ionised F, thus providing an explanation for the vigour of the reactions in acid solutions.

The scheme as given in equations 3.9. to 3.11., where 'AH' represents the acid, is suggested by de Jong and de Jonge(75).



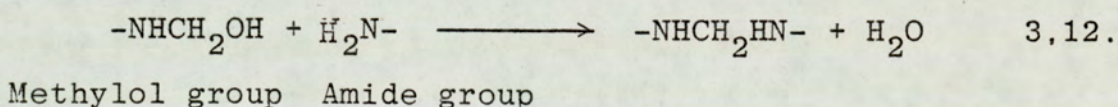


### 3.2.2. CONDENSATION REACTIONS OF UF

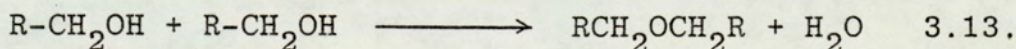
Condensation reactions in aqueous UF solutions follow different paths depending on the pH of the mixture and are reversible in nature during the early stages of reaction.

The condensation mechanism in acid solutions follows a different course to that in basic or neutral solutions due to the different reactivities of the chemical groups involved.

Generally, there are two possible routes for condensation in aqueous solutions of U and F. In the first instance combination of a methylol group with urea would result in condensation products as outlined in equation 3.12.



The other possibility for condensation is the reaction between two methylol groups thus:

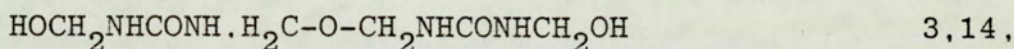


The preference in choice of routes is governed by the acidity or alkalinity of the solution. For this reason the condensation reactions in alkaline and acid solutions are presented separately in the following sections.

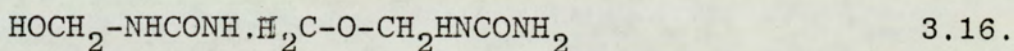
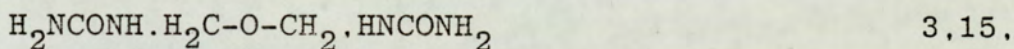
## CONDENSATION REACTIONS IN ALKALINE SOLUTIONS

In neutral or alkaline solutions condensation occurs almost exclusively by interaction of methylol groups as outlined in Equation 3.13. Equation 3.13, also shows that the link between the two methylol groups is a " $-\text{CH}_2, \text{O}, \text{CH}_2-$ " formation known as a "methylene ether bridge".

As an example, DMU condenses in mildly alkaline solutions to give:



and MMU under the same conditions produces two compounds with structures as shown in 3.15. and 3.16, below:



These compounds were isolated by Zigeuner(94,95,96) who developed degradative techniques which enabled him to distinguish between methylene ether bridges which are described above and the methylene bridges which have a formation " $-\text{CH}_2-$ " and are the linkage groups for condensation products of methylol and amide groups as outlined in equation 3.12. Having developed the above technique he was able to confirm that condensation in neutral or alkaline solutions was mainly by mutual reactions of methylol groups.

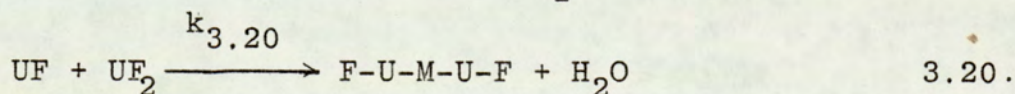
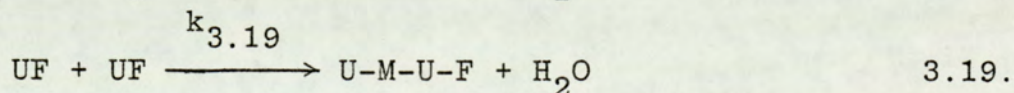
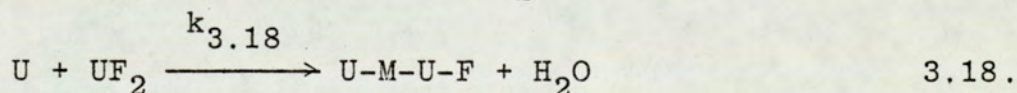
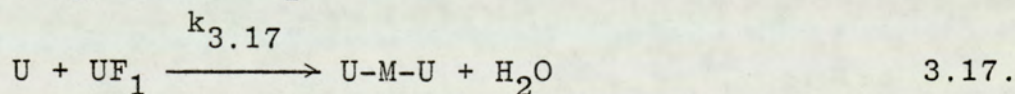
As will be shown in the following section, in acid solutions however, condensation occurs almost exclusively by the mechanism of Equation 3.12.

## CONDENSATION REACTIONS IN ACID SOLUTIONS

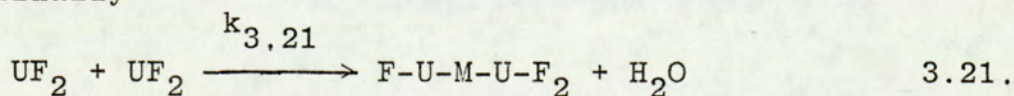
While methylolureas condense in alkaline solutions almost exclusively by mutual interaction of methylol groups to form methylene-ether bridges, in acid solutions the exclusive condensation reaction is that of Equation 3.12, where methylol and amide groups combine to produce methylene bridges.

Zigeuner(94,95,96) continued his studies of "linkage groups" to cover weak acid solutions pH 4-7, and acid solution pH less than 4. His main conclusions were that although in weak acid solutions the slight possibility of methylene ether linkage existed, in acid solutions methylene bridges alone are formed. De Jong and de Jonge(78) confirm this in their extensive kinetic study and add that the reaction mechanism suggested in Equation 3.12, is bimolecular. On this basis they studied five possible reactions between U, MMU and DMU.

If -M- denotes the methylene bridge  $-\text{CH}_2-$  and with  $\text{MMU} \equiv \text{UF}_1$ ,  $\text{DMU} \equiv \text{UF}_2$

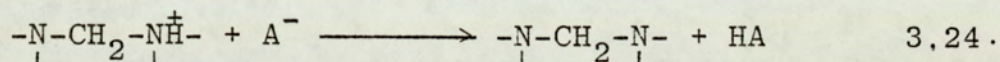
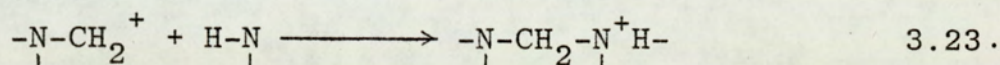
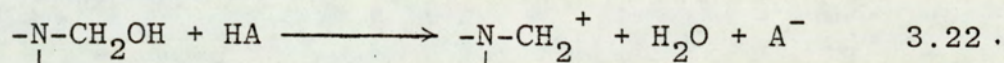


and finally



The F,U, methylene bridge and extra hydrogens at each end of the chain can be distinguished as before.

De Jong and de Jonge believe that the mechanism for all of the above reactions is the same and suggest the following scheme(78),



Experimentally the reactions were followed by measuring the decrease in methylol group concentration. This enabled them to establish the order of the reactions and evaluate the rate constants which are given in Table 3.3,

The techniques used for detection of methylol groups involved analysis for combined F by iodimetric evaluations. The conditions under which the reactions proceeded were so chosen that dissociation of methylolureas was relatively small and its effects could be neglected.

RATE CONSTANT k	VALUE AT 35°C pH.4 1/MOL S
$k_{3.17}$	$2.3 \times 10^{-4}$
$k_{3.18}$	$2.0 \times 10^{-4}$
$k_{3.19}$	$0.85 \times 10^{-4}$
$k_{3.20}$	$0.5 \times 10^{-4}$
$k_{3.21}$	less than $0.03 \times 10^{-4}$

TABLE 3.3.

RATE CONSTANT VALUES FOR POSSIBLE  
CONDENSATION REACTIONS

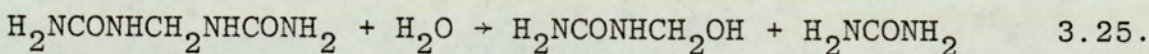
From Table 3.3, and under the experimental conditions of de Jong and de Jonge(78), it can be concluded that the reaction of Equation 3.21. is either extremely slow or does not occur at all, indicating that methylol groups do not readily combine with a substituted amide group. Furthermore, the methylol group in MMU is seen to be more reactive than in DMU, while the  $-NH_2$  group in MMU is less reactive than in U.

The other significant result from this investigation was that while the UF addition reactions are generally acid-base catalysed; the condensation reactions, or more specifically the rate constants for these reactions, are only subject to specific hydrogen ion catalysis(78).

Experiments showed that elevation in temperature in

each case caused an increase in the rate of reaction, as can be expected, and activation energies of about 15 Kcal/mol for each of the reactions 3.17 to 3.21 were found.

To add to the complexity of the situation, the chemical reactions so far described are not the only ones involved, in fact all the condensation products can undergo further changes in the solution with increased time. Taking the simplest condensation product, methylenebisurea (U-M-U) as an example, it can undergo hydrolysis in solution in accordance with equation 3.25.



and, in solution, also behaves in a manner analogous to U, forming addition and condensation products with F and MMU(97,98). Following the same pattern as in the previous case the addition reactions are subject to general acid-base catalysis while the condensation reactions are subject to specific hydrogen ion catalysis. The rate constants for these reactions are identical to those of the corresponding reactions of U.

Detailed examination of equation 3.25. has shown it to be first-order, the rate constant being directly proportional to hydrogen ion concentration. From this it can be concluded that the condensation reaction between MMU and U and probably the process of methylene link formation in general is reversible in acid solutions. The activation energy for the reaction in 3.25. is 19.5 Kcal/mol (81). This shows the condensation

reaction to be exothermic to the extent of  
 $-19.5 + 15 = -4.5$  Kcal/mol.

One of the major deductions from analysis of these systems is that the state of progress of condensation reactions in aqueous solutions can be closely controlled by adjustment of pH and temperature of the system and this is important and invaluable in terms of process conditions for production of UF resins.

### 3.2.3. THE UF RESINS

UF resins are produced by a solution of U in formalin containing between one to three molecules of F to one molecule of U. Under mildly acid conditions the solution is boiled under reflux and polymerisation is characterised by the following changes(99).

"initially on cooling the solution, white amorphous solids are precipitated. As heating proceeds, the temperature at which the solids separate falls until a point is eventually reached when the condensation products remain dissolved at room temperature. The cold solution at this stage is infinitely miscible with water. On further heating, the syrup diminishes in water tolerance, increases in viscosity and in due course sets to an insoluble and irreversible gel". "However, prior to gelation the reaction can be arrested at any convenient stage by addition of alkali in excess of the acid present". The syrup in this form is then vacuum evaporated to remove water to any required degree and the

resin used for application.

The above sequence of events can be explained in the light of the chemistry of UF reactions discussed in the previous sections. The excess F to U ratio is to ensure the production of methylolureas and the acidity of the solution to render condensation possible. The high temperature speeds the reaction and the progress of the polymerisation reaction can be observed by the increase in viscosity and eventually gelation. The adjustment of pH so that it falls in the alkaline range virtually stops the polymerisation at any required stage and thereafter water removal is achieved under vacuum so that low temperatures are dominant and the possibility of further reaction is reduced.

Industrially, the resins are produced in two stages. In the first stage the UF mixture mentioned above is heated under neutral or mildly alkaline conditions to ensure methylolurea formation. Thereafter the solution is made slightly acid and condensation to the required degree effected. The resin is then vacuum concentrated, if necessary, as described above.

#### THEORIES OF UF RESIN FORMATION

The theory of functionality (100) states that, three

dimensional networks can only be formed when, at least, one of the constituent molecules has three or more reactive points, in order that molecular chains can cross-link. Since the production of thermosets requires cross-linking between molecular chains, then it follows that UF resins which exhibit thermosetting characteristics must possess initial constituents with three or more reactive points.

The same theory states that where molecules have two reactive points each, straight or branch-chained formations are the only possibility. From the addition products of U and F, MMU has four reactive points. However, the reactive points in all methylolureas are the hydroxyl groups and the hydrogen atoms attached to the nitrogen. Therefore, the MMU system is not truly 4,4 since each hydroxyl group must have a corresponding hydrogen in another molecule to react with.

This suggests therefore that MMU is only capable of producing straight or branched chain polymers which generally exhibit thermoplastic rather than thermosetting characteristics(101).

DMU on the other hand contains two reactive hydrogen atoms and two reactive hydroxyl groups per molecule rendering a true 4,4 system and therefore the mutual interaction of its molecules provide ample opportunity for cross-linking. The formation of DMU is achieved by increasing the F to U ratio to above 1:1 and therefore U F mixtures with these molar ratio characteristics produce cross-linked and hence thermosetting resins.

The exact nature of the chemical reactions and progress to complex cross-linked structures from low molecular weight products is far from understood. The several theories put forward are based on a knowledge of structures at the early stages of the reaction, the behaviour of apparently similar chemical systems and the experimental measurement of the rate of water and F liberation and consumption during the reaction.

The theories put forward to date can be divided into three categories, in general. These are described briefly under different headings. It will become apparent that the theory of "chain growth" has most support and gives the best explanation of the sequence of observations made in the preparation of this kind of resin.

#### THE CHAIN GROWTH THEORY

This theory is based on the work of many investigators (65,102,103) who performed their studies separately and in different periods. The recent work of Zigeuner(94,95) and the extensive studies of de Jong and de Jonge tend to support it, providing the most widely accepted explanation of the practical observations made during the preparation of the resin.

The theory postulates the initial growth of molecular chains of varying lengths, consisting of condensed methylolurea molecules with the structure of 3.26.



A detailed discussion of this theory can be found elsewhere(9). The principles of the theory are similar to the methylene and methylene ether bridge formations discussed in Section 3.2.2.

#### THE TRIMERISATION THEORY

This theory now little supported, was first put forward by Marvel(105), in 1941. It postulates that U acting as both amine and amide, first condenses with F to give a cyclic trimer, which on further condensation with F yields a spatial network.

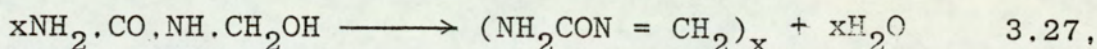
Alternatively, Thurston(106) suggests cyclisation of MMU and DMU, followed by cross-linking of heterocyclic rings by condensation of N-methylol groups with -NH- groups.

Conceptions such as these would adequately account for the high degree of branching and cross-linking which exists in cured UF resins, but are speculative and lack rigorous experimental proof(106). Moreover, the recent work of Zigeuner(94,95), de Jong and de Jonge and others provide considerable evidence confirming the presence of molecular chains in the early stages of condensation and absence of ring structures.

#### THE AZOMETHINE THEORY

This theory postulates that methylol compounds dehydrate to unsaturated azomethine or methylenimine

groups as in 3.27., from which branched or cross-linked structures build up by addition polymerisation (104).

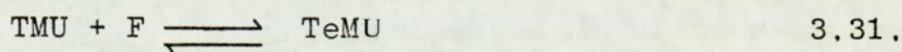


The above concept suffers from the same limitations as that of the trimerisation theory, namely, lack of experimental evidence. In fact, as mentioned before, the experimental evidence so far gathered seems to point towards the "chain-growth" theory as the most plausible explanation of the mechanism of UF resin formation.

#### 3.2.4. SUMMARY OF UF REACTIONS

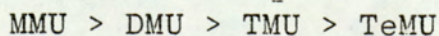
The reaction between U and F can be summarised in the following way.

In the first steps of the reaction, F can add from one to four molecules to one molecule of U to form the methylolureas in the stepwise manner shown in equations 3.28. to 3.31.



The addition reactions possess the following properties:

- (i) The reactions proceed with increasing difficulty such that the formation of methylolureas will have the order of ease of



- (ii) The extent of reaction is dependant on the U:F molar ratio.
- (iii) All reactions are second-order forward and first-order reverse,
- (iv) All reactions are acid and base catalysed.
- (v) All reactions are exothermic.
- (vi) The rate constants are independant of pH in the pH range 4-9.
- (vii) Rate constants increase with temperature following the Arrhenius law.
- (viii) Concentration has little effect on the value of rate constants.

The UF condensation reactions can take place between any two of the constituents of equations 3.28. to 3.31. The condensation reactions investigated possess the following properties:

- (i) The mechanism of condensation in acid solutions is by way of methylene bridge formation. The mechanism of condensation in alkaline solutions is by the way of methylene ether bridge formation.
- (ii) The methylol group's reactivity is in the order MMU>DMU>TMU while the reactivity of  $-NH_2$  group is in the order of TMU>DMU>MMU.
- (iii) Reactions are second-order forward and first-order reverse, for the early stages of the reaction.
- (iv) The reactions are subject to specific hydrogen ion catalysis.



(v) Reactions are exothermic.

(vi) Equilibrium constants are independent of pH.

The UF resins are produced by allowing the above reactions to take place under suitable conditions. The chain-growth theory provides the most generally accepted explanation of the observations which can be made during preparation of UF resins.

### 3.3. EVALUATION OF RATE OF REACTION AT LOW TEMPERATURES

The rate of reaction can be defined mathematically as:

$$R_{P_c} = \pm \frac{dc}{dt} \quad 3.32.$$

where  $c$  is the concentration of a reaction constituent in a reaction mixture. The negative sign denotes the consumption of a species and the positive sign denotes the production of a species.

The numerical value of the expression 3.32. can be found from a plot of concentration versus time ( $c-t$  curve) where the gradient of the resultant curve at any given time is a measure of the rate of reaction (Fig. 3.3.)

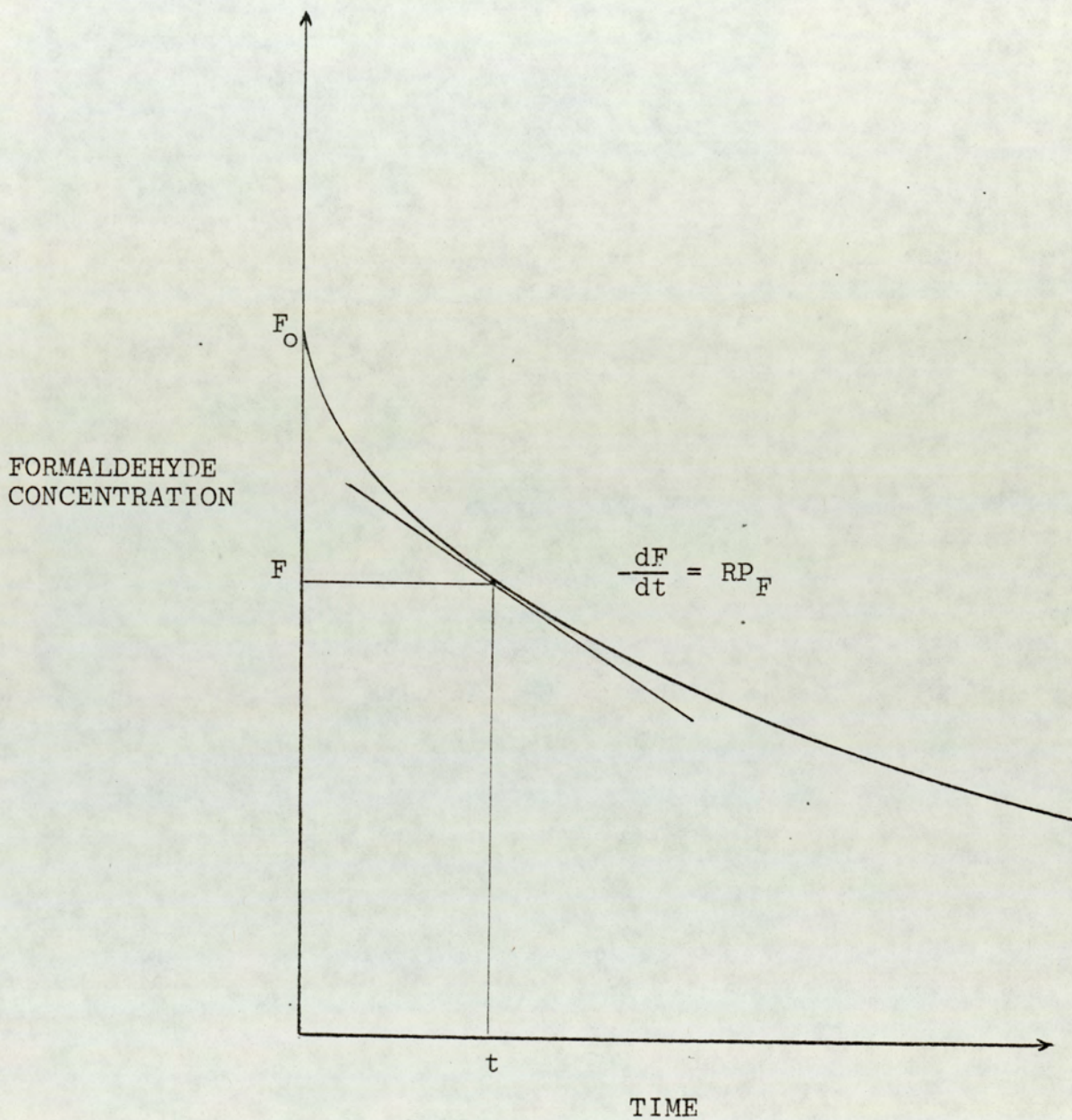


FIG. 3.3.

DEFINITION OF RATE OF REACTION

Therefore the steps required for the evaluation of rate of reaction are as follows:

- (i) Observations of c-t curves under the required conditions.
- (ii) Representation of the c-t curves mathematically.
- (iii) Evaluation of the rate of reaction from the mathematical expression by differentiation of concentration with respect to time.

It may be suggested at this point that if the curves are available, it would be possible to evaluate the gradient at a given point either graphically or by approximation techniques. However, in most cases c-t curves are of the exponential form and graphical or approximation techniques would prove to be inaccurate. The above three steps therefore, provide the best approach to the investigation of the kinetics.

### 3.3.1. DEVELOPMENT OF CONCENTRATION-TIME CURVES

Details of c-t data which were made available are given in Table 3.4. and Fig. 3.4.(107). Concentration of F was evaluated using the acidimetric sulphite method described in Appendix 9. The experiments were performed in standard open glass reactors, equipped with a stirrer for agitation and a condenser to prevent escape of volatile materials. 36% formalin of industrial specifications (Appendix 6) was used in all experiments. The experimental investigation covered a temperature range of 20<sup>o</sup>-80<sup>o</sup>C at a U:F molar ratio of 1:1.33. See Fig. 3.4.

TEMP., T °C	TIME, t MIN	CONC. F <sub>O</sub> , F %
25	0	23.40
	60	13.10
	120	9.90
	240	6.60
	360	4.75
40	0	23.40
	15	14.50
	30	11.30
	60	7.60
	120	4.70
	240	2.25
	300	1.75
60	0	23.40
	10	8.80
	20	5.40
	30	3.75
	60	1.90
	120	1.00
	240	0.50
	360	0.25
80	0	23.40
	5	7.40
	10	3.75
	20	1.70
	30	1.00
	60	0.70
	120	0.60
	240	0.50
	360	0.50

TABLE 3.4.

CONCENTRATION-TIME DATA FOR FORMALDEHYDE

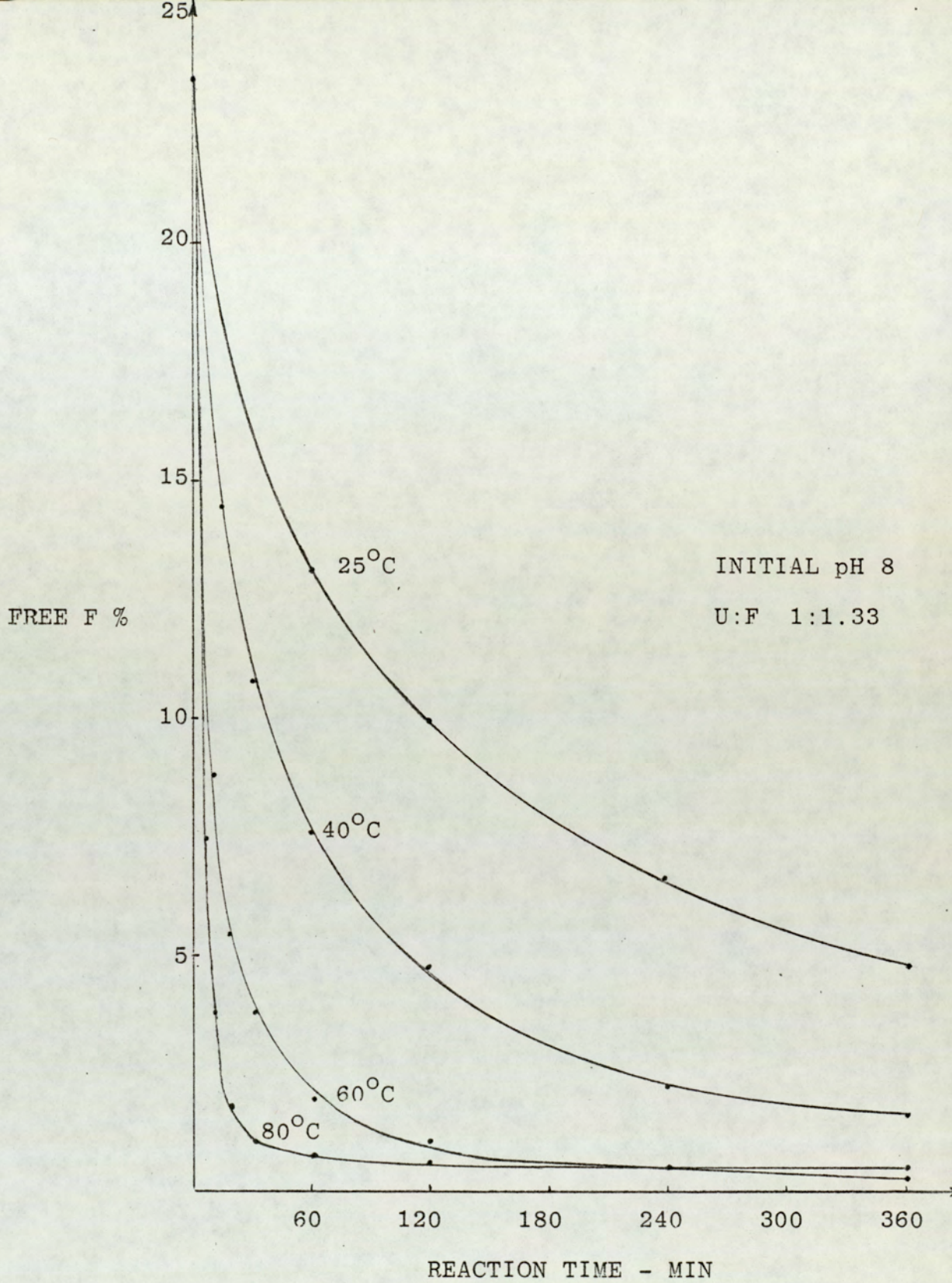


FIG. 3.4.

CONCENTRATION - TIME CURVES FOR FORMALDEHYDE

### 3.3.2. MATHEMATICAL REPRESENTATION OF CONCENTRATION - TIME CURVES

There are several techniques which can be applied to fit mathematical equations to the c-t curves. Since the curves exhibit exponential form, equations of the type 3.33. to 3.36. may be used for fitting the data.

$$F = +ae^{-bt} \quad \text{where } t > 0 \quad 3.33.$$

$$F = +at^{-b} \quad 3.34.$$

$$\log \log \frac{F_0}{F} = A \log \log t + B \quad 3.35.$$

$$\log \log \frac{F_0}{F - F_{EQ}} = A \log \log t + B \quad 3.36.$$

Plots of  $\log F$  versus  $t$  from equation 3.33, gave a number of straight lines which possessed sharp discontinuities.

Plots of  $\log F$  versus  $\log t$  from equation 3.34, resulted in straight lines covering the middle region of each set of data, turning into sharp curves at extremes.

Plots of equations 3.35, and 3.36., which were used by Landquist(87) to present his data at 20°C, resulted in straight lines covering 85-90% of the range covered by each set of data. However the range of applicability fell with increase in temperature. Furthermore, use of equations 3.35. and 3.36. can be criticised on the grounds that the effect of employing a loglog scale is to reduce the relative magnitude of the divergence of data from straight line plots. In fact the above plots at 80°C were so inaccurate that a back substitution of time into the final equation produced free F concentrations which

were approximately 50% in error,

A second approach to this sort of problem is the use of approximation techniques and elementary curve fitting principles. In this connection the method of least squares was applied to equations 3.33. and 3.34. to force a mathematical fit. Again the result, evaluated on a Honeywell 316 computer was to achieve fits over regions of data at each temperature. The method generally failed in attempting to cope with the sharp turn towards equilibrium in the c-t curves at high temperatures. Polynomial fits of the forms of equations 3.37. and 3.38. were also examined on the same computer.

$$F = a + bt + ct^2 + dt^3 + ft^4 + \dots \quad 3.37.$$

$$F = a + bt + ct^2 + g e^{-mt} \quad 3.38.$$

By using terms as high as  $t^4$ , in equation 3.37., fits were obtained which covered the data range at 20°C and 40°C with an average accuracy of 4% difference between experimental and predicted values of free F. However the accuracy dropped sharply with rise in temperature.

Examination of equation 3.38. proved somewhat more successful giving 1.5% maximum difference at 25°C, with the difference rising to 5% maximum at 80°C.

In conclusion of the above investigation the following points became evident.

- (i) Comparatively poor accuracy in the equations developed to describe the data.
- (ii) Absence of any temperature dependance in the equations so that each temperature examined

was represented by a single equation.

- (iii) Increasing inaccuracy of developed equations as reaction temperatures are elevated.
- (iv) The fits being confined to prediction of c-t curves for F only.

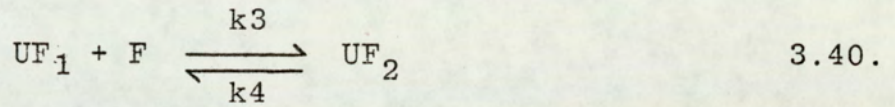
The above considerations resulted in a search for a technique for providing better fits to the data. This was achieved by considering the reaction mechanism between U and F.

With reference to the literature on the chemistry of UF the following relevant points can be deduced:

- (i) The combination of F with U begins with a series of addition reactions followed by condensation reactions.
- (ii) The speed and extent of reaction are dependant on the temperature, pH and the U:F molar ratio,
- (iii) In the pH range 4-9 the reaction rate remains constant at any given temperature.
- (iv) U and F in the ratio of between 1:1 and 1:2.5 react to produce only MMU and DMU as the addition products, the amount of TMU being negligible.

In addition to the above points it should be emphasised that the function of the reactor is to effect the methylation of U with F thereby achieving the first step in the manufacture of the industrial resins (Section 3.2.3.). The bulk of condensation reactions is achieved in later processing. With U:F molar ratios of interest being 1:1.33 and 1:2,2 and with pH range of

operation being well within the band 4-9, it is reasonable to suggest that the reactions taking place are:



where

$UF_1 = MMU = \text{Monomethylolurea}$

$UF_2 = DMU = \text{Dimethylolurea}$

$k_1$  and  $k_3$  are rate constants for second-order forward reactions.

$k_2$  and  $k_4$  are rate constants for first-order reverse reactions.

From equations 3.39. and 3.40. the rates of reaction for F and U can be written as:

$$RP_F = \frac{dF}{dt} = k_1.U.F - k_2.UF_1 + k_3.F.UF_1 - k_4.UF_2 \quad 3.41.$$

$$RP_U = -\frac{dU}{dt} = k_1.U.F - k_2.UF_1 \quad 3.42.$$

where U, F,  $UF_1$  and  $UF_2$  denote concentrations of U, F,  $UF_1$  and  $UF_2$  respectively.

A mass balance on the system can also be written as:

$$F + UF_1 + 2UF_2 = F_0 \quad 3.43.$$

$$U + UF_1 + UF_2 = U_0 \quad 3.44.$$

where  $UF_1$  in this case denotes the concentration, in moles per unit volume, of F in  $UF_1$  etc.

Solution of 3.43. and 3.44. for  $UF_1$  and  $UF_2$  in terms of  $U_0$  and  $F_0$  gives:

$$UF_1 = 2(U_0 - U) - (F_0 - F) \quad 3.45.$$

$$UF_2 = (U - F) - (U_0 - F_0) \quad 3.46.$$

Substitution of 3.45. and 3.46. into 3.41. and 3.42. results in:

$$\begin{aligned} RP_F = -\frac{dF}{dt} = & k_1 \cdot U \cdot F - k_2 \{2 \cdot (U_0 - U) - (F_0 - F)\} \\ & + k_3 \cdot F \{2 \cdot (U_0 - U) - (F_0 - F)\} \\ & - k_4 \{(U - F) - (U_0 - F_0)\} \end{aligned} \quad 3.47.$$

$$RP_U = -\frac{dU}{dt} = k_1 \cdot U \cdot F - k_2 \{2 \cdot (U_0 - U) - (F_0 - F)\} \quad 3.48.$$

For solution of equations 3.47. and 3.48. values of  $k_1$ ,  $k_2$ ,  $k_3$  and  $k_4$  have to be specified. These were obtained by evaluating the data of de Jong and de Jonge (75,76) plotted as  $\log k$  versus  $\frac{1}{T}$ , using the Arrhenius equation as in 3.49. and 3.50.

$$k = A e^{-\Delta E/RT} \quad 3.49.$$

$$\ln k = \ln A - \frac{\Delta E}{R} \cdot \frac{1}{T} \quad 3.50.$$

The slopes of the curves were calculated from a knowledge of the activation energies. This helped to reduce the error in estimation of the intercept ( $\ln A$ ).

The values obtained are:

$$k_1 = 10^{5.81} \text{ EXP}(-6542.5/T) \text{ lit/mol s} \quad 3.51.$$

$$k_2 = 10^{6.31} \text{ EXP}(-9562.15/T) \text{ s}^{-1} \quad 3.52.$$

$$k_3 = 10^{4.26} \text{ EXP}(-7045.8/T) \text{ lit/mol s} \quad 3.53.$$

$$k_4 = 10^{7.15} \text{ EXP}(-9562.15/T) \text{ s}^{-1} \quad 3.54.$$

Using the above values for the rate constants, the system of second-order non-linear simultaneous differential

equations 3.47. and 3.48, were integrated on a Honeywell 316 computer using the computer package, ASTON SIMULATION PROGRAM (ASP)(108) and the Runge-Kutta fourth-order routine(130). Details of the program and the package can be found in Appendix 7. A flow sheet is given in Fig. 3.5.

This provided values for F and U concentrations versus time.

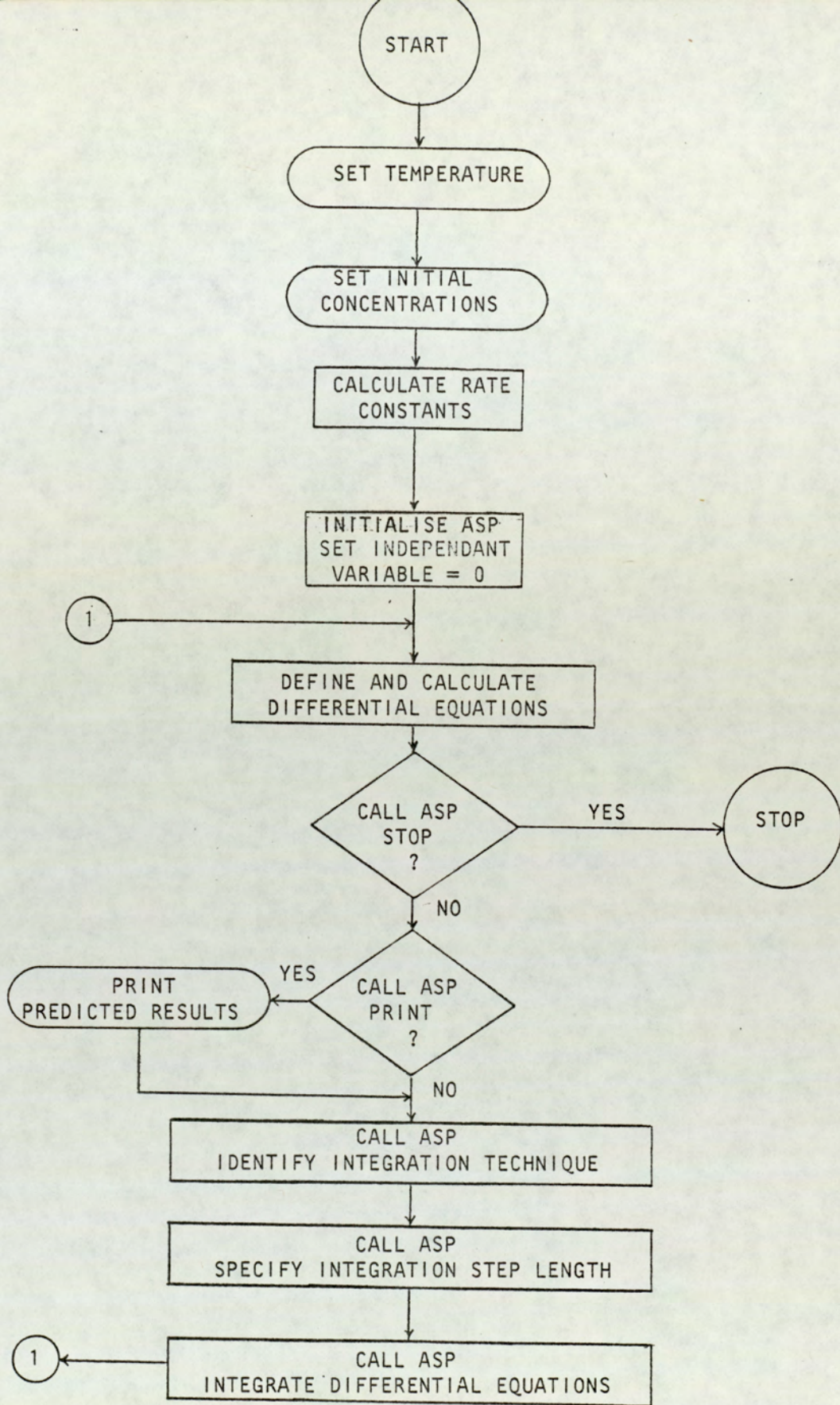


FIG.3.5.

LOGIC DIAGRAM FOR SOLUTION OF KINETICS

### 3.3.3. RESULTS AND DISCUSSION OF RESULTS

The results are shown graphically in figures 3.6. and 3.7. The experimental curves are those described in section 3.3.2.

As can be seen in Fig. 3.6., excellent prediction of the experimental c-t curves are produced at 20°C and 40°C. However, as can be seen in Fig. 3.7. at 80°C there is originally close agreement between experimental and predicted results but divergence in the middle region, the curves converging again towards equilibrium.

The discrepancies in the middle regions of Fig. 3.7. can be explained by consideration of the following points.

(i) The unreliability of experimental results at higher temperatures due to possible losses of formaldehyde from 'open' reactions.

(ii) Mode of operation i.e. charge reactor, heat to required temperature, then sample at chosen intervals. Reaction during the initial heating period cannot be avoided and must affect the results, particularly at higher temperatures.

(iii) Possible inadequacy of the reaction mechanism hypothesised at higher temperatures including the omission of any of the side reactions taking place.

Furthermore, Sato(109), in a paper published in 1967 studied the thermodynamics of the reaction between U and F. The kinetics confirmed that the constancy range of the rate constants is, in general, confined to narrow conversion limits. This, he concluded, was due to

the change in the functionality of U with progress of the reaction.

U reduces its functionality as the reaction progresses on reaction with F and the loss of its reactive points.

The above finding by Sato could explain the reason for the divergence in the mid-regions of Fig. 3.7. A sensitivity analysis on the rate constants at this point showed that in fact the predicted curves could be shifted to represent the experimental data at the higher temperatures with the same orders of accuracy achieved for the curves at 25° and 40°C,

However, the main conclusion from this exercise was that confident extrapolation to the temperatures of use in the reactor operation was still not possible.

It therefore became evident that the high temperature reaction between U and F under the conditions of interest had to be investigated.

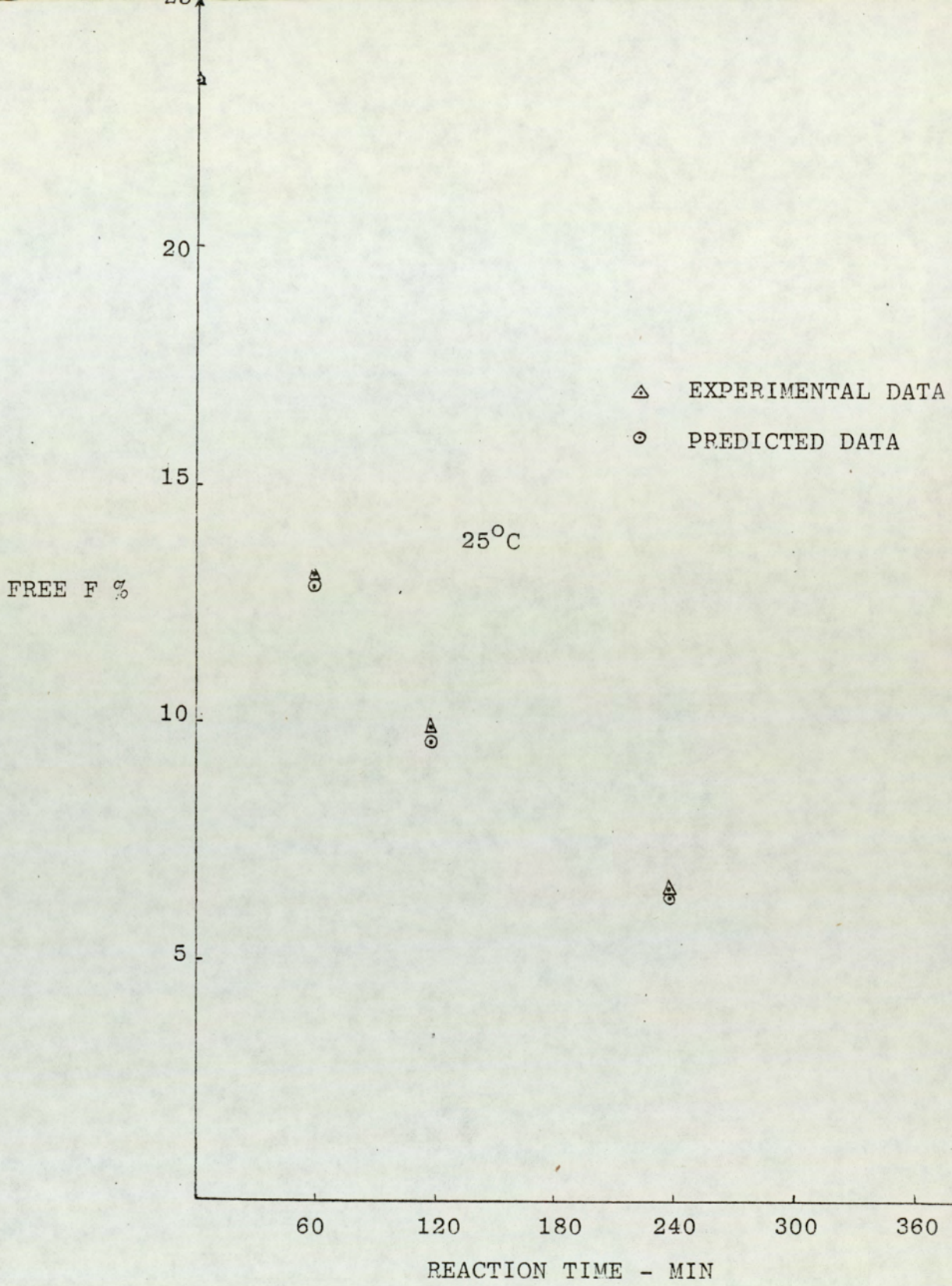


FIG. 3.6.

PREDICTION OF LOW TEMPERATURE UF KINETICS

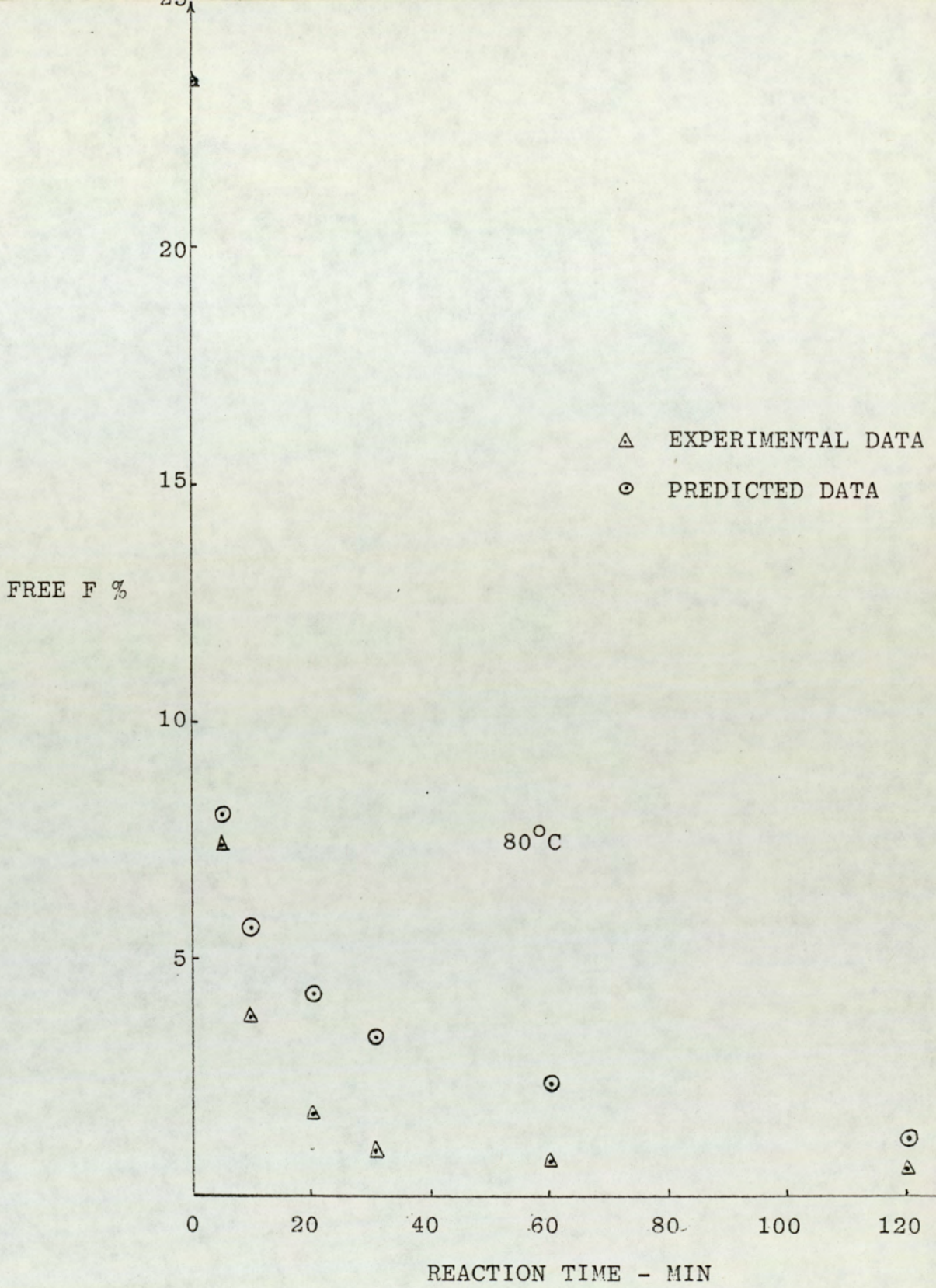


FIG.3.7.

PREDICTION OF LOW TEMPERATURE UF KINETICS

### 3.4. INVESTIGATION OF HIGH TEMPERATURE UF KINETICS

In Chapter One, it was emphasised that in order to be able to use high temperatures for the reaction of U with F, the vapour pressure problems, presented by the presence of water in the system, have to be overcome. The same problem is encountered in the kinetic investigation of high temperature UF reactions.

There is virtually no previous work published in this domain. Gorbunov et. al.(110) described a crude experimental technique for evaluation of the UF reactions in the temperature range 140<sup>o</sup>-160<sup>o</sup>C.

A solution of urea in water was prepared in a test tube. A calculated quantity of Formalin with a set pH value was added to the U and some of the mixture transferred into an ampoule. The ampoule was sealed and immersed in a heating oil bath. The reaction time was measured from the time the ampoules were immersed in the bath. On completion of the reaction the ampoules were removed and cooled in a stream of cold water. The ampoules were then broken and analysed for extent of reaction. The above work can be vigorously criticised on the following points,

(i) The reaction times can be extremely inaccurate. No allowance was made for the temperature of the reaction mixture to reach that of the bath. Obviously this could not have been possible with the technique used. Furthermore, as the reactions went to completion in between 2-4 minutes, the heating time and the cooling

time compared to the reaction time could introduce errors of the order of 300-400% in the timing.

(ii) There was no agitation in the ampoules so that their results were not compatible with the published data.

It was therefore necessary to develop a novel technique for investigation of the kinetics of UF at high temperatures. The technique would ideally possess the following features.

- (i) The reactions have to be examined in sealed vessels.
- (ii) Provisions should be made to allow accurate determination of the reaction time.
- (iii) Provisions should be made for adequate mixing.

#### 3.4.1. THE EXPERIMENTAL TECHNIQUE

The reactor designed for this purpose is shown in Fig. 3.8. It is a Y-shaped glass vessel with two charging arms. Formalin solution of a chosen pH value is charged through one arm, while prilled urea is charged through the other. This has the effect of keeping the reactants separate until they reach the reaction temperature upon immersion in the constant temperature bath. On completion of charging, the arms are sealed by a flame. The seals are produced on very small areas so that the pressure force on the seal points remains small and therefore the possibilities of

leakage and breakage are reduced. The sealed reactor is then held by a clamp which also acts as the shaft to a suitable electric stirrer. The stirrer motor is repositioned carefully such that the reactor is well immersed in the constant temperature bath. Sufficient time is allowed for U and F to reach the bath temperature, during which, a very small portion of formalin solution evaporates so that the vapour pressure in the small volume keeps the rest of the reactants in the liquid phase; hence one reason for the small size of the reactor.

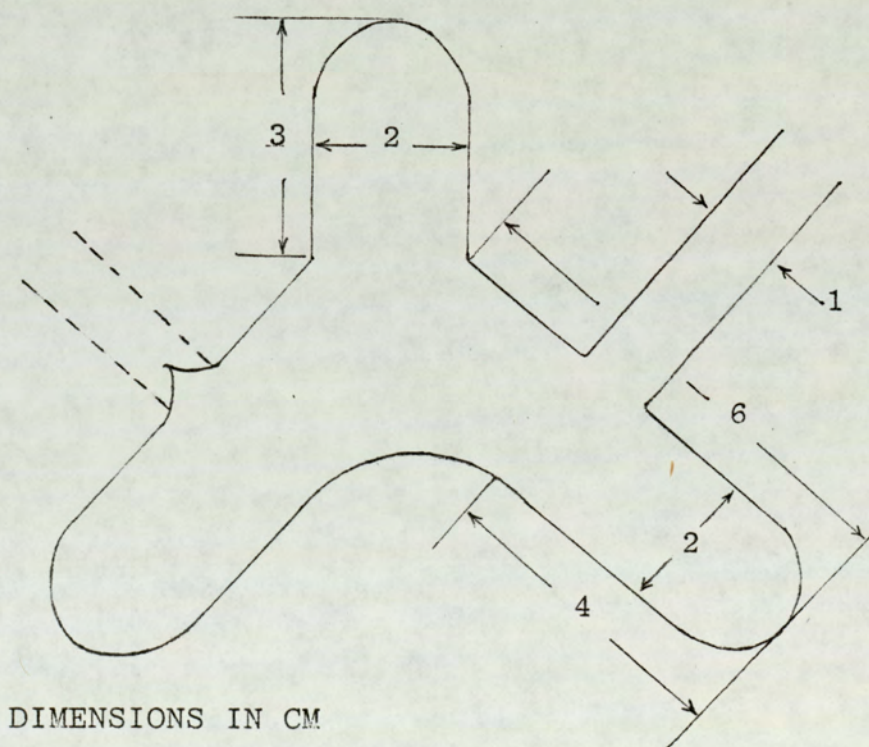


FIG. 3.8.

REACTION VESSEL FOR INVESTIGATION  
OF HIGH TEMPERATURE UF KINETICS

The motor is started at the same time as a stop-watch used to monitor the reaction time. The vessel at this stage is rotating around the axis projected by the stirrer shaft (clamp) and behaving as a 'Y-cone mixer'. After the required reaction time has elapsed the motor is stopped. The reactor is removed and immediately broken into a quantity of ice-water which helps to kill the reaction. (The ice-water serves as part of the water which has to be used in the analytical technique. See Appendix 9). The resultant mix is then directly analysed by the acidimetric sulphite method for free F (Appendix 9).

The weight of reactants are chosen to suit the analytical method, this being the other reason for the small size of the reaction vessel. The round ends of each limb of the reactor are designed to stand the high pressures which could be generated in the system at the higher temperatures.

#### 3.4.2. RESULTS AND DISCUSSION OF RESULTS

The above experimental procedure and technique proved successful in the first part of the experimental investigation(111) even though minor modifications were made to the reaction vessel for ease of operation. Investigation of the reaction between U and F at 25°C and 80°C, under the conditions of Table 3.4, and Fig. 3.4. produced comparable results for free F which were on average 1% higher than those in Table 3.4.

This was explained by the fact that use of sealed

vessels prevented any possible loss of free F. Having proved and perfected the technique, further work was done(112) to produce c-t curves for molar ratios of 1:1.33 and 1:2.2 in the temperature range 20° to 160°C, with the pH in the band 4-9. The results are tabulated in Table 3.5. to 3.8.

Examination of the results shows good agreement between Tables 3.5, and 3.6, and in comparison with Table 3.4, thereby confirming that the technique used was successful in concept and operation. The data at 100°C in Table 3.8, show signs of inaccuracy near equilibrium which can also be seen in some other tables. This could be due to the decreasing accuracy of the analytical technique at low concentrations of free F. It also seems evident from Table 3.8, that the equilibrium concentrations at 160°C show higher values than those at 120°C. This clearly establishes that the Le Chatelier's principle does apply to the case of UF reactions. The reason this effect cannot be seen throughout the data can be attributed to the fact that not enough time was allowed for the equilibrium to be reached at lower temperatures.

RESULTS FOR U:F MOLAR RATIO 1:1.33

TEMP., T °C	TIME, t MIN	CONC. F <sub>O</sub> , F %	CONC. F <sub>O</sub> , F MOL/LIT
25	0	23.32	9.1867
	60	12.98	5.1052
	120	10.04	3.9490
	240	6.75	2.6549
	360	5.78	2.2733
40	0	23.32	9.1867
	60	7.87	3.0953
	120	5.43	2.1357
	180	3.47	1.3648
	240	2.45	0.9636
	360	1.63	0.6411
60	0	23.32	9.1867
	10	8.75	3.4415
	20	6.15	2.1489
	30	4.50	1.7699
	60	2.57	1.0108
	90	1.42	0.5585
	120	1.21	0.4759
	180	0.58	0.2281

TABLE 3.5.

CONCENTRATION-TIME DATA FOR UF MIXTURES

RESULTS FOR U:F MOLAR RATIO 1:1.33

TEMP., T °C	TIME, t MIN	CONC. F <sub>O</sub> , F %	CONC. F <sub>O</sub> , F MOL/LIT
80	0	23.32	9.1867
	5	6.38	2.5093
	10	3.61	1.4199
	20	1.88	0.7394
	30	1.36	0.5394
	60	0.98	0.3854
	120	0.86	0.3382
120	0	23.32	9.1867
	1.17	2.96	1.1642
	2.5	1.49	0.5860
	5	0.60	0.2160
	10	0.33	0.1284
	20	0.32	0.1259
	30	0.15	0.0590
160	0	23.32	9.1867
	1	0.95	0.3736
	5	0.82	0.3325
	10	0.72	0.2832
	20	0.62	0.2438
	30	0.62	0.2438

TABLE 3.6.

CONCENTRATION-TIME DATA FOR UF MIXTURES

RESULTS FOR U:F MOLAR RATIO 1:2.2

TEMP., T °C	TIME, t MIN	CONC. F <sub>0</sub> , F %	CONC. F <sub>0</sub> , F MOL/LIT
40	0	27.12	10.4970
	5	21.96	8.4998
	10	21.10	8.1669
	20	18.29	7.0793
	60	14.10	5.4575
	90	11.35	4.3931
	120	10.95	4.2383
60	0	27.12	10.4970
	5	20.17	7.7988
	10	15.89	6.1439
	20	13.20	5.1038
	30	11.44	4.4233
	60	7.92	3.0623
	120	7.97	3.0816
80	0	27.12	10.4970
	5	6.24	2.4127
	30	5.29	2.0454
	60	3.91	1.5118
	120	4.10	1.5853

TABLE 3.7.

CONCENTRATION-TIME DATA FOR UF MIXTURES

RESULTS FOR U:F MOLAR RATIO 1:2.2

TEMP., T °C	TIME, t MIN	CONC. F <sub>O</sub> , F %	CONC. F <sub>O</sub> , F MOL/LIT
100	0	27.12	10.4970
	1.25	5.78	2.2348
	5.50	1.72	0.6651
	10	1.19	0.4600
	20	1.19	0.4600
	30	1.17	0.4524
	60	1.19	0.4600
120	0	27.12	10.4970
	1.1	1.92	0.7424
	5	0.77	0.2977
	10	0.47	0.1817
	20	0.32	0.1237
	30	0.17	0.0657
160	0	27.12	10.4970
	1	3.73	1.4412
	5	2.77	1.0727
	10	2.20	0.8492
	20	1.60	0.4470
	30	0.92	0.3577

TABLE 3.8.

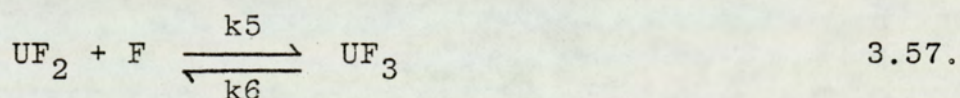
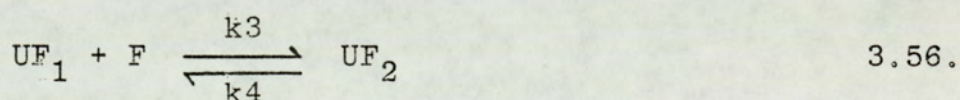
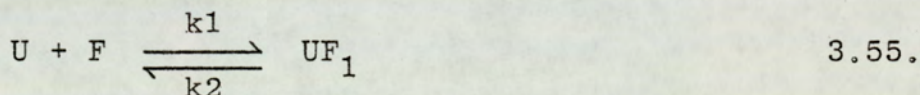
CONCENTRATION-TIME DATA FOR UF MIXTURES

3.5. REPRESENTATION OF KINETIC DATA OVER THE  
TEMPERATURE RANGE

The final curve fitting technique of Section 3.3.2. was applied to the results of tables 3.5. to 3.8. It became evident that the descriptions were not adequate for representing the entire temperature range. This could be attributed to two main factors:

- (i) Inadequacy of the reaction mechanism hypothesised, especially at higher temperatures.
- (ii) The variation in the value of rate constants with reaction time as well as reaction temperature as suggested by Sato(109).

The first problem was resolved by including the third addition reaction to the reaction mechanism such that the reactions became:



where  $UF_3 = TMU$

Hypothesising the reactions as such results in the rate equations being:

$$RP_F = -\frac{dF}{dt} = k_1.U.F. - k_2.UF_1 + k_3.F.UF_1 - k_4.UF_2 + k_5.F.UF_2 - k_6.UF_3 \quad 3.58.$$

$$RP_U = -\frac{dU}{dt} = k_1.U.F - k_2.UF_1 \quad 3.59.$$

$$RP_{UF_1} = \frac{dUF_1}{dt} = + k_2.UF_1 - k_1.U.F. + k_3.F.UF_1 - k_4.UF_2 \quad 3.60.$$

with the mass balance:

$$U + UF_1 + UF_2 + UF_3 = U_0 \quad 3.61.$$

$$F + UF_1 + 2.UF_2 + 3.UF_3 = F_0 \quad 3.62.$$

so that

$$UF_2 = 3(U_0 - U) + (F - F_0) - 2.UF_1 \quad 3.63.$$

$$UF_3 = 2(U - U_0) + (F_0 - F) + UF_1 \quad 3.64.$$

Substitution of 3.63. and 3.64. into 3.58., 3.59. and 3.60. would provide the necessary rate equations for F, U and  $UF_1$ . The inclusion of a rate equation for  $UF_1$  is necessary for solution of the above system of differential equations.

To complete the above description, it remains to specify values for  $k_5$  and  $k_6$  in equation 3.57. Due to lack of data it was not possible to calculate  $k_5$  and  $k_6$  in the same way as for the previous rate constants. However de Jong and de Jonge(78) give approximate values for  $k_5$  and the equilibrium constant of equation 3.57. at 35°C.

Using these values  $k_5$  and  $k_6$  can be written as:

$$k_5 = \frac{1.2}{9} \times k_1 \quad 3.65.$$

$$k_6 = \frac{1}{9} \times k_1 \quad 3.66.$$

The value of the equilibrium constant ( $k = \frac{k_5}{k_6}$ ) from 3.65. and 3.66. will always remain at 1.2 although  $k_5$  and  $k_6$  change with temperature. The above is not strictly

correct thermodynamically (i.e. the equilibrium constant must change with temperature since  $\Delta H \neq 0$ ) but as will become apparent from the treatment of rate constants which follows, the above values will be adequate as approximate starting points for the calculation of more accurate constants which would represent the experimental data.

### 3.5.1. NON-LINEAR REGRESSION ANALYSIS

Dealing with the problem of variation in the value of the rate constants over the temperature range is more complex. Solution to this problem necessitates a simultaneous search for 4 to 6 rate constant values at each temperature. This search must therefore go on until the values found give the closest prediction of the experimental data. Such a search is called a multivariable unconstrained non-linear optimisation problem. The object of the optimisation is therefore to minimise the difference between the predicted and experimental values over the prediction range by varying the values of the 4 or 6 rate constants simultaneously. This exercise is also sometimes referred to as "Non-linear regression analysis" or curve fitting to non-linear data.

Therefore use of the above technique should be made at each particular temperature to find the best values of the rate constants which would predict the experimental data within a specified limit of accuracy.

It must also be assumed that a fit provided for a particular temperature will also be accurate in predicting the c-t data over a band around that temperature. For instance it may be assumed that the equations predicting the data at 40°C will hold in accuracy over the temperature range 30°C-50°C. With the above in mind the steps which would have to be taken towards a solution are:

- (i) Use of either equations 3.47. and 3.48. or equations 3.58. to 3.60. to predict the c-t data.
- (ii) Comparison of predicted and experimental data to find whether the specified accuracy is satisfied.
- (iii) If accuracy is not satisfactory; use of optimisation routine to calculate new values for rate constants.
- (iv) Repetition of the cycles (ii) and (iii) until the required accuracy is reached.

Investigation of points (i) and (ii) above lead to the results of Table 3.9, which were obtained on a Honeywell 316 computer.

MOLAR RATIO U:F	TEMP., T °C	REACTION MECHANISM PROVIDING ADEQUATE PREDICTION
1:1.33	25	$U+F \xrightleftharpoons[k_2]{k_1} UF_1$ $UF_1+F \xrightleftharpoons[k_4]{k_3} UF_2$
1:1.33	40	"
1:1.33	60	"
1:1.33	80	"
1:1.33	120	$U+F \xrightleftharpoons[k_2]{k_1} UF_1$ $U+UF_1 \xrightleftharpoons[k_4]{k_3} UF_2$ $UF_2+F \xrightleftharpoons[k_6]{k_5} UF_3$
1:1.33	160	"
1:2.2	40	"
1:2.2	60	"
1:2.2	80	"
1:2.2	100	"
1:2.2	120	"
1:2.2	160	"

TABLE 3.9.

CHEMICAL MECHANISMS FOR DESCRIPTION OF UF REACTIONS

Furthermore, in this context, the accuracy criteria for convergence of data was defined as  $F_{\text{EXP}} - F_{\text{PRE}} < \text{the experimental error in determination of free F.}$  3.67.

where

$F_{\text{EXP}}$  = Experimental free F at time t

$F_{\text{PRE}}$  = Predicted free F at time t

With the experimental error in determination of percent free F being  $\pm 0.1\%$  (Appendix 9) equation 3.67, becomes

$$F_{\text{EXP}} - F_{\text{PRE}} < \text{ABS}(0.1) \quad 3.68.$$

Having specified the reaction mechanisms for prediction at each temperature and the accuracy criteria it remains to assess an optimisation routine to search for the best 'k' values, at each temperature.

#### THE OPTIMISATION ROUTINE

A computer package in Fortran was used for the optimisation exercise (113). The package makes use of an improved simplex search routine, due to Nelder and Mead (114), to minimise an objective function. Details of the package can be found elsewhere (113). A logic diagram for the package is given in Fig.3,9.

The inputs required for using the program are as follows:

(i) A subroutine for description of the objective function to be minimised.

(ii) The following variables:

Number of independent variables

Initial starting values for the rate constants

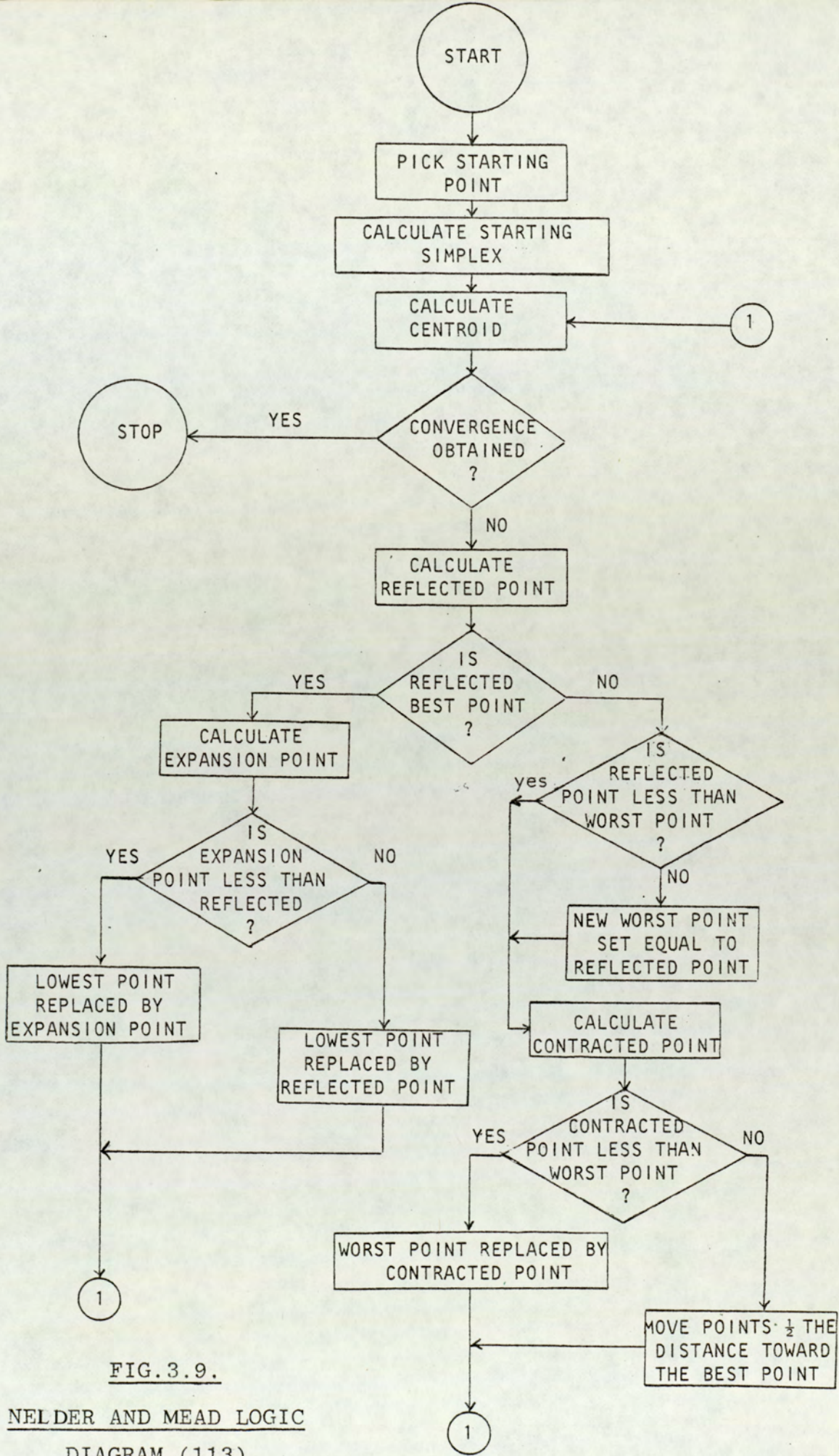


FIG. 3.9.

NELDER AND MEAD LOGIC  
DIAGRAM (113)

Side length of simplex  
Reflection coefficient  
Contraction coefficient  
Expansion coefficient  
Accuracy

The objective function to be minimised was defined as

$$S = \sum_{J=1}^{J=K} (E_J - F_J)^2$$

where

$E_J$  = Experimental value of free F for the Jth observation.

$F_J$  = Predicted value of free F for the Jth observation.

K = Number of experimental points.

S = Sum squared error function.

The values of free F were predicted by solution of the appropriate systems of equation of Table 3.9. at each temperature. The solution technique is as described in Section 3.3.2.

In general the package, solved on an ICL 1904S machine, was found to be slow in convergence. Due to the high cost of computing and the lack of available funds the following three steps were taken.

(i) The prediction range was narrowed to shorter reaction times which caused direct-savings in computer simulation time. This was justified by the short residence times in the tubular reactor. At least two experimental points were included in the prediction range.

(ii) Since simulation results produced predictions

at equal reaction time intervals it was necessary to interpolate some of the experimental data from the experimental curves. Failure to do so would result in print intervals as low as 6 seconds which would increase computer costs.

(iii) The initial values of the rate constants were improved using an interactive Honeywell 316 computer. This reduced the optimisation times as the starting values for rate constants were much closer to the final results. In fact in some cases the Honeywell simulations predicted results which satisfied the accuracy requirements.

For these cases no further optimisation was attempted as the cost did not justify the overall improvement in accuracy.

Details of the program and the subroutine for prediction of F concentrations which also defines the objective function to be minimised can be found in Appendix 7.

A logic diagram for the subroutine is presented in Fig. 3.10.

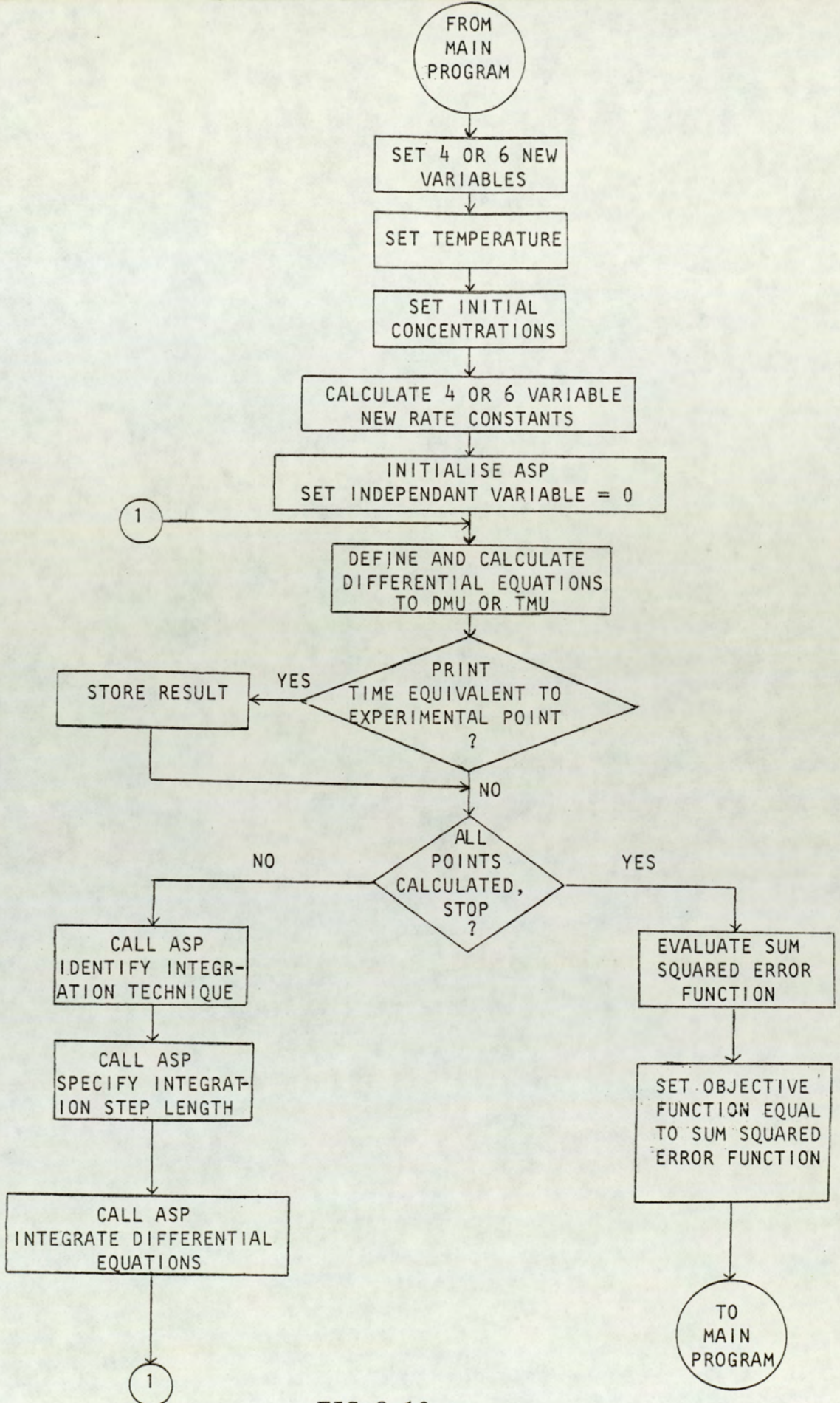


FIG. 3.10.

LOGIC DIAGRAM FOR SUB-ROUTINE TO DEFINE OBJECTIVE FUNCTION FOR MINIMISATION

### 3.5.2. RESULTS AND DISCUSSION OF RESULTS

The results are tabulated in Tables 3.10. to 3.21.

The values of the rate constants are given as multiples of the original rate constants, which were defined as:

$$k_1 = 10^{5.18} \text{ EXP } (-6542.5/T) \text{ lit/mol s}$$

$$k_2 = 10^{6.31} \text{ EXP } (-9562.15/T) \text{ s}^{-1}$$

$$k_3 = 10^{4.26} \text{ EXP } (-7045.8/T) \text{ lit/mol s}$$

$$k_4 = 10^{7.15} \text{ EXP } (-9562.15/T) \text{ s}^{-1}$$

$$k_5 = \frac{1.2}{9} \times 10^{5.18} \text{ EXP } (-6542.5/T) \text{ lit/mol s}$$

$$k_6 = \frac{10^{5.18}}{9} \times \text{EXP } (-6542.5/T) \text{ s}^{-1}$$

As an example  $k_1 = 0.8534 \times k_1$  refers to  $k_1 = 0.8534 \times 10^{5.18} \text{ EXP } (-6542.5/T) \text{ lit/mol s}$ . The error at each data point is given by  $\Delta E_r$ , where  $\Delta E_r = \text{Experimental value} - \text{Predicted value}$ . The error criteria for convergence of data was defined in Section 3.51. as

$$\Delta E_r = \pm 0.1\% \quad \text{or} \quad \Delta E_r = \pm 0.0394 \text{ mol/lit}$$

Assuming seven data points on each curve, the maximum value for the sum squared error function becomes

$$S = (0.0394)^2 \times 7 = 0.011 \text{ mol/lit}$$

Therefore the convergence criteria became

$$S \leq 0.0108 \text{ mol/lit}$$

Appropriate values of 'S' were calculated for cases where the number of data points was not equal to seven.

The temperature range for application of each model is

assigned as follows:

<u>Molar Ratio</u> <u>U:F</u>	<u>Temperature of</u> <u>Prediction °C</u>	<u>Temperature of</u> <u>application °C</u>
1:1.33	25	T<30
1:1.33	40	30-50
1:1.33	60	50-70
1:1.33	80	70-90
1:1.33	120	90-130
1:1.33	160	T>130
1:2.2	40	T<50
1:2.2	60	50-70
1:2.2	80	70-90
1:2.2	100	90-110
1:2.2	120	110-130
1:2.2	160	T>130

RATE CONSTANTS

k1 = 0.8534 x k1  
k2 = 1.0034 x k2

k3 = 0.1034 x k3  
k4 = 1.0144 x k4

TEMP., T °C	TIME, t MIN	CONCENTRATIONS F <sub>O</sub> , F MOL/LIT	
		EXPERIMENTAL	PREDICTED
25	0.0	9.1867	9.1867
	10.0	7.9500	7.9590
	20.0	7.0500	7.0626
	30.0	6.3750	6.3801
	40.0	5.8875	5.8437
	50.0	5.4750	5.4114
	60.0	5.1052	5.0561

U:F MOLAR RATIO 1:1.33      S = 0.0047

TABLE 3.10.

COMPARISON OF EXPERIMENTAL AND PREDICTED RESULTS

RATE CONSTANTS

k1 = 0.9030 x k1  
k2 = 1.0034 x k2

k3 = 1.0034 x k3  
k4 = 1.0144 x k4

TEMP., T °C	TIME, t MIN	CONCENTRATIONS F <sub>O</sub> , F MOL/LIT	
		EXPERIMENTAL	PREDICTED
40	0.0	9.1867	9.1867
	10.0	6.3750	6.3454
	20.0	5.0250	4.9933
	30.0	4.2750	4.2033
	40.0	3.7500	3.6858
	50.0	3.3750	3.3208
	60.0	3.0953	3.0494

U:F MOLAR RATIO 1:1.33      S = 0.0161

TABLE 3.11.

COMPARISON OF EXPERIMENTAL AND PREDICTED RESULTS

RATE CONSTANTS

$k1 = 1.0068 \times k1$   
 $k2 = 1.0068 \times k2$

$k3 = 4.0068 \times k3$   
 $k4 = 1.0289 \times k4$

TEMP., T °C	TIME, t MIN	CONCENTRATIONS $F_{O_2}, F$ MOL/LIT	
		EXPERIMENTAL	PREDICTED
60	0.0	9.1867	9.1867
	10.0	3.4415	3.4306
	20.0	2.1489	2.1930
	30.0	1.7699	1.6078
	40.0	1.2750	1.2524
	50.0	1.0500	1.0090
	60.0	1.0108	0.8307

U:F MOLAR RATIO 1:1.33      S = 0.0580

TABLE 3.12.

COMPARISON OF EXPERIMENTAL AND PREDICTED RESULTS

RATE CONSTANTS

$k1 = 1.0136 \times k1$   
 $k2 = 1.0136 \times k2$

$k3 = 5.0136 \times k3$   
 $k4 = 5.0578 \times k4$

TEMP., T °C	TIME, t MIN	CONCENTRATIONS $F_{O_2}, F$ MOL/LIT	
		EXPERIMENTAL	PREDICTED
80	0.0	9.1867	9.1867
	5.0	2.5093	2.4630
	10.0	1.4109	1.3902
	15.0	0.9900	0.9305
	20.0	0.7394	0.6821
	25.0	0.6000	9.5341
	30.0	0.5349	0.4413

U:F MOLAR RATIO 1:1.33      S = 0.0229

TABLE 3.13.

COMPARISON OF EXPERIMENTAL AND PREDICTED RESULTS

RATE CONSTANTS

$k1 = 1.0000 \times k1$      $k3 = 5.0000 \times k3$      $k5 = 0.8333 \times k5$   
 $k2 = 1.0000 \times k2$      $k4 = 1.0000 \times k4$      $k6 = 1.2000 \times k6$

TEMP., T °C	TIME, t MIN	CONCENTRATIONS F <sub>O</sub> , F MOL/LIT	
		EXPERIMENTAL	PREDICTED
120	0.0	9.1867	9.1867
	2.5	0.3860	0.6138
	5.0	0.2160	0.2011
	7.5	0.1350	0.1332
	10.0	0.1284	0.1208
	12.5	0.1195	0.1185
	15.0	0.1048	0.1176

U:F MOLAR RATIO 1:1.33      S = 0.0021

TABLE 3.14.

COMPARISON OF EXPERIMENTAL AND PREDICTED RESULTS

RATE CONSTANTS

$k1 = 1.0000 \times k1$      $k3 = 8.0000 \times k3$      $k5 = 0.8333 \times k5$   
 $k2 = 1.0000 \times k2$      $k4 = 4.0000 \times k4$      $k6 = 1.2000 \times k6$

TEMP., T °C	TIME, t MIN	CONCENTRATIONS F <sub>O</sub> , F MOL/LIT	
		EXPERIMENTAL	PREDICTED
160	0.0	9.1867	9.1867
	1.0	0.3736	0.3761
	2.0	0.3562	0.3423
	3.0	0.3375	0.3330
	4.0	0.3337	0.3292
	5.0	0.3325	0.3275
	6.0	0.3287	0.3268

U:F MOLAR RATIO 1:1.33      S = 0.0021

TABLE 3.15.

COMPARISON OF EXPERIMENTAL AND PREDICTED RESULTS

RATE CONSTANTS

k1 = 1.0000 x k1      k3 = 1.0000 x k3      k5 = 0.8333 x k5  
k2 = 1.0000 x k2      k4 = 1.0000 x k4      k6 = 1.2000 x k6

TEMP., T °C	TIME, t MIN	CONCENTRATIONS F <sub>O</sub> , F MOL/LIT	
		EXPERIMENTAL	PREDICTED
40	0.0	10.4970	10.4970
	10.0	8.1669	8.0954
	20.0	7.0793	7.0166
	30.0	6.5250	6.4295
	40.0	6.0750	6.0714
	50.0	5.7750	5.8345
	60.0	5.4575	5.6665

U:F MOLAR RATIO 1:2.2      S = 0.0263

TABLE 3.16.

COMPARISON OF EXPERIMENTAL AND PREDICTED RESULTS

RATE CONSTANTS

k1 = 0.6000 x k1      k3 = 5.0000 x k3      k5 = 16.6667 x k5  
k2 = 5.0000 x k2      k4 = 10.0000 x k4      k6 = 24.0000 x k6

TEMP., T °C	TIME, t MIN	CONCENTRATIONS F <sub>O</sub> , F MOL/LIT	
		EXPERIMENTAL	PREDICTED
60	0.0	10.4970	10.4970
	2.5	8.9625	8.8844
	5.0	7.7988	7.7547
	7.5	6.8875	6.8982
	10.0	6.1439	6.2200

U:F MOLAR RATIO 1:2.2      S = 0.01395

TABLE 3.17.

COMPARISON OF EXPERIMENTAL AND PREDICTED RESULTS

RATE CONSTANTS

$k1 = 5.0000 \times k1$      $k3 = 40.0000 \times k3$      $k5 = 0.0083 \times k5$   
 $k2 = 5.0000 \times k2$      $k4 = 40.0000 \times k4$      $k6 = 0.0120 \times k6$

TEMP., T °C	TIME, t MIN	CONCENTRATIONS F <sub>O</sub> , F MOL/LIT	
		EXPERIMENTAL	PREDICTED
80	0.0	10.4970	10.4970
	5.0	2.4127	2.4430
	10.0	2.2050	2.1210
	15.0	2.1375	2.0690
	20.0	2.0775	2.0579
	25.0	2.0550	2.0535
	30.0	2.0454	2.0504

U:F MOLAR RATIO 1:2.2      S = 0.0131

TABLE 3.18.

COMPARISON OF EXPERIMENTAL AND PREDICTED RESULTS

RATE CONSTANTS

$k1 = 1.0000 \times k1$      $k3 = 80.0000 \times k3$      $k5 = 16.6667 \times k5$   
 $k2 = 1.0000 \times k2$      $k4 = 30.0000 \times k4$      $k6 = 12.0000 \times k6$

TEMP., T °C	TIME, t MIN	CONCENTRATIONS F <sub>O</sub> , F MOL/LIT	
		EXPERIMENTAL	PREDICTED
100	0.0	10.4970	10.4970
	1.25	2.2348	2.2965
	2.50	1.1625	1.0890
	3.75	0.9075	0.8134
	5.00	0.7424	0.7207
	6.25	0.6300	0.6743
	7.50	0.5475	0.6443
	8.75	0.5100	0.6227
	10.00	0.4600	0.6062

U:F MOLAR RATIO 1:2.2      S = 0.0639

TABLE 3.19.

COMPARISON OF EXPERIMENTAL AND PREDICTED RESULTS

RATE CONSTANTS

k1 = 1.2000 x k1      k3 = 150.0000 x k3      k5 = 50.0000 x k5  
k2 = 1.0000 x k2      k4 = 40.0000 x k4      k6 = 12.0000 x k6

TEMP., T °C	TIME, t MIN	CONCENTRATIONS F <sub>O</sub> , F MOL/LIT	
		EXPERIMENTAL	PREDICTED
120	0.0	10.4970	10.4970
	1.0	0.7575	0.7643
	2.0	0.4125	0.4949
	3.0	0.3337	0.4312
	4.0	0.3000	0.3980
	5.0	0.2977	0.3774

U:F MOLAR RATIO 1:2.2      S = 0.0237

TABLE 3.20.

COMPARISON OF EXPERIMENTAL AND PREDICTED RESULTS

RATE CONSTANTS

k1 = 0.7000 x k1      k3 = 8.0000 x k3      k5 = 1.0833 x k5  
k2 = 1.0000 x k2      k4 = 4.0000 x k4      k6 = 1.5600 x k6

TEMP., T °C	TIME, t MIN	CONCENTRATIONS F <sub>O</sub> , F MOL/LIT	
		EXPERIMENTAL	PREDICTED
160	0.0	10.4970	10.4970
	1.0	1.4412	1.4869
	2.0	1.2740	1.1963
	3.0	1.2000	1.1500
	4.0	1.1175	1.1395
	5.0	1.0727	1.1369
	6.0	1.0125	1.1363

U:F MOLAR RATIO 1:2.2      S = 0.0307

TABLE 3.21.

COMPARISON OF EXPERIMENTAL AND PREDICTED RESULTS

## DISCUSSION OF RESULTS

Tables 3.10. to 3.21. show good prediction of experimental data.

However it must be emphasised that the predictive chemical mechanisms have no chemical significance. Although the predicted data are a true representation of what happens in the experiments, no theoretical significance can be attached to the chemical mechanisms from which the data were predicted. Discussing the case of U:F molar ratio 1:1.33 at 160°C (Table 3.15.) as an example, excellent prediction of the experimental data is achieved. Yet it cannot be assumed that the reaction between U and F progressing to the stage of TMU formation is strictly true. It is very likely that other reactions are taking place at such high temperatures. Some condensation is inevitable. Also side reactions such as formation of formic acid by Cannizzaro's reaction should be significant at this temperature (Appendix 6).

Therefore to be able to attach chemical significance to the work above much more detailed research is necessary.

A discussion of the behaviour of the systems at the various temperatures can be found elsewhere (111,112).

## C H A P T E R 4

### SOLUTION OF MATHEMATICAL MODELS

This Chapter presents the solution of the mathematical models developed in Chapter 2 and utilises the kinetic data evaluated in Chapter 3. The solution of the plug-flow models is followed by the description of a novel technique for the more complicated solution of the complex models. Flow diagrams elucidating the computer solutions are included where appropriate. Listing of the programs is given in Appendix 7.

#### 4.1. SOLUTION OF PLUG-FLOW MODELS

The plug-flow models developed in Chapter 2 are:-  
(see 2.4).

$$V_o \frac{\partial F}{\partial x} = -RP_F \quad 4.1.$$

$$V_o \frac{\partial U}{\partial x} = RP_U \quad 4.2.$$

$$V_o \frac{\partial UF_1}{\partial x} = -RP_{UF_1} \quad 4.3.$$

$$V_o \frac{\partial T}{\partial x} = \frac{4.364 K_M}{R^2 \cdot \rho_M S} (T_w - T) - \frac{\Delta H R_F R P_F}{\rho_M S} \quad 4.4.$$

From Chapter 3 and depending on the U:F molar ratio and temperature the following equations can be written:

(i) For cases where the reaction progresses to formation of DMU (Dimethylolurea).

$$RP_F = -\frac{\partial F}{\partial t} = k1.U.F. - k2.UF_1 + k3.U.UF_1 - k4.UF_2 \quad 4.5.$$

$$RP_U = -\frac{\partial U}{\partial t} = k1.U.F - k2.UF_1 \quad 4.6.$$

where

$$UF_1 = 2(U_0 - U) - (F_0 - F) \text{ and } UF_2 = (U - F) - (U_0 - F_0)$$

(ii) For cases where the reaction progresses to formation of TMU (Trimethylolurea).

$$RP_F = -\frac{\partial F}{\partial t} = k1.U.F - k2.UF_1 + k3.UF_1.F - k4.UF_2 + k5.UF_2.F - k6.UF_3 \quad 4.7.$$

$$RP_U = -\frac{\partial U}{\partial t} = k1.U.F - k2.UF_1 \quad 4.8.$$

$$RP_{UF_1} = -\frac{\partial UF_1}{\partial t} = -k1.U.F + k2.UF_1 + k3.UF_1.F - k4.UF_2 \quad 4.9.$$

where

$$UF_2 = (F - F_0) - 3(U - U_0) - 2UF_1 \quad \text{and}$$

$$UF_3 = (F_0 - F) + 2(U - U_0) + UF_1$$

Substitution of equations 4.5. and 4.6. into equations 4.1., 4.2. and 4.4. defines the plug-flow models which have to be solved where reactions proceed to formation of DMU. Thus

$$V_0 \frac{\partial F}{\partial x} = -k1.U.F + k2.UF_1 - k3.UF_1.F + k4.UF_2 \quad 4.10.$$

$$V_0 \frac{\partial U}{\partial x} = -k1.U.F + k2.UF_1 \quad 4.11.$$

$$V_0 \frac{\partial T}{\partial x} = \frac{4.364 K_M}{\rho_M \cdot S \cdot R^2} (T_w - T) - \frac{\Delta H R F \cdot R P F}{\rho_M \cdot S} \quad 4.12.$$

Where the value of  $RP_F$  in 4.12. is calculated from 4.5.

Substitution of equations 4.7., 4.8. and 4.9. into equations 4.1., 4.2., 4.3. and 4.4. defines the plug-flow

models which have to be solved where reactions proceed to formation of TMU. Thus

$$V_o \frac{\partial F}{\partial x} = k_1.U.F + k_2.UF_1 - k_3.UF_1.F + k_4.UF_2 - k_5.UF_2.F + k_6.UF_3 \quad 4.13.$$

$$V_o \frac{\partial U}{\partial x} = -k_1.U.F + k_2.UF_1 \quad 4.14.$$

$$V_o \frac{\partial UF_1}{\partial x} = k_1.U.F - k_2.UF_1 - k_3.UF_1.F + k_4.UF_2 \quad 4.15.$$

$$V_o \frac{\partial T}{\partial x} = \frac{4,364 K_M}{\rho_M \cdot S \cdot R^2} (T_w - T) - \frac{\Delta H R_F \cdot R \cdot P_F}{\rho_M \cdot S} \quad 4.16.$$

where the value of  $RP_F$  in 4.16, is calculated from 4.7.

The system of simultaneous partial differential equations 4.10. to 4.12. and 4.13. to 4.16. was solved using Aston Simulation Program (ASP) (Appendix 7) in conjunction with the Runge-Kutta 4th order technique of integration. The boundary conditions for solution were as described in 2.4. The logic for the solution can be given in the following steps:

- (i) Read the required data, including initial boundary conditions at tube entrance (see 2.4.).
- (ii) Initialise ASP (set independent variable, distance, equal to zero).
- (iii) Check distance along the reactor. If distance exceeds 30ft change diameter of the tube and velocity.
- (iv) Check temperature.
- (v) Set appropriate values of rate constants and note whether the model to be used is the 6 rate constant or the 4 rate constant model.
- (vi) Choose and define the differential equations

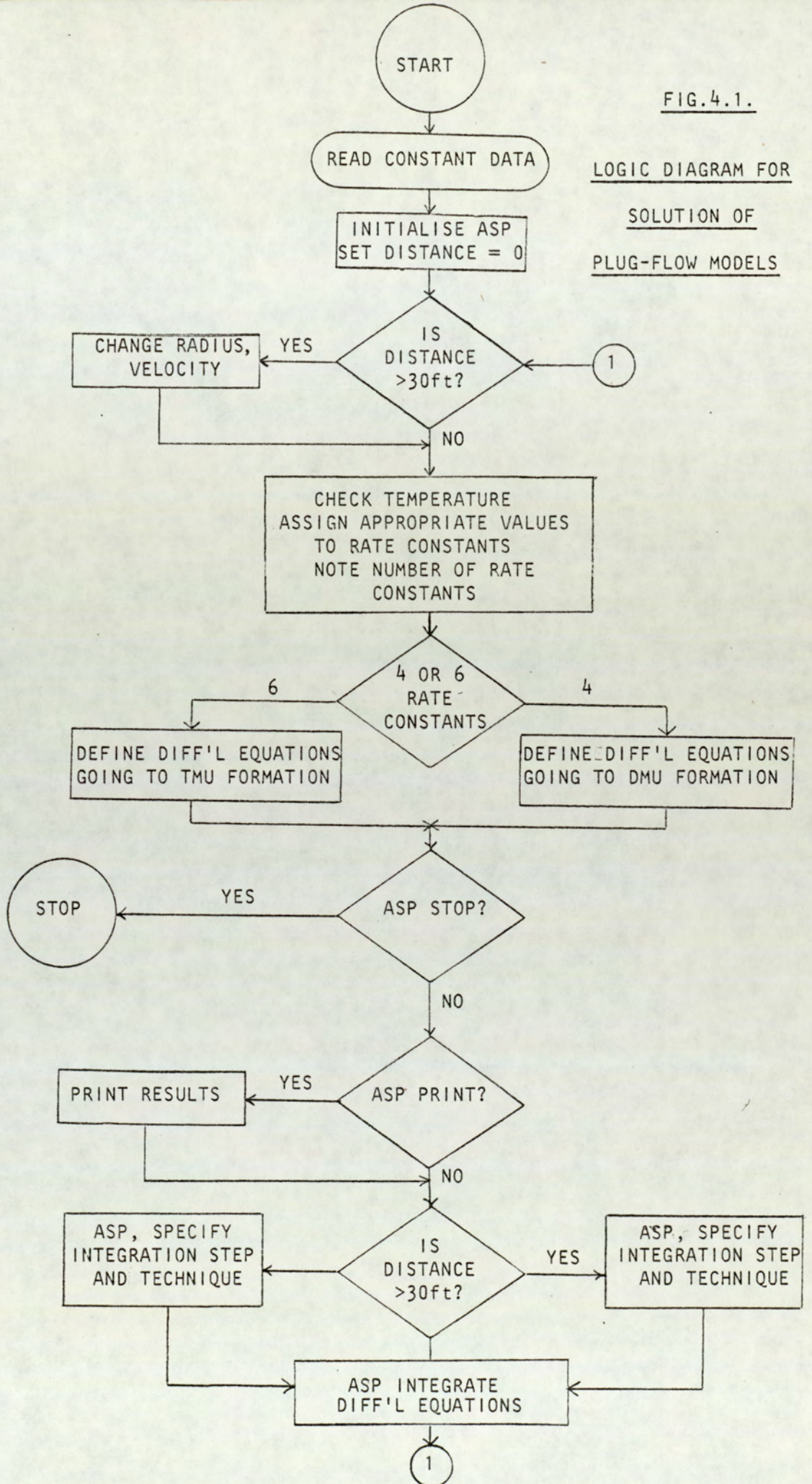
to be solved on basis of number of rate constants set.

- (vii) Check distance along the reactor. If distance exceeds 30ft specify step length and integrate technique for use with the 5/8" i.d. tube.
- (viii) If distance does not exceed 30ft specify step length and integration technique to be used with the 1/4" i.d. tube.
- (ix) Integrate the chosen differential equations for new values of concentrations and temperature (ASP).
- (x) Check on print time and termination point (ASP).
- (xi) If termination point is not reached repeat steps (iii) onwards using new values of variables.

A logic diagram on the basis of the above points is given in Fig.4.1. A listing of the program, written in Basic and solved on a Honeywell 316 Computer can be found in Appendix 7.

FIG.4.1.

LOGIC DIAGRAM FOR  
SOLUTION OF  
PLUG-FLOW MODELS



## EFFECT OF CHOICE OF STEP LENGTH ON ACCURACY OF RESULTS

The choice of step length for integration is the most significant factor in the accuracy of the results. In general, the accuracy of results is improved with decrease in step length. However, excessively small step lengths result in high job times and therefore computer costs.

For the case of the solution of the plug flow models, a step length of 10cm resulted in approximation and round-off errors which caused numerical over flow on the computer. However the difference in accuracy for the step lengths 5cm and 1cm were in the second decimal place of the results only. Therefore the step length of integration chosen was 5cm for the  $\frac{1}{4}$ " i.d. tube. Similarly for the longer diameter tube the acceptable step length was found to be 1cm. Using the above values a solution time of 35 minutes was obtained on the Honeywell 316 computer. This can be compared to a solution time of 65 minutes for a step length of 1cm along the whole of the reactor, on the same computer.

### 4.2. SOLUTION OF COMPLEX MODELS

The dimensionless complex models developed in Chapter 2 are:

$$V'_{x(r)} \frac{\partial F'}{\partial x'} = \frac{1}{Pe_F} \cdot \frac{L}{R} \left( \frac{\partial^2 F'}{\partial r'^2} + \frac{1}{r'} \frac{\partial F'}{\partial r'} \right) - Da_{IF} \quad 4.17.$$

$$V'_{x(r)} \frac{\partial U'}{\partial x'} = \frac{1}{Pe_U} \cdot \frac{L}{R} \left( \frac{\partial^2 U'}{\partial r'^2} + \frac{1}{r'} \frac{\partial U'}{\partial r'} \right) - Da_{IU} \quad 4.18.$$

$$V'_{x(r)} \frac{\partial UF1'}{\partial x'} = \frac{1}{Pe_{UF1}} \cdot \frac{L}{R} \left( \frac{\partial^2 UF1'}{\partial r'^2} + \frac{1}{r'} \frac{\partial UF1'}{\partial r'} \right) - Da_{IUF1} \quad 4.19.$$

$$V'_{x(r)} \frac{\partial T'}{\partial x'} = \frac{1}{Pe_t} \left( \frac{\partial^2 T'}{\partial r'^2} + \frac{1}{r'} \frac{\partial T'}{\partial r'} \right) - Da_{III} \quad 4.20.$$

where

$$V' = 1 - (r')^2 \quad 4.21.$$

For solutions of complex models either equations 4.17., 4.18. and 4.20. or equations 4.17. to 4.20. are chosen. The choice is made on the basis of the progress of reaction as described in section 4.1. with the inclusion of the appropriate rate equations.

Therefore the task is to solve a set of three or four simultaneous, second order partial differential equations. The most frequent approach to the numerical solution of this problem is by the application of finite differences in both radial and axial directions. The result is a set of first order ordinary differential equations of the initial value type, the solution of which can be described as follows:

Since only two independent variables are involved in the problem, the concept of solution can be represented on a two dimensional plane as shown in Fig.4.2.

With reference to Fig.4.2. the following approximations for the radial constituents of equation 4.17. can be written using finite differences:

$$\frac{\partial^2 F'}{\partial r'^2} = \frac{F'(N+1,M) - 2F'(N,M) + F'(N-1,M)}{(\Delta r')^2} \quad 4.27.$$

$$\frac{\partial F'}{\partial r'} = \frac{F'(N+1,M) - F'(N-1,M)}{2 \cdot \Delta r'} \quad 4.28.$$

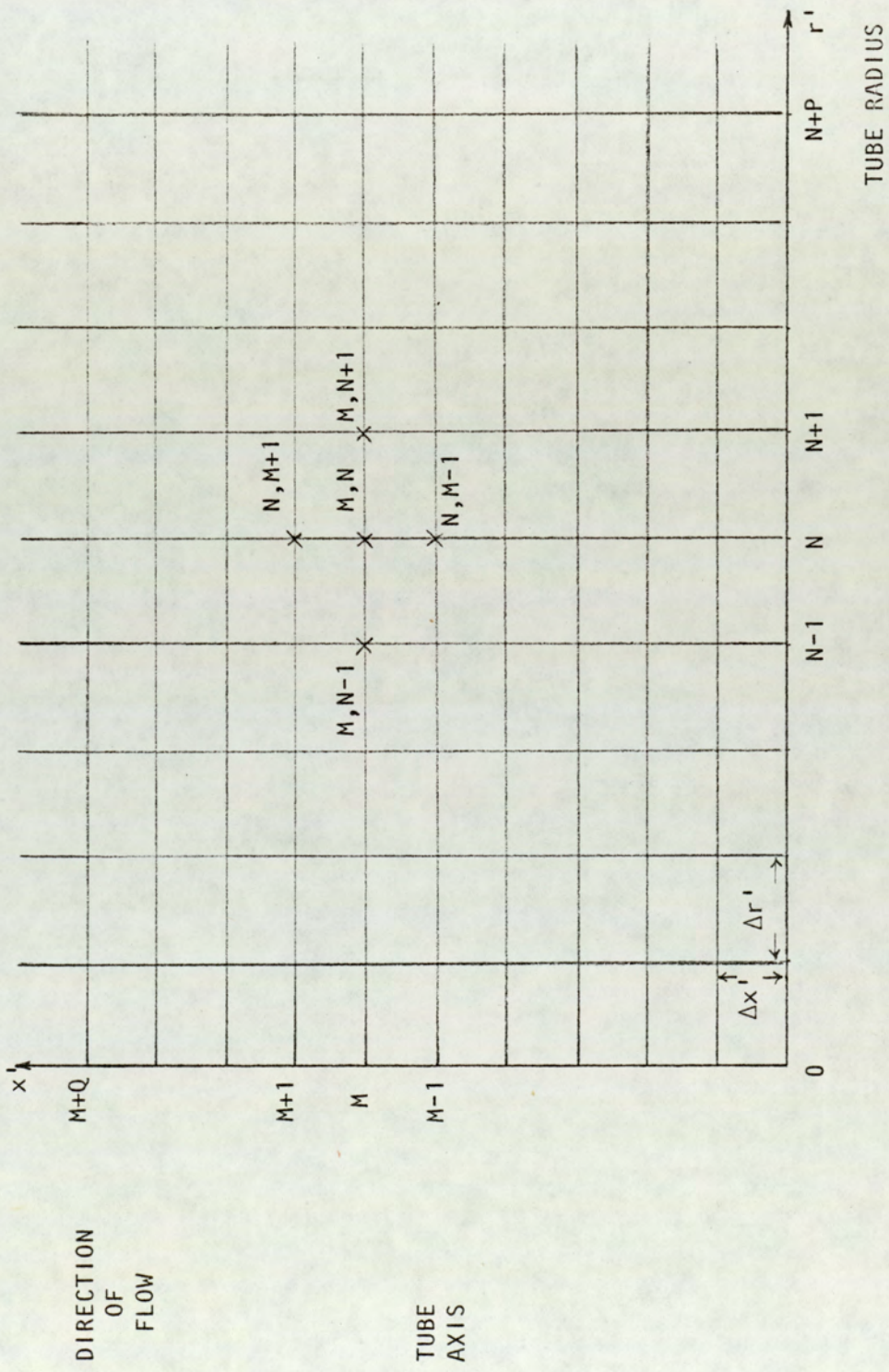


FIG. 4.2.

CLASSIFICATION OF GRID POINTS USED FOR SOLUTION OF

COMPLEX MODELS

also  $N, \Delta r' = r'$

so that  $\frac{1}{r'} = \frac{1}{N, \Delta r'}$

Substitution of equations 4.27, and 4.28. or finite difference descriptions of higher orders, into equation 4.17. and writing the term  $\frac{\partial F'}{\partial x'}$  as:

$$\frac{\partial F'}{\partial x'} = \frac{F'(N, M+1) - F'(N, M)}{\Delta x'}$$

renders the final finite difference equation. Similar treatment of equations 4.18. to 4.20. results in a set of finite difference equations which can be expressed such that the following two solutions become possible:

- (i) An explicit solution, where the value of each pivotal grid point (Fig.4.2.) is calculated from the values of known pivotal points.
- (ii) An implicit solution, where the value of each pivotal point on the grid (Fig. 4.2.) is calculated from the solution of a set of simultaneous equations.

Although implicit techniques of solution, such as the Crank-Nicolson iterative method (130) are much more complicated. They have the following two advantages:

- (i) Stability : stability meaning that errors evolved during the numerical solution of difference equations do not grow exponentially but damp out.
- (ii) Convergence : convergence meaning that the numerical solution approaches the exact

solution as the values of  $\Delta r'$  and  $\Delta x'$  approach zero.

Hence in general the implicit methods are superior in approach and are considered as standard.

The essential difference between the technique used and the standard approach is that finite difference equations are only used in the radial direction. The approximation technique of using first order finite differences for integration in the axial direction is replaced by the Runge-Kutta fourth order integration routine. This is expected to give higher accuracy for solution of complex models, considering the parabolic profiles which are used. The equation for solution therefore becomes:

$$V'_{x(r)} \frac{dF'(N,M)}{dx'} = \frac{1}{Pe_F} \left\{ \frac{F'(N+1,M) - 2F'(N,M) + F'(N-1,M)}{(\Delta r')^2} + \frac{F'(N+1,M) - F'(N-1,M)}{2N(\Delta r')^2} \right\} - Da_I \quad 4.29.$$

Equation 4.29, has an infinite value at the centre line of the tube where  $N=0$ . Hence a separate equation must be found to represent the tube axis.

Applying La'Hopital's rule:

$$\lim_{r \rightarrow 0} \frac{1}{r'} \frac{\partial F'}{\partial r'} = \frac{\partial^2 F'}{\partial r'^2} \quad 4.30.$$

The equation to represent the tube axis becomes

$$V'_{x(r)} \frac{\partial F'(0,M)}{\partial x'} = \frac{2}{Pe_F} \left\{ \frac{F'(1,M) - 2F'(0,M) + F'(-1,M)}{(\Delta r')^2} \right\} - Da_{IF} \quad 4.31.$$

To assign a value to the term  $F'(-1,M)$  use is made of the boundary condition (section 2.4.).

$$\frac{\partial F'}{\partial r'} = 0 \quad \text{at} \quad r = 0 \quad 4.32.$$

Boundary condition 4.32, can be written as

$$\frac{F'(1,M) - F'(-1,M)}{2(\Delta r')} = 0 \quad 4.33.$$

So that

$$F'(1,M) = F'(-1,M)$$

Hence the equation for the tube centre line is:

$$V'_{x(r)} \frac{\partial F'(0,M)}{\partial x'} = \frac{4}{Pe_F} \left\{ \frac{F'(1,M) - F'(0,M)}{(\Delta r')^2} \right\} - Da_{IF} \quad 4.34.$$

For values of dimensionless formaldehyde concentrations at the wall boundary condition (Section 2.4.) is used.

$$F' = \frac{F_{EQ}}{F_0} \quad \text{at} \quad r' = 1 \quad 4.35.$$

This completes the development of the required algorithms for solution of formaldehyde concentration models.

Similar analysis can be made on equations 4.18, to 4.20.

The resulting equations correspond to 4.31. for general positions in the tube, to 4.34. for centre line position

in the tube with replacement of appropriate dependant variables and equation constants. Equations 4.18, and

4.19. use constant concentration boundary conditions

for the wall (Section 2.4.) while equation 4.20. has

a constant temperature boundary condition for some length

of tube. The constant temperature boundary condition is

replaced by the boundary condition which allows heat

transfer when the temperature inside the tube exceeds the steam temperature.

The system of algorithms so developed can now be programmed for solutions using the technique described above. It remains to specify the value of ' $\Delta r$ ' and the

step length for integration.

The reactor was divided into five increments in the radial direction giving

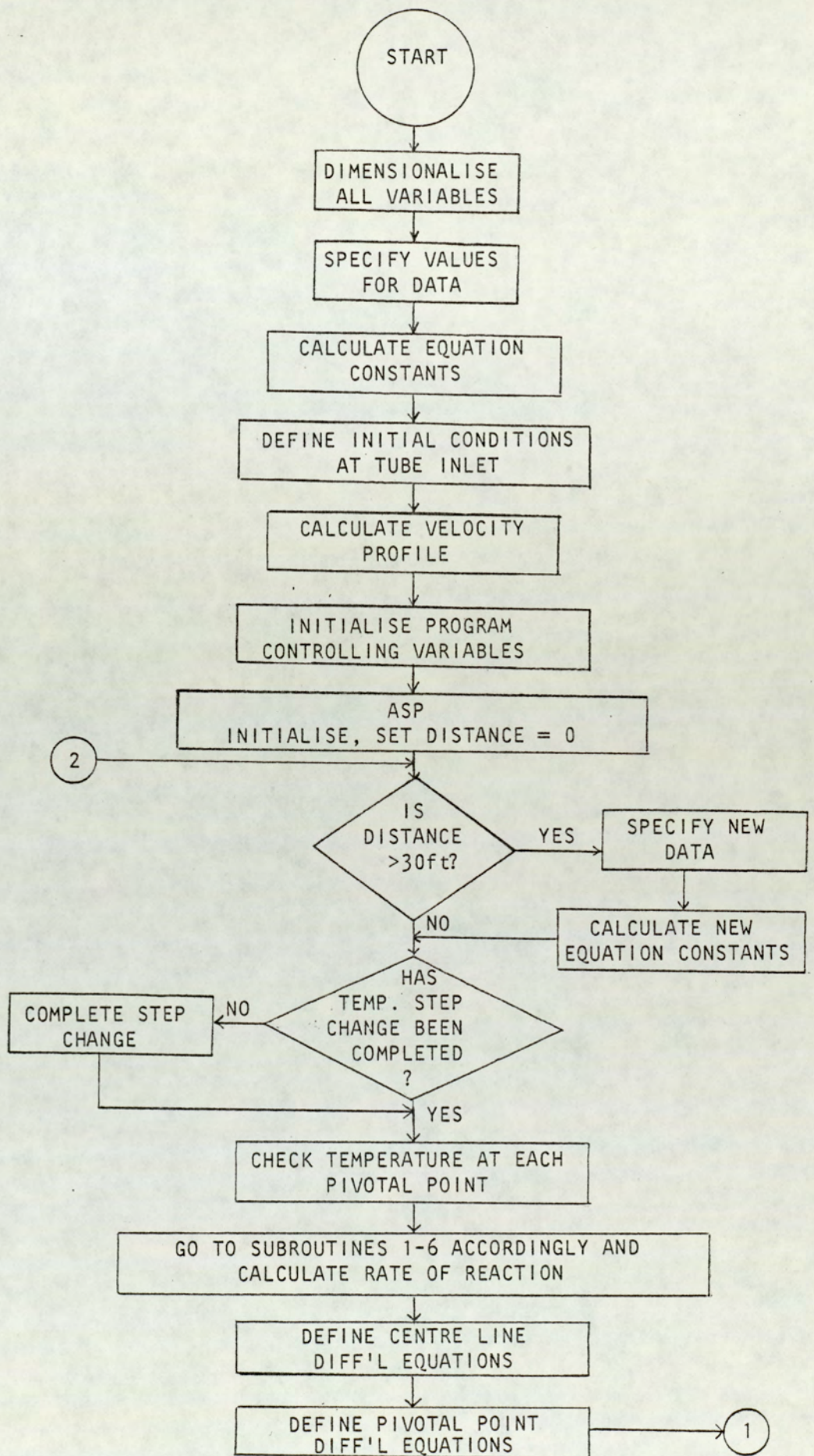
$$\Delta r' = 0.2$$

$$\text{or } \Delta r = 0.0655 \text{ cm}$$

This increment size was expected to be sufficiently small for accurate results. Furthermore, a maximum of twenty equations (four at each pivotal point on the radius) are solved simultaneously which exactly equals the capacity of ASP. Therefore use of smaller increments in the radial direction meant modification of ASP to cope with a higher number of simultaneous differential equations. Although possible, the small gain in accuracy did not seem to merit the modification of ASP. However, if the tube radius is enlarged excessively the above exercise may become necessary.

The choice of step length for integration by the Runga-Kutta fourth-order routine is governed by the same factors discussed in Section 4.1. A step length of 0.002 (2.316cm) was used for the  $\frac{1}{4}$ " i.d. tube and 0.001 (1.158cm) for the  $\frac{5}{8}$ " i.d. tube, giving average job times of 247 seconds on the ICL machine. Furthermore, to increase accuracy the large step change from room temperature to steam temperature at the reactor wall was introduced in smaller increments over the first four steps along the reactor.

The logic of solution is analogous to that described in Section 4.1. A logic diagram is shown in Fig.4.3., while the listing of the program written in Fortran and processed on an ICL 1904S computer can be found in Appendix 7.



Continued .....

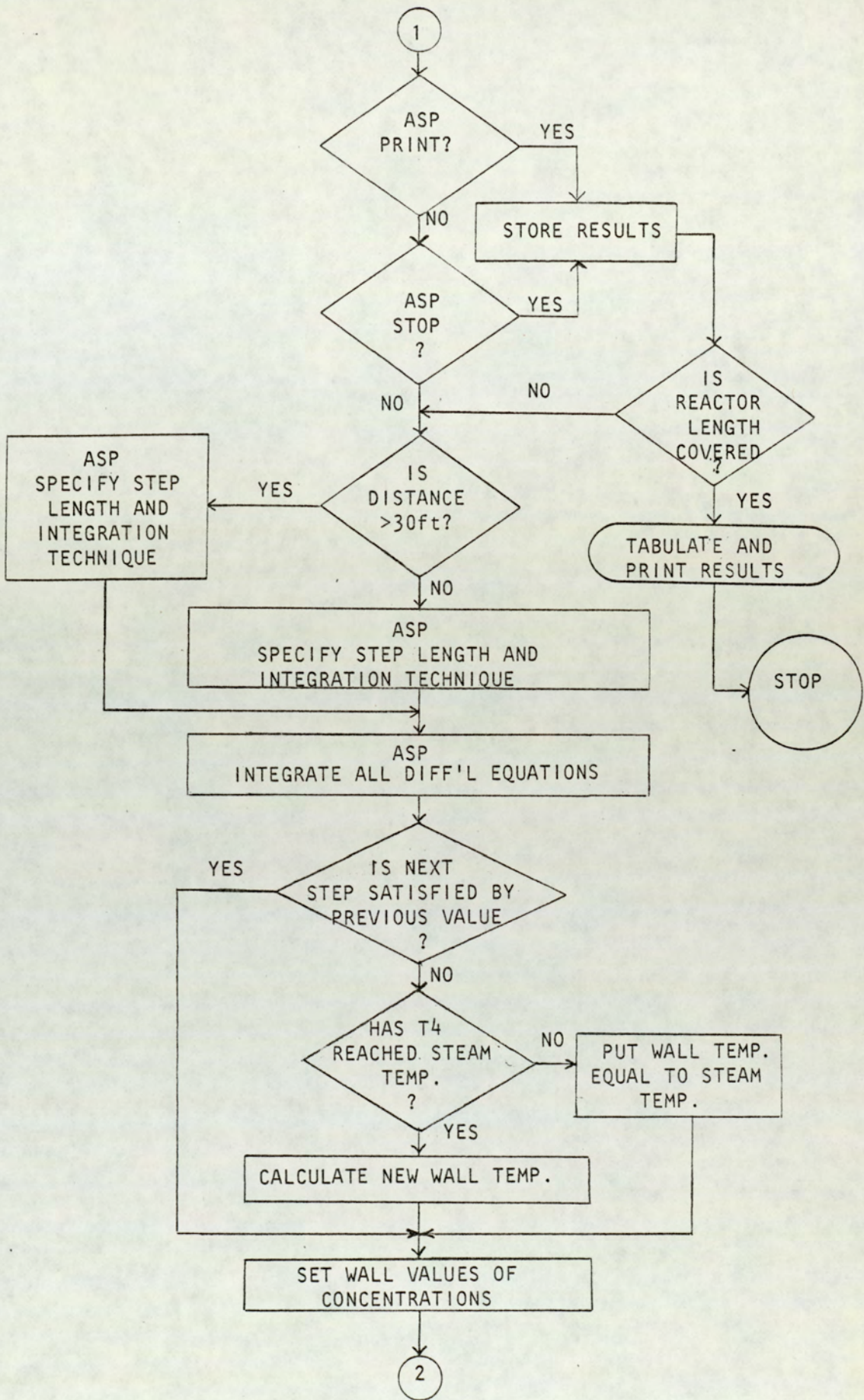


FIG. 4. 3.

LOGIC DIAGRAM FOR SOLUTION OF COMPLEX MODELS

## C H A P T E R 5

### EXPERIMENTAL

Chapter 5 describes the experimental pilot tubular reactor. A brief account of the original rig is followed by a discussion which highlights the necessity of some radical modifications.

The compatibility of the modifications with the existing system is verified and the equipment, as used for the collection of experimental data, specified. The start-up and shut-down procedures are listed with particular reference to the novel sampling technique.

The choice of the quantitative analytical technique is discussed and justified. The scope of the experimental investigation is then described and the range of operating variables specified. The chapter is terminated with sections tabulating the experimental results.

#### 5.1. DESCRIPTION AND OPERATING PROCEDURE FOR THE ORIGINAL RIG

The rig description starts with the raw materials mixing tank and proceeds through the equipment in the order that the feed flows. A simplified flow diagram for the original layout is shown in Fig.5.1.

Prilled urea is added to formalin, in the required

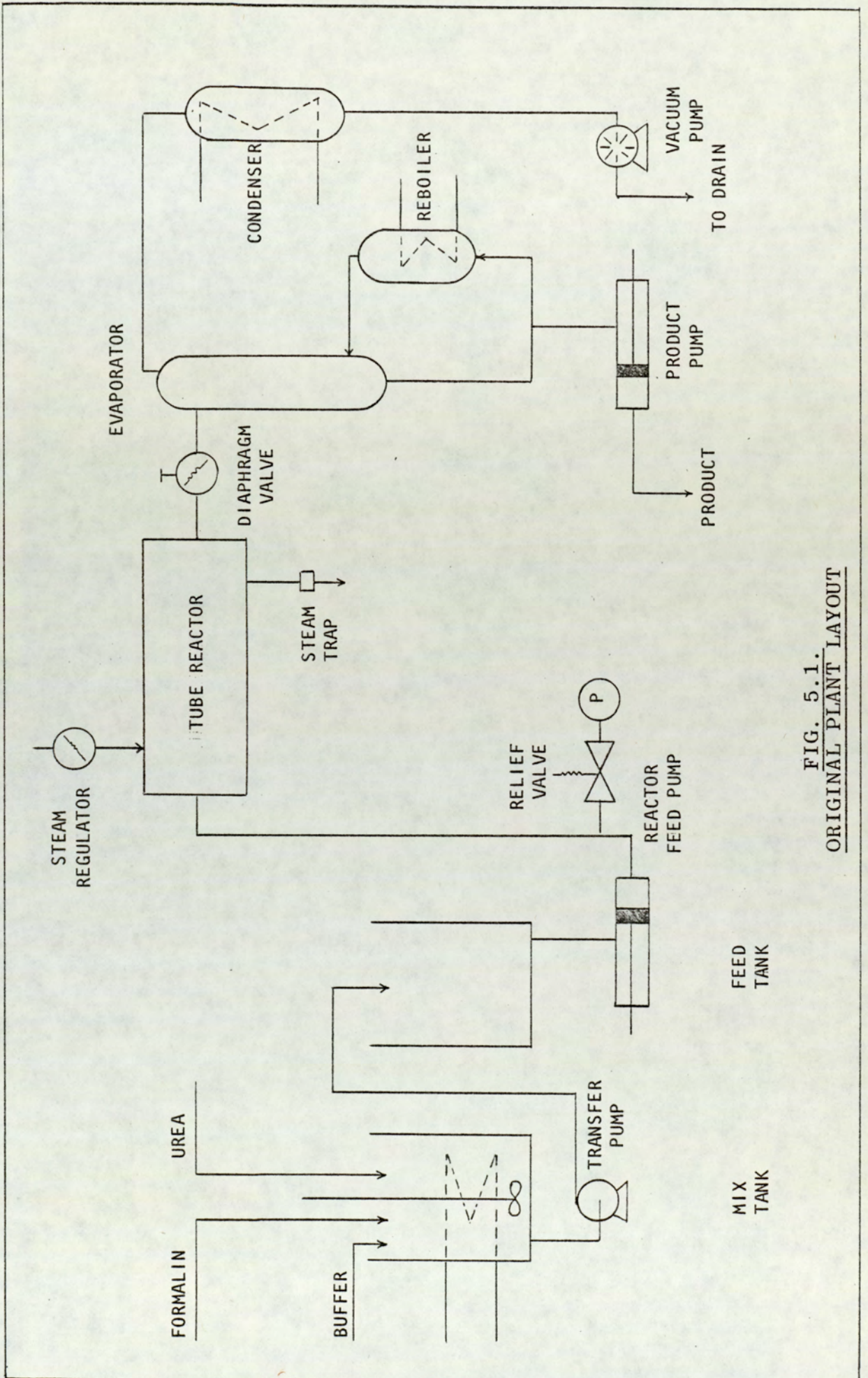


FIG. 5.1.  
ORIGINAL PLANT LAYOUT

U:F molar ratio, in the mix tank. Buffer is added as necessary and the urea is dissolved with the aid of agitation and heat transfer through a heating/cooling copper coil. The direction of the heat transfer is governed by the choice of the U:F molar ratio. For a U:F molar ratio of 1:1.33 the endothermic heat of solution of urea in water causes a sharp drop in temperature and slows the dissolution of urea significantly. Therefore heat is supplied to the mix to speed up the solution step. For a U:F molar ratio of 1:2.2, the heat release of the preliminary UF reaction compensates for the endothermic heat of urea going into solution and the initial sharp drop in temperature is rapidly recovered. However, the rise in temperature and therefore the rate of UF reaction becomes significant once the urea has dissolved. To avoid excessive reaction at this stage, cooling is applied to the mix to maintain a low temperature.

On completion of dissolution the mix is transferred to the feed tank ready for processing. It remains for up to two hours in some cases, until required as feed to the reactor. No heat transfer facilities existed in the feed tank. Meanwhile, a further batch can be prepared.

The feed is then pumped through the reactor tube using a 'Milroyal' metering pump, the capacity of which is set on a vernier scale to give the required residence time. Regulated steam at the required pressure is introduced into the reactor jackets and the diaphragm

valve at the reactor outlet is closed until the required pressure is developed in the tubes.

The material leaving the reactor enters the evaporator which is operating under vacuum. The sudden change in pressure causes flash vapourisation of a significant quantity of water at low temperatures. This water is passed through a condenser and leaves the system. Further vapourisation of the volatile solvent can be achieved using the reboiler. The product leaves the system through the product pump.

## 5.2. NECESSITY OF MODIFICATIONS

The above description of the original plant, which was set up as the pilot rig for resin production gives rise to two critical questions which have to be answered satisfactorily before the plant can be used for the collection of experimental data. These are:

- (i) Observation of the behaviour of the feed mix indicates some UF reaction in the mixing stage and further reaction while the mix is residing in the feed tank. The extent and significance of these reactions has to be investigated.
- (ii) Valves for taking representative samples from the reactor for chemical analysis, were not fitted to the reactor. Therefore a sampling device and technique had to be developed.

### 5.2.1. INVESTIGATION OF THE FEED TO THE REACTOR

The feed to the reactor was investigated for the U:F molar ratio of 1:2.2. This was expected to represent the less vigorously reactive feed to the reactor because of its lower concentration. The plant conditions were simulated in the laboratory where prilled urea was added to 36% formalin in the molar ratio of 1:2.2 with adequate agitation and a cooling coil to prevent excessive rise in the feed temperature. The results presented in the form of a concentration and a temperature history can be seen in Fig.5.2. The analytical technique for determination of free formaldehyde was that used throughout the investigations in this project (Appendix 9).

From the concentration history of Fig.5.2. it can be concluded that after two hours, which is the normal residence time for the feed, more than half the free formaldehyde has reacted.

Furthermore, as there are no heat transfer provisions in the feed tank it can be assumed that the extent of reaction is more in the actual plant system. From the above it becomes obvious that the mix and the feed tanks behave as batch reactors for the feed to the tube reactor. This means that the feed is not consistent, which results in a non-uniform material leaving the reactor. This introduces an additional complication in the overall modelling of the tubular reactor since the modelling of the batchwise feed system becomes necessary. Therefore, inevitably the feed system had to be modified

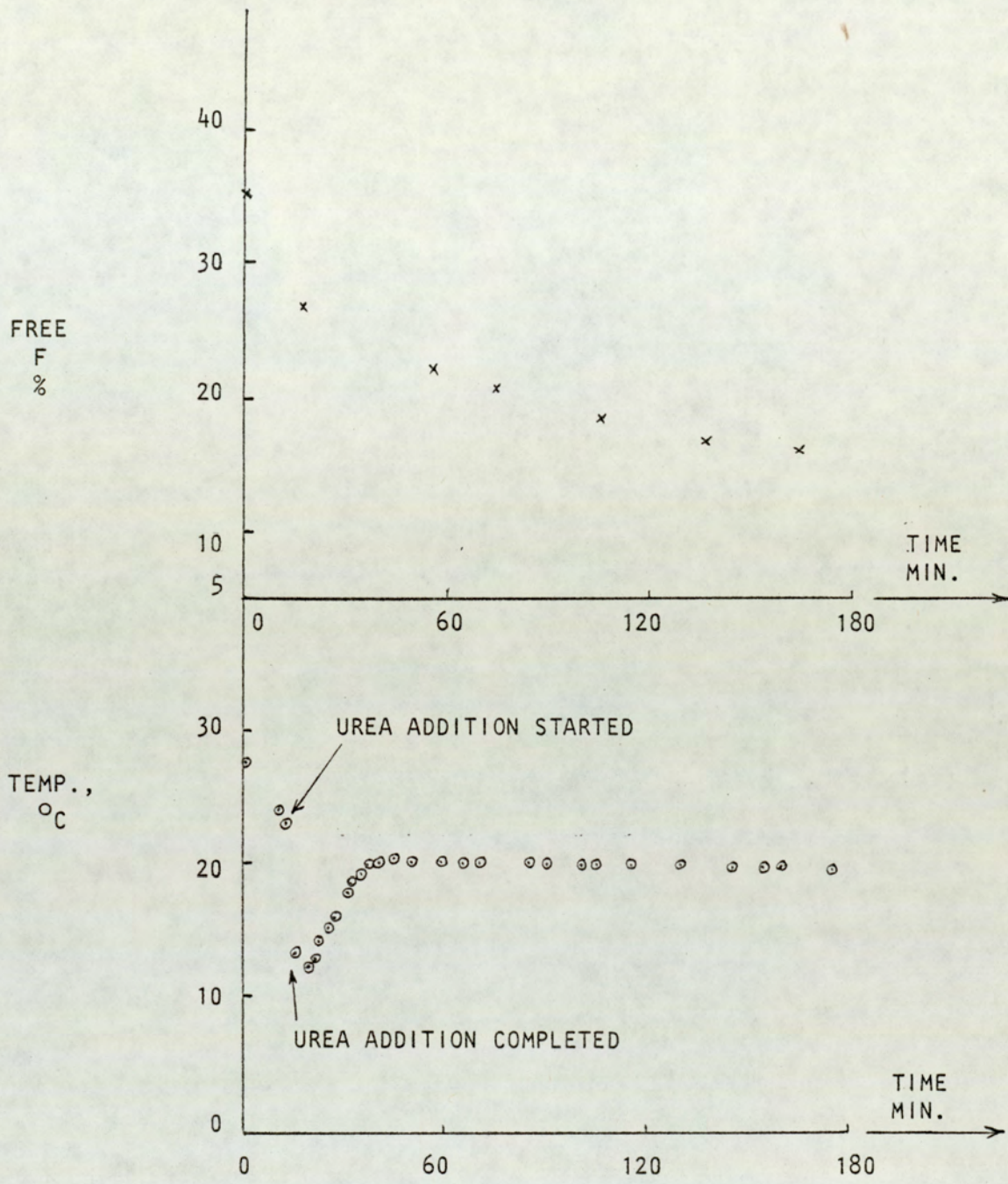


FIG. 5.2.

CONCENTRATION AND TEMPERATURE HISTORY  
CURVES FOR THE FEED TO THE REACTOR

to ensure a consistent, known feed to the reactor.

#### MODIFICATION OF THE FEED SYSTEM

The objectives to be achieved by the modified feed system can be listed as:

- (i) To keep the reactants apart until they mix at the inlet to the reactor tube.
- (ii) To achieve adequate mixing in the correct molar ratio at the reactor inlet.

Satisfying the first objective meant dissolving the urea prills in water and pumping the resultant solution to meet the Formalin-Buffer mixture at a T-junction at the reactor inlet. This system of feeding the reactor offers the advantages of consistency in feed, a known composition to the reactor and avoids a time-dependant feed composition. Conversely, one main objection to this system, in the industrial case, would be the additional introduction of water in the aqueous urea, which has to be removed at a later stage. However this objection may not be as critical as it seems. Urea is readily soluble in cold water and even more so in hot water. As a result, highly concentrated solutions of urea can be prepared. The excess water introduced, therefore becomes small in quantity as compared to that introduced by formalin and will either be flash evaporated with the bulk of the water or can be driven off using the reboiler.

The second objective is harder to achieve, considering

the use of two piston feed pumps and the problems of phasing of the pumps so that the two pistons perform simultaneously. Due to variation of slip factors in pumps it is highly unlikely that the two pumps could ever be synchronised for simultaneous performance. It is possible to use a two pump combination driven by the same motor (mechanical coupling) to achieve the above requirement. However as this was not available the following steps were taken to ensure the correct and adequate mixing of the reactants.

The tee at the reactor entrance was enlarged (Section 5.3.) so that the increased volume allowed better mixing of the two feeds. The extent of mixing was examined using refractive indices. This was done by comparing the refractive index of the material coming out of the tee, over an extended period, to that of a fresh well mixed laboratory sample with the same characteristics. An Abbe Refractometer (Bellingham and Stanley) was used and standardised with a glass test-piece of  $N = D 1.5173$  using Monobromonaphthalene as cement. No attempts were made to phase the two feed pumps. The results given in Table 5.1. are averages of ten readings over an hour of testing. From Table 5.1. it can be concluded that adequate mixing and the correct molar ratio is obtained and therefore the feed system was adopted as such.

MATERIAL	REFRACTIVE INDEX AT 25°C		$\Delta E_r$
	LABORATORY	PILOT PLANT	
50% w/w Urea Solution	1.4130	1.4128	0.0002
36% F	1.3739	1.3739	0.0000
UF Feed U:F Molar Ratio 1:2.2	1.3891	1.3890	0.0001

TABLE 5.1.

ADEQUACY OF MIXING FOR THE MODIFIED  
FEED SYSTEM

5.2.2. SAMPLING FROM THE REACTOR

In the description of the original plant layout it was emphasised that no provisions for sampling from the reactor were available.

In addition to satisfying the safety requirements at reactor pressures of between 100-200 psig, any sampling device to be used must possess unique properties due to the nature of resins produced in the reactor. Furthermore, the high pressure makes removal of representative

samples very difficult as the material leaving the device will undergo physio-chemical change due to the sudden reduction in pressure.

However, to test the mathematical models conveniently it is desirable that the material in the reactor should be sampled at frequent intervals along the reactor so that several residence times can be examined in each run carried out. From the above consideration the desired sampling device should possess the following properties.

- (i) Safety of operation
- (ii) No dead spaces; as the resins would gel (solidify) in such spaces
- (iii) Ability to provide samples without physio-chemical change due to the differential pressure.

As a result of the above specifications, no such device was found readily available on the market and therefore the sampling device had to be designed, constructed and finally tested on the reactor. The sampling device developed is shown in Fig.5.3. and consists of:

A main tube (EN58J Stainless Steel) passing through the valve which is the same size as the reactor tube and is inserted in the line (Reactor tube) by means of Hermeto couplings (Fig.5.6.). The valve thus becomes part of the reactor tube. A PTFE shaft is sealed perfectly on a hole  $\frac{1}{8}$  inch diameter thus resulting in a small area, ensuring exertion of a small force on it and alleviating the problems of leakage.



The PTFE shaft is threaded against the top body (EN56 AM Stainless Steel) which has two seals on the main body (EN58J Stainless Steel) with gaskets sealing the inner compartment. The PTFE shaft increases in diameter for a small length ( $\frac{1}{4}$ " ) immediately before the seal closest to the reactor tube. This restricts the movement of the shaft such that it cannot be removed from the system. A compartment is produced as a result of the position of this protrusion in the top body of the valve. This compartment is sealed using 'O' rings. The inclusion of this protrusion serves as a safety measure for cases where the valve is used carelessly or where the PTFE thread against the top body is damaged and fails. Thus the central plug could not eject hazardously under reactor pressure. The top body is bolted tightly to the main body at four points. Other dimensions of the valve are included in Fig.5.3.

On opening the valve the mix flows into the small valve compartment under the differential pressure and through the outlet which is submerged in a collecting vessel filled with ice water. The collection technique minimises any physio-chemical change which may occur as a result of the differential pressure (see Section 5.4.1.). Once the sample collection is completed, the valve is closed. Provisions are made for wash water and compressed air to wash and dry the inner compartment of the valve after each sample collection (Fig.5.3.). This avoids any possibility of gel formation due to any stagnant resin remaining in the sampling device.

The device so constructed was tested with the reactor operating at 250-300 psig and a steam temperature of 160°C with water flowing through the tubes. Under these severe conditions the sampling valve performance was found to be satisfactory and the operation simple. Four such valves were therefore manufactured and inserted in the reactor tube at various points. The full description of the usage of the valve can be found in Section 5.4.1,

### 5.3. THE MODIFIED PLANT DESCRIPTION

The flow and instrumentation diagram, for the final equipment layout used in this work, appears in Fig.5.4. The description of the items of the plant follows:

#### FORMALIN TANK

The formalin tank was a 45 litre ( $0.045\text{m}^3$ ) QVF glass vessel. The stirrer system was made of stainless steel and included 4 baffles close to the vessel wall. The stirrer was driven by a 0-3000 RPM Gast MFG Corp. variable speed motor. The heating/cooling coil was made of  $\frac{1}{2}$  inch i.d. copper tubing and was connected to the steam and cold water lines via  $\frac{1}{2}$ " gate valves. The wash water line to the tank and the drain line were made of  $\frac{1}{2}$ " flexible tubing and controlled by  $\frac{1}{2}$ " gate valves. The outlet to the formalin pump was 1" i.d. pressure-tubing. A  $\frac{1}{2}$ " flexible tubing water line joined this line via a  $\frac{1}{2}$ " gate valve at a Tee. The tank temperature was checked manually using a -10 to 110°C

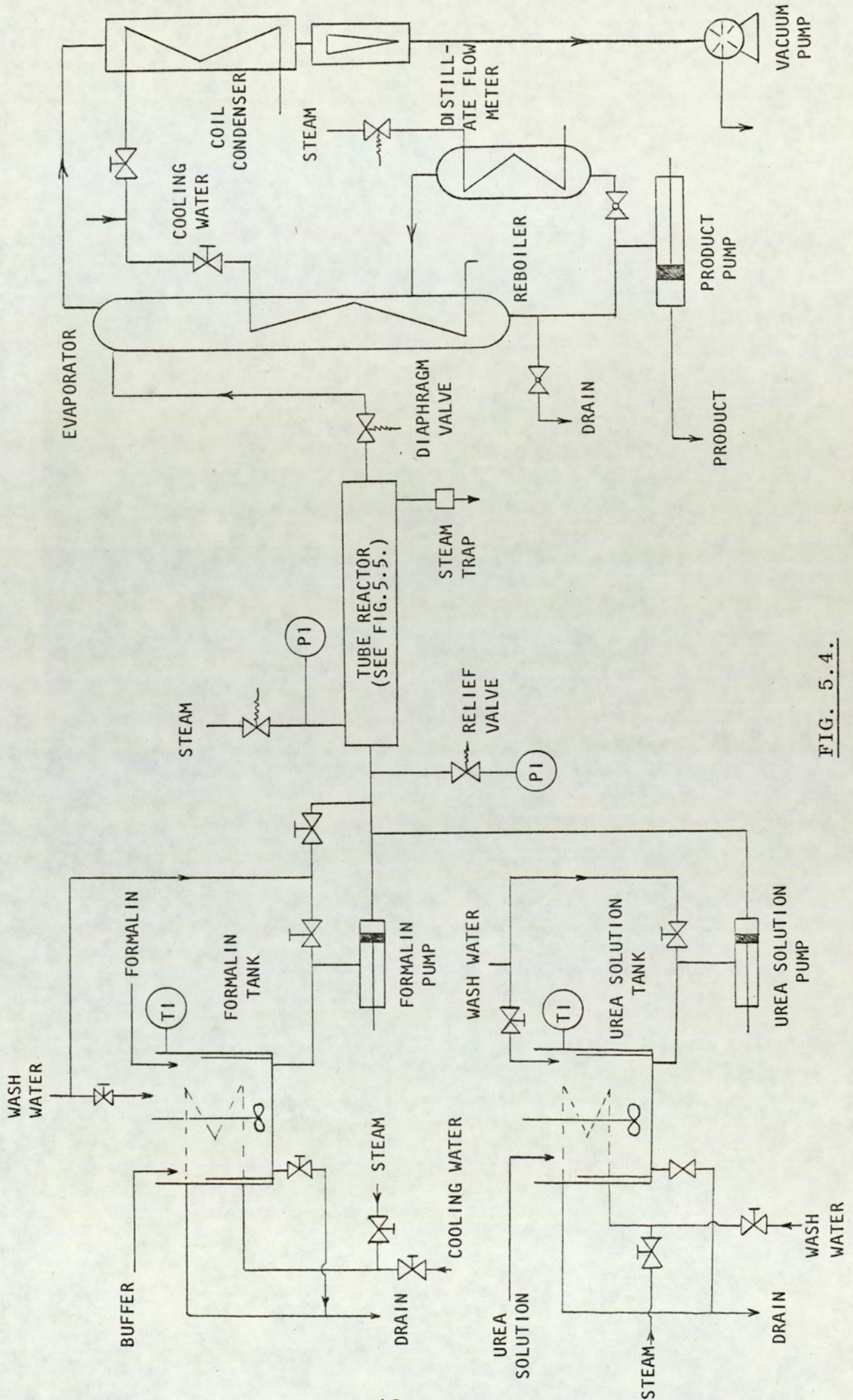


FIG. 5.4. EXPERIMENTAL PLANT FLOW AND INSTRUMENTATION DIAGRAM

Mercury-in-glass thermometer,

#### FORMALIN PUMP

The formalin pump was a variable capacity 'Milroyal' metering pump having a maximum capacity of 40 GPH ( $0.1818\text{m}^3\text{h}^{-1}$ ) made of stainless steel. On the suction side the line was 1" i.d. pressure tubing with wash water facilities as described above. On the process side the line was made of a  $\frac{1}{4}$ " i.d. EN58J (type 316) stainless steel tube leading to the Tee at the reactor entrance. A calibration chart for the formalin pump can be found in Appendix 8.

#### UREA TANK

The urea tank was a 40 litre ( $0.04\text{m}^3$ ) opaque PVC vessel. The agitation system, the heating/cooling coil arrangement, the wash water and drain lines were as specified for the formalin tank. The outlet to the urea pump was also as specified for the formalin tank. The large i.d. tube avoided pump starvation on the suction side. The temperature was checked manually in the same manner as described for the formalin tank.

#### UREA PUMP

The urea pump was a variable capacity "Milroyal" metering pump of 80 GPH ( $0.3636\text{m}^3\text{h}^{-1}$ ) maximum capacity. On the suction side the line was a 1" i.d. pressure tubing with a  $\frac{1}{2}$ " flexible wash water line joining it via a  $\frac{1}{2}$ " gate valve at a Tee. On the process side the

line was a  $\frac{1}{4}$ " i.d. EN58J (type 316) stainless steel tube leading to the tee at the reactor entrance. A calibration chart for the urea pump is included in Appendix 8.

#### THE REACTOR TEE AND REACTOR ENTRANCE

The tee where urea and formaldehyde solutions met at the reactor entrance was a  $\frac{3}{4}$ " stainless steel tee reduced on all three sides to accommodate  $\frac{1}{4}$ " i.d. lines from the formalin pump, from the urea pump and to the reactor. This increase in size gave the required volume for good mixing of the reactant solutions. Between the tee and the reactor entrance a wash water line joined the reactor tube via a  $\frac{1}{2}$ " gate valve. This line was a safety measure such that the resin could be washed out of the reactor in case both pumps failed. Also before the reactor entrance a tee in the reactor line lead to a  $\frac{1}{2}$ " diaphragm spring loaded relief valve and a pressure indicator. The stainless steel relief valve could be manually set to release the reactor contents at a given pressure. The pressure indicator was a "Budenberg" stainless steel diaphragm type with a range of 0-1000 psig.

#### THE REACTOR

A detailed layout of the reactor is shown in Fig.5.5. The reactor consisted of three 10 feet lengths of  $\frac{1}{4}$  inch i.d. (18 SWG) and one 8 feet length of  $\frac{3}{8}$  inch i.d. (18 SWG) EN58J type 316 stainless steel tubes. The tubes were joined consecutively by means of small bends and Ermeto couplings, so that each tube could be easily

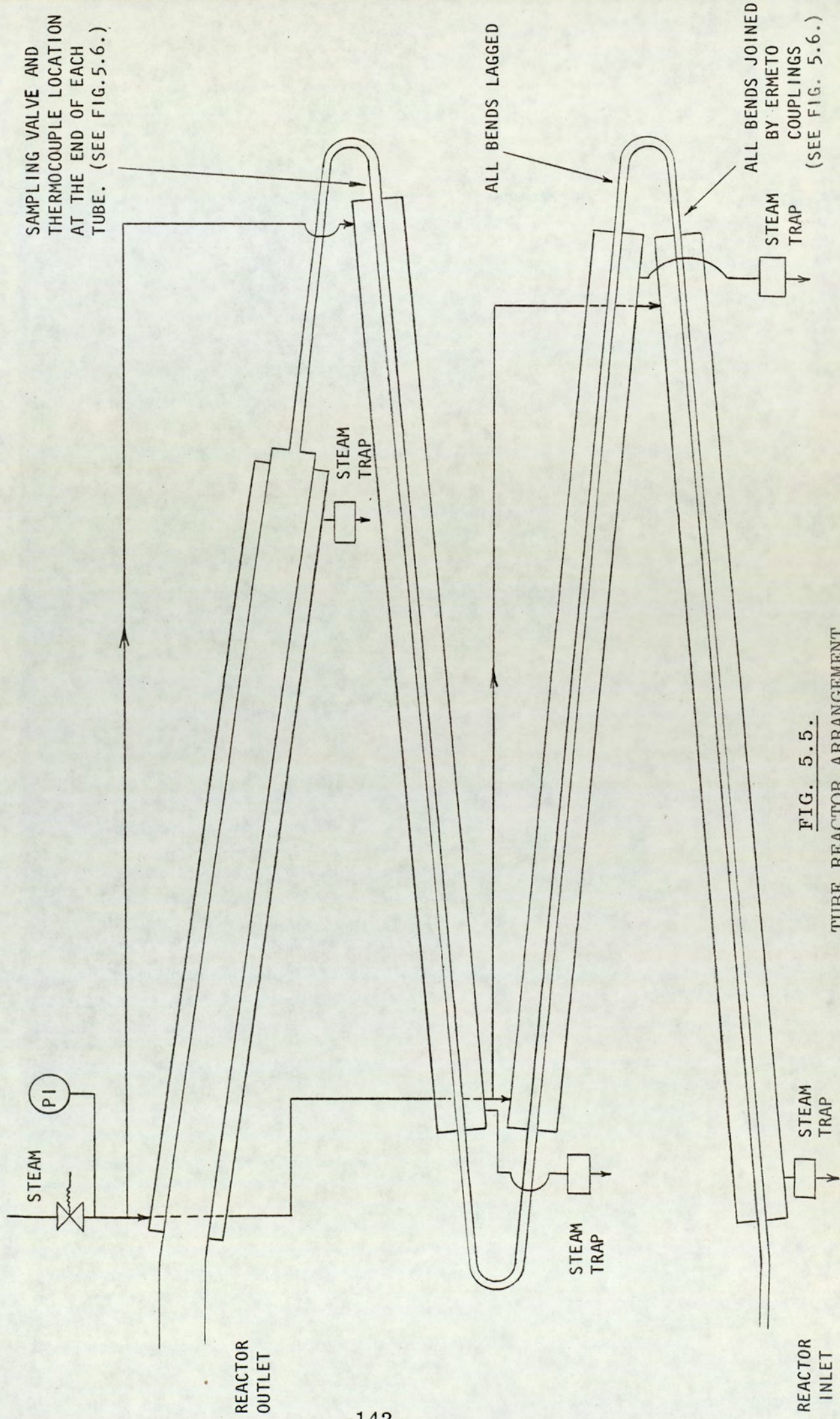


FIG. 5.5.  
TUBE REACTOR ARRANGEMENT

isolated if required. The actual formation of the tubes is shown in Fig.5.5. Each length of the tube was placed concentrically in a 4 inch i.d. mild steel pipe which constituted the thermal jackets. The bends connecting the tubes, including the sampling valves, were lagged using glass fibre wool and cloth.

There are two separate lengths of the reactor to be considered in subsequent calculations. The effective reactor length as far as the reaction is concerned was assumed to be 38 feet (11.5824m) with a volume of 47.1 in<sup>3</sup> (30ft at  $\frac{1}{4}$ " i.d. and 8ft at  $\frac{3}{8}$ " i.d.)( $7.7 \times 10^{-4}$  m<sup>3</sup>). This meant that those sections of the tube (bends) which were not affected by isothermal heat transfer were assumed to be of little significance as reaction zones. The reactor length as used for calculations of residence time and pump delivery rates (Appendix 8) was 49.84 feet (15.1912m) with a volume of 55.41 in<sup>3</sup> ( $9.08 \times 10^{-4}$  m<sup>3</sup>). This was accounted for as follows:

Reactor tee to reactor entrance	=	7.6"
First tube	=	10'
First bend	=	2'6"
Second tube	=	10'
Second bend	=	2'9.4"
Third tube	=	10'
Third bend	=	5'5.9"
Fourth tube	=	8'
Line between end of fourth tube and sample valve	=	5.2"
Total length	=	49'10.1" = 49.84' (15.1912m)

$$\begin{aligned} \text{Volume (41'4.9" @ } \frac{1}{4} \text{'' i.d. and 8'5.2" @ } \frac{5}{8} \text{'' i.d.)} \\ = 55.41 \text{ in}^3 \text{ (} 9.08 \times 10^{-4} \text{ m}^3 \text{)} \end{aligned}$$

Although the urea and formalin pumps were not equidistant from the tee, the lengths of the tubes between the pumps and the tee will not effect the calculations (Appendix 8).

The pressure of the steam supply to the jackets was controlled using a Spirax Sarco (Type BRV) reduction valve. The steam pressure indicator was a David Harcourt Ltd., phosphore-bronze tube type gauge with a range of 0-200 psig. The steam was introduced into the jacket at the more elevated side of each particular jacket. The condensate from each jacket left separately via a steam trap, located at the lowest point of each jacket.

## REACTOR SAMPLING VALVES

The details of the sampling valves are given in Section 5.2.2. and Fig.5.3. Four sampling valves were inserted in the line immediately after each tube length and before each bend using Ermeto couplings. The diagrammatic detail is shown in Fig.5.6.

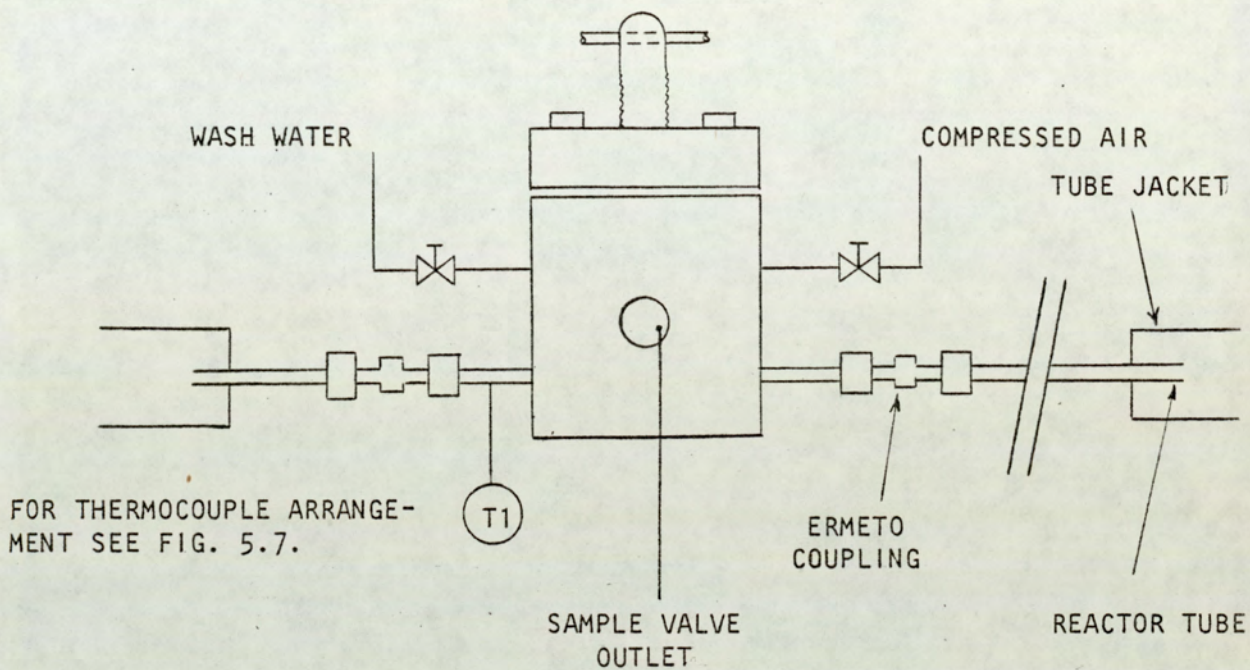
## REACTOR TEMPERATURE MEASUREMENT

Four thermocouples were situated adjacent to each sampling valve. The junction of each thermocouple was dropped into a depression made in the main reactor tube as shown in Fig.5.7(a). This ensured good contact at the wall. A copper strip covered each thermocouple keeping it in position and ensuring representative temperature distribution (Fig.5.7(b)). Each assembly was lagged with fibre glass wool and cloth.

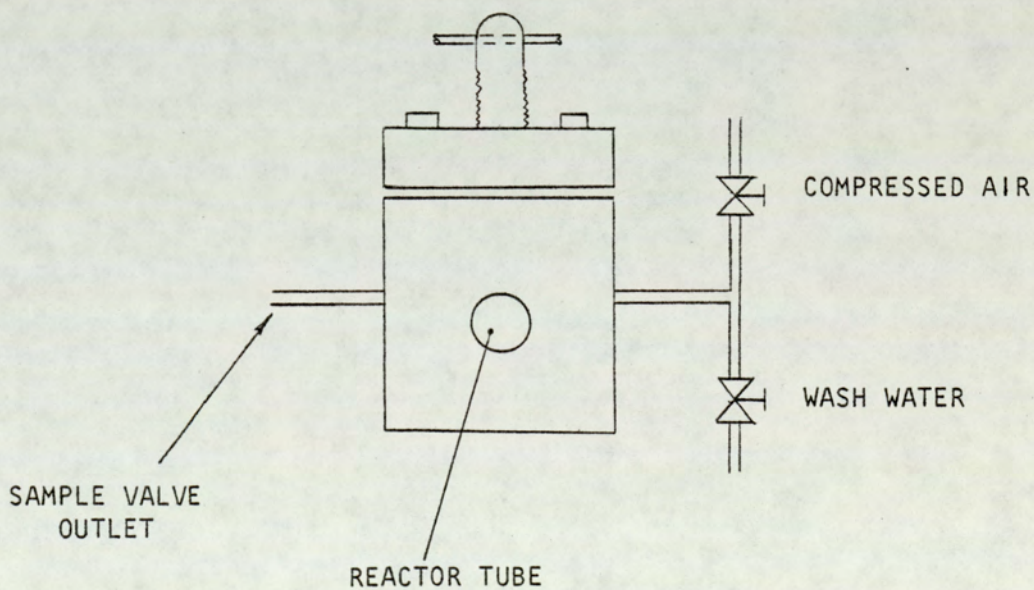
The four thermocouples were connected to a 6 channel Kent (Mode Mark 3) recorder with a range of 0-200°C. No cold junction for reference was required as the recorder had a compensation facility. The recorder was calibrated to BS1818.

## REACTOR OUTLET DIAPHRAGM VALVE

The reactor outlet spring loaded diaphragm valve was a ½" stainless steel (EN58J type 316) construction of 38 GPH capacity. It was manually operated and set by trial and error to give the required pressure in the reactor. The diaphragm was made of PTFE.



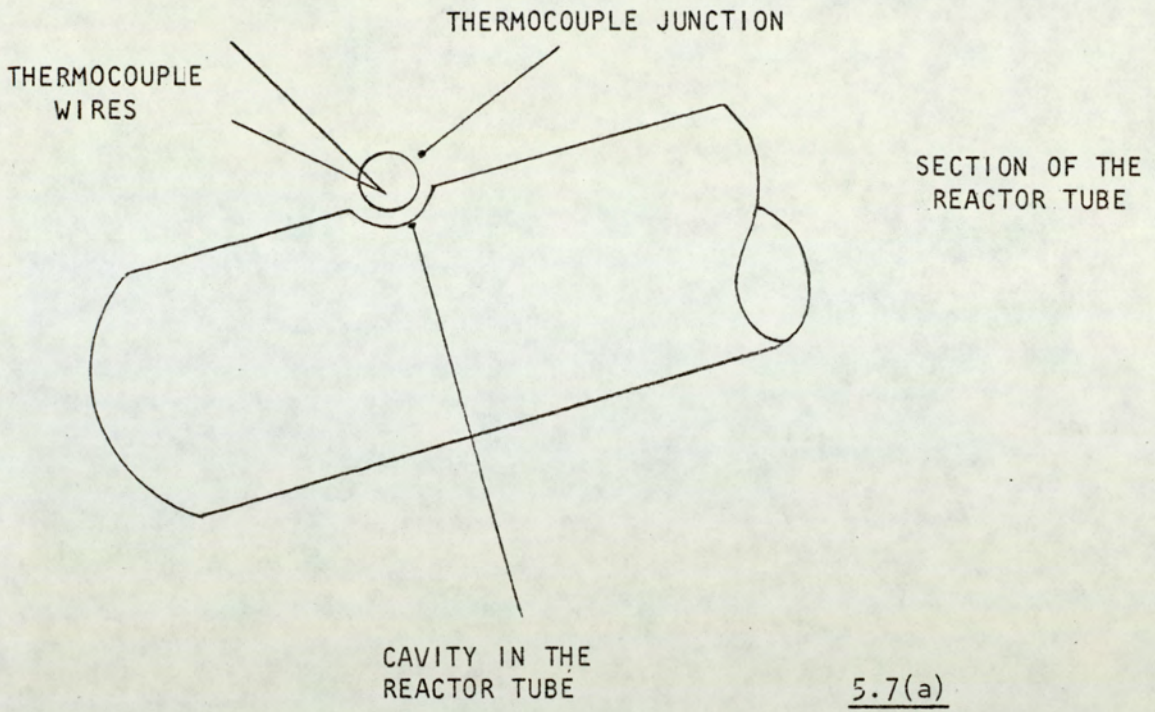
SAMPLE VALVE LINE ARRANGEMENT



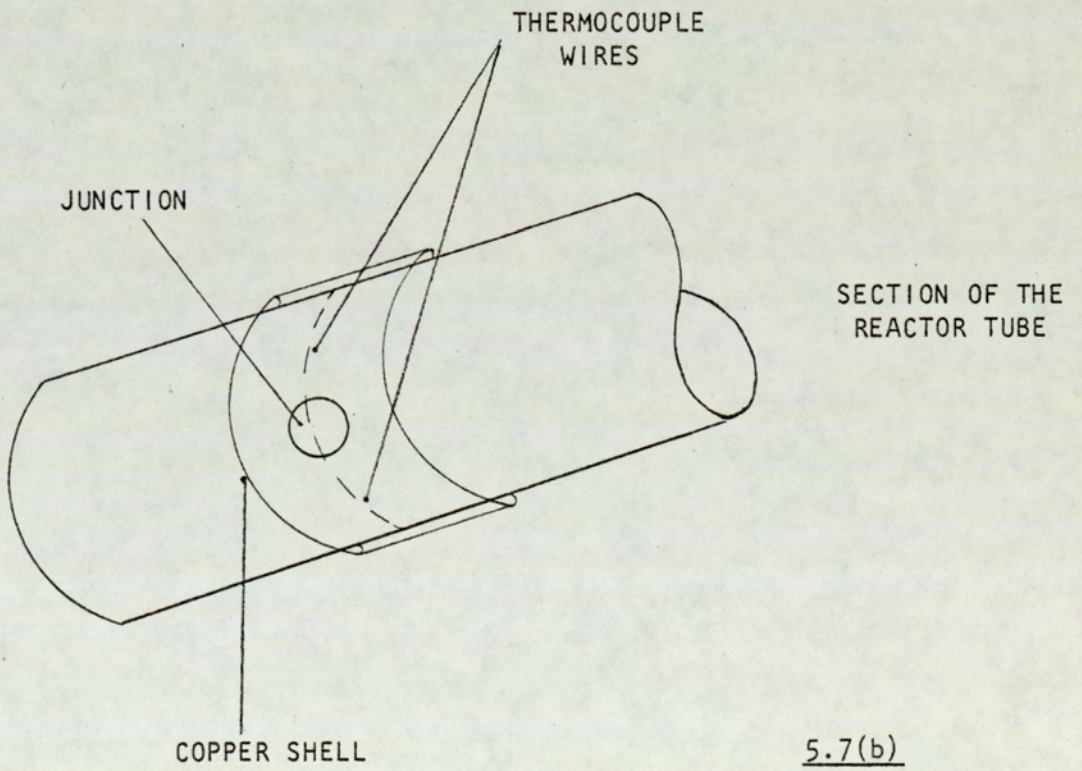
SAMPLE VALVE SERVICE LINES

FIG. 5.6.

SAMPLING VALVE ARRANGEMENT



5.7(a)



5.7(b)

FIG. 5.7.  
THERMOCOUPLE ARRANGEMENT

## THE PRODUCT REMOVAL SYSTEM

The remainder of the equipment shown in Fig.5.4. is ordinarily used for flash evaporating and concentrating the resin. However in this work the system was used to collect and cool the product from the reactor ready for disposal. For this reason the details of this part of the rig are not of relevance to the work carried out in this project and are therefore omitted.

### 5.4. PLANT OPERATION AND EXPERIMENTAL PROCEDURE

With reference to Fig.5.4. the plant operation and experimental procedure were as follows:

The required w/w urea solution was prepared in the urea tank. The heating coil was used to compensate for the endothermic dissolution of urea in water and therefore speed the dissolution. The temperature of the solution was measured and stabilised. The pH of the particular batch of formalin of the required strength was measured at the formalin's stabilised temperature. A small amount of the required U:F molar ratio mix was prepared from the above solutions. The pH was recorded and the temperature of the mix noted as that at which the mix would enter the reactor. In cases where the pH of the above mix was less than 7.5, the formalin would have been adjusted with either 10% NaOH solution for U:F molar ratio 1:2.2 or Hexamine for U:F molar ratio 1:1.33, such that the pH of the mix fell in the range

7.5-8.5. This initial pH was therefore at the more alkaline end of the correct range (Chapter 3) and compensated for the acidity developed as a result of the Cannizzaro's reaction, keeping the pH within the required band throughout the reactor. However such cases did not arise in any of the systems which were investigated in this work. The temperature of the urea solution and formalin were monitored continuously.

The formalin pump was started and the vernier set to give the required delivery for the desired U:F molar ratio and residence time in the tube. The urea pump was then similarly set (Appendix 8).

The delivery of each pump was checked before and several times during each experimental run.

The reactor relief valve was fully opened and the reactor outlet diaphragm valve fully closed. The relief valve was adjusted to open at a safe pressure of approximately 100 psig higher than that which would develop in the tubes. The diaphragm valve was then opened to such an extent that half the required pressure developed in the tubes.

Steam was gradually allowed into the reactor jacket. Meanwhile cooling water to the evaporator and condenser was turned on to cool the product leaving the tubes. The steam pressure was then slowly adjusted using the reduction valve until the required pressure was developed. Time was allowed for the pressure to stabilise.

Monitoring of reactor temperatures was started. At the same time all sampling valves were checked for

services and cleared.

Once the reactor temperatures stabilised, approximately 10 to 20 minutes were allowed to elapse for all systems to reach steady state (Appendix 1). All variables were monitored continuously for any disturbances during this period.

Once steady state was reached with all the equipment performing satisfactorily, the sampling sequence was initiated. Two samples were taken on every occasion because of the constraints imposed by the analytical techniques.

Samples were removed from consecutive valves always starting with the one closest to the reactor outlet so that chances of disturbing the flow downstream were small.

Once the first two samples were removed the operation of the reactor was continued until time was available for the next two samples to be accommodated in the analytical sequence. Thus unmonitored reactions during storage, sampling and analysing were avoided. During this period all the parameters were rechecked for possible disturbances and monitored to ensure consistency of conditions.

On completion of the run steam was turned off first. When the reactor temperatures dropped to below 50°C the tube pressure was released. Wash water to the reactor was opened at this point and the two pumps stopped. The urea and formalin tanks were then cleared and filled with water. The wash water to the reactor

was then closed and the two pumps restarted so that water was pumped through the pumps and reactor thereby cleaning the whole system. Finally the relief valve was fully opened so that it could be cleaned by passage of water through it.

Once the equipment was clean, the shut down was completed by turning the equipment and services off systematically.

A sample calculation to specify the equipment and services performance is given in Appendix 8.

#### 5.4.1. THE SAMPLING TECHNIQUE

In Section 5.2.2, it was emphasised that sample collection was to be achieved without any physio-chemical change to the reactor mix, likely to occur as a result of the differential pressure.

The arrangement for sample collection is shown in Fig.5.8.

On opening the valve the resin flowed from the reactor tube into the valve compartment (Fig.5.3.). The small size of the compartment pressurised the bulk of the sample which flowed through the outlet tube into the test tube of Fig.5.8. The size of the test tube and the level of water in it was chosen in the trial runs such that under the most severe conditions of pressure and temperature any vapour entering the test tube in the form of rising bubbles would not reach the liquid surface.

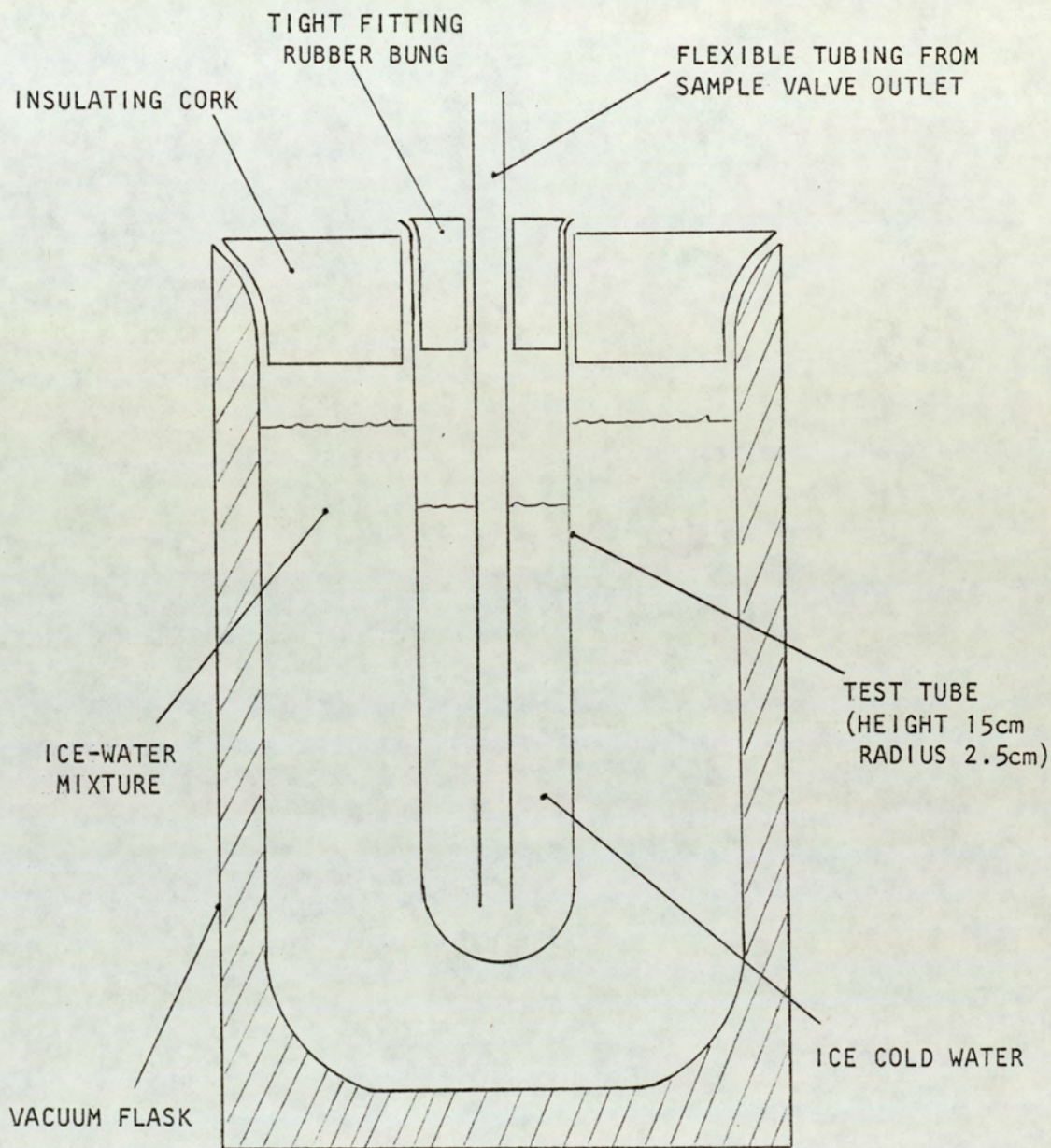


FIG. 5.8.

SAMPLE COLLECTION ARRANGEMENT

No vapour left any other part of the valve. This was confirmed in the trials where the valve was covered with soap water and its behaviour inspected for any possible vapour leakage through the other joints.

The experiments showed that at a jacket steam temperature of 120°C no bubbles of vapour entered the test tube. The resin could be seen entering the test tube and rising to the top as a result of its higher temperature. At a jacket temperature of 160°C, however, bubble formation was apparent. The level of liquid used proved to be adequate as no bubbles travelled more than half-way up the test tube.

Frequent use of the valves made it possible to judge the approximate weight of resin required. The ice water in the test tube as well as quenching the reaction by a drop in temperature and dilution was used as some of the water which is added to the resin as part of the analytical technique. Each sample removal took approximately 1-2 minutes to complete. The samples were immediately analysed on removal. Details of the technique and calculations required for the analysis are given in the following section and Appendix 9.

#### 5.5. THE ANALYTICAL TECHNIQUE

In general, the primary purpose of any chosen analytical technique would be to differentiate between the constituents of the reaction mixture of urea and formaldehyde. These constituents can be listed as:

- (i) Unreacted urea, "Free Urea".
- (ii) Unreacted formaldehyde, "Free Formaldehyde".
- (iii) Urea-formaldehyde addition products (Methylolureas).
- (iv) Urea-formaldehyde condensation products  
(Methylene bridged or Methylene ether bridged)  
of various molecular weights depending on the  
reaction conditions and the degree of progress  
of reaction.

A literature survey on the methods capable of analysing the urea-formaldehyde reaction mixtures showed that five different techniques were available. These, in chronological order of development are:

- (i) Quantitative Analysis (71,72,83).
- (ii) Polarography (71,72,83,123).
- (iii) Paper Chromotography (124).
- (iv) Thin layer chromatography (125,126).
- (v) Gel-permeation chromatography (127,128).

Therefore it became necessary to select one of the above techniques for application to the analysis of the reactor products. In order to be able to make this selection, the most important requirements of the technique to be used in conjunction with the reactor had to be identified. These requirements were of critical importance if the method was to be successful and are listed below.

#### a. SPEED OF THE ANALYTICAL TECHNIQUE

The reason for this can be associated with the

reactivity of the UF systems under acidic, basic or neutral conditions, even at low temperatures. Therefore the speed of the analytical technique is critical.

#### b. REQUIREMENTS OF SMALL SAMPLE VOLUMES

This arises as a result of the sampling valve construction. Although removal of large quantities of sample is possible, it is not advisable to do so as the flow pattern in the reactor tube could be significantly disturbed.

#### c. ECONOMIC FEASIBILITY

Methods (iii) and (iv) were discarded due to their lengthy procedures. Methods (ii) and (v) were suitable and could be adapted for successful use giving results of good accuracy. In particular, gel permeation chromatography seemed a powerful analytical tool as it could analyse the constituents of the urea-formaldehyde reaction mixture as well as differentiate between the various molecular weight condensation products. However both of the above techniques (methods (ii) and (v)) had to be excluded for economic considerations.

#### 5.5.1. THE QUANTITATIVE ANALYTICAL METHOD

Having concluded the above investigation with the choice of quantitative analysis, it remained to identify

the different routes required to analyse the different constituents of the reaction mixture.

Assuming that since formaldehyde is in excess, all of the urea in the reaction mixture undergoes reaction, and also that formaldehyde is present in the mix in the form of:

- (a) free, uncombined formaldehyde
- (b) methylol groups ( $-\text{CH}_2\text{OH}$ ), and
- (c) methylene groups ( $-\text{CH}_2-$ )

Then by application of the following analytical technique it is possible to determine the percentage of formaldehyde present in each of these three forms.

The 'total-formaldehyde', i.e. (a)+(b)+(c) can either be estimated as the input formaldehyde or obtained analytically by, for example, distilling a sample of the mix with phosphoric acid. By the latter procedure, all formaldehyde residues are converted into free formaldehyde which can be estimated by a number of methods such as those described later in this section.

Free-formaldehyde (a) can be estimated in a number of different ways, the essence of which is the reaction of formaldehyde with an agent such that acid or base is released. Titration is then used to measure the amount of acid or base produced which is a measure of the formaldehyde in the mix.

The formaldehyde in the form of methylol groups together with the free formaldehyde i.e. (a)+(b) can be determined by using techniques such as the Iodimetric methylol analysis or the mild alkaline hydrolysis (129).

Having obtained (a), (a)+(b), and (a)+(b)+(c), appropriate subtractions give the individual values of (b) and (c).

The most important analysis in the above analytical procedure is the determination of free formaldehyde. This is because the free formaldehyde results are directly comparable to the results of the reactor model simulations.

Since it has been assumed that all of the urea has reacted, then on the basis of the assumptions used for derivation of the kinetics (Chapter 3), the extent of reaction of formaldehyde is also the extent of formation of the methylolureas. For this reason the techniques for analysis of free formaldehyde were surveyed in detail and are presented in the next section. However, in the interest of completion and to provide a basis for judging the accuracy of the assumptions, the Iodimetric methylol analysis was used to evaluate the extent of methylation and methylene bridge formation (condensation) as described above. The choice was made in preference to the mild alkaline hydrolysis technique because the latter is less accurate in as much as it cannot differentiate between methylol and methylene ether groups. The details of the procedures are given in Appendix 9.

The total formaldehyde was assumed to be the input formaldehyde. To ensure that no loss of formaldehyde occurred, the formaldehyde content of the formalin feed was checked on several occasions as described in Appendix 9 under 'Standardisation of Formalin'. No

appreciable loss of formaldehyde was detected during the operation time of the reactor which was a maximum of two hours at a time.

#### 5.5.2. FREE FORMALDEHYDE ANALYSIS

Walker (116) in "Formaldehyde" lists eight different quantitative analytical methods for determination of free formaldehyde. Of these the most accurate and suitable is the 'sulphite method'. Of the other techniques some are moderate in accuracy, some use hazardous chemicals such as cyanide and some possess lengthy procedures. Furthermore the sulphite method was selected as it satisfied the two criteria of selection which were described in Section 5.5, namely speed of test and requirement of small sample quantity. A sample weight of between 2 and 3 grams is required using this technique, the analysis time, for an experienced operator, being between 2 and 3 minutes.

There are two versions of the sulphite method, these being:

- (i) The acidimetric sulphite method
- (ii) The iodimetric sulphite method.

The acidimetric sulphite method uses excess sodium sulphite solution which when added to the sample to be analysed liberates alkali which is titrated with standard acid. However, in the presence of urea, accuracy may be greatly reduced because of the alkaline catalysis of the U-F addition reaction.

De Jong and de Jonge(77), rejected the acidimetric sulphite method, on the above basis, and developed a modification of the common sulphite assay known as the iodimetric sulphite method.

From the work of de Jong and de Jonge, it may be concluded that the acidimetric sulphite method would generally give low results for free formaldehyde. However Landqvist(83) compared the acidimetric sulphite method with the polarographic method and found excellent agreement between the two methods. Furthermore, the iodimetric method takes longer and is therefore more susceptible to error even though the pH of the analytical mixture is kept around the neutral region. It should also be mentioned that the reaction mixtures under investigation are well advanced in addition reactions and therefore with formaldehyde in excess the possibility of any unreacted urea in the solution is small.

Assuming that the polarographic technique is the more accurate of the above three methods and from the above discussion, it is justifiable to select the acidimetric sulphite method as the best available. The details of the procedures are given in Appendix 9.

To conclude this section it must be emphasised that inspection of the acidimetric sulphite procedure shows that exactly one minute elapses between the addition of excess neutral sodium sulphite and the back titration of the excess acid.

This is necessary for standardisation of the method so that all the results become comparable on the same

basis. The implication of the above is that the technique becomes comparative and not absolute. However the discrepancy is not expected to be sufficiently great to adversely effect the aims of this project.

#### 5.6. SCOPE AND RANGE OF EXPERIMENTAL INVESTIGATION

The experimental operating variables which influence the final properties of the reactor product and which have been investigated in this work are:

- (i) Steam temperature in the jacket.
- (ii) Residence time in the tubes.
- (iii) U:F molar ratio.
- (iv) Concentration of the feed.

The scope and range of variation in each of the above parameters is discussed in this section. One major parameter, the tube radius, whose variation would affect the product properties significantly has not been investigated experimentally.

#### RANGE OF JACKET TEMPERATURES

This range was chosen to cover cases of industrial significance. The lowest jacket temperature was 120°C while the highest was 160°C. The upper limit was partly imposed by the very short residence times and partly by the investigation of the UF kinetics which was conducted to 160°C. The former was noted when early experiments showed that in cases where the residence

time was very low, the reactor contents did not have much time to reach the jacket temperature and left the reactor at 20 to 40°C below the jacket temperature. The low temperature limit was chosen so as to represent a realistically high temperature of operation such that savings in reaction time, as compared to the batch process (Chapter 1), became worthwhile.

As a result, the reactor jacket temperature band of operation was 120 to 160°C with the three temperatures (120°C, 140°C, 160°C) being investigated experimentally.

#### RANGE OF RESIDENCE TIMES

Two residence times of industrial importance exist depending on the properties of the product required. One is in the range of 0-30 seconds and the other between 1 and 3 minutes. It was originally hoped that the conditions could be so chosen to cover both these ranges. However, the capacity of the formalin and urea pumps, the only pumps available, were such that only the shorter residence time range could be accurately covered. Furthermore, since four sampling valves were installed in the reactor line the choice of one overall residence time meant that four different residence times could be investigated simultaneously. The maximum residence time obtained with the use of the above pumps was in the region of 60 seconds for the overall reactor length. It was therefore decided to choose two overall residence times which, due to the non-uniform geometry of the

reactor, encompassed only one overlapping residence time. In this way more comparative results could be gathered and also the consistency of the runs could be checked.

The lowest residence time achievable was 26.75 seconds which fixed the second residence time at 53.50 seconds for one overlap. These two residence times on break down covered the industrial range of interest. This made the investigation of the following residence times (RT) possible, (for calculations see Appendix 5).  
overall RT = 26.75 s giving RT of 3.34, 6.68, 10.02, 26.75  
overall RT = 53.50 s giving RT of 6.68, 13.36, 20.04, 53.50

#### RANGE OF U:F MOLAR RATIOS

Two molar ratios of U:F which were of significance were investigated.

These were:

- (i) U:F 1:1.33, which represents the optimum reacting ratio for formation of methylolureas to DMU, and
- (ii) U:F 1:2.20, which ensures the formation of methylolureas higher than DMU.

#### RANGE OF FEED CONCENTRATION

The main purpose of investigation of this parameter was to assess the effect of variations in commercial formalin strength (36% w/w and 44% w/w) and the urea solution strengths on the product. The following

combinations were therefore investigated.

- (i) Combination of 36% w/w formalin and 50% w/w urea solution.
- (ii) Combination of 36% w/w formalin and 25% w/w urea solution.
- (iii) Combination of 44% w/w formalin and 50% w/w urea solution.

### 5.7. EXPERIMENTAL ERROR

Before presenting the experimental results it is worth examining the sources of experimental error.

Error is likely to arise in the following areas.

- (i) Quantitative analysis
- (ii) Measurements and Readings
- (iii) Calculations

It is attempted to quantify the error where possible. However in cases where this cannot be done with any certainty, the fact is reported. Each area is discussed separately.

#### 5.7.1. ANALYTICAL TECHNIQUES

The error of the quantitative analysis arises in determination of total formaldehyde, free formaldehyde and methylol plus free formaldehyde.

## TOTAL FORMALDEHYDE

The total formaldehyde i.e. formaldehyde present in the formalin solution was assumed as the input formaldehyde in the feed. Furthermore the formaldehyde in the formalin solution was assumed to be at the manufactured concentration i.e. 36% w/w or 44% w/w. The variation of concentration of formaldehyde in the formalin solution at the time of this investigation was found to be a maximum of  $\pm 1\%$ , when results are expressed as percentage of total solution analysed, i.e. the concentrations were  $36 \pm 1\%$  w/w and  $44 \pm 1\%$  w/w.

## FREE FORMALDEHYDE AND METHYLOL PLUS FREE FORMALDEHYDE

Duplicate analysis of several samples established the reproducibility of these techniques to be within  $\pm 0.1\%$ , when results are expressed as per cent of total solution. However, as it was emphasised earlier in this Chapter (Section 5.5.2.) both of these techniques are comparative and therefore no absolute error of technique can be quoted.

### 5.7.2. MEASUREMENT

The errors of measurement could arise in assuming the jacket steam pressure constant, averaging the temperature recorders output over the experiment time and finally assuming that the delivery of the two pumps

remain constant.

The use of steam regulator and steam traps allowed the steam pressure to remain constant within  $\pm 1$  psi absolute at steady state conditions. This infers that the steam pressure of 15 psig to give a jacket temperature of  $120^{\circ}\text{C}$  gave jacket temperatures of  $120 \pm 1.2^{\circ}\text{C}$ . Applying the same technique, the accuracy of the temperatures investigated are as follows:

$$120 \pm 1.2^{\circ}\text{C}$$

$$140 \pm 1.0^{\circ}\text{C}$$

$$160 \pm 0.5^{\circ}\text{C}$$

The recorder output temperature was generally constant under steady state conditions and was assumed representative. However, it is difficult to quantify the error between the thermocouples response and the actual wall temperature. This is an even more critical argument in this particular case because of the thermocouples being positioned in the lagged sections of the reactor.

The error associated with the pump deliveries and therefore accuracy of residence times is easier to explain yet harder to remedy. The pumps output varied considerably due to pump drifts which could only be associated with the age of the pumps. This problem became especially acute at lower capacities which were predominantly used due to the excessive size of the pumps. An attempt was made to avoid any drifts by repetitive checks and calibration before each experiment. Unfortunately, even with the above checks the consistent

performance of the two pumps can not be certified.

### 5.7.3. CALCULATIONS

There are errors involved in the calculation of residence times due to the use of densities and conversion factors (Appendix 8). However the significance of these errors as compared to those discussed previously can be neglected.

### 5.8. EXPERIMENTAL RESULTS

The logic of the experimental runs was as follows: For one set of given conditions the reproducibility of the results was established by repeating the experiment. Tables 5.2, and 5.3. show these results.

The effect of variation in temperature at seven residence times with constant U:F molar ratio and concentration was then investigated, Tables 5.2., 5.4, and 5.5. exhibit the results of this investigation. The molar ratio was changed and the above repeated. The results for the investigation at this molar ratio are given in Tables 5.6. and 5.7. Finally the effect of variation in concentration was investigated at seven residence times with constant U:F molar ratio and temperature. These results can be found in Tables 5.8. and 5.9.

The experiments are numbered so that the results can be clearly discussed with reference to particular

experiments. Tables showing the comparisons possible between the results of the various experiments together with full discussion of the implications of the results are presented in the next Chapter,

PARAMETERS	EXPERIMENT REFERENCE NUMBER			
	E1	E2	E3	E4
MOLAR RATIO, U:F	1:2,2	1:2,2	1:2.2	1:2,2
UREA SOLUTION STRENGTH/ FORMALIN STRENGTH, % W/W	50/36	50/36	50/36	50/36
JACKET TEMP., °C	160	160	160	160
RESIDENCE TIME, S	6,68	13,36	20,04	53,50
INPUT F., %	21,77	21,77	21,77	21,77
(FREE & METHYLOL) F., %	21,22	19,69	17,12	17,01
FREE F., %	19,76	13,82	8,49	5,72
METHYLOL F., %	1,46	5,87	8,63	11,29
METHYLENE F., %	0,55	2,08	4,65	4,76
REACTOR LENGTH, cm	304,8	609,6	914,4	1158,24
REACTOR WALL TEMP., °C	124	158	168	166

INLET TEMP. = 35°C

TABLE 5.2.

EXPERIMENTAL RESULTS

PARAMETERS	EXPERIMENT REFERENCE NUMBER			
	E5	E6	E7	E8
MOLAR RATIO, U:F	1:2.2	1:2.2	1:2.2	1:2.2
UREA SOLUTION STRENGTH/ FORMALIN STRENGTH, % W/W	50/36	50/36	50/36	50/36
JACKET TEMP., °C	160	160	160	160
RESIDENCE TIME, S	6.68	13.36	20.04	53.50
INPUT F., %	21.77	21.77	21.77	21.77
(FREE & METHYLOL) F., %	21.42	19.12	17.03	17.86
FREE F., %	19.72	13.63	8.05	6.34
METHYLOL F., %	1.70	5.49	8.98	11.52
METHYLENE F., %	0.35	2.65	4.74	3.91
REACTOR LENGTH, cm	304.8	609.6	914.4	1158.24
REACTOR WALL TEMP., °C	126	157	168	165

INLET TEMP. = 35°C

TABLE 5.3.

EXPERIMENTAL RESULTS

PARAMETERS	EXPERIMENT REFERENCE NUMBER			
	E9	E10	E11	E12
MOLAR RATIO, U:F	1:2.2	1:2.2	1:2.2	1:2.2
UREA SOLUTION STRENGTH/ FORMALIN STRENGTH, % W/W	50/36	50/36	50/36	50/36
JACKET TEMP., °C	120	120	120	120
RESIDENCE TIME, S	3.34	6.68	10.02	26.75
INPUT F., %	21.77	21.77	21.77	21.77
(FREE & METHYLOL) F., %	21.70	20.50	19.84	18.17
FREE F., %	21.12	19.98	18.65	11.87
METHYLOL F., %	0.58	0.52	1.19	6.30
METHYLENE F., %	0.07	0.27	1.93	3.60
REACTOR LENGTH, cm	304.8	609.6	914.4	1158.24
REACTOR WALL TEMP., °C	68	102	108	138

INLET TEMP. = 35°C

TABLE 5.4.

EXPERIMENTAL RESULTS

PARAMETERS	EXPERIMENT REFERENCE NUMBER			
	E13	E14	E15	E16
MOLAR RATIO, U:F	1:2.2	1:2.2	1:2.2	1:2.2
UREA SOLUTION STRENGTH/ FORMALIN STRENGTH, % W/W	50/36	50/36	50/36	50/36
JACKET TEMP., °C	140	140	140	140
RESIDENCE TIME, S	6.68	13.36	20.04	53.50
INPUT F., %	21.77	21.77	21.77	21.77
(FREE & METHYLOL) F., %	20.00	19.84	18.60	15.90
FREE F., %	19.73	14.89	11.29	7.36
METHYLOL F., %	0.27	4.95	7.31	8.54
METHYLENE F., %	1.77	1.93	3.17	5.87
REACTOR LENGTH, cm	304.8	609.6	914.4	1158.24
REACTOR WALL TEMP., °C	103	135	154	152

INLET TEMP. = 25°C

TABLE 5.5.

EXPERIMENTAL RESULTS

PARAMETERS	EXPERIMENT REFERENCE NUMBER			
	E17	E18	E19	E20
MOLAR RATIO, U:F	1:1.33	1:1.33	1:1.33	1:1.33
UREA SOLUTION STRENGTH/ FORMALIN STRENGTH, % W/W	50/36	50/36	50/36	50/36
JACKET TEMP., °C	120	120	120	120
RESIDENCE TIME, S	3.34	6.68	10.02	26.75
INPUT F., %	17.30	17.30	17.30	17.30
(FREE & METHYLOL) F., %	17.17	16.20	14.96	13.71
FREE F., %	16.89	16.13	14.93	12.60
METHYLOL F., %	0.28	0.07	0.03	1.11
METHYLENE F., %	0.13	1.10	2.34	3.59
REACTOR LENGTH, cm	304.8	609.6	914.4	1158.24
REACTOR WALL TEMP., °C	68	88	108	132

INLET TEMP. = 34°C

TABLE 5.6.

EXPERIMENTAL RESULTS

PARAMETERS	EXPERIMENT REFERENCE NUMBER			
	E21	E22	E23	E24
MOLAR RATIO, U:F	1:1.33	1:1.33	1:1.33	1:1.33
UREA SOLUTION STRENGTH/ FORMALIN STRENGTH, % W/W	50/36	50/36	50/36	50/36
JACKET TEMP., °C	140	140	140	140
RESIDENCE TIME, S	6.68	13.36	20.04	53.50
INPUT F., %	17.30	17.30	17.30	17.30
(FREE & METHYLOL) F., %	17.19	15.54	10.98	6.94
FREE F., %	16.61	12.81	6.26	1.40
METHYLOL F., %	0.58	2.73	4.72	5.54
METHYLENE F., %	0.11	1.76	6.32	10.36
REACTOR LENGTH, cm	304.8	609.6	914.4	1158.24
REACTOR WALL TEMP., °C	106	135	161	159

INLET TEMP. = 34°C

TABLE 5.7.

EXPERIMENTAL RESULTS

PARAMETERS	EXPERIMENT REFERENCE NUMBER			
	E25	E26	E27	E28
MOLAR RATIO, U:F	1:2.2	1:2.2	1:2.2	1:2.2
UREA SOLUTION STRENGTH/ FORMALIN STRENGTH, % W/W	25/36	25/36	25/36	25/36
JACKET TEMP., °C	140	140	140	140
RESIDENCE TIME, S	6.68	13.36	20.04	53.50
INPUT F., %	15.61	15.61	15.61	15.61
(FREE & METHYLOL) F., %	16.61	14.92	14.68	12.12
FREE F., %	15.17	11.87	9.98	6.16
METHYLOL F., %	1.44	3.05	4.70	5.96
METHYLENE F., %	0.00	0.69	0.93	3.49
REACTOR LENGTH, cm	304.8	609.6	914.4	1158.24
REACTOR WALL TEMP., °C	101	132	134	149

INLET TEMP. = 34°C

TABLE 5.8.

EXPERIMENTAL RESULTS

PARAMETERS	EXPERIMENT REFERENCE NUMBER			
	E29	E30	E31	E32
MOLAR RATIO, U:F	1:2.2	1:2.2	1:2.2	1:2.2
UREA SOLUTION STRENGTH/ FORMALIN STRENGTH, % W/W	50/44	50/44	50/44	50/44
JACKET TEMP., °C	140	140	140	140
RESIDENCE TIME, S	3.34	6.68	10.02	26.75
INPUT F., %	24.44	24.44	24.44	24.44
(FREE & METHYLOL) F., %	23.34	24.16	24.10	20.19
FREE F., %	23.29	22.20	18.20	10.41
METHYLOL F., .	0.05	1.96	5.91	9.78
METHYLENE F., %	1.10	0.28	0.34	4.25
REACTOR LENGTH, cm	304.8	609.6	914.4	1158.24
REACTOR WALL TEMP., °C	72	102	136	162

INLET TEMP. = 34°C

TABLE 5.9.

EXPERIMENTAL RESULTS

## C H A P T E R 6

### DISCUSSION AND COMPARISON OF RESULTS

In Chapter 6, experimental and predicted results are discussed and compared. Initially, the experimental results reported in Chapter 5 are examined, discussing the effects of the variations in parameters investigated. These results are then compared with the plug-flow model predictions and the accuracy of the predictions estimated. The comparison of the experimental results with the complex model simulation then follows with a parallel treatment. The chapter terminates with sections summarising the major conclusions, suggesting the more appropriate model for use under the conditions specified in this investigation.

#### 6.1. DISCUSSION OF EXPERIMENTAL RESULTS

The experimental results presented in Tables 5.2. to 5.9. are discussed in the following sections. Beginning with an examination of the reproducibility of the results, the work develops to discuss the effect of variations in temperature, molar ratio, concentration and residence time on the performance of the tubular reactor.

### 6.1.1. REPRODUCIBILITY OF EXPERIMENTAL RESULTS

The reproducibility of the experimental results for a given set of conditions can be assessed by examination of the experiments detailed in Table 6.1.

EXPERIMENTS TO BE COMPARED	CONDITIONS			
	RT., Seconds	MR., U:F	SS., U%/F%	T., °C
E1 Vs E5	6.68	1:2.2	50/36	160
E2 Vs E6	13.36	1:2.2	50/36	160
E3 Vs E7	20.04	1:2.2	50/36	160
E4 Vs E8	53.50	1:2.2	50/36	160

RT., : Residence Time

SS., : Solutions Strengths, w/w

MR., : Molar Ratio

T., : Temperature

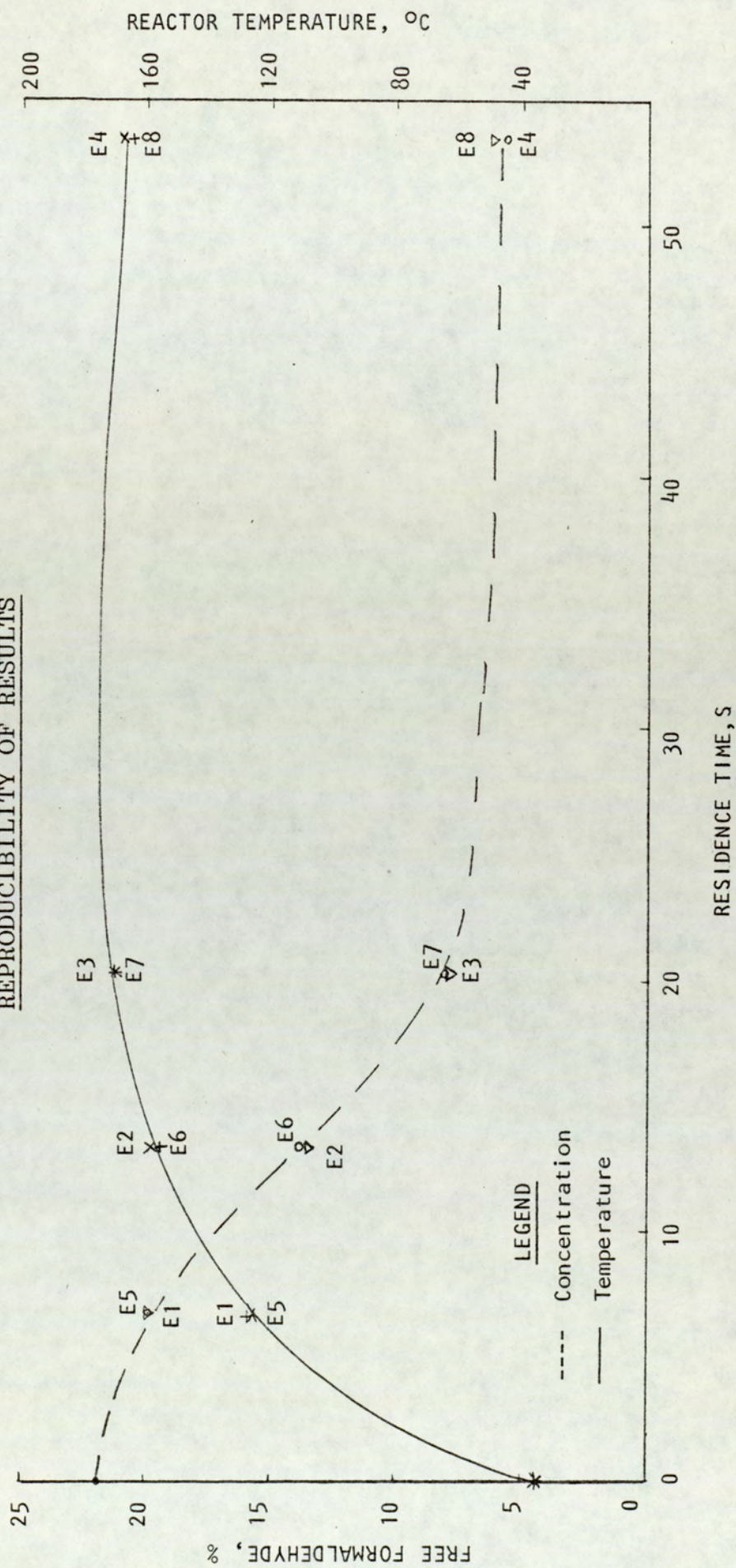
TABLE 6.1.

### REPRODUCIBILITY OF RESULTS

An adequate number of data points, for one given set of conditions, were not obtained (due to limits on availability of equipment) to permit a meaningful statistical analysis for means and standard deviations. However, comparison of the data obtained for the conditions outlined in Table 6.1. shows good reproducibility

FIG. 6.1.

REPRODUCIBILITY OF RESULTS



of the results. The reproducibility of the more important of these data, namely, free formaldehyde and temperature is shown graphically in Fig.6.1.

#### 6.1.2. EFFECT OF VARIATIONS IN STEAM TEMPERATURE

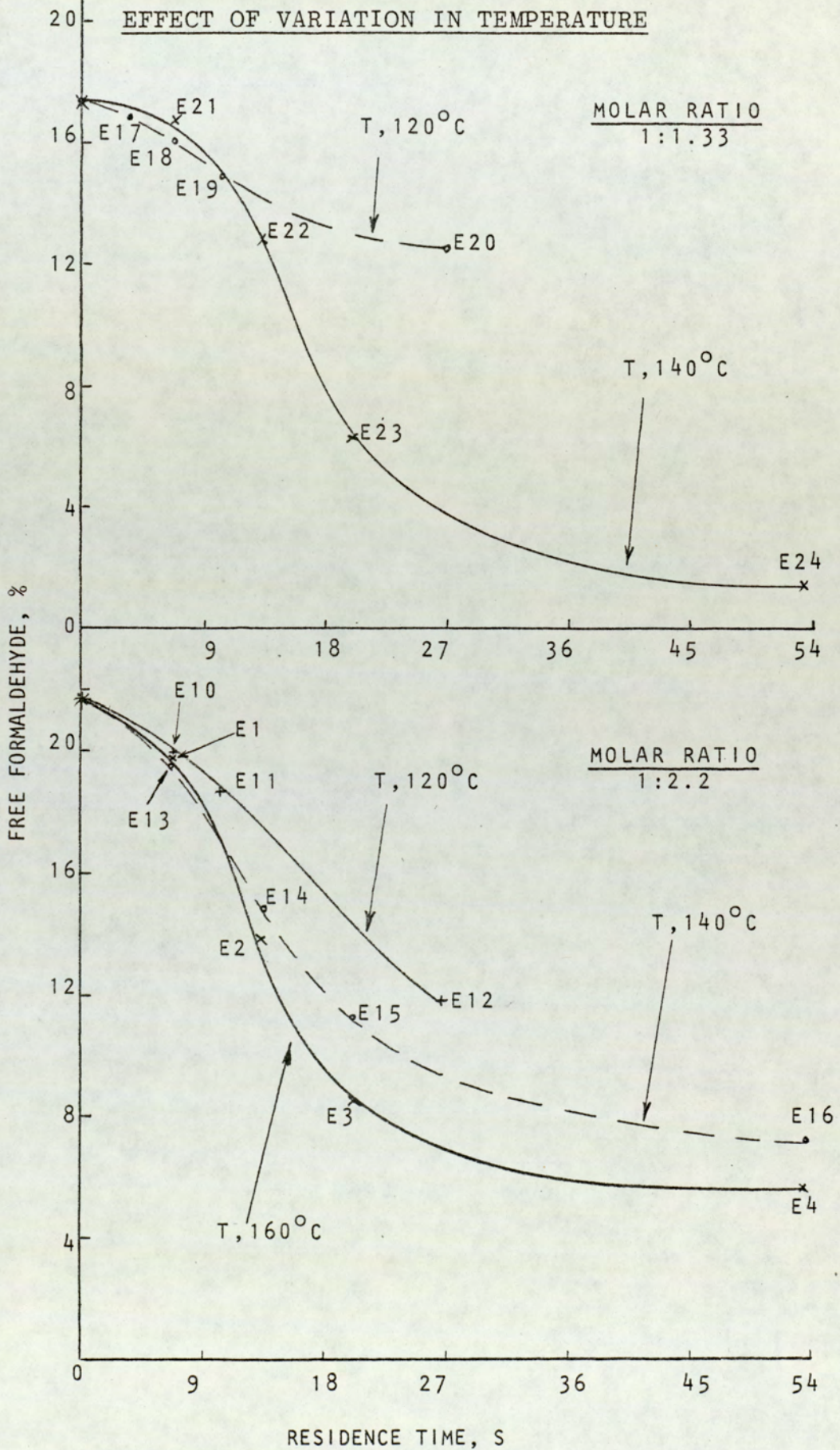
The effect of variations in steam temperature can be examined by comparison of the experiments detailed in Table 6.2.

EXPERIMENTS TO BE COMPARED	CONDITIONS			
	RT., Seconds	MR., U:F	SS., U%/F%	T., °C
E1 Vs E13 Vs E10	6.68	1:2.2	50/36	160 140 120
E2 Vs E14	13.36	1:2.2	50/36	160 140
E3 Vs E15	20.04	1:2.2	50/36	160 140
E4 Vs E16	53.50	1:2.2	50/36	160 140
E18 Vs E21	6.68	1:1.33	50/36	120 140

TABLE 6.2.

EFFECT OF VARIATION IN STEAM TEMPERATURE

FIG. 6.2.



For ease of comparison, the free formaldehyde concentrations in these experiments are presented in Fig.6.2. From an examination of Fig.6.2. in conjunction with the above experiments, the following points can be deduced.

a. FREE FORMALDEHYDE CONCENTRATIONS

(i) The effect of an increase in steam temperature is to speed the rate of reaction of formaldehyde. This is valid for both molar ratios investigated. From Fig.6.2. the only exceptions seem to be the data points represented by E17 and E18. For the above statement to be true E17 and E18 should have values higher than E21.

This suggests that these two data points are in error by 0.7 to 0.9%, but since the value of this discrepancy is well within the degree of reproducibility and experimental error, it can be concluded that the temperature effect proposed is valid.

(ii) The increase in the speed of reaction caused by increase in steam temperature from 120 to 160°C seems to be negligible for up to 6.68 seconds residence time at both molar ratios (E1,E10,E13) and (E18,E21), (See also iii).

The effect of the increase in speed of reaction however becomes progressively more significant with increasing residence time for both molar ratios (E4 Vs E16 and E23 Vs E20).

(iii) The shapes of the curves in Fig.6.2. suggest

a reaction initiation lag after which the bulk of the formaldehyde reactions occur in a comparatively short time. The curves are then seen to flatten towards equilibrium.

(iv) Higher steam temperatures attain lower values of equilibrium concentration of formaldehyde (E4 Vs E16). Furthermore the reaction positions of points E4 and E16 suggest that further reactions, of the condensation type, take place at the higher temperature. This statement seems valid since if the same reactions occurred at both 140°C and 160°C, it would be expected that the curve at 160°C would cross the curve at 140°C near equilibrium heading towards a higher equilibrium value, of unconverted formaldehyde as a result of the Le Chataillier's principle (Appendix 5). As the shape of the curves represented by E1, E2, E3, E4 and E13, E14, E15, E16 do not exhibit any such tendency, it must be concluded that the extent of condensation reaction at 160°C is higher than at 140°C.

#### b. METHYLOLS AND METHYLENES

(i) Higher temperatures favour a faster conversion of formaldehyde to methylols for U:F molar ratio of 1:2.2. This is particularly valid for shorter residence times as the ratio of methylol formaldehyde to methylene formaldehyde appears to decrease with increasing residence times (series E1 to E4, E13 to E16 and E9 to E12).

Lower temperatures cause slower methylation and therefore permit some of the methylols produced to be converted to methylenes (E9-E12). Although high residence times suggest that methylol formation is well in excess of methylene linkage, the data shows that the extent of formation of methylene compounds is significant and cannot be assumed negligible (E3,E4,E16).

(ii) For molar ratio of 1:1.33 at low temperatures, almost all of the methylols formed convert immediately to methylene (E17 to E20). At higher temperatures however, the speed of methylol formation seems to be faster than the condensation reaction at lower residence times. However an increase in residence time results in the bulk of methylols being converted to methylene (E21 to E24). This can be explained by the more vigorous reaction at this molar ratio due to the higher concentration of reactants.

### c. REACTOR WALL TEMPERATURES

The wall temperature at some point along the reactor exceeds the steam temperature due to the exothermic nature of the reaction. Beyond that point, cooling occurs, as shown in the longer residence time experiments where the wall temperature approaches the steam temperature near the reactor outlet. This effect however cannot be detected at lower residence times because of the poor cooling characteristics of steam. As a result of the above it could be said that the exotherm

of the reaction coupled with heat transfer from the steam to the resin will always result in the wall temperature exceeding the steam temperature if adequate time is allowed. The wall temperature will then drop slowly to reach the steam temperature at which point a constant wall and steam temperature can be retained.

### 6.1.3. EFFECT OF VARIATION IN MOLAR RATIO

Table 6.3. gives the details of the experiments which can be compared for an assessment of the effect of variation of molar ratio on the reactor performance.

The free formaldehyde concentrations of the experiments listed in Table 6.3. are shown in Fig.6.3. Some of the effects of change in molar ratio were discussed in Section 6.1.2., in conjunction with the effect of variations in temperature. The additional points which can be deduced from Fig.6.3. are listed below.

#### a. FREE FORMALDEHYDE

(i) The shape of the curves in Fig.6.3. suggest that the reaction mechanism is the same for both molar ratios.

(ii) Each molar ratio exhibits a reaction initiation lag both at 120°C and at 140°C, (E9,E17,E13,E21).

(iii) The reaction stage shows a faster rate of reaction at the molar ratio of 1:1.33 (E13,E14,E15, Vs

EXPERIMENTS TO BE COMPARED	CONDITIONS			
	RT., Seconds	MR., U:F	SS., U%/F%	T., °C
E13 Vs E21	6.68	1:2.2 1:1.33	50/36	140
E14 Vs E22	13.36	1:2.2 1:1.33	50/36	140
E15 Vs E23	20.04	1:2,2 1:1.33	50/36	140
E16 Vs E24	53.50	1:2,2 1:1.33	50/36	140
E9 Vs E17	3.34	1:2.2 1:1.33	50/36	120
E10 Vs E18	6.68	1:2.2 1:1.33	50/36	120
E11 Vs E19	10.02	1:2.2 1:1.33	50/36	120
E12 Vs E20	26.75	1:2.2 1:1.33	50/36	120

TABLE 6.3.

EFFECT OF VARIATION IN MOLAR RATIO

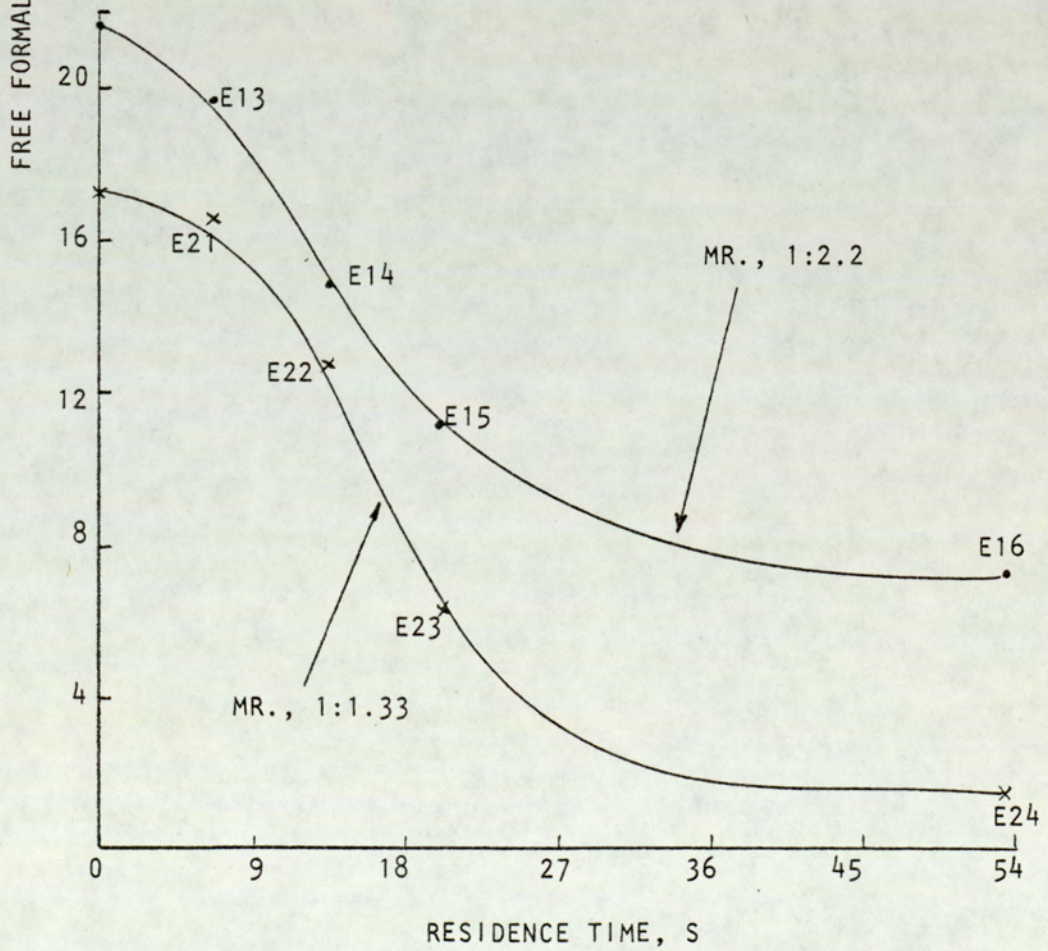
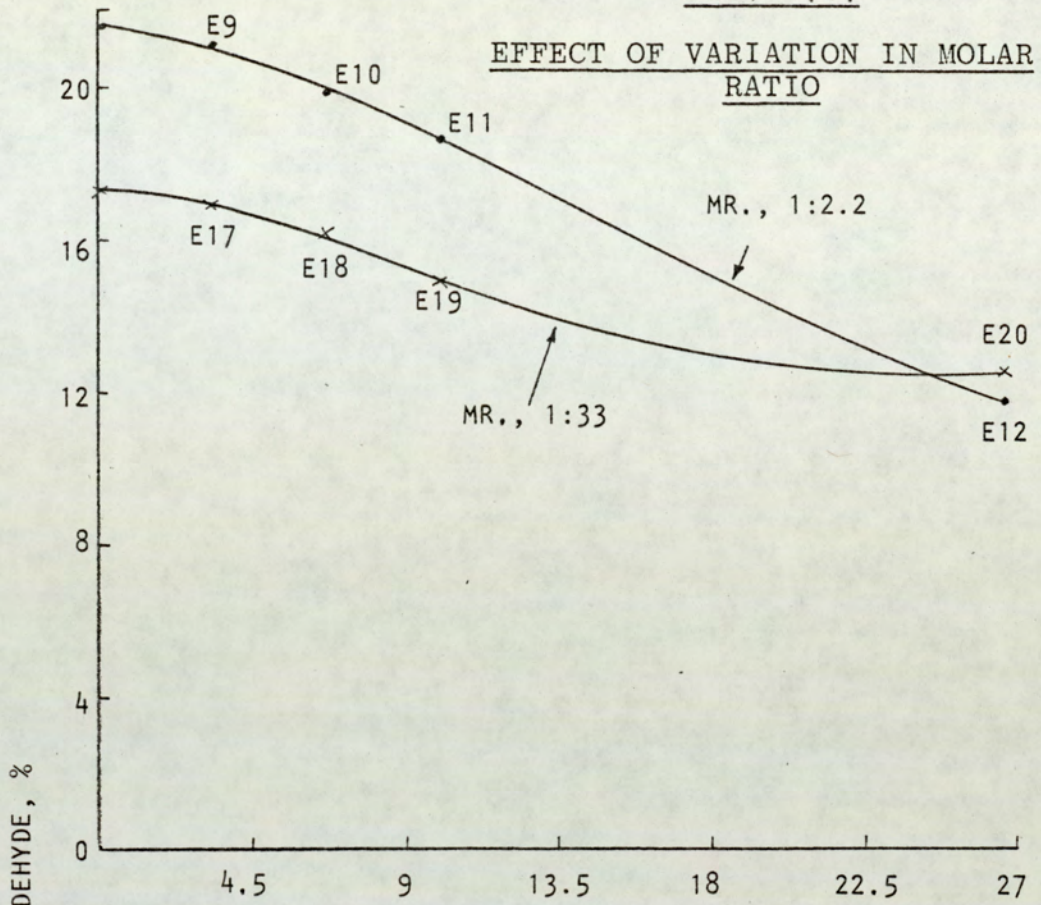
E21,E22,E23). This is as a result of the higher concentration of the reactants at this ratio.

(iv) A higher equilibrium concentration of free formaldehyde is attained at the higher molar ratio. This can be attributed to the excess formaldehyde present at the molar ratio of 1:2.2. However, the drop in concentration of free formaldehyde at this molar ratio seems to be small with increasing residence times once the bulk of the reaction has taken place (E15,E16 and E23,E24). This implies that free formaldehyde takes little part in the condensation reactions which follow.

(v) A close examination of the curves of Fig.6.3. suggests that irrespective of the starting molar ratio, it is possible to arrive at the same resin composition, as far as free formaldehyde concentration is concerned, by the choice of the correct residence time at a given temperature (E14 Vs E22 and E12 Vs E20). This can be explained by the fact that while the resin at a molar ratio of 1:2.2 has passed its reaction initiation lag and is well into the process of reaction, the resin with the molar ratio of 1:1.33 has just started its reaction stage and hence the concentrations of free formaldehydes virtually coincide. A further implication from the above is that the reaction initiation lag for the higher molar ratio takes less time while the rate of reaction is slower at the higher molar ratio.

FIG. 6.3.

EFFECT OF VARIATION IN MOLAR RATIO



## b. METHYLOLS AND METHYLENES

The formation of methylol and methylene compounds is greatly influenced by the molar ratio employed. At a molar ratio of 1:2.2, at shorter residence times, up to 20.04 seconds, methylolurea formation seems predominant, although some methylene bridges are formed during the process (e.g. E2,E3). Increase of residence time causes a significant conversion of methylol to methylene compounds (E16,E12). At a molar ratio of 1:1.33 any methylols formed seem to be immediately consumed by condensation reactions (E17,E18,E19,E22). This effect becomes more pronounced with increases in residence time where the condensation reactions become predominant (E24). From the above it can be concluded that the lower the molar ratio, the less the time lag between the addition and the condensation reactions, to the extent that the two reactions become virtually simultaneous.

## c. TEMPERATURE

The wall temperature variations reflect the increase in speed of the reaction as the molar ratio is lowered.

A faster reaction results in faster heat release which in turn results in higher wall temperatures for the same residence time and steam temperatures. This can be verified by comparison of E15 and E23 where at a residence time of 20.04 seconds and a jacket temperature of 140°C, the 1:1.33 molar ratio shows a wall temperature

of 161°C, whereas the 1:2.2 molar ratio shows a wall temperature of 154°C.

Furthermore, the implication that the reaction initiation lag takes a shorter time at the higher molar ratios seems to be confirmed by the wall temperatures of E9, E10, E11 and E12 as compared to those of E17, E18, E19 and E20. This comparison shows E10 to have a value 14°C higher than E18. Finally, in general, at lower residence times and higher temperatures not much difference can be detected between the wall temperatures produced by either molar ratio. This could be as a result of a decrease in the significance of the reaction initiation lag with increasing temperatures (E13, E14 Vs E21, E22).

#### 6.1.4. EFFECT OF VARIATION IN CONCENTRATION

The effects which would be manifested as a result of a change in concentration of the reactants will correspond to those described for variations in molar ratio. Since an increase in molar ratio of F:U corresponds to a decrease in concentration of the reactants, the changes observed as a result of an increase in molar ratio of F:U will therefore correspond to the changes which would result if the concentration of the reactants were reduced.

Comparison of the experiments tabulated in Table 6.4. confirms the above as well as the conclusions which were arrived at in association with changes in the molar ratio,

discussed in the previous section.

EXPERIMENTS TO BE COMPARED	CONDITIONS			
	RT., Seconds	MR., U:F	SS., U%/F%	T., °C
E13 Vs E30	6.68	1:2.2	50/36 50/44	140
E13 Vs E25	6.68	1:2.2	50/36 25/36	140
E14 Vs E26	13.36	1:2.2	50/36 25/36	140
E15 Vs E27	20.04	1:2.2	50/36 25/36	140
E16 Vs E28	53.50	1:2.2	50/36 25/36	140

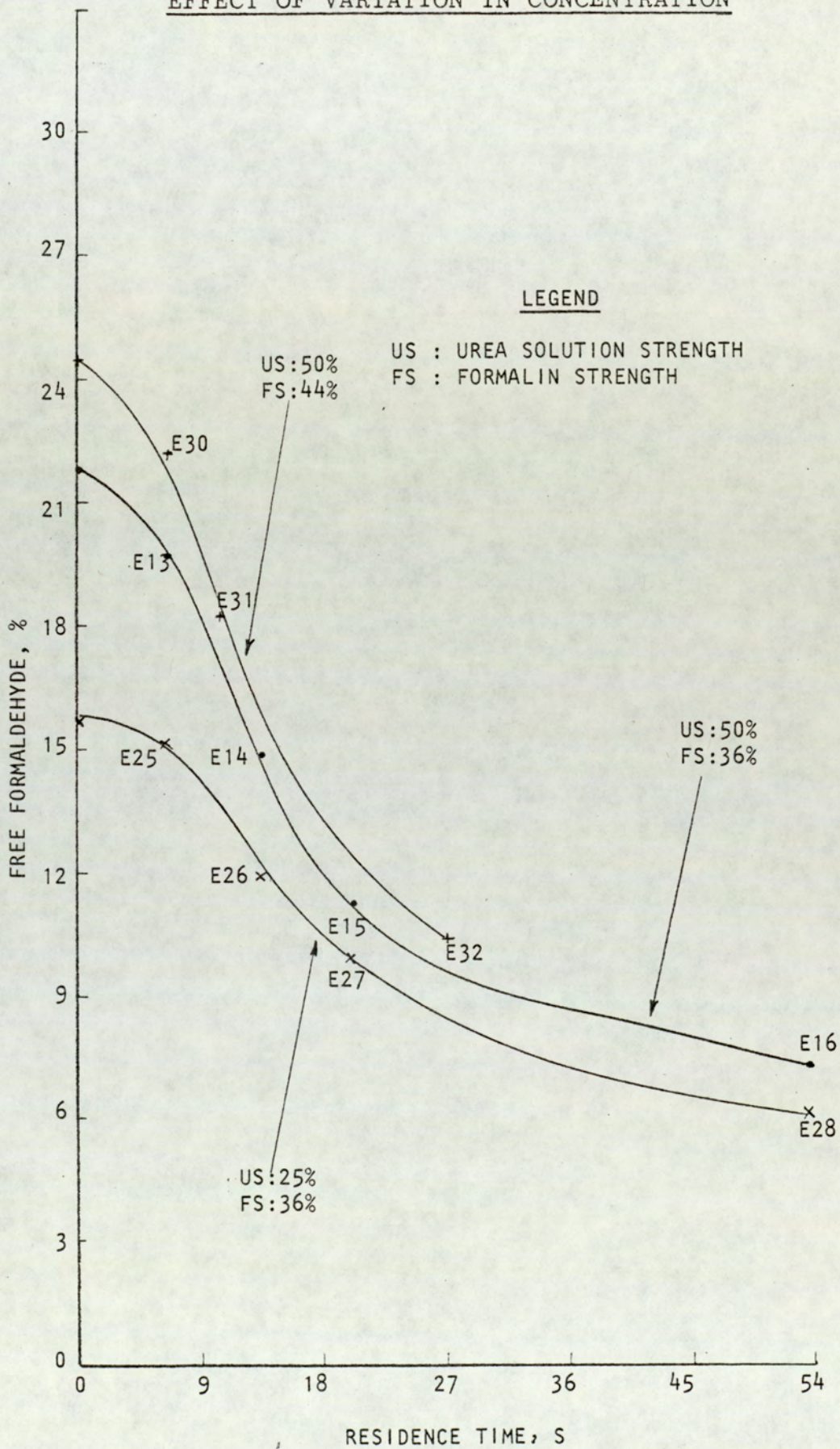
TABLE 6.4.

EFFECT OF VARIATION IN CONCENTRATION

The free formaldehyde concentrations of the experiments detailed in Table 6.4. are shown graphically in Fig.6.4. Comparison of Fig.6.4. with Fig.6.3. confirms the points discussed in Section 6.1.3. with

FIG. 6.4.

EFFECT OF VARIATION IN CONCENTRATION



respect to free formaldehyde reactions. Some further points, however, may be deduced from comparisons of experiments listed in Table 6.4, as outlined below:

(i) The best conditions for conversion of formaldehyde to methylolureas with the avoidance of significant condensation at a given temperature is achieved by a combination of low concentration and shorter residence times. This seems evident when experiments (E25,E26,E27 and E30,E31) are compared with experiments E21 to E24. The above point can also be deduced by comparing E14 and E15 with E22 and E23. Increase in either concentration of the reactants or residence time results in the conversion of methylols to methylenes. Decrease in temperature also adversely affects the minimum formation of methylenes (See 6.12).

(ii) Comparison of the experiments of Table 6.4 confirms that the reactor wall temperature reflects the speed and extent of reaction. At high concentrations a temperature rise above that of the steam and subsequent cooling suggests that the bulk of the formaldehyde reactions have been completed and the resin is undergoing condensation reactions.

The confirmation of the validity of the above statement can be deduced from E21 to E24, E13 to E16 and also generally elsewhere through the data.

#### 6.1.5. EFFECT OF VARIATION IN RESIDENCE TIME

The effects of variations in residence time on the reactor performance have been discussed in conjunction with the effect of variations in other parameters through 6.1.2. to 6.1.4.

#### 6.1.6. SOME CONCLUSIONS OF EXAMINATION OF EXPERIMENTAL RESULTS

Some of the more important conclusions of the examination of the experimental results, presented in the previous sections, can be summarised as follows:-

- (i) The experiments are reproducible with a good degree of consistency.
- (ii) Experimental evidence suggests a reaction initiation lag, which precedes the reactions which consume the bulk of free formaldehyde.
- (iii) The reaction initiation lag takes a shorter time at higher U:F molar ratios.
- (iv) Low residence times and high temperatures seem to reduce the significance of the reaction initiation lag between the two molar ratios investigated.
- (v) Wall temperatures reflect the speed of the reaction and at high concentrations the extent of the reaction.
- (vi) The reactor wall temperature at some point along the reactor tube will always exceed

the steam temperature, if adequate residence time is allowed. Subsequently the temperature will drop and attain a constant value equal to the steam temperature. The extent of the wall temperature rise above that of the steam depends on residence time and concentration of reactants.

- (vii) A higher degree of reaction is achieved as the steam temperature is elevated.
- (viii) The reaction mechanism follows the same pattern at both molar ratios investigated.
- (ix) The reaction is accomplished faster at lower molar ratios (F:U) and higher concentrations.
- (x) High molar ratios (F:U), low concentrations, short residence times and high temperatures favour the addition reactions. Increase in residence time increases the extent of condensation.
- (xi) At lower molar ratios (F:U) (higher concentrations), the addition and condensation reactions seem to take place simultaneously. Increase in temperature at these ratios causes addition reactions to become faster as compared to the condensation reactions. However, both methylols and methylene compounds are formed extensively.
- (xii) For a given temperature, it is possible to arrive at the same resin composition, with respect to free formaldehyde, irrespective

of the starting molar ratio, with the right choice of residence time.

(xiii) At a given temperature the best conditions for conversion of free formaldehyde to methylols with no significant condensation are low residence times, low concentrations and high molar ratios (F:U).

(xiv) Free formaldehyde takes little part in the condensation reactions.

## 6.2. COMPARISON OF EXPERIMENTAL RESULTS WITH PLUG-FLOW MODEL PREDICTIONS

In this section the experimental results are compared to the results of the plug-flow model simulations.

The plug-flow models were simulated for the conditions of tables 5.2. to 5.9, of Chapter 5. With reference to Chapter 4 and Appendix 7, the models were programmed for output of free formaldehyde concentration and reactor wall temperatures with respect to tube length. The model outputs were printed at 10cm intervals along the reactor, This was to economise on the operation time as shorter output intervals extended the simulation times significantly.

Minor modification to the program (Appendix 7) would permit the print-out of other variables measured experimentally (e.g. methylenes and methylols). However, significantly longer simulation times are required for this evaluation. Unfortunately adequate time and

budget were not available for this exercise.

The comparisons are tabulated in Tables 6.5. to 6.12.

The abbreviations listed below are used throughout the Tables:

RL., : Reactor length  
FFC., : Free formaldehyde concentrations  
T., : Temperature  
 $\Delta F.$ , : Absolute difference between experimental  
and predicted results for free formaldehyde  
 $\Delta T.$ , : Absolute difference between experimental  
and predicted results for temperature  
EXP., : Experimental data point  
PRE., : Predicted data point  
MR., : Molar ratio (U:F)  
ST., : Steam/jacket temperature  
US., : Urea solution strength  
FS., : Formalin solution strength

The experiments are numbered in the tables for ease of reference to Tables 5.2. to 5.9.

Generally, the plug-flow models are seen to provide excellent prediction of free formaldehyde concentration and reactor wall temperatures. The patterns and accuracy of prediction of the plug-flow models and complex models are discussed together later in this Chapter (6.4.)

CONDITIONS

MR., U:F : 1:2.2  
ST., °C : 160  
US., % W/W : 50  
FS., % W/W : 36

EXPERIMENT NUMBER	RL., cm	FFC., %		$\Delta F$ %	T., °C		$\Delta T$ °C
		EXP.	PRE.		EXP.	PRE.	
E1	304.8	19.76	19.70	0.06	124	116.39	7.61
E2	609.6	13.82	14.10	0.28	158	159.80	1.80
E3	914.4	8.49	9.24	0.75	168	175.31	7.31
E4	1158.24	5.72	6.02	0.30	166	176.0	10.0

MAXIMUM T., 182.9°C AT 990 cm

TABLE 6.5.

PLUG FLOW PREDICTIONS

CONDITIONS

MR., U:F : 1:2.2  
ST., °C : 120  
US., % W/W : 50  
FS., % W/W : 36

EXPERIMENT NUMBER	RL., cm	FFC., %		$\Delta F$ %	T., °C		$\Delta T$ °C
		EXP,	PRE.		EXP.	PRE.	
E9	304.8	21.72	21.71	0.01	68	65.70	2.30
E10	609.6	19.98	20.34	0.36	102	90.86	11.14
E11	914.4	18.65	19.20	0.55	108	105.97	2.03
E12	1158.24	11.87	11.20	0.67	138	141.70	3.70

TABLE 6.6.

PLUG FLOW PREDICTIONS

CONDITIONS

MR., U:F : 1:2.2  
ST., °C : 140  
US., % W/W : 50  
FS., % W/W : 36

EXPERIMENT NUMBER	RL., cm	FFC., %		$\Delta F$ %	T., °C		$\Delta T$ °C
		EXP.	PRE.		EXP.	PRE.	
E13	304.8	19.73	20.45	0.72	103	97.82	5.18
E14	609.6	14.89	15.69	0.80	135	138.03	3.03
E15	914.4	11.29	12.22	0.93	154	150.67	3.33
E16	1158.24	7.36	6.16	1.20	152	163.60	11.60

MAXIMUM T., 166.80 °C AT 1050 cm

TABLE 6.7.

PLUG FLOW PREDICTIONS

CONDITIONS

MR., U:F : 1:1.33

ST., °C : 120

US., % W/W : 50

FS., % W/W : 36

EXPERIMENT NUMBER	RL., cm	FFC., %		$\Delta F$ %	T., °C		$\Delta T$ °C
		EXP.	PRE.		EXP.	PRE.	
E17	304.8	16.89	17.22	0.33	68	66.68	1.32
E18	609.6	16.13	16.87	0.74	88	88.15	0.15
E19	914.4	14.93	15.99	1.06	108	102.84	5.16
E20	1158.24	12.60	11.27	1.33	132	137.90	5.90

TABLE 6.8.

PLUG FLOW PREDICTIONS

CONDITIONS

MR., U:F : 1:1.33

ST., °C : 140

US., % W/W : 50

FS., % W/W : 36

EXPERIMENT NUMBER	RL., cm	FFC., %		$\Delta F$ %	T., °C		$\Delta T$ °C
		EXP.	PRE.		EXP.	PRE.	
E21	304.8	16.61	16.58	0.03	106	101.48	4.52
E22	609.6	12.81	12.59	0.22	135	138.10	3.10
E23	914.4	6.26	6.96	0.70	161	157.53	3.47
E24	1158.24	1.40	1.45	0.05	159	161.73	2.73

MAXIMUM T., 171.2°C AT 1010 cm

TABLE 6.9.

PLUG FLOW PREDICTIONS

CONDITIONS

MR., U:F : 1:2,2

ST., °C : 140

US., % W/W : 25

FS., % W/W : 36

EXPERIMENT NUMBER	RL., cm	FFC., %		$\Delta F$ %	T., °C		$\Delta F$ °C
		EXP.	PRE.		EXP.	PRE.	
E25	304.8	15.17	14.82	0.35	101	99.24	1.76
E26	609.6	11.87	11.97	0.10	132	132.82	0.82
E27	914.4	9.98	10.26	0.28	134	142.61	8.61
E28	1158.24	6.16	5.70	0.46	149	155.51	6.51

TABLE 6.10PLUG FLOW PREDICTIONS

CONDITIONS

MR., U:F : 1:2.2

ST., °C : 140

US., % W/W : 50

FS., % W/W : 44

EXPERIMENT Number	RL., cm	FFC., %		$\Delta F$ %	T., °C		$\Delta T$ °C
		EXP.	PRE.		EXP.	PRE.	
E29	304.8	23.29	24.28	0.99	72	72.83	0.83
E30	609.6	22.20	22.59	0.39	102	103.50	1.50
E31	914.4	18.20	18.62	0.42	136	132.83	3.17
E32	1158.24	10.41	9.03	1.38	162	173.76	11.76

TABLE 6.11.

PLUG FLOW PREDICTIONS

### 6.3. COMPARISON OF EXPERIMENTAL RESULTS WITH COMPLEX MODEL PREDICTIONS

The complex models were simulated for the conditions of tables 5.2. to 5.9. With reference to Chapter 4 and Appendix 7 the models were solved in their dimensionless form. The outputs were the dimensionless free formaldehyde and reactor temperatures at each grid point (Chapter 4). The output table consisted of 11 points (including zero) along the axis of the reactor tube and 6 points (including zero) across the radius of the tube. This made the longitudinal print interval 115.824 cm. Since there are no integer multiples of the longitudinal print interval which would permit a direct comparison with the first three sample valve positions in the tubes (304.8cm, 609.6cm, 914.4cm), interpolation of the results becomes necessary for comparison purposes.

Minor modifications to the program would permit any desired print interval such that direct comparison becomes possible. However, a large storage bank is required for this purpose causing a significant rise in the computational costs,

Furthermore, the program is capable of giving outputs of other variables measured experimentally. However, the limitation of computing budget prevented the modification of the program for this purpose.

Based upon the above discussion the experimental and complex model predicted results are shown graphically

through Figs.6.5. to 6.11., with the interpolated results being tabulated in Tables 6.12. to 6.18.

### 6.3.1. CALCULATION OF AVERAGE REACTOR CONCENTRATIONS

Since the concentration of free formaldehyde is given at six radial points for each longitudinal print interval, it is necessary to calculate an average concentration so that direct comparison can be made with the experimental results. The same criteria however does not apply to temperature outputs, as the only logical comparison should be made at the reactor wall.

The average concentration of free formaldehyde at any given distance from the reactor inlet can be expressed by:

$$F_{\text{av}} = \frac{\int_{r=0}^{r=R} F r dr}{\int_{r=0}^{r=R} r dr} \quad 6.1.$$

The denominator of 6.1. is given by:

$$\int_{r=0}^{r=R} r dr = \frac{R^2}{2} \quad 6.2.$$

The numerator of 6.1. can be numerically integrated by Simpson's rule (130). The Cote's coefficients for a six point Simpson's formula (131) are:

$$\int_0^{5h} y dx = \frac{5h}{288} \{19y_0 + 75y_1 + 50y_2 + 50y_3 + 75y_4 + 19y_5\} \quad 6.3.$$

where  $h = \frac{R}{5}$

Applying 6.3. to the numerator of 6.1.

$y$  is replaced by  $Fr$

$y_0$  is replaced by  $F_0 r_0$

$y_1$  is replaced by  $F_1 r_1$  etc.

and since the radius is divided into five equal intervals,

then

$r_0 = 0, r_1 = \frac{R}{5}, r_2 = \frac{2R}{5}$  etc.

gives

$$\int_{r=0}^{r=R} F r dr = \frac{R^2}{288} \{15F_1 + 20F_2 + 30F_3 + 60F_4 + 19F_5\}$$

and 6.1. then becomes

$$F = \frac{1}{144} \{15F_1 + 20F_2 + 30F_3 + 60F_4 + 19F_5\} \quad 6.4.$$

Equation 6.4. was used to calculate the average concentration of formaldehyde at the longitudinal intervals.

FIG. 6.5.  
COMPARISON OF EXPERIMENTAL AND  
PREDICTED RESULTS

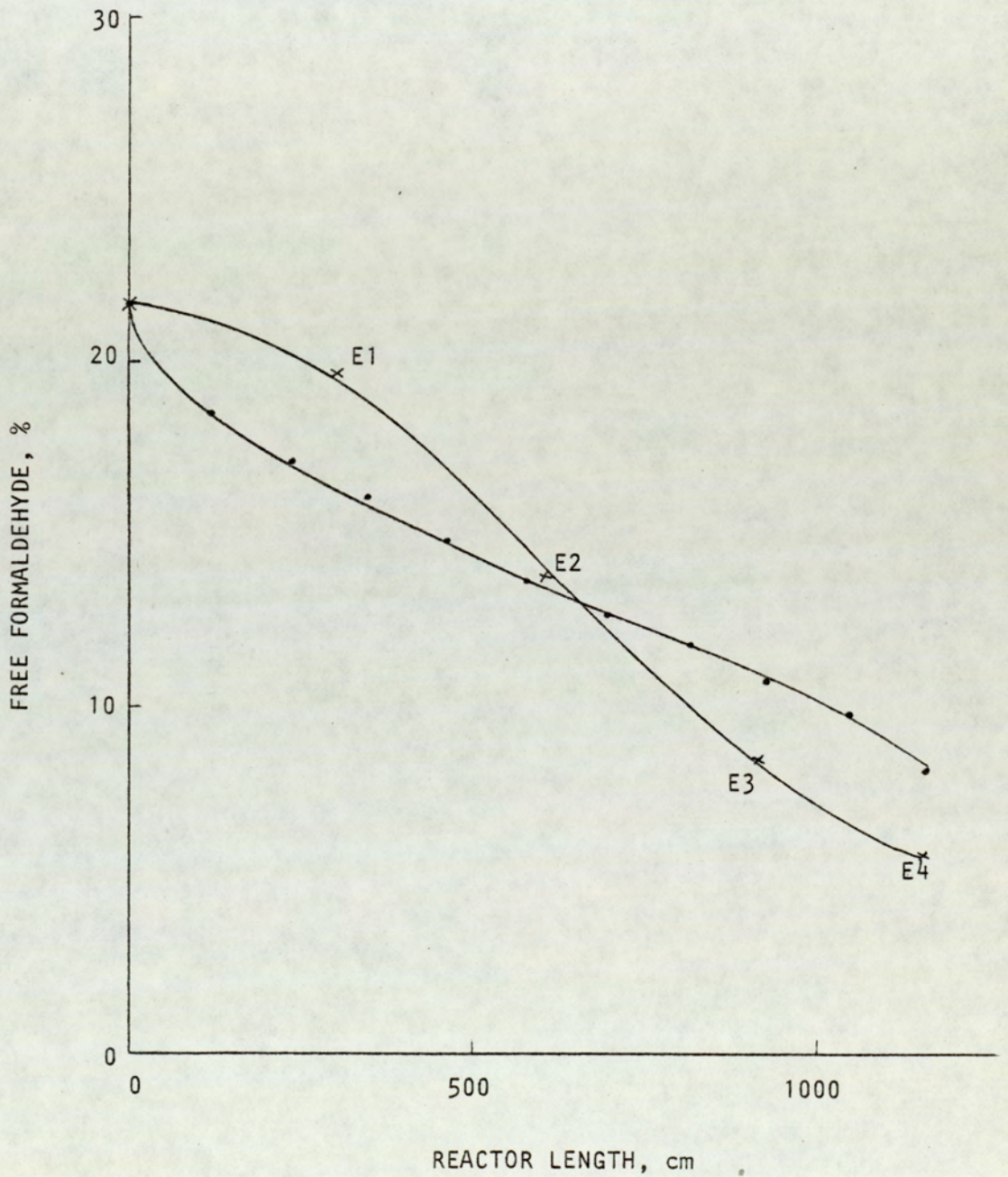


FIG. 6.6.

COMPARISON OF EXPERIMENTAL AND

PREDICTED RESULTS

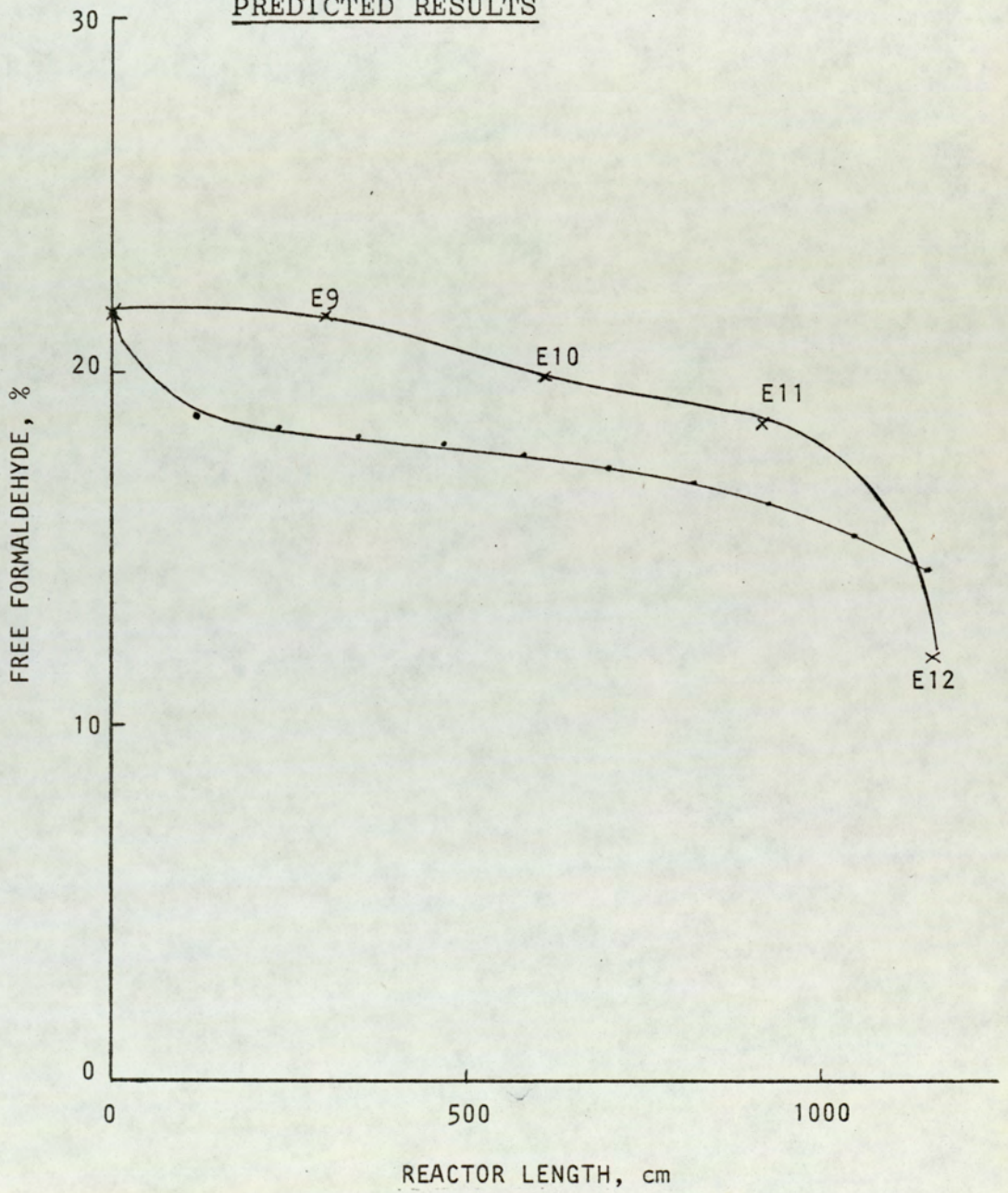


FIG. 6.7.  
COMPARISON OF EXPERIMENTAL AND  
PREDICTED RESULTS

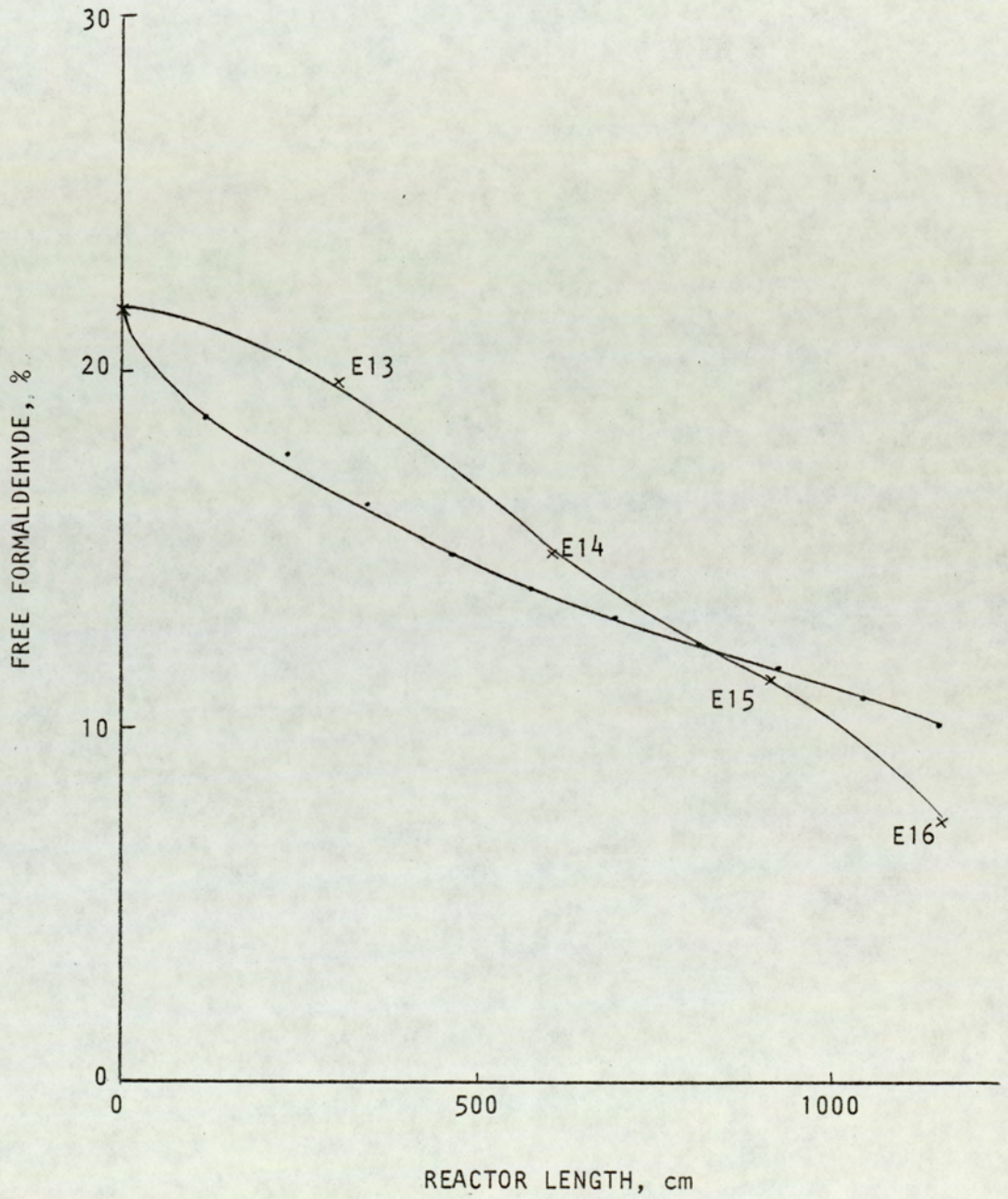


FIG. 6.8.  
COMPARISON OF EXPERIMENTAL AND  
PREDICTED RESULTS

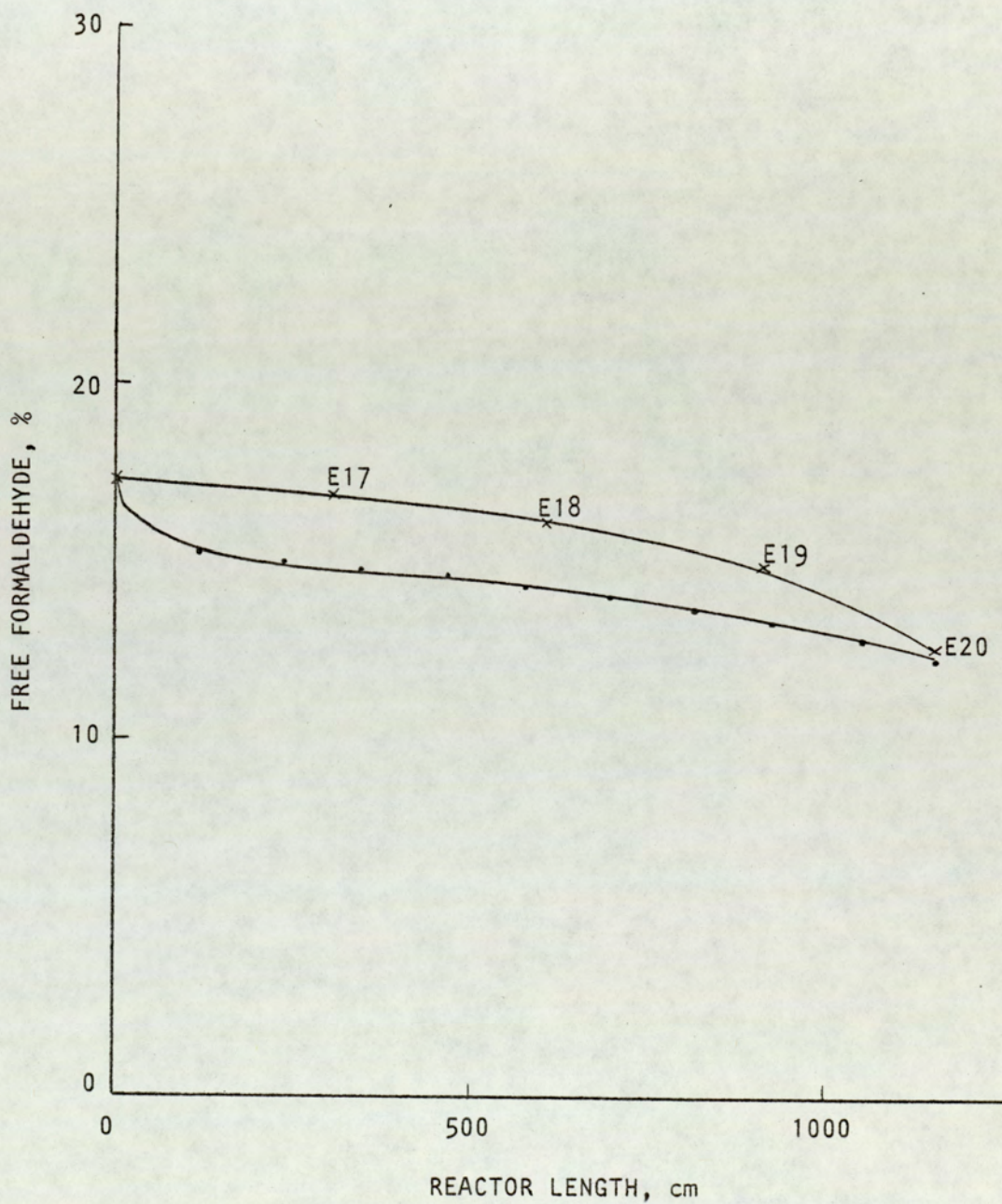


FIG. 6.9.  
COMPARISON OF EXPERIMENTAL AND  
PREDICTED RESULTS

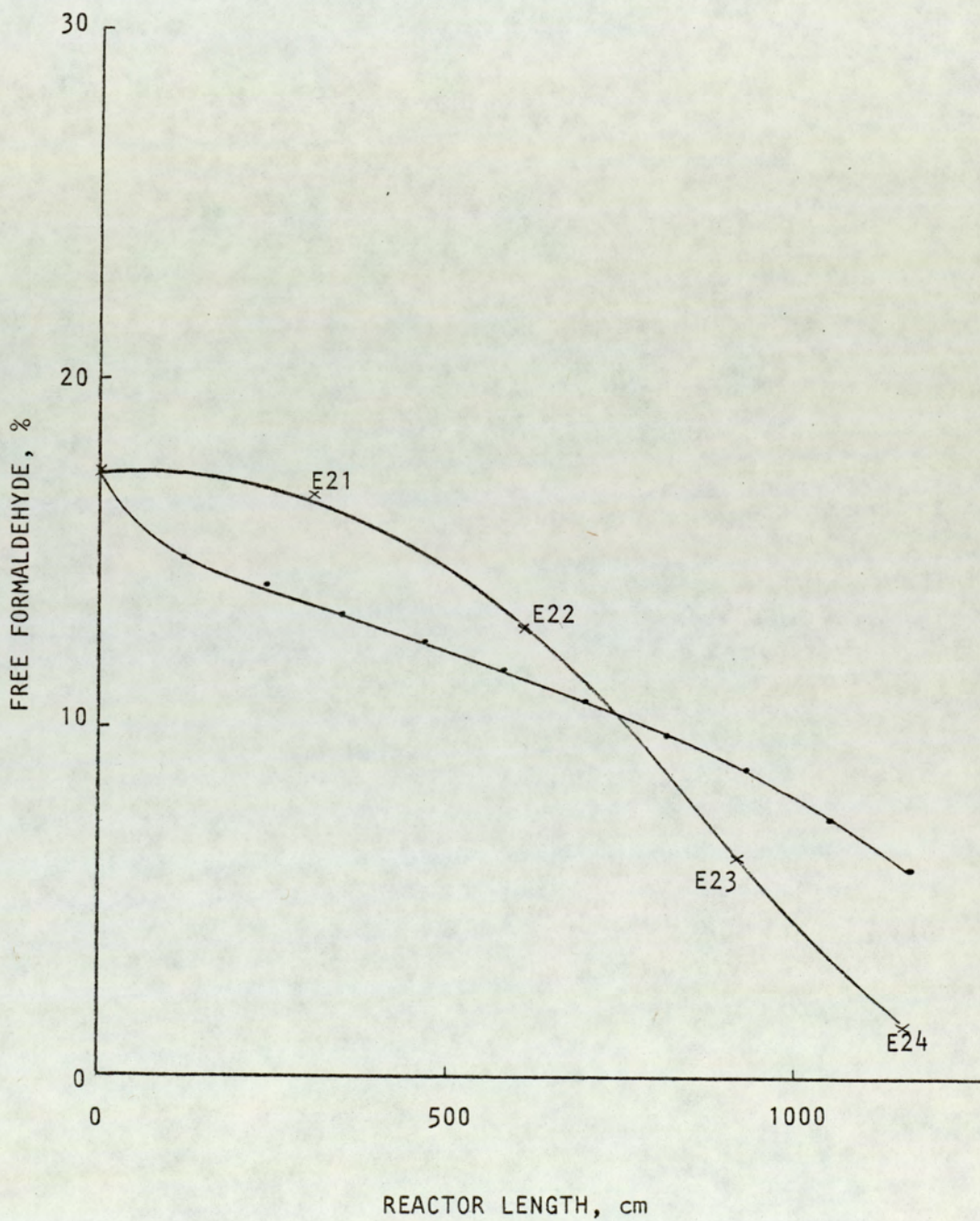


FIG. 6.10.

COMPARISON OF EXPERIMENTAL AND  
PREDICTED RESULTS

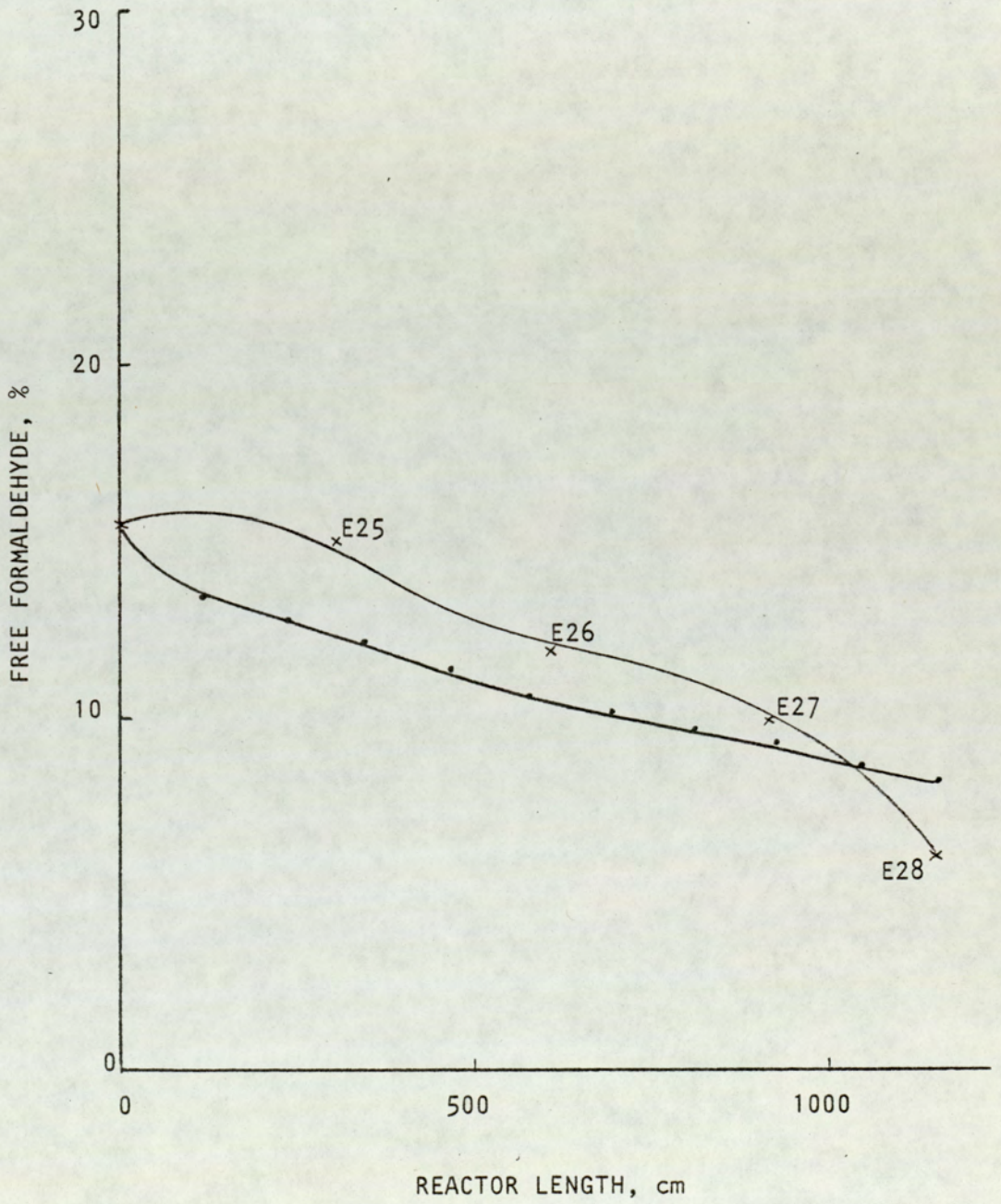
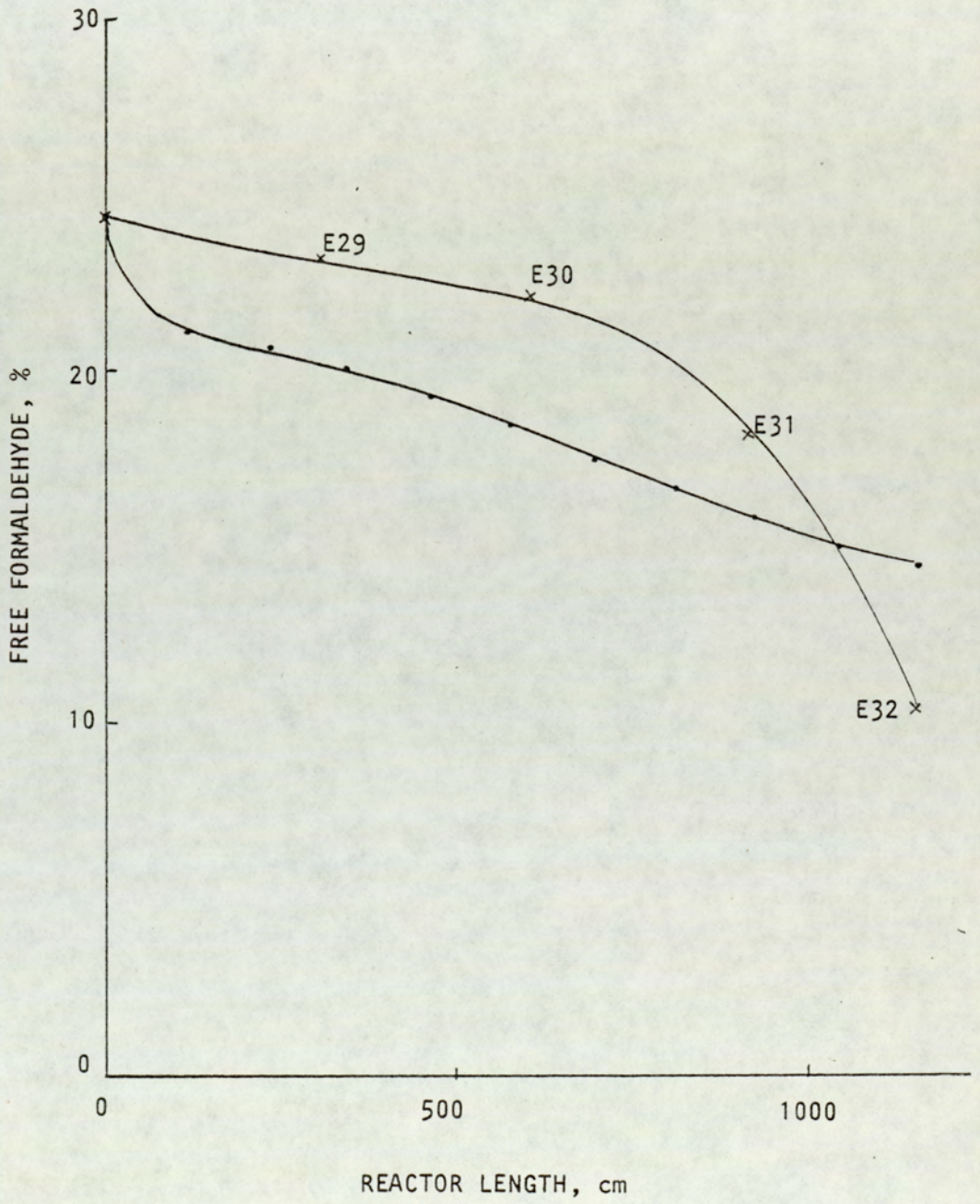


FIG. 6.11.  
COMPARISON OF EXPERIMENTAL AND  
PREDICTED RESULTS



CONDITIONS

MR., U:F : 1:2.2  
ST., °C : 160  
US., % W/W : 50  
FS., % W/W : 36

EXPERIMENT NUMBER	RL., cm	FFC., %		$\Delta F$ %	T., °C		$\Delta T$ °C
		EXP.	PRE.		EXP.	PRE.	
E1	304.8	19.76	16.40	3.36	124	160	36
E2	609.6	13.82	13.60	0.22	158	160	2
E3	914.4	8.49	11.00	2.51	168	160.74	7.26
E4	1158.24	5.72	8.35	2.63	166	171.29	5.29

MAXIMUM T., 182.9°C AT 990 cm

TABLE 6.12.

COMPLEX MODEL PREDICTIONS

CONDITIONS

MR., U:F : 1:2,2  
ST., °C : 120  
US., % W/W : 50  
FS., % W/W : 36

EXPERIMENT NUMBER	RL., cm	FFC., %		$\Delta F$ %	T., °C		$\Delta T$ °C
		EXP.	PRE.		EXP.	PRE.	
E9	304.8	21.72	18,2	3.52	68	120	52
E10	609.6	19.98	17.7	2.28	102	120	18
E11	914.4	18.65	16.25	2,3	108	120	12
E12	1158.24	11.87	14,42	2.55	138	122.83	15.17

TABLE 6.13.

COMPLEX MODEL PREDICTIONS

CONDITIONS

MR., U:F : 1:2,2  
ST., °C : 140  
US., % W/W : 50  
FS., % W/W : 36

EXPERIMENT NUMBER	RL., cm	FFC., .		$\Delta F$ %	T., °C		$\Delta T$ °C
		EXP.	PRE.		EXP.	PRE.	
E13	304.8	19.73	16.60	3.13	103	140	37
E14	609.6	14.89	15.70	0.81	135	140	5
E15	914.4	11.29	11.60	0.31	154	142.9	11.1
E16	1158.24	7.36	10.07	2.71	152	146.6	5.4

MAXIMUM T., 166.80°C AT 1050 cm

TABLE 6.14.

COMPLEX MODEL PREDICTIONS

CONDITIONS

MR., U:F : 1:1.33

ST., °C : 120

US., % W/W : 50

FS., % W/W : 36

EXPERIMENT NUMBER	RL., cm	FFC., %		$\Delta F$ %	T., °C		$\Delta T$ °C
		EXP.	PRE.		EXP.	PRE.	
E17	304.8	16.89	14.8	2.09	68	120	52
E18	609.6	16.13	14.3	1.83	88	120	32
E19	914.4	14.93	13.5	1.43	108	120	12
E20	1158.24	12.60	12.30	0.3	132	120	12

TABLE 6.15

COMPLEX MODEL PREDICTIONS

CONDITIONS

MR., U:F : 1:1.33

ST., °C : 140

US., % W/W : 50

FS., % W/W : 36

EXPERIMENT NUMBER	RL., cm	FFC., %		$\Delta F$ %	T., °C		$\Delta T$ °C
		EXP.	PRE.		EXP.	PRE.	
E21	304.8	16.61	13.50	3.11	106	140	34
E22	609.6	12.81	11.40	1.41	135	140	5
E23	914.4	6.26	8.80	2.54	161	140.6	20.4
E24	1158.24	1.40	6.14	4.74	159	153.8	5.2

MAXIMUM T., 171.2°C AT 1010 cm

TABLE 6.16.

COMPLEX MODEL PREDICTIONS

CONDITIONS

MR., U:F : 1:2.2

ST., °C : 140

US., % W/W : 25

FS., % W/W : 36

EXPERIMENT NUMBER	RL., cm	FFC., %		$\Delta F$ %	T., °C		$\Delta T$ %
		EXP.	PRE.		EXP.	PRE.	
E25	304.8	15.17	12.4	2.77	101	140	39
E26	609.6	11.87	10.6	1.27	132	140	8
E27	914.4	9.98	9.30	0.6	134	140	6
E28	1158.24	6.16	8.32	2.16	149	140.7	8.3

TABLE 6.17.COMPLEX MODEL PREDICTIONS

CONDITIONS

MR., U:F : 1:2,2

ST., °C : 140

US., % W/W : 50

FS., % W/W : 44

EXPERIMENT NUMBER	RL., cm	FFC., .		$\Delta F$ %	T., °C		$\Delta T$ °C
		EXP.	PRE.		EXP.	PRE.	
E29	304.8	23.29	20.4	2.89	72	140	68
E30	609.6	22.20	18.3	3.90	102	140	38
E31	914.4	18.20	16.0	2.20	136	140	4
E32	1158.24	10.41	14.52	4.11	162	140	22

TABLE 6.18.

COMPLEX MODEL PREDICTIONS

## 6.4. DISCUSSION OF MODEL PREDICTIONS

### 6.4.1. PLUG FLOW MODEL PREDICTIONS

Examination of Tables 6.5. to 6.11. shows that the prediction of the reactor performance in terms of free formaldehyde concentrations and reactor temperatures by the plug flow models is of good accuracy.

The maximum absolute difference between predicted and experimental results for concentration of free formaldehyde is 1.38% (E32), but the predictions in general show much better accuracy. The minimum absolute difference for the above case is 0.01% (E9).

Defining the best fit for a series of four data points, collected under one particular experimental condition, as the minimum value of the standard deviation

$$\sqrt{\frac{\sum_{J=1}^{J=4} (\Delta F_J)^2}{4}}$$

and the worst fit, the maximum value of the standard deviation, the best and worst fits for concentrations are given by experiment series E25 to E28 and E17 to E20 respectively. These two are shown graphically in Figs.6.12. and 6.13.

Also defining the standard deviation for the 28 experiments (excluding E5 to E8) as

$$\sqrt{\frac{\sum_{J=1}^{J=28} (\Delta F_J)^2}{28}}$$

FIG. 6.12.

BEST PLUG FLOW CONCENTRATION PREDICTION

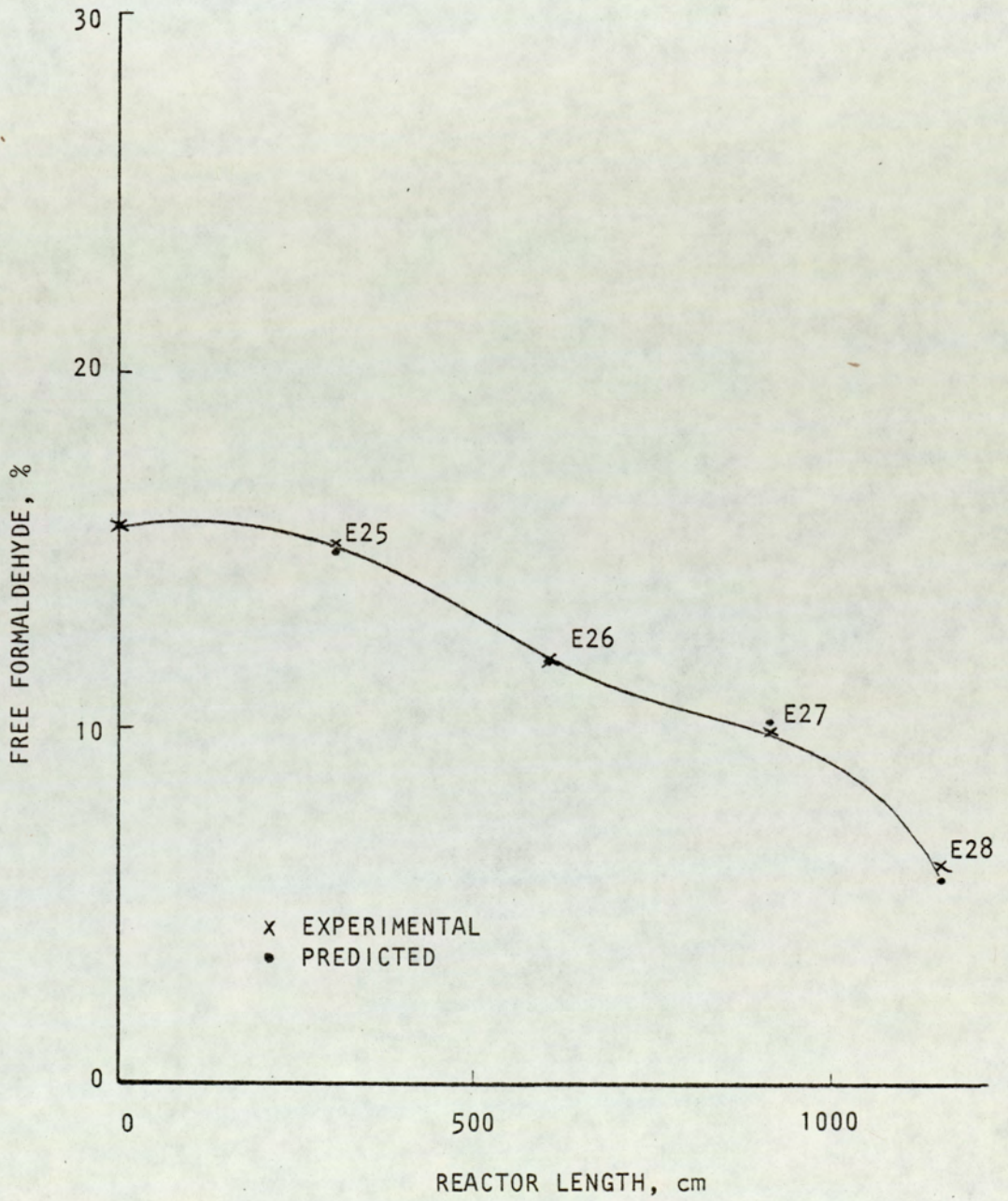
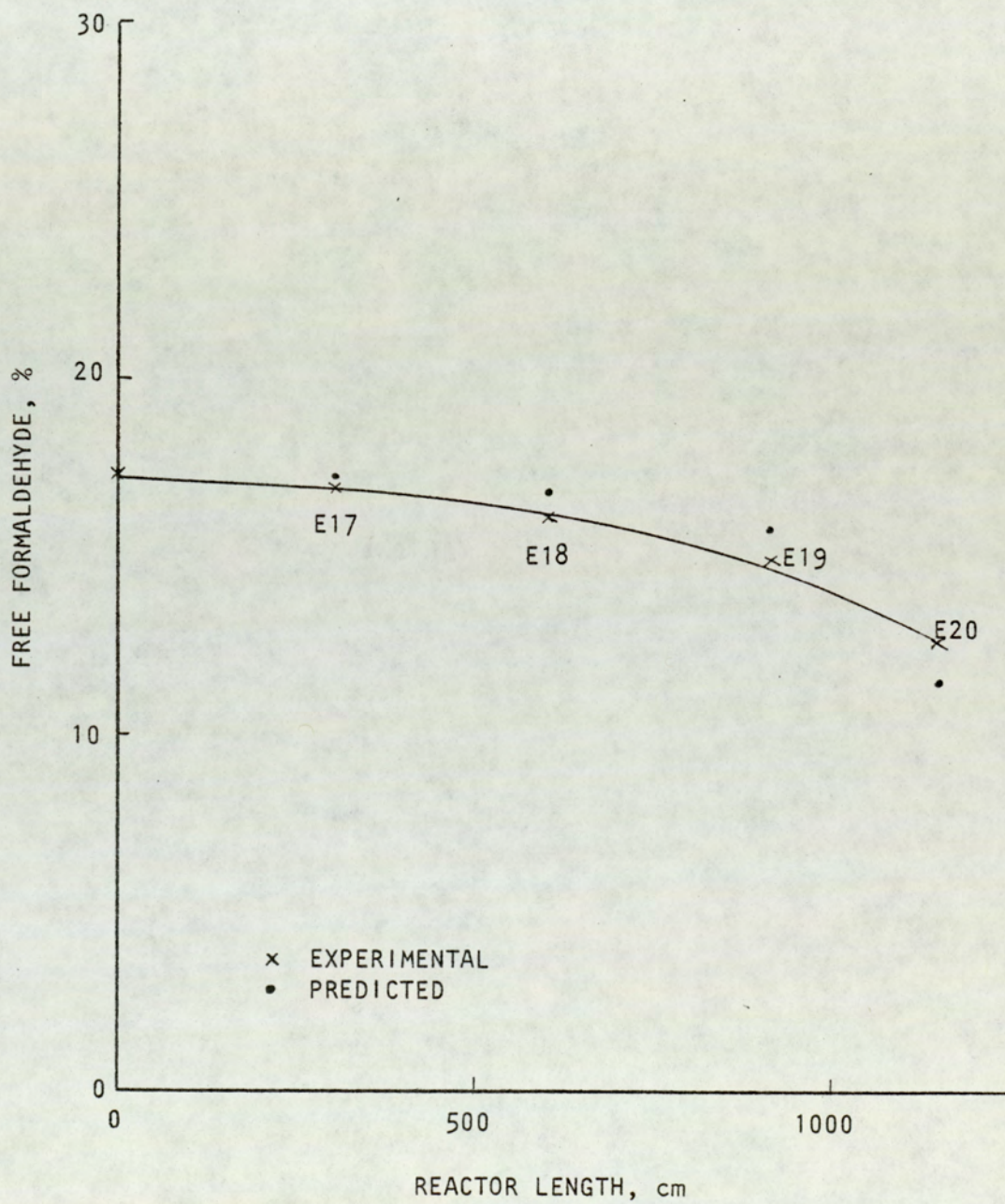


FIG. 6.13.

WORST PLUG FLOW CONCENTRATION PREDICTION



a value of 0.65 is obtained. This gives the average accuracy of the plug flow model predictions of concentrations as  $\pm 0.65\%$  when results are expressed as % free formaldehyde.

For the case of temperature predictions the maximum absolute difference is found to be  $11.76^{\circ}\text{C}$  (E32), whereas the minimum absolute difference is  $0.15^{\circ}\text{C}$  (E18). The worst fit is given by experiment series E13 to E16, while the best fit is given by the experiment series E21 to E24. These are shown graphically in Figs. 6.14. and 6.15.

The standard deviation of temperature for all the experiments is calculated to be  $5.75^{\circ}\text{C}$ . This gives the accuracy of the plug flow temperature predictions as  $\pm 5.75^{\circ}\text{C}$ .

The pattern of the plug flow model predictions generally confirm the conclusions of the examination of experimental results (6.16.). In particular the reaction initiation lag seems to be confirmed as the predicted results show that the resin temperature in the reactor has to rise to a certain value, depending on the conditions, before a significant amount of reaction starts to take place.

Tables 6.5. to 6.11. also show that at the end of the first tube the predicted reactor temperature is lower than the experimental temperature in all cases except one (E29), suggesting that the value of the thermal conductivity used in the plug flow model is not quite representative and has to be determined more

FIG. 6.14.

BEST PLUG FLOW TEMPERATURE PREDICTION

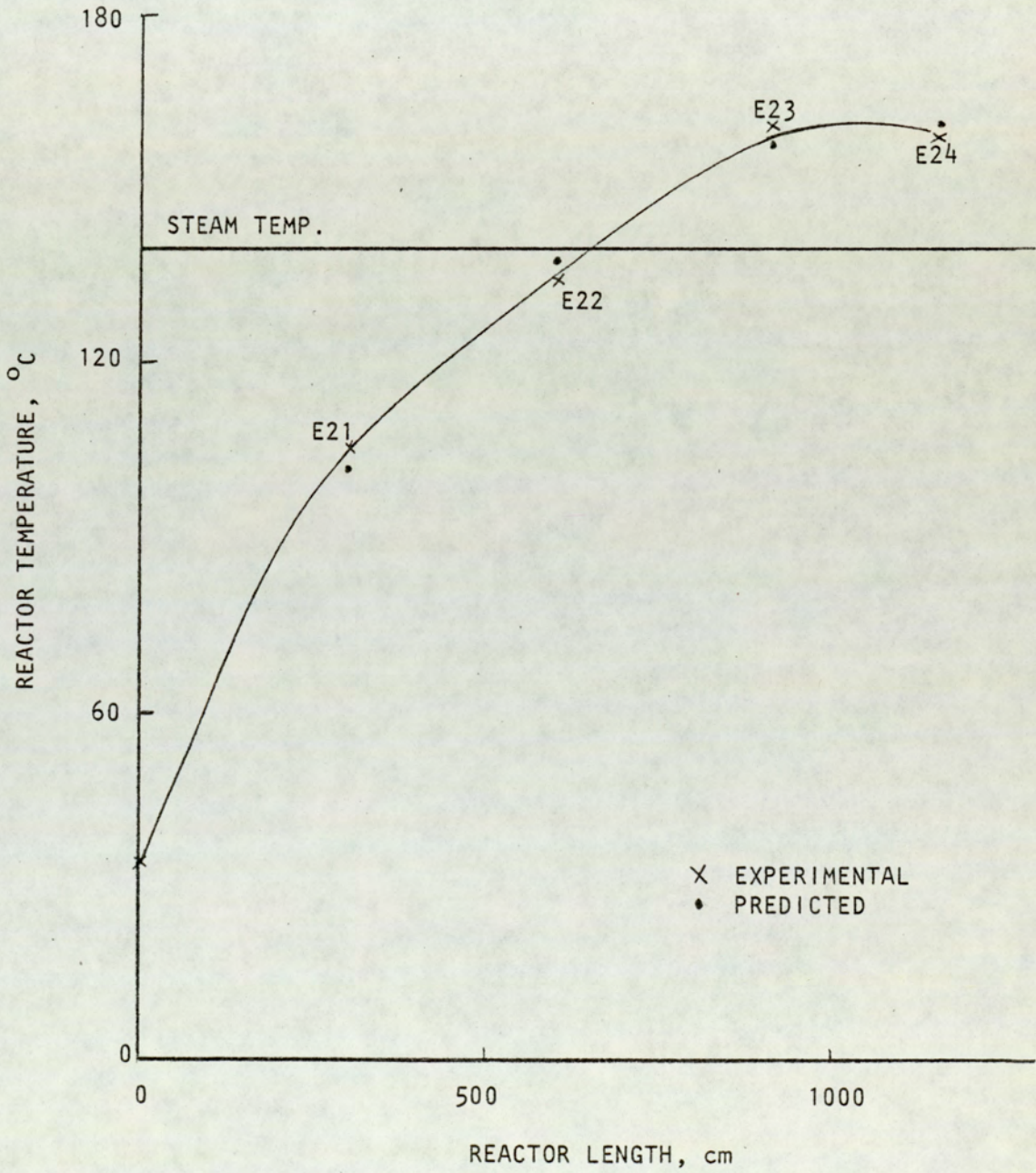
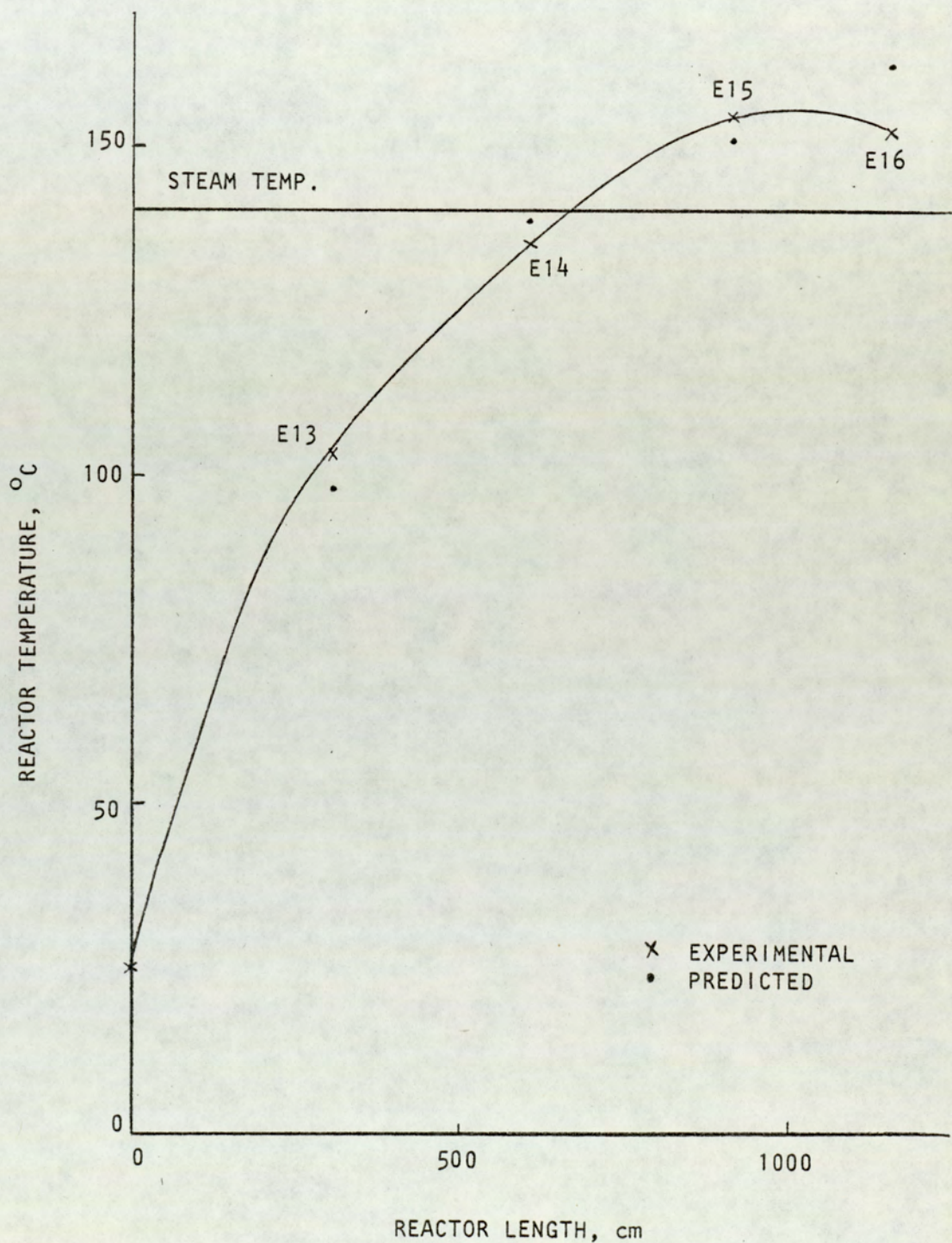


FIG. 6.15.

WORST PLUG FLOW TEMPERATURE PREDICTION



accurately. The low values of predicted temperatures cause low values of predicted concentrations in the corresponding experiments as compared to the experimental results.

Furthermore, with reference to Chapters 3 and 4, the models do not include any condensation reactions. The experimental data however show an appreciable amount of condensation. Yet the predictions remain good, implying that formaldehyde takes little part in the condensation reactions. This was also concluded from the pattern of the experimental data in 6.1.6.

Examination of Tables 6.5. to 6.11. also shows that the predicted concentration results are lower than the experimental results in all cases except one (E4), at the end of the 4th tube. This is probably due to the enlargement of the diameter of the fourth tube (Chapter 4). For this case, although the models carry on the reaction in the same manner as for the other tubes, experimentally it seems that the heat transfer could be effected by the larger diameter resulting in slower rate of reaction. This is confirmed by examining the temperature predictions where higher temperatures are predicted in all cases for the last tube. A further possibility is that while good mixing in the first three tubes results in good prediction by the plug flow models, the velocity drop (drop in Reynolds number) in the fourth tube as a result of its larger diameter may necessitate the use of laminar flow and parabolic velocity profile for better predictions.

To conclude the above discussion a plausible explanation should be given for the good predictions of the plug flow model, noting that the Reynolds numbers are quite low. A number of reasons could be given for the good mixing in the reactor at the low Reynolds numbers. These are:

(i) The reactor feed pumps were of the metering (piston displacement) type (Chapter 5). This results in intermittent (pulsating) flow of resin which could cause disturbances in a developed velocity profile and increase the amount of mixing. Although the use of such pumps would produce continuous flow in some cases, visual observation showed that the flow was pulsating under all the conditions of investigation where the resin was seen to leave the reactor outlet diaphragm valve in intermittent bursts.

(ii) The high temperature difference between the wall and the tube centre could result in convection which could enhance mixing.

(iii) The shape of the reactor (Chapter 5) could be detrimental to any developed velocity profile. The reactor bends are likely to disturb the profiles and cause good mixing in the reactor.

(iv) The enlargement of the tube diameter at the end of the third tube would probably completely deform any developed profile with the result of more mixing.

Consideration of the above points would explain the reason for the good prediction of plug flow models at such low Reynolds numbers.

#### 6.4.2. COMPLEX MODEL PREDICTIONS

Figs. 6.5. to 6.11. and Tables 6.12. to 6.18. show the results of the complex model predictions. For these models the maximum absolute difference between the predicted and experimental results of concentration is 4.74% (E24) while the minimum difference is 0.22% (E2).

With reference to the definitions of 6.4.1. the best concentration fit is given by the experiment series E17 to E20, while the worst concentration fit is given by experiment series E29 to E32. These can be seen in Figs. 6.8. and 6.11. The standard deviation of the complex model predictions of concentration is calculated at  $\pm 2.55\%$ , when results are expressed as % free formaldehyde.

For the case of temperature predictions the maximum absolute difference is  $68^{\circ}\text{C}$  (E29) while the minimum is  $2^{\circ}\text{C}$  (E2). The worst fit is given by the experiment series E29 to E32, while the best fit is given by the experiment series E1 to E4. These can be seen graphically in Figs. 6.16. to 6.17.

The discussions in 6.4.1. explaining the reasons for good mixing in the reactor and the good accuracy of the plug flow predictions would also explain the failings of the complex model predictions and the poor accuracy of the predicted results for this case. However, examination of the results of the complex model predictions throws further light on the behaviour

FIG. 6.16,

WORST COMPLEX TEMPERATURE PREDICTION

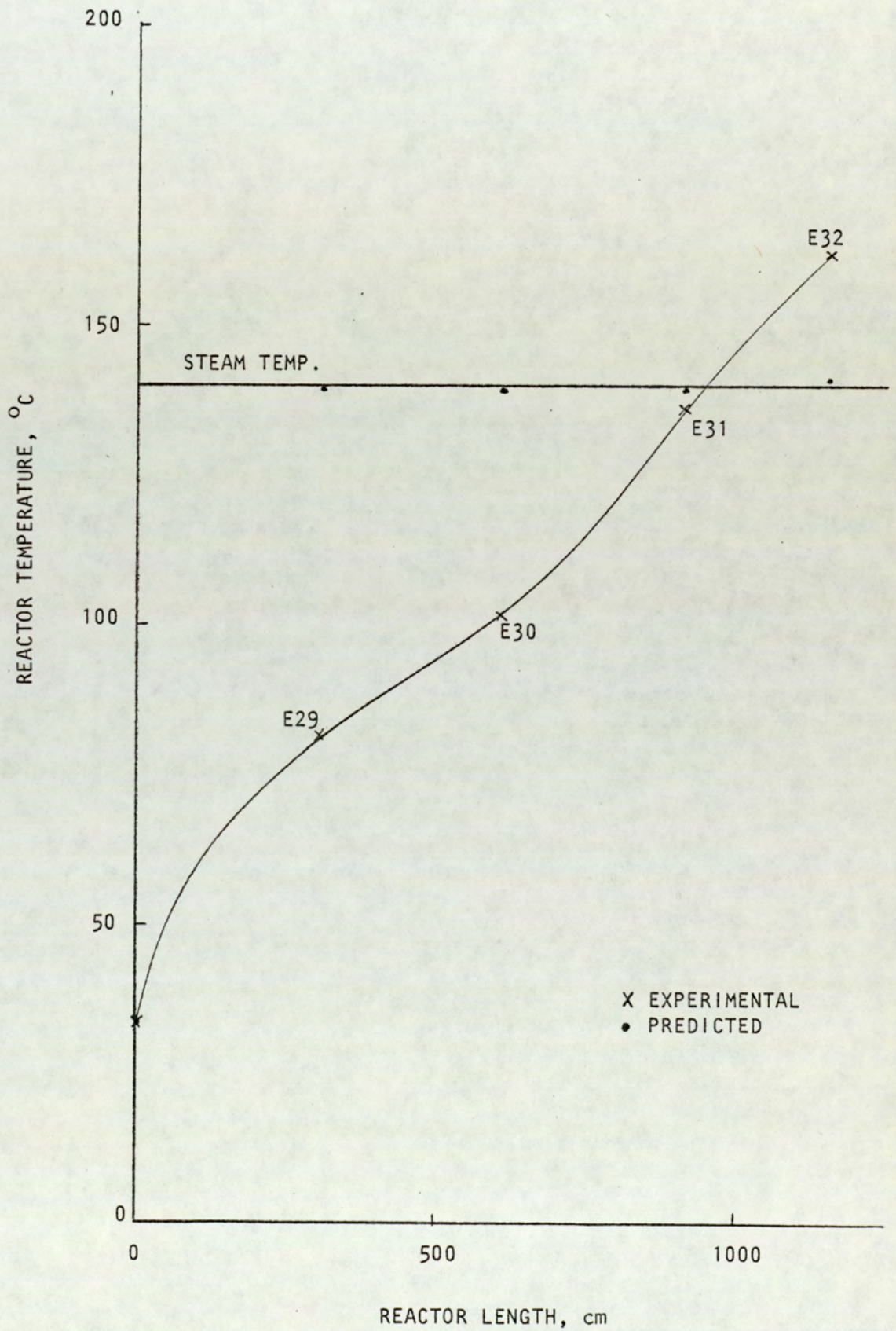
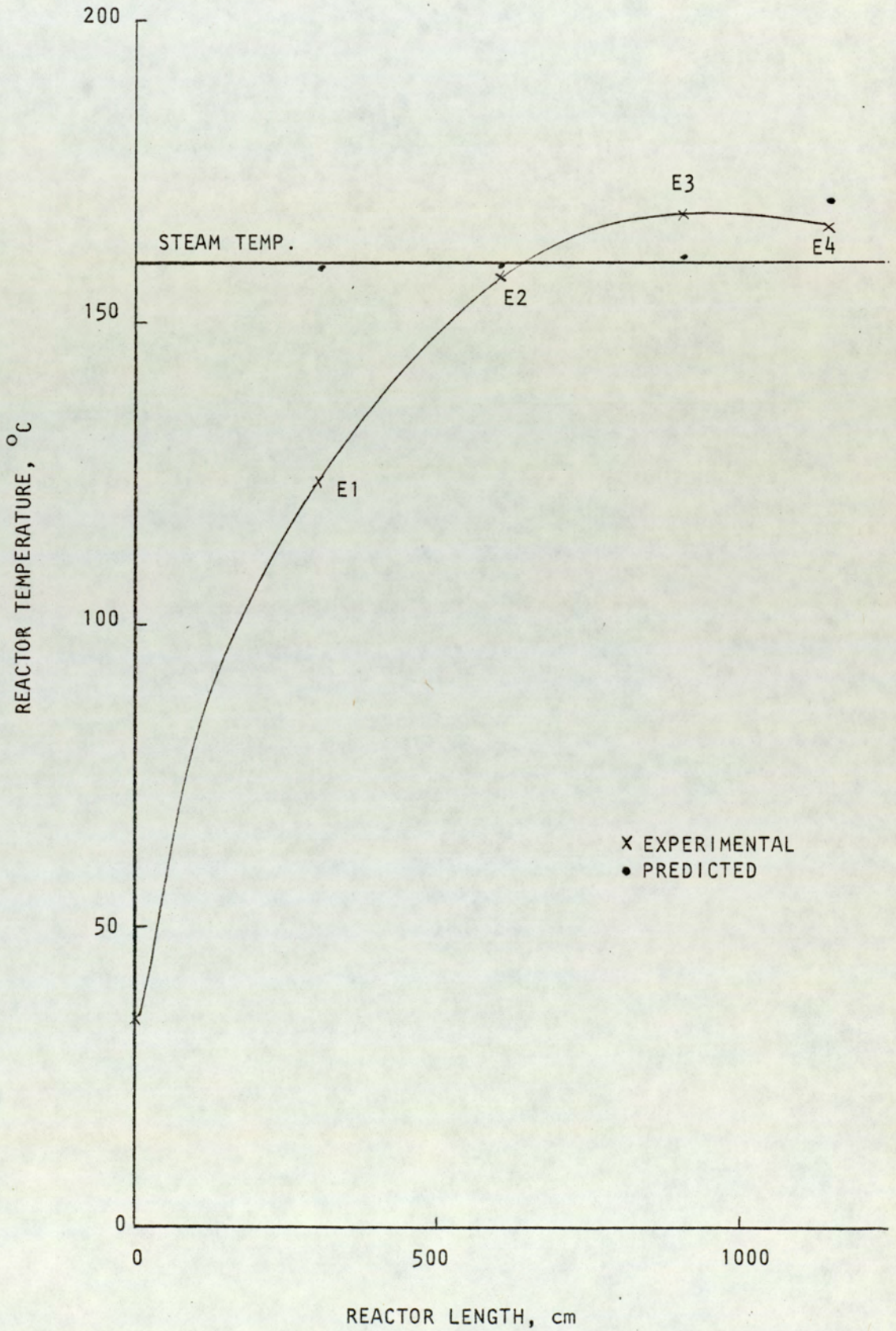


FIG. 6.17.

BEST COMPLEX TEMPERATURE PREDICTION



of the reactor,

The rather large differences of temperature between the predicted and experimental results is a direct consequence of the assumption that the velocity profile is laminar and that the wall temperature reaches the steam temperature almost immediately. This discrepancy arises because the experimental temperatures are measured in the lagged sections of the reactor bends where one can assume that the tube wall is initially at room temperature and is heated up only by transfer from the resin's sensible heat. Therefore the assumption that the wall temperature is equal to the steam temperature although true in the jacketed sections of the tube, cannot be true for the lagged sections. Experimental evidence confirms this, where all the first two temperatures in all the experimental series are lower than the steam/wall temperature as assumed by the models. The above also explains the shape of the curves in Figs. 6.5. to 6.11. As a result of the high assumed initial temperature the concentrations are much lower when compared to the experimental results until the wall temperature reaches the steam temperature. Once the wall temperature has reached the steam temperature the predicted concentrations are consistently higher in value, suggesting that there is better mixing in the reactor than expressed by these models. The accuracy of the temperature predictions improves considerably after the wall temperature reaches the steam temperature and isothermal heat transfer begins.

## 6.5. POSSIBLE IMPROVEMENT OF MODELS

The plug flow models, although giving excellent prediction can be improved in accuracy. Some of the physical data such as thermal conductivity and specific heat were estimated (Appendix 3). These should be evaluated accurately. Also regions of adiabatic operation should be included in these models to cover the lagged lengths of the reactor bends.

The complex models also require the improvements suggested for the plug flow models. In addition further work in the following areas would increase the accuracy of these models for cases where the flow is continuous (not intermittent) and the reactor cross-section uniform.

(i) Better estimation of the equilibrium concentrations at the reactor wall for urea, formaldehyde and methylolureas (Appendix 5).

(ii) Replacement of the thermal boundary condition  $T_w = T_s$  by an equation capable of allowing heat transfer for this section of the tube where the resin temperature is lower than the steam temperature. On the basis of this equation more accurate wall temperatures could be predicted which would also improve the accuracy of the predicted concentrations.

## C H A P T E R 7

### CONCLUSIONS AND RECOMMENDATIONS

The analysis of the experimental data generated in this investigation and comparison with the predictions obtained by numerical solutions of the mathematical models describing the reactor behaviour lead to the following general conclusions:

#### 7.1. CONCLUSIONS

##### 7.1.1. Conclusions relating to the chemical investigation

###### i. Adequacy of available kinetic data

Although the kinetic data relating to the chemical reaction between urea and formaldehyde were adequate to represent the low temperature reaction between them (less than 60°C), this investigation shows that extrapolation of the data is not adequate to represent the high temperature (up to 160°C) kinetics of urea-formaldehyde reactions.

###### ii. Novel high temperature kinetic investigation of UF kinetics.

The novel technique developed in this investigation

for the high temperature investigation of UF kinetics is concluded to be adequate, reliable and practical, producing check results at the lower temperatures comparable to those generated by standard routes at the lower temperature range (up to 60°C).

iii. Mathematical representation of kinetic data over the entire temperature range.

The representation of the kinetic data over the temperature and time ranges of interest was achieved with excellent accuracy using the chemical mechanisms postulated and solving and optimising the resulting differential equations. However it was also concluded that the above procedure was of mathematical significance only and no particular chemical significance could be attached to the stoichiometric systems as a result of the above work.

7.1.2. Conclusions relating to the experimental performance of the tubular reactor

- (i) The reactor was shown to be capable of consistent and reproducible operation.
- (ii) The sampling valve proved reliable in operation and satisfactory for the purposes of sample removal.
- (iii) Experimental evidence implies the presence of a reaction initiation lag, the significance of which is reduced with increase in concentra-

- tion and temperatures and reduction in residence time.
- (iv) Reactor wall temperatures reflect the speed of the reaction.
  - (v) The pattern of the behaviour of the reactor wall temperature in relation to the steam temperature in the jacket is governed by the concentrations of the reactants and the residence time.
  - (vi) The reaction mechanism follows the same pattern at both molar ratios investigated. However, the reaction is accomplished faster at lower molar ratios (F:U) and higher concentrations.
  - (vii) A higher degree of reaction is achieved as the steam temperature is elevated.
  - (viii) High molar ratios, low concentrations, short residence times and high temperatures favour the addition reactions. Increase in residence time increases the extent of condensation.
  - (ix) At lower molar ratios of F:U (higher concentrations), the addition and condensation reactions seem to take place simultaneously. Increase in temperature at these ratios causes addition reactions to become faster as compared to the condensation reactions. However, both methylols and methylene compounds are formed extensively.
  - (x) At a given temperature the best conditions for conversion of free formaldehyde to methylols

with no significant condensation are low residence times, low concentrations and high molar ratios.

- (xi) Free formaldehyde takes little part in the condensation reactions.

### 7.1.3. Conclusions relating to the mathematical model predictions

- (i) The plug-flow models predicted the reactor performance with excellent accuracy providing free formaldehyde concentrations averaging to within  $\pm 0.65\%$  (when results are expressed as % F) and reactor wall temperatures averaging to within  $\pm 5.75^{\circ}\text{C}$ .
- (ii) The novel technique developed for solution of complex models proved to be very satisfactory and straight forward in use.
- (iii) The complex models were much poorer in accuracy, providing free formaldehyde concentrations averaging to within  $\pm 2.55\%$  and reactor wall temperatures averaging to within  $\pm 26.87^{\circ}\text{C}$ .
- (iv) It was concluded that the reactor geometry was the main reason for the good prediction of the plug-flow models and the poor accuracy of the complex model predictions. This resulted from the extensive mixing which took place in the reactor due to the mechanical

design of the equipment leading to deformation of a laminar parabolic velocity profile. Inadequacy of the complex energy model to deal with the wall boundary condition for the initial lengths of the reactor tube also detracted from the effectiveness of the model.

## 7.2. RECOMMENDATIONS

### 7.2.1. Recommendations with regard to improvement of the chemical kinetic investigation

- (i) The novel technique developed in this investigation should be extended to obtain further high temperature UF kinetic information. In this context the chemical investigation should be conducted at  $10^{\circ}\text{C}$  intervals over the range  $20^{\circ}$  to  $160^{\circ}\text{C}$  to narrow the range of application of each particular model and also to complete some of the gaps in the data. The technique can then be exploited further to evaluate other molar ratios and concentrations to throw some light on the overall behaviour of the system.
- (ii) The mathematical representation of the kinetic data could be improved by looking at other techniques which could represent the data with the same degree of accuracy.

Work could also be directed towards finding a mathematical relationship to account for the pattern of change of the rate constants, thereby facilitating the data prediction process.

Finally, other chemical reactions which are likely to take place under the conditions of each investigation could be implemented in the existing kinetic models and their accuracy of prediction examined against experimental data. As a result of this further work some chemical significance could perhaps be attached to the mathematical description.

#### 7.2.2. Recommendations with regard to the extension of the experimentation program

- (i) The reactor could be modified to give a uniform shape with reasonably smooth bends and the experimental program repeated to investigate any possible changes in the results as compared to either model prediction.
- (ii) The experimental program could be extended to cover the effects of change of radius on the reactor performance and the scaling-up possibilities of the process. The accuracy of the model predictions could then be investigated for scaling-up purposes.

- (iii) Use of alternative analytical techniques which could provide a more complete analysis of the resins including identification of the condensation products.

### 7.2.3. Recommendations with regard to improvement of mathematical models

- (i) Some of the physical data input to the models merit a more accurate estimation. This will improve the general accuracy of both models.
- (ii) The complex energy model can be reviewed and replaced by a more representative model possessing a wall boundary condition allowing for heat transfer for that length of the tube where steam behaves as a heating medium.
- (iii) The equilibrium concentrations of urea, formaldehyde and monomethylolurea should be measured experimentally to improve the accuracy of the complex model predictions.
- (iv) Finally, the plug-flow models, in their present form, could be simulated to give concentration outputs for the condensation products. This could serve as a basis for further model improvements in this direction.

A P P E N D I C E S

## APPENDIX 1

### VALIDITY OF BASIC ASSUMPTIONS

#### 1. ASSUMPTION OF STEADY STATE

Experiments show that steady state conditions are reached very quickly with the systems under consideration. In addition the following theoretical approach can also be given in support of the above statement.

Consider laminar flow in a tube with a parabolic velocity profile, having annuli of variable velocity  $V_x$ .

Then

for 1 residence time all annuli with velocity

$$V_x \geq V_0 \text{ have eluted}$$

for 2 residence times all annuli with velocity

$$2V_x \geq V_0 \text{ have eluted}$$

for 3 residence times all annuli with velocity

$$3V_x \geq V_0 \text{ have eluted}$$

so that

for  $n$  residence times all annuli with velocity

$$nV_x \geq V_0 \text{ have eluted}$$

Since the velocity profile is parabolic for a Newtonian fluid

$$V_x = 2V_0 \left(1 - \left(\frac{r}{R}\right)^2\right) \quad \text{A.1.1.}$$

$$\text{Let } \frac{r}{R} = \theta$$

Hence the substitution of  $nV_x \geq V_o$  in A.1.1. results in

$$\frac{V_o}{n} = 2V_o \left(1 - \left(\frac{r}{R}\right)^2\right) = 2V_o (1 - \theta^2)$$

or on manipulation

$$\theta \leq \left(\frac{2n-1}{2n}\right)^{\frac{1}{2}} \quad \text{A.1.2.}$$

The non equality A.1.2. suggests that all the material in the tube within  $\theta=0$  and the variable  $\theta=\frac{r}{R}$  has escaped.

Now the volume flow through an annulus of thickness  $dr$  at radius  $r$  is given by

$$2\pi r V_x dr \quad \text{A.1.3.}$$

also

$$r = R\theta \quad \text{and} \quad R d\theta = dr$$

So that A.1.3. becomes

$$2\pi R^2 \theta V_x d\theta$$

and substituting for  $V_x$  from A.1.1. in the above results in

$$\begin{aligned} & 2\pi R^2 \theta (2V_o (1 - \theta^2)) d\theta \\ & = 4\pi R^2 \theta (1 - \theta^2) d\theta \end{aligned} \quad \text{A.1.4.}$$

Hence the volume of the material which has left the reactor between radii  $\theta=0$  and

$$\theta = \left(\frac{2n-1}{2n}\right)^{\frac{1}{2}} \text{ is given by}$$

$$4\pi V_o R^2 \int_0^{\left(\frac{2n-1}{2n}\right)^{\frac{1}{2}}} \theta (1 - \theta^2) d\theta \quad \text{A.1.5.}$$

Integrating A.1.5, and substituting the integration limits gives

$$\Pi V_0 R^2 \left( \left( \frac{2n-1}{n} \right) - \frac{(2n-1)^2}{4n^2} \right) \quad \text{A.1.6.}$$

To express this quantity as a fraction of the total volume which has left the reactor between  $\theta=0$  and  $\theta=1$  ( $r=R$ ), the total volume has to be found.

This is given by:

$$4\Pi V_0 R^2 \int_0^1 \theta(1-\theta^2) d\theta \quad \text{A.1.7.}$$

Integration of A.1.7. and substitution of limits yields

$$\Pi V_0 R^2$$

Hence the fraction of material which has left the reactor after  $n$  residence times is:

$$\frac{\Pi V_0 R^2 \left( \left( \frac{2n-1}{n} \right) - \frac{(2n-1)^2}{4n^2} \right)}{\Pi V_0 R^2} = \left( \frac{2n-1}{n} \right) - \frac{(2n-1)^2}{4n^2} \quad \text{A.1.8.}$$

Tabulating the results we have:

No. of Residence Times, $n$	% Initial Feed Discharged
1	75.0
2	93.7
3	97.2
4	98.4
5	99.0

TABLE A.1.1.

TIME REQUIRED TO REACH STEADY STATE

So it can be concluded that the steady state condition is closely approached after four to five residence times, as the incremental gains for the extra numbers of residence times become progressively smaller.

The residence times used for the experiments in this investigation are all less than one minute, so that steady state conditions are reached after four to five minutes assuming that all the services to the reactor are at steady state condition. Inclusion of radial diffusion in the above analysis would decrease the residence time for the same per cent elution as plug flow conditions are approached.

Instability at the entrance need not be considered in the light of the investigation by Ulrichson and Schmitz (36), which is discussed in the literature survey.

## 2. ASSUMPTION OF FLOW IN ONE DIRECTION ONLY

Although radial velocities can exist in all systems of this type even at low Reynolds numbers, the fact that they are not considered will not effect the results significantly due to the relative small magnitude of these velocities as compared to those in the axial direction.

## 3. ASSUMPTION OF CONSTANT DENSITY

This assumption is justified with regard to the most susceptible case when the variation in density is expected to be highest.

The density of the feed to the reactor, for U:F molar ratio of 1:2.2, using prilled urea dissolved in 36% formalin solution is known to be  $1.16 \text{ g/cm}^3$ . The resin, after leaving the reactor, is flash evaporated and as such possesses a density of  $1.18 \text{ g/cm}^3$ . This gives rise to a 1.7% variation. However much of the rise in density occurs during flash evaporation where the bulk of the water is removed. As a result the per cent rise in density at reactor outlet can be expected to be significantly lower. Accepting the figure of 1.7% as a conservative maximum, the variation in density can be assumed negligible for all practical purposes.

It must be emphasised that this assumption has to be considered carefully for different systems, as changes in excess of approximately 15% would require variable density models.

#### 4. ASSUMPTION OF NO NATURAL CONVECTION

This assumption is based on the argument that the small tube diameter does not allow significant distortion to the velocity profile because of variation in density caused by buoyancy effects. However, enlarging the tube diameter enhances the effects of natural convection resulting in serious distortions in velocity profile. This effect has been discussed with regard to the work of Lynn and Huff(27) in the literature survey (Section 2.2.),

## 5. ASSUMPTION ON EFFECTS OF RADIATION

The effect of the mechanism of radiation on heat transfer can be neglected for all practical purposes due to its relative magnitude as compared to convective and diffusional heat transfers.

## 6. ASSUMPTION ON VISCOUS ENERGY DISSIPATION

This assumption is justifiable as the reaction is of a primary stage (Chapter 3) and although the viscosity of the fluid increases substantially, it does not rise to such an extent that a significant amount of energy is dissipated through its flow.

## 7. ASSUMPTION OF LAMINAR FLOW AND PARABOLIC VELOCITY PROFILE EVALUATION OF REYNOLDS NUMBER

In the development of the complex momentum model the flow was assumed to be laminar and the velocity profile parabolic in shape, i.e. Reynolds number less than 2100. The Reynolds number evaluated for the least viscous feed to the reactor, at the highest velocity confirms the above assumption.

The least viscous feed to the reactor was made up of 25% urea solution mixed with 36% formalin in the molar ratio 1:2.2 and its viscosity, as measured on a Ferranti Viscometer at 20°C, was found to be 0.115 poise. Hence,

with the following values:

$$\rho_M = 1.0820 \text{ g/cm}^3$$

$$V_o = 91.13 \text{ cm/s}$$

$$d_i = 0.655 \text{ cm}$$

$$\mu = 0.115 \text{ poise}$$

The Reynolds number is:

$$Re = \frac{\rho_M V_o d_i}{\mu} = 561$$

All other feeds to the reactor had higher viscosities and therefore lower Reynolds numbers.

It was further assumed that the decrease in viscosity as a result of increase in temperature, as the mixture passes along the reactor, is less critical than the increase in viscosity as a result of progress in reaction. It is not possible to measure the actual viscosity of the mix at the reactor outlet, due to immediate flash evaporation, to confirm this assumption numerically. However, visual observation supports this consideration.

## APPENDIX 2

### EVALUATION OF HEAT TRANSFER COEFFICIENT

In tube laminar-flow the convection heat transfer coefficient is usually defined by (51),

$$\text{Local heat flux} = q'' = h(T_w - T_b)$$

where  $T_w$  is the wall temperature

$T_b$  is the bulk temperature which may be calculated from

$$T_b = \frac{\int_0^R 2\rho_M V_x(r) S T r dr}{\int_0^R 2\rho_M V_x(r) S r dr} \quad \text{A.2.1.}$$

The numerator of equation A.2.1. represents the total energy flow through the tube and the denominator the product of mass flow and specific heat integrated over the flow area.

The bulk temperature is therefore representative of the total energy flow at the particular location, and is sometimes referred to as the "cup mixing temperature".

From equation A.2.1.

$$T_b = T_c + \frac{7}{96} \frac{V_0 R^2}{\alpha} \frac{\partial T}{\partial x} \quad \text{A.2.2.}$$

where,

$T_c$  is the temperature at the centre of the tube

$\alpha$  is the molecular diffusivity of heat

and for the wall temperature

$$T_w = T_c + \frac{3}{16} \frac{V_0 R^2}{\alpha} \frac{\partial T}{\partial x} \quad \text{A.2.3.}$$

The heat transfer coefficient is calculated from:

$$q = hA(T_w - T_b) = K_M A \left( \frac{\partial T}{\partial x} \right)_{r=R} \quad \text{A.2.4.}$$

resulting in

$$h = \frac{K_M \left( \frac{\partial T}{\partial r} \right)_{r=R}}{(T_w - T_b)} \quad \text{A.2.5.}$$

The temperature gradient is then given by

$$\left( \frac{\partial T}{\partial r} \right)_{r=R} = \frac{V_0}{\alpha} \frac{\partial T}{\partial x} \left( \frac{r}{2} - \frac{r^3}{4R^2} \right)_{r=R} = \frac{V_0 R}{4\alpha} \frac{\partial T}{\partial x} \quad \text{A.2.6.}$$

Substituting equations A.2.2., A.2.3. and A.2.5. into equation A.2.4. gives

$$h = \frac{24K_M}{11R}$$

or expressing the result in terms of Nusselt number

$$\text{Nud} = \frac{h(2R)}{K_M} = 4.364$$

or

$$h = \frac{4.364K_M}{2R}$$

This result is in agreement with an exact calculation by Sellars, Tribus and Klein(52).

### APPENDIX 3

#### PHYSICAL DATA AND EVALUATION OF DIFFUSION EFFECTS

##### A. PHYSICAL DATA

##### 1. DENSITY ( $\rho_M$ )

The densities of the various feed compositions to the reactor were measured and are given in Table A.3.1. and have been used where appropriate.

An average density of  $1.0992 \text{ g/cm}^3$  is used for the calculation of the thermal diffusion coefficient ( $D_{TH}$ ).

FEED COMPOSITION			DENSITY $\text{g/cm}^3$
MOLAR RATIO U:F	UREA SOLUTION STRENGTH % W/W	FORMALIN SOLUTION STRENGTH % W/W	
1:1.33	50	36	1.1165
1:2.2	50	36	1.1140
1:2.2	50	44	1.1135
1:2.2	25	36	1.0820

TABLE A.3.1.

DENSITIES OF FEEDS TO REACTOR

2. HEAT CAPACITY (S)

A value of 0.4 cal/g °C is used(53). Although this value is given for finished UF resins, it can be used for the mixture in the reactor as a good and conservative approximation.

3. THERMAL CONDUCTIVITY (K<sub>M</sub>)

A value of  $14 \times 10^{-4}$  cal/cm s °C for the finished resin is quoted in (53). This value is used with the same arguments in 2 above applying.

4. TUBE LENGTH (L) AND RADIUS (R)

The tube length is 38ft (1158.24cm). The radius of the tube is  $\frac{1}{8}$  inch internal for the first 30ft and expands to  $\frac{5}{16}$  inch internal for the remaining 8ft. Full details can be found in Chapter 5.

5. AVERAGE VELOCITY (V<sub>O</sub>)

The average velocity is calculated from a knowledge of the residence time in the tubes. The overall residence times used in this investigation are 53.5 and 26.75 seconds, resulting in average velocities of:

For 53.5 seconds residence time:

$$\frac{1}{4}'' \text{ i.d. tube } V_o = \frac{304.8}{6.68} = 45.6 \text{ cm/s}$$

$$5/8" \text{ i.d. tube } V_o = \frac{243.84}{33.46} = 7.3 \text{ cm/s}$$

For 26.75 seconds residence time

$$1/4" \text{ i.d. tube } V_o = \frac{304.8}{3.34} = 91.1 \text{ cm/s}$$

$$5/8" \text{ i.d. tube } V_o = \frac{243.84}{16.73} = 14.6 \text{ cm/s}$$

## 6. DIFFUSION COEFFICIENTS

### Thermal Diffusion Coefficient ( $D_{TH}$ )

A value for  $D_{TH}$  is calculated from

$$D_{TH} = \frac{KM}{S\rho_M}$$

$$= \frac{14 \times 10^{-4}}{0.4 \times 1.0992} = 31.84 \times 10^{-4} \text{ cm}^2 \text{ s}^{-1}$$

### MOLECULAR DIFFUSION COEFFICIENT FOR FORMALDEHYDE ( $D_{MF}$ )

Since formaldehyde exists in water as methylene glycol and reacts as such, its diffusion coefficient will correspond to that calculated for methylene glycol.

The molecular diffusion coefficient for methylene glycol can be estimated with a 4% deviation and a maximum 16% deviation from (60).

$$\frac{DL\mu}{T} = 7.4 \times 10^{-8} \frac{(\text{X.M.})^{0.5}}{V_o^{0.6}} \quad \text{A.3.1.}$$

where

$DL$  = diffusion coefficient in  $\text{cm}^2/\text{s}^2 = D_{MF}$

$\mu$  = viscosity of solvent in centipoise = 1 cp for  
water

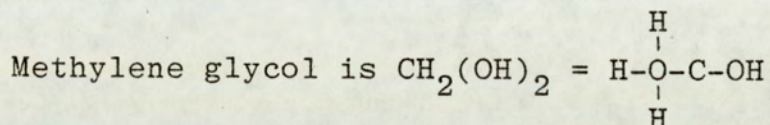
$T$  = absolute temperature of solution in  $^{\circ}\text{K} = 293^{\circ}\text{K}$   
at  $20^{\circ}\text{C}$

X = association parameter for solvent = 2,6 for  
water(54)

M = molecular weight of solvent = 18 for water

Vo = molar volume of solute

Vo can be calculated from the atomic volumes of the atoms of methylene glycol as follows:



The atomic volumes are therefore (54),

$$\text{C} = 14.8$$

$$\text{H} = 3.7$$

$$\text{O} = 9.9 \text{ for oxygen bounded to two different atoms}$$

Hence

$$\text{Vo} = \text{C} + 4(\text{H}) + 2(\text{O})$$

$$\text{Vo} = 14.8 + 4 \times 3.7 + 2 \times 9.9 = 49.4 \text{ cm}^3/\text{g}$$

Substitution of these values in equation A.3.1. will result in

$$D_{\text{MF}} = T \times 4.876 \times 10^{-8} \text{ cm}^2/\text{s}^2$$

or at 20°C

$$D_{\text{MF}} = 1.43 \times 10^{-5} \text{ cm}^2/\text{s}^2$$

#### MOLECULAR DIFFUSION COEFFICIENT FOR UREA (DMU)

This is quoted as  $1.14 \times 10^{-5} \text{ cm}^2 \text{ s}^{-1}$  for urea in water (55). As the formalin is a 36% solution, it is assumed that it behaves substantially as water and therefore the value given above is fairly representative.

J.H. Arnold(56) states an observed value of  $0.96 \text{ cm}^2 \text{ Day}^{-1}$  ( $1.01 \times 10^{-5} \text{ cm}^2 \text{ s}^{-1}$ ) which is in close agreement

with the above, A value of  $1.16 \times 10^{-5} \text{ cm}^2 \text{ s}^{-1}$  has also been calculated from (56),

$$D_M = \frac{B\sqrt{1/M_1 + 1/M_2}}{A_1 A_2 Z_2^{1/2} S^2}$$

where

A = a proportionality constant

B = a universal constant

M = molecular weight

$S = V_1^{0.33} + V_2^{0.33}$  (V being molar volumes)

Z = solvent viscosity in centipoises

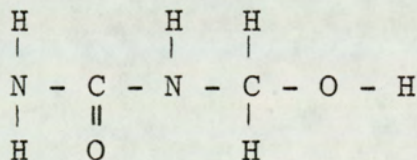
Subscript 1 refers to the diffusing substance

Subscript 2 refers to the solvent medium

Since all the above values are close in magnitude, the value of  $1.14 \times 10^{-5} \text{ cm}^2 \text{ s}^{-1}$  will be used in the calculations as representative.

#### MOLECULAR DIFFUSION COEFFICIENT FOR MONOMETHYLOLUREA ( $D_{MUFI}$ )

The chemical formula for monomethylolurea is



This gives a molar volume of  $93.7 \text{ cm}^3/\text{g}$  for monomethylolurea. Insertion of this figure into equation A.3.1. and substitution of the other relevant parameters gives the molecular diffusion coefficient of monomethylolurea as  $0.97 \times 10^{-5} \text{ cm}^2/\text{s}$  at  $20^\circ\text{C}$ .

## B. EVALUATION OF SIGNIFICANCE OF DIFFUSIONAL EFFECTS

### 1. AXIAL DIFFUSION

a : Heat

Kramers and Westerterp(57) state that if  $V_o \frac{L}{D_{TH}}$  is much greater than unity, then axial conduction of heat may be neglected. Using the values of velocity and length which give the minimum value of the above quantity,

$$V_o \frac{L}{D_{TH}} = 7.3 \frac{243.84}{31.84 \times 10^{-4}} = 0.56 \times 10^6$$

and therefore axial conduction of heat may be neglected.

b : Mass

If  $V_o \frac{L}{D_M}$  is much greater than unity then axial mass diffusion may be neglected (57). Similarly the minimum value is given by:

$$V_o \frac{L}{D_M} = 7.3 \frac{243.84}{1.43 \times 10^{-5}} = 1.24 \times 10^8$$

and therefore axial diffusion of mass may be neglected.

### 2. RADIAL DIFFUSION

Radial temperature gradients are accounted for in the models and therefore only mass diffusion in the radial direction will be considered.

If  $\frac{D_M}{V_o} \cdot \frac{L}{R^2}$  is very small and tends to zero then radial diffusion of mass may be neglected (57). The maximum value of the above quantity is given by,

$$\frac{D_M L}{V_o R^2} = \frac{1.43 \times 10^{-5}}{45.6} \cdot \frac{914.4}{(0.3175)^2} = 0.00284$$

This number is small but could not be considered as tending to zero. Hence radial diffusion of mass is included in the model.

## APPENDIX 4

### EVALUATION OF BOUNDARY CONDITIONS

#### FOR COMPLEX ENERGY MODEL

The exothermic nature of the reactions under investigation and in general most polymerisation reactions require the development of a unique tube wall boundary condition. This is because the fluid reaction mixture first absorbs heat from the steam heated tube wall and then gives up heat to the wall as its temperature rises above the steam temperature due to the reaction heat release.

Therefore steam behaves as both a heating medium in the early stages of the reaction and a coolant in the later stages, and the boundary condition has to be changed accordingly. The analysis can be presented as follows:

#### 1. STEAM AS A HEATING MEDIUM

In this case steam condenses to heat the fluid in the reactor. Therefore heat transfer takes place through a liquid film. The heat transfer coefficient will have a very high value and this would give rise to boundary condition:

$$T_w = T_s$$

ignoring the thermal resistance of the tube wall,

## 2. TRANSITION POINT

The transition point is defined as the point where the fluid temperature closest to the wall reaches the temperature of steam (wall). A reverse effect starts at this point whereby steam acts as a coolant thereafter.

The point of change over is therefore:

$$T_4 = T_w$$

where

$T_4$  is the temperature closest to the wall on a mesh grid used for solution of models (Chapter 4).

## 3. STEAM AS A COOLING MEDIUM

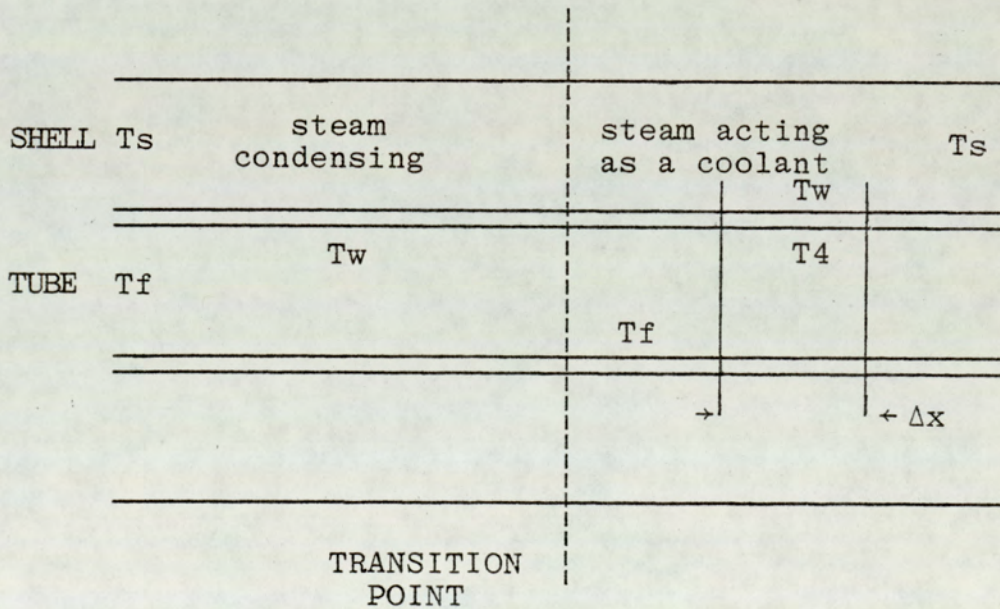


FIG. A.4.1.

## SHELL-TUBE HEAT TRANSFER

With reference to Fig. A.4.1., the balance on an incremental element of length  $\Delta x$  gives:

$$dq = \Pi d_o \Delta x h_{cs} (T_w - T_s) = \Pi d_i \Delta x h_f (T_4 - T_w)$$

giving

$$T_w = \frac{h_f T_4 + \phi h_{cs} T_s}{h_f + h_{cs} \phi} \quad \text{A.4.1.}$$

where

$h_f$  = tube side film coefficient

$h_{cs}$  = shell side film coefficient

$\phi$  = ratio of external to internal diameter

The two film coefficients can be calculated as follows:-

#### Prediction of 'hcs'

"hcs" refers to a heat transfer coefficient on the outside which is of "free convective nature".

This arises from the consideration that although steam is stagnant and at a constant pressure and hence temperature, free convection takes place under the temperature difference between steam adjacent to the tube wall and the bulk steam temperature.

Using the equation by Chilton and Colburn(58), a value for the film coefficient can be obtained which is accurate for the case of heat transfer through tubes.

Hence

$$h_{cs} = 116 \left\{ \left( \frac{K_f^3 \rho_f^2 S_f \beta}{\mu_f} \right) \left( \frac{\Delta T}{d_o} \right) \right\}^{\frac{1}{4}} \quad \text{A.4.2.}$$

where

$$\beta = \text{coefficient of thermal expansion} \frac{\frac{1}{\rho_{t2}} - \frac{1}{\rho_{t1}}}{(t_2 - t_1) \frac{1}{\rho_{fav}}}$$

$\Delta T = (t_2 - t_1) =$  Temperature difference between steam  
and fluid at reactor outlet

Subscript f refers to the steam temperature

Rewriting hcs as

$$hcs = 116 \left\{ \frac{K_f^3 \rho_{fav}^2 S_f \beta}{\mu_f} (\Delta T) \right\}^{\frac{1}{4}} \left\{ \frac{1}{d_o} \right\}^{\frac{1}{4}} \quad A.4.3.$$

two values can be computed for the two sizes of reactor tube (Chapter 5). The values of the various parameters in A.4.3. for steam at an average temperature of 140°C (284°F) in British units, and viscosity,  $\mu_f$ , in centipoises are (58):

$$K_f = \text{thermal conductivity} = 0.015 \text{ Btu/hr ft } ^\circ\text{F}$$

$$\rho_{fav} = \text{average density} = 0.1352 \text{ lb/ft}^3$$

$$S_f = \text{specific heat} = 0.45 \text{ Btu/lb } ^\circ\text{F}$$

$$\beta = \text{coefficient of thermal expansion} = 0.0146 \text{ } ^\circ\text{F}^{-1}$$

$$\mu_f = \text{viscosity in centipoises} = 0.014 \text{ cp}$$

$$\Delta T = \text{average temperature difference} = 12.6 \text{ } ^\circ\text{F} \text{ (7} ^\circ\text{C)}$$

(Chapter 5)

$$d_o = \text{outside tube diameter in inches} =$$

$$\frac{5}{8} + 2(0.049) \text{ in or } \frac{1}{4} + 2(0.049) \text{ in}$$

Computing the above results using the following values for the two reactor tubes, for  $\frac{1}{4}$ " i.d. reactor tube

$$hcs = 3.71 \quad \text{Btu/hr ft}^2 \text{ } ^\circ\text{F}$$

$$= 0.0005027 \text{ cal/s cm}^2 \text{ } ^\circ\text{C}$$

$$= 21.0665 \quad \text{w/m}^2 \text{ deg } ^\circ\text{C}$$

for 5/8" i.d. reactor tube

$$\begin{aligned} hcs &= 3.09 \quad \text{Btu/hr ft}^2 \text{ } ^\circ\text{F} \\ &= 0.004186 \text{ cal/s cm}^2 \text{ } ^\circ\text{C} \\ &= 17.5459 \text{ w/m}^2 \text{ deg C} \end{aligned}$$

#### Prediction of "hf"

The value of the film coefficient on the tube side can be evaluated from the Sieder and Tate equation (58).

$$\begin{aligned} \frac{hfd_i}{k_f} &= 1.86 \left\{ \left( \frac{d_i G_f}{\mu_f} \right) \left( \frac{S_f \mu_f}{K_f} \right) \left( \frac{d_i}{L} \right) \right\}^{1/3} \left( \frac{\mu}{\mu_w} \right)^{0.14} \\ &= 1.86 \left\{ \frac{4ws_f}{\pi K_f L} \right\}^{1/3} \left( \frac{\mu}{\mu_w} \right)^{0.14} \end{aligned} \quad \text{A.4.4.}$$

where

- w = mass flow of fluid in lb/hr
- $\mu_f$  = viscosity at caloric temperature in lb/ft hr
- $\mu_w$  = viscosity at wall temperature in lb/ft hr
- $d_i$  = inside diameter in ft

A.4.4. can be written as

$$hf = 1.86 \left\{ \frac{K_f^2 S_f}{d_i L} \right\}^{1/3} \{V_o\}^{1/3} \text{ Btu/ft}^2 \text{ hr } ^\circ\text{F} \quad \text{A.4.5.}$$

Using the relevant data of Appendix 3, in British units and the above information, four values of hf can be computed for the four velocities in the two sizes of the reactor tubes. These are calculated in the relevant computer programs of Appendix 7.

In the above calculation the differential change in viscosity has been taken to be unity, resulting in

$$\left( \frac{\mu}{\mu_w} \right)^{0.14} = 1$$

This is due to the small variations of temperature over the radius of the tube. Along the axis the ratio would give a value of 0.88 with the highest differential temperature, justifying the above assumption for all practical purposes.

Substitution of the relevant values of 'hcs' and 'hf' in c.g.s. units and the two temperatures in degrees Kelvin into A.4.1., would give the final boundary condition as:

$$T_w = \frac{hfT_4 + \phi hcsT_s}{hf + hcs\phi}$$

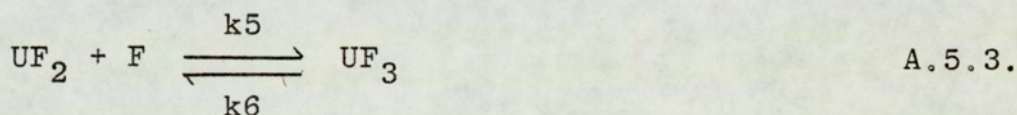
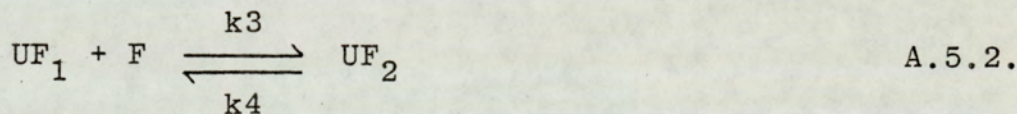
## APPENDIX 5

### ESTIMATION OF EQUILIBRIUM CONCENTRATIONS OF UREA-FORMALDEHYDE REACTION MIXTURES

It is expected that the reaction mixture at the reactor wall will reach equilibrium rapidly, due to the high residence time and temperature.

Appendix 5 presents a technique for estimation of equilibrium concentrations of the various reactants.

Assuming the reaction scheme is given by (Chapter 3):



Then the respective equilibrium constants may be expressed as:

$$K_1 = \frac{k_1}{k_2} = \frac{(UF_1)_e}{(U)_e (F)_e} \quad \text{A.5.4.}$$

$$K_2 = \frac{k_3}{k_4} = \frac{(UF_2)_e}{(UF_1)_e (F)_e} \quad \text{A.5.5.}$$

$$K_3 = \frac{k_5}{k_6} = \frac{(UF_3)_e}{(UF_2)_e (F)_e} \quad \text{A.5.6.}$$

where the parentheses denote concentrations of various components and the subscript e refers to equilibrium conditions.

Relations A.5.4. to A.5.6. can be written as:

$$(UF_1)_e = K_1(U)_e(F)_e \quad A.5.7.$$

$$(UF_2)_e = K_2(UF_1)_e(F)_e \quad A.5.8.$$

$$(UF_3)_e = K_3(UF_2)_e(F)_e \quad A.5.9.$$

Combining A.5.7. to A.5.9. results in:

$$(UF_1)_e = K_1(U)_e(F)_e \quad A.5.10.$$

$$(UF_2)_e = K_1K_2(U)_e(F)_e^2 \quad A.5.11.$$

$$(UF_3)_e = K_1K_2K_3(U)_e(F)_e^3 \quad A.5.12.$$

Also, a molar material balance at equilibrium yields:

$$U_o = (U)_e + (UF_1)_e + (UF_2)_e + (UF_3)_e \quad A.5.13.$$

$$F_o = (F)_e + (UF_1)_e + 2(UF_2)_e + 3(UF_3)_e \quad A.5.14.$$

In equation A.5.13.,  $(UF_1)_e$ ,  $(UF_2)_e$ ,  $(UF_3)_e$  can be replaced by A.5.10. to A.5.12. resulting in:

$$(U)_e = \frac{U_o}{1 + K_1(F)_e + K_1K_2(F)_e^2 + K_1K_2K_3(F)_e^3} \quad A.5.15.$$

Substitution of A.5.15. into A.5.14. results in a relationship for the equilibrium concentration of formaldehyde, thus:

$$F_o - (F)_e = \frac{U_o \{K_1(F)_e + 2K_1K_2(F)_e^2 + 3K_1K_2K_3(F)_e^3\}}{1 + K_1(F)_e + K_1K_2(F)_e^2 + K_1K_2K_3(F)_e^3} \quad A.5.16.$$

In fact relations A.5.15. and A.5.16. can be mathematically generalised for similar reactions going to  $UF_M$ , thus:

$$(U)_e = \frac{U_0}{1 + \sum_{J=1}^{J=M} \{(F)_e \prod_{K=1}^J KJ\}} \quad \text{A.5.17.}$$

and

$$F_0 - (F)_e = \frac{U_0 \sum_{J=1}^{J=M} \{J(F)_e \prod_{K=1}^J KJ\}}{1 + \sum_{J=1}^{J=M} \{(F)_e \prod_{K=1}^J KJ\}} \quad \text{A.5.18.}$$

A knowledge of the values of initial concentrations of urea,  $U_0$ , formaldehyde,  $F_0$ , and rate constants  $K1$ ,  $K2$  and  $K3$  would permit the solution of the quartic equation in  $(F)_e$  represented by A.5.16. Once the equilibrium concentration of formaldehyde has been estimated, use can be made of equations A.5.15. and A.5.10. consecutively to obtain estimations for concentrations of urea and mono-methylol urea, respectively, at equilibrium.

Both analytical (132) and numerical solutions (Newton-Raphson (130)) of equations A.5.18. produced some irregular results. For some conditions no positive result for the concentration of  $(F)_e$  could be found. In some of the other cases two close roots in the range of interest were obtained whereas only one sensible root would normally be expected. The latter result was attributed to the accumulated round-off errors in the analytical solution and approximations in the numerical solution.

Furthermore, the following three points can be cited to highlight the deficiencies of the above estimation technique.

(i) Equation A.5.16, is derived theoretically and does not allow for any other reactions which could influence the equilibrium concentration of formaldehyde, e.g. condensation reactions.

(ii) Equation A.5.16. is not strictly correct thermodynamically. Since the forward reactions in A.5.1. to A.5.3. are all second order, thermodynamics require that the reverse reactions should also be second order at equilibrium (133). This criterion is not allowed for in the above mathematical derivations.

(iii) The equilibrium constants  $K_1$ ,  $K_2$  and  $K_3$  used in the above calculations are optimised in Chapter 3 for particular experimental conditions and have definite ranges of application. Extrapolation of these values to cover equilibrium conditions could introduce errors.

The dubious nature of the results considering the above points, caused a reluctance in pursuing this course of estimation.

The problem was, however, resolved by making use of the approximate equilibrium values of  $(F)_e$  found in the course of investigations described in Chapter 3. These values were expected to be close to the real equilibrium values of formaldehyde as well as representing the real situation inclusive of all side reactions. Equation A.5.15. was then used to evaluate approximate values for equilibrium concentration of urea, based on experimental

values of  $(F)_e$  and optimised values of  $K_1$ ,  $K_2$  and  $K_3$ . Relation A.5.10. gave the value of  $(UF_1)_e$ . These values are tabulated in Table A.5.1.

CONDITIONS		EQUILIBRIUM CONCENTRATIONS					
MOLAR RATIO U:F	STEAM/ WALL TEMP °C	EXPERIMENTAL MOL/LIT		CALCULATED MOL/LIT		CALCULATED MOL/LIT	
		$F_0$	$(F)_e$	$U_0$	$(U)_e$	$UF_{10}$	$(UF_1)_e$
1:2.2	160	10,497	0.3577	4.771	0.16	0	3.17
1:2.2	140	10,497	0,2177	4.771	0.20	0	3.47
1:2.2	120	10,497	0.066	4.771	0.28	0	3.51
1:1.33	160	9,1867	0,2438	6.9072	0.27	0	5.22
1:1.33	140	9,1867	0,1514	6.9072	0.32	0	5.46
1:1.33	120	9,1867	0.0590	6.9072	0.54	0	5.63

TABLE A.5.1.

EQUILIBRIUM CONCENTRATIONS

Table A.5.1. shows increasing equilibrium concentrations of formaldehyde with increasing temperature. This can be explained by consideration of Le Chatelier's principle. Since the forward reactions are exothermic, an increase in temperature will shift the reactions such that heat is absorbed by the system. As a result the dissociation mechanism becomes more significant than the reaction mechanism. Consequently the concentration of

formaldehyde increases with increasing temperature. This is exhibited experimentally where results at 160°C show a higher equilibrium concentration than results at 120°C (Chapter 3).

In conclusion, a further source of error should be considered. While Table A.5.1. is representative of the systems investigated in Chapter 3, where formalin and prilled urea were the reactants, in the reactor operation prilled urea was replaced by urea solutions of various concentrations (Chapter 5). This infers that the actual equilibrium concentrations would possess lower values in the reactor system. However, the discrepancy discussed is expected to be of little significance.

## APPENDIX 6

### SPECIFICATION OF RAW MATERIALS AND CHEMICALS

#### 1. FORMALDEHYDE

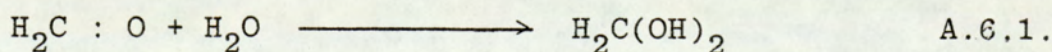
##### INTRODUCTION

Generally formaldehyde solutions can be divided into two distinct categories.

- (i) Solutions in which the dissolved formaldehyde is present in the monomeric form,
- (ii) Solutions in which the solute is chemically combined with the solvent.

Solutions of the former type are obtained with non-polar solvents such as chloroform and toluene. The latter type, which includes water solutions, are obtained with polar solvents.

Research on the state of formaldehyde in aqueous solution may be summarised as showing that the dissolved aldehyde is present as an equilibrium mixture of the monohydrate, methylene glycol according to equation A.6.1., and a series of low molecular weight polymeric hydrates, or polyoxymethylene glycols, having the type formula  $\text{HO} \cdot (\text{CH}_2\text{O})_n \cdot \text{H}$

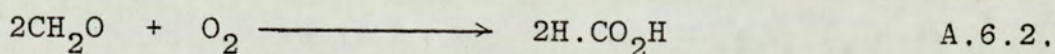


The state of equilibrium is governed by temperature

and concentration of formaldehyde. Low temperatures and high concentrations favour the polymeric hydrates, which will gradually precipitate, while high temperatures and low concentrations favour the monohydrate (115,116,117, 118,119).

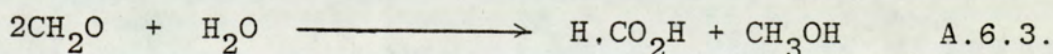
#### COMMERCIAL FORMALDEHYDE

Commercial formaldehyde is generally marketed under the trade name "Formalin" (F) which is an aqueous solution containing 36-37 per cent by weight dissolved formaldehyde plus sufficient methanol to prevent precipitation of solid polymer under ordinary conditions of storage and industrial use. Formalin also contains small amounts of formic acid formed by oxidation of formaldehyde:



The character of the final resin product is appreciably dependant on the proportions of these impurities and close limits of specifications in the composition of formalin are usually observed.

On heating formalin develops increased acidity as a result of the Cannizzaro reaction:



The formalin used for this work is industrial formalin with specifications as outlined in Table A.6.1. The specifications of Table A.6.1, differ from the usual industrial formalin in two respects. In the first instance, the low methanol content (c.f. 7-15% w/w generally) is due to the fact that prolonged storage is not required.

However, in cases where lengthy storage becomes necessary, the formalin can be kept clear for long periods at a temperature of between 25-30°C. Secondly, the low acid content (c.f. 0.2% w/w generally) is required for resin production where acidity is usually avoided. Buffers are added to check both the low existing acidity and also to provide the neutralising agent for further acidity developed on heating due to Cannizzaro's reaction.

STRENGTH	.36-37% w/w Formaldehyde
METHANOL CONTENT	2-3% w/w Methanol
ACIDITY	less than 15 ppm Formic
IRON	Trace
COPPER	Trace
ALUMINIUM	Trace
HEAVY METALS	Trace

TABLE A.6.1.

FORMALIN SPECIFICATIONS

PHYSICAL PROPERTIES

The relevant physical properties of formalin, namely density and viscosity depend on methanol content as well as temperature.

There is an apparent lack of agreement on the physical properties of formalin in the published literature. This however can be accounted for by the failure of some of the

early authors (120,121) to realise the presence of varying quantities of methanol in commercial formalin.

The density of formalin containing up to 15% methanol at temperatures in the region of 18°C can be obtained from equation A,6.4. (116),

$$\rho_F = 1.00 + F \cdot \frac{3}{1000} - M \cdot \frac{2}{1000} \quad \text{A.6.4.}$$

where

$\rho_F$  = density of formalin g/cm<sup>3</sup>

F = per cent weight of formaldehyde

M = per cent weight of methanol

This gives a density of 1.107 g/cm<sup>3</sup> at 25°C which can be compared with the accurate value of 1.105 g/cm<sup>3</sup> from data of Natta and Baccaredda(122),

The presence of methanol in formalin causes a slight increase in viscosity of formalin. A value corresponding to about 4.0 centipoises at 20°C for the specified formalin is given in "Formaldehyde" (116),

It is believed that temperature dependance of the above properties are not significant as formalin is mixed at about room temperature where all the above data vary due to the presence of the added urea.

A comprehensive collection of physical properties of formalin can be found in "Formaldehyde" (116).

## 2. UREA

Urea is a white crystalline compound with the chemical

formula  $\text{CO}(\text{NH}_2)_2$  and molecular weight 60.06.

It is commercially produced from liquid carbon dioxide and ammonia and marketed in different grades.

The urea used in this case is a high grade urea (47.4% nitrogen) in the form of prills. Although there is slight variation in its specification depending on where it is purchased, the following data are reasonably representative.

It contains a maximum of 170 ppm ammonia and ammonium salts and has a melting point of  $130\text{--}132^\circ\text{C}$  (107) (c.f.  $132.6^\circ\text{C}$  for pure urea),

A 10% aqueous solution of the above urea gives a pH of 7.5-10.5 at  $20^\circ\text{C}$  (107) suggesting mild alkalinity. It is highly soluble in cold water (104.7 g per 100 g water) and even more so in hot. Density of urea is given as  $1.335\text{ g/cm}^3$  (53).

### 3. ANALYTICAL REAGENTS

All reagents used for chemical analysis were of AR grade with the following exceptions.

Thymolphthalien	pH 9.3 - 10.5
Sodium Sulphite	Technical Grade Crystals
Hydrochloric Acid, N	AVS Grade

Alcohol used in some of the analyses (Appendix 9) was of industrial grade. However any available grade can be used as 'Blanks' are carried out in the analytical procedure.

## APPENDIX 7

### LISTING OF COMPUTER PROGRAMS

Appendix 7 includes the listing of the following programs.

1. Aston simulation program (ASP)
2. Program for solution of UF kinetics for reactions going to TMU formation.
3. Program for solution of UF kinetics for reactions going to DMU formation.
4. Program for optimisation of rate constants for reaction going to TMU formation.
5. Program for optimisation of rate constants for reactions going to DMU formation.
6. Program for solution of plug-flow models for U:F molar ratio of 1:1.33.
7. Program for solution of plug-flow models for U:F molar ratio of 1:2.2.
8. Program for solution of complex models for U:F molar ratio of 1:1.33.
9. Program for solution of complex models for U:F molar ratio of 1:2.2.

Most of the programs are self explanatory. Logic diagrams for the programs are presented in Chapters 3 and 4.

The symbols used in the programs correspond with those used in the text wherever possible. However, where

this could not be done the symbols have been defined, with the exception of the program for solution of complex models which has the following list of symbols.

DP, DQ, DR and DS referring to various diffusivities, EL to reactor lengths, R1 to internal tube radius, R2 to density, ROU to external tube radius and Q, Z, HP and Y to dimensionless quantities of F, U, UF1 and T.

A S T O N S I M U L A T I O N P R O G R A M

LISTING OF PROGRAM USED FOR SOLUTION OF A SET OF  
DIFFERENTIAL EQUATIONS.

SUBROUTINE FOR INITIALISATION OF INDEPENDANT VARIABLE.

```
SUBROUTINE ZERO(TD)
COMMON/CINT/T,DT,JS,JN,DXA(20),XA(20),IO,JS4
T=0.
JS=0
JS4=0
TD=0.
DO 1 I=1,20
DXA(I)=0.
XA(I)=0.
1 CONTINUE
RETURN
END
```

SUBROUTINE FOR PRINT INTERVAL AND EXIT CONDITION  
SPECIFICATION

```
SUBROUTINE PRINTF(PRI,FNR,I1,I2)
COMMON/CINT/T,DT,JS,JN,DXA(20),XA(20),IO,JS4
IF(T.EQ.0.) GO TO 4
IF((T.GE.TPRNT-DT/2.).AND.((JS.EQ.2).OR.(JS4.EQ.4))) GOTO 5
I2=1
RETURN
4 I1=1
TPRNT=0.
5 I2=2
TPRNT=TPRNT+PRI
IF(T.GE.FNR) GOTO 6
RETURN
```

```

6 TPRNT=0.
  T=0.
  I1=2
  RETURN
  END

```

SUBROUTINE FOR SPECIFICATION OF INTEGRATION STEP LENGTH AND TECHNIQUE.

```

SUBROUTINE INTI(TD,DTD,K5)
COMMON/CINT/T,DT,JS,JN,DXA(20),XA(20),IO,JS4
IO=K5
JN=0
IF(IO.EQ.4) GOTO 1
JS=JS+1
IF(JS.EQ.3) JS=1
IF(JS.EQ.2) RETURN
DT=DTD
TD=TD+DT
T=DT
RETURN
1 JS4=JS4+1
  IF(JS4.EQ.5) JS4=1
  IF(JS4.EQ.1) GOTO 2
  IF(JS4.EQ.3) GOTO 4
  RETURN
2 DT=DTD/2.
  GO TO 3
4 TD=TD+DT
  DT=2.*DT
  T=TD
  RETURN
  END

```

SUBROUTINE FOR INTEGRATION OF DEPENDANT VARIABLES.

```

SUBROUTINE INTX(X,DX)
COMMON/CINT/T,DT,JS,JN,DXA(20),XA(20),IO,JS4
JN=JN+1
IF(IO.EQ.4) GOTO 3
GOTO (1,2),JS
1 DXA(JN)=DX
  X=X+DX*DT
  RETURN
2 X=X+(DX-DXA(JN))*DT/2.
  RETURN
3 GOTO (4,5,6,7),JS4
4 XA(JN)=X
  DXA(JN)=DX
  X=X+DX*DT
  RETURN
5 DXA(JN)=DXA(JN)+2.*DX
  X=XA(JN)+DX*DT
  RETURN
6 DXA(JN)=DXA(JN)+2.*DX
  X=XA(JN)+DX*DT

```

```
RETURN
7 DXA(JN)=(DXA(JN)+DX)/6
X=XA(JN)+DXA(JN)*DT
RETURN
END
FINISH
```

```

1  REM          "SOLUTION OF KINETIC EQUATIONS"
2  REM
3  REM          "PROGRAM FOR REACTIONS GOING TO TMU FORMATION"
4  REM
5  REM          "SYMBOLS GENERALLY AS DESCRIBED IN TEXT"
6  REM          "TIME UNITS-MIN., CONCENTRATION-MOL/LIT"
7  REM          "TEMPERATURE-K"
8  REM          "COMPUTER-HONEYWELL 316, LANGUAGE-BASIC"
25  T1=80
30  T2=T1+273
31  REM
32  REM
33  REM          "RATE CONSTANTS SPECIFICATION"
34  REM
35  REM
45  G1=-6542.5
47  G2=-9562.15
49  G3=-7045.8
51  G4=-9562.15
60  K1=((10+5.18)*EXP(G1/T2))*60
70  K2=((10+6.31)*EXP(G2/T2))*60
80  K3=((10+4.26)*EXP(G3/T2))*60
90  K4=((10+7.15)*EXP(G4/T2))*60
100  K6=K1/9
110  K5=(1.2/9)*K1
113  REM
114  REM
115  REM          "INITIAL CONDITIONS"
116  REM
117  REM
120  F0=10.497
130  U0=4.767
135  F=F0
137  U=U0
140  M1=0
150  M2=0
155  PRINT
160  PRINT
165  PRINT TAB(5);"T";TAB(20);"F";TAB(35);"U";TAB(50);"MMU"
170  REM
171  REM
172  REM          "INITIALISATION SECTION"
173  REM
174  REM
200  CALL (1,T)
204  REM
205  REM          "DIFFERENTIAL EQUATIONS
206  REM
210  A=(-K1*U*F)+(M1*(K2-(K3*F)))
220  A1=(3*(U0-U)+(F-F0)-2*M1)
230  B=A1*(-K4+(K5*F))
240  B1=(2*(U-U0)+(F0-F)+M1)
250  C=K6*B1
260  D1=(A-B)+C
270  D2=((-K1*U)*F)+(K2*M1)
280  C1=(K1*U)*F
290  C2=K4*A1
300  C3=(K2+(K3*F))*M1
310  D3=(C1-C3)+C2

```

```

314 REM
315 REM          "PRINT INTERVAL AND EXIT CONDITIONS"
316 REM
320 CALL (2,5,35,L1,L2)
330 IF L1=2 THEN 450
340 IF L2=2 THEN 360
350 GOTO 390
360 PRINT
370 PRINT T,TAB(15);F;TAB(23);U;TAB(45);M1
380 PRINT
384 REM
385 REM          "STEP LENGTH AND INTEGRATION TECHNIQUE"
386 REM
390 CALL (3,T,.1,4)
394 REM
395 REM          "INTEGRATION SECTION"
396 REM
400 CALL (4,F,D1)
410 CALL (4,U,D2)
420 CALL (4,M1,D3)
430 GOTO 210
450 IF T1>60 THEN 500
460 T1=T1+25
470 GOTO 30

```

```

1 REM "SOLUTION OF KINETIC EQUATIONS"
2 REM
3 REM "PROGRAM FOR REACTIONS GOING TO DMU FORMATION"
4 REM
5 REM "SYMBOLS GENERALLY AS DESCRIBED IN TEXT"
6 REM
7 REM "TIME UNITS-MIN., CONCENTRATION-MOL/LIT"
8 REM "TEMPERATURE-K"
9 REM "COMPUTER - HONEYWELL 316, LANGUAGE - BASIC"
10 REM T1=40
11 T2=T1+273
12 PRINT TAB(25);"FOR TEMPERATURE=";T1;"CELSIUS"
13 REM "RATE CONSTANTS SPECIFICATION"
14 K1=((1015.18)*EXP(-6542.5/T2))*60
15 K2=((1016.31)*EXP(-9562.15/T2))*60
16 K3=((1014.26)*EXP(-7045.8/T2))*60
17 K4=((1017.15)*EXP(-9562.15/T2))*60
18 REM "INITIAL CONDITIONS"
19 U0=6.90732
20 F0=9.1867
21 M1=0
22 M2=0
23 PRINT
24 PRINT
25 PRINT TAB(5);"T";TAB(20);"F";TAB(35);"U";TAB(50);"MMU";TAB(65);"DMU"
26 PRINT
27 U=U0
28 F=F0
29 REM "INITIALISATION SECTION"
30 CALL (1,I
31 REM "DIFFERENTIAL EQUATIONS"
32 REM
33 REM
34 REM
35 A=-K1*U*F-K3*F*((F-2*U)+(2*U0-F))
36 B=K2*((F-2*U)+(2*U0-F))+K4*((U-F)-(U0-F))
37 D1=A+B
38 D2=-K1*U*F+K2*(2*(U0-U)-(F0-F))
39 C=K1*U*F-K2*(2*(U0-U)-(F0-F))

```

```

40 E=K4*((F0-F)-(U0-U))-K3*F*(2*(U0-U)-(F0-F))
41 D3=C+E
42 D4=K3*F*((F-2*U)+(2*U0-F0))-K4*((U-F)+(F0-U0))
43 REM
44 REM          "PRINT INTERVAL AND EXIT CONDITIONS"
45 CALL (2,10,120,L1,L2)
50 IF L1=2 THEN 85
55 IF L2=2 THEN 65
60 GOTO 70
65 PRINT
66 PRINT T,TAB(15);F;TAB(30);U;TAB(45);M1;TAB(60);M2
67 PRINT
68 PRINT
69 REM          "STEP LENGTH AND INTEGRATION TECHNIQUE"
70 CALL (3,T,.2,4)
71 REM
72 REM          "INTEGRATION SECTION"
73 REM
74 CALL (4,F,D1)
75 CALL (4,U,D2)
76 CALL (4,M1,D3)
77 CALL (4,M2,D4)
80 GOTO 35
85 IF T1>60 THEN 110
90 T1=T1+20
100 GOTO 12
110 STOP

```

CURVE FITTING USING HELDER AND HEAD MINIMISATION ROUTINE

PROGRAM TO OPTIMIZE RATE CONSTANTS  
FOR REACTIONS GOING TO TMU FORMATION.

DIMENSION X(7,7),XCEN(7,7),XREF(7,7),XCON(7,7),XEX(7,7),Z(7),E(12)

NI=1  
NO=2

001 READ(NI,001) N,ITHAX,IPRINT  
FORMAT(8I110)

NP1=N+1

READ(NI,002) ALFA,BETA,GAM,ACC,A

READ(NI,002) (X(1,J), J=1,N)

WRITE(NO,002) (X(1,J), J=1,N)

READ(NI,002) (E(J), J=1,7)

WRITE(NO,002) (E(J), J=1,7)

002 FORMAT(8F10.4)

Q=(A/N\*(2.\*\*.5))\*((N+1)\*\*.5+1.)

P=(A/N\*(2.\*\*.5))\*((N+1)\*\*.5+N\*1.)

M=N+1

DO 130 I=2,N

AP=1.0

DO 120 J=1,N

AP=AP+1

IF(I.EQ.AP)GO TO 135

X(I,J)=X(1,J)+Q

GO TO 120

135 X(I,J)=X(1,J)+P

120 CONTINUE

130 CONTINUE

```

IF(ALFA.EQ.0.)ALFA=1.
IF(BETA.EQ.0.)BETA=.5
IF(GAM.EQ.0.)GAM=2.
IF(ACC.EQ.0.)ACC=.0001

```

```

WRITE(NO,003)
003 FORMAT(1H1,10X,28HHELDER AND MEAD OPTIMISATION )
WRITE(NO,004)
004 FORMAT(/,2X,10HPARAMETERS )
WRITE(NO,005) N,ACC,ALFA,BETA,GAM
005 FORMAT(/,2X,4H1 = ,I2,4X,11HACCURACY = ,E10.4,/,2X,8HALPHA = ,
1E10.4,4X,7HBETA = ,E10.4,4X,8HGAMMA = ,E10.4)
WRITE(NO,007)
007 FORMAT(/,10X,16HSTARTING SIMPLEX )
DO 140 I=1, NP1
WRITE(NO,006) (I,J,X(I,J), J=1,N)
006 FORMAT(/,5(2X,2HX(,I2,1H,,I2,4H) = ,1PE12,5))
140 CONTINUE
ITR=0
150 DO 155 I=1, NP1
CALL FUNC(I,X,Z,N,NP1,E)
155 CONTINUE
ITR=ITR+1
IF(ITR.GE.ITMAX)GO TO 145.
IF(IPRINT)158,162,158
158 WRITE(NO,008)ITR
008 FORMAT(/,2X,17HITERATION NUMBER ,I3)
DO 160 J=1, NP1
160 WRITE(NO,006) (J,I,X(J,I), I=1,N)
WRITE(NO,009) (I,Z(I), I=1, NP1)
009 FORMAT(/,3(2X,2HF(,I2,4H) = ,E16.8))

162 ZHI=AMAX1(Z(1),Z(2),Z(3),Z(4),Z(5),Z(6),Z(7))
ZLO=AMIN1(Z(1),Z(2),Z(3),Z(4),Z(5),Z(6),Z(7))
DO 165 I=1, NP1
IF(ZHI.EQ.Z(I))GO TO 170
165 CONTINUE

170 K=I
EN=N
DO 180 J=1, N
SUM=0.
DO 175 I=1, NP1
IF(K.EQ.I)GO TO 175
SUM=SUM+X(I,J)
175 CONTINUE
180 XCEN(K,J)=SUM/EN
I=K
CALL FUNC(I,X,Z,N,NP1,E)
ZCEN=Z(I)
SUM=0.
DO 185 I=1, NP1
IF(K.EQ.I)GO TO 185
SUM=SUM+(Z(I)-ZCEN)*(Z(I)-ZCEN)/EN
185 CONTINUE
EJ=SQRT(SUM)
IF (EJ.LT.ACC)GO TO 998
IF (ZHI.LT.0.01) GO TO 700
DO 190 J=1, N
XREF(K,J)=XCEN(K,J)+ALFA*(XCEN(K,J)-X(K,J))
190 CONTINUE
I=K
CALL FUNC(I,X,Z,N,NP1,E)
ZREF=Z(I)
DO 200 I=1, NP1
IF(ZLO.EQ.Z(I))GO TO 205
200 CONTINUE

```

```

205 L=1
   IF(ZREF.LT.Z(L))GO TO 240
   DO 207 I=1,NP1
   IF(ZREF.LT.Z(I))GO TO 208
207 CONTINUE
   GO TO 215
208 DO 210 J=1,N
210 X(K,J)=XREF(K,J)
   GO TO 150
215 DO 220 J=1,N
220 XCON(K,J)=XCEN(K,J)+BETA*(X(K,J)-XCEN(K,J))
   I=K
   CALL FUNC(I,X,Z,N,NP1,E)
   ZCON=Z(I)
   IF(ZCON.LT.Z(K))GO TO 230
   DO 225 J=1,N
   DO 225 I=1,NP1
225 X(I,J)=(X(I,J)+X(L,J))/2.
   GO TO 150
230 DO 235 J=1,N
235 X(K,J)=XCON(K,J)
   GO TO 150
240 DO 245 J=1,N
245 XEX(K,J)=XCEN(K,J)+GAM*(XREF(K,J)-XCEN(K,J))
   I=K
   CALL FUNC(I,X,Z,N,NP1,E)
   ZEX=Z(I)
   IF(ZEX.LT.Z(L))GO TO 255
   DO 250 J=1,N
250 X(K,J)=XREF(K,J)
   GO TO 150
255 DO 260 J=1,N
260 X(K,J)=XEX(K,J)
   GO TO 150
950 FORMAT(///,10X,38HLEAST SQUARE ERROR CRITERIA SATISFIED. )
700 WRITE(NO,950)
   GO TO 998

145 WRITE(NO,011)ITNAX
011 FORMAT(///,10X,20HDID NOT CONVERGE IN ,I5,11HITERATIONS. )
998 WRITE(NO,012)ZLO
012 FORMAT(//,2X,21HOPTIMUM VALUE OF F = ,E16.8)
   WRITE(NO,013)
013 FORMAT(//,2X,27HOPTIMUM VALUE OF VARIABLES. )
   DO 300 I=1,N
300 WRITE(NO,014) I,X(NP1,I)
014 FORMAT(/,2X,2HX(,I2,4H) = ,1PE16.8)
   END

```

SUBROUTINE TO SPECIFY OBJECTIVE  
FUNCTION FOR MINIMISATION.

SUBROUTINE FUNC (I,X,Z,N,NP1,E)

```

DIMENSION X(7,7),Z(7),E(12),Q(12)
X1=X(I,1)
X2=X(I,2)
X3=X(I,3)
X4=X(I,4)
X5=X(I,5)
X6=X(I,6)
K=0
S = 0.0
T1=30.0
T2=T1+273.

```

```

R1=((10.**5.18)*EXP(-6542.5/T2))*60.
R2=((10.**6.31)*EXP(-9562.15/T2))*60.
R3=((10.**4.26)*EXP(-7045.8/T2))*60.
R4=((10.**7.15)*EXP(-9562.15/T2))*60.
R5=R1*(1.2/0.)
R6=R1/9.
U0=4.7670
F0=10.4970
G1=0.0
U=U0
F=F0
C1=X1*R1
C2=X2*R2
C3=X3*R3
C4=X4*R4
C5=X5*R5
C6=X6*R6

CALL ZERO(T)
20 A=(-C1*U*F)+(G1*(C2-(C3*F)))
A1=(3.0*(U0-U)+(F-F0)-2.0*G1)
B=A1*(-C4+(C5*F))
B1=(2.0*(U-U0)+(F0-F)+G1)
C=C6*B1
D1=(A-B)+C
D2=((-C1*U)*F)+(C2*G1)
V1=(C1*U)*F
V2=C4*A1
V3=(C2+(C3*U))*G1
D3=(V1-V3)+V2

CALL PRNTE(5.,30.,L1,L2)
IF(L2.EQ.1) GO TO 50
30 K=K+1
Q(K)=F
WRITE(NO,70) K,Q(K)
70 FORMAT(/,2X,2HQ(,I3,4H) = ,E16.8)
50 CONTINUE
IF (L1.EQ.2) GO TO 80
CALL INTI(T,0.1,4)

CALL INTX(F,D1)
CALL INTX(U,D2)
CALL INTX(G1,D3)
GO TO 20

80 DO 90 J=1,7
S=S+(Q(J)-E(J))**2
90 CONTINUE
WRITE(NO,60) S
60 FORMAT(/,2X,14H S VALUE IS = ,E16.8)
Z(I)=S
RETURN
END
FINISH

```

CURVE FITTING USING NELDER AND MEAD MINIMISATION ROUTINE

PROGRAM TO OPTIMISE RATE CONSTANTS  
FOR REACTIONS GOING TO DMU FORMATION.

DIMENSION X(5,5),XGEN(5,5),XREF(5,5),XCON(5,5),XEX(5,5),Z(5),E(12)

NI=1  
NO=2

001 READ(NI,001) N,ITMAX,IPRINT  
FORMAT(G110)

NP1=N+1

READ(NI,002) ALFA,BETA,GAM,ACC,A

READ(NI,002) (X(1,J), J=1,N)

WRITE(NO,002) (X(1,J), J=1,N)

READ(NI,002) (E(J), J=1,7)

WRITE(NO,002) (E(J), J=1,7)

002 FORHAT(QF10.4)

Q=(A/N\*(2.\*\*.5))\*(N+1)\*\*.5+1.)

P=(A/N\*(2.\*\*.5))\*(N+1)\*\*.5+N-1.)

M=N+1

DO 130 I=2,M

AP=1.0

DO 120 J=1,N

AP=AP+1

IF(I.EQ.AP)GO TO 135

X(I,J)=X(1,J)\*Q

GO TO 120

135 X(I,J)=X(1,J)\*P

120 CONTINUE

130 CONTINUE

```

IF(ALFA.EQ.0.)ALFA=1.
IF(BETA.EQ.0.)BETA=.5
IF(GAM.EQ.0.)GAM=2,
IF(ACC.EQ.0.)ACC=.0001

WRITE(N0,003)
003 FORMAT(1H1,10X,28HNELDER AND HEAD OPTIMISATION )
WRITE(N0,004)
004 FORMAT(/,2X,10HPARAMETERS )
WRITE(N0,005) N,ACC,ALFA,BETA,GAM
005 FORMAT(/,2X,4HN = ,I2,4X,11HACCURACY = ,E10.4,/,2X,8HALPHA =
1E10.4,4X,7HBETA = ,E10.4,4X,8HGAMMA = ,E10.4)
WRITE(N0,007)
007 FORMAT(/,10X,16HSTARTING SIMPLEX )
DO 140 I=1, NP1
WRITE(N0,006) (I,J,X(I,J), J=1,N)
006 FORMAT(/,5(2X,2HX(,I2,1H,,I2,4H) = ,1PE12,5))
140 CONTINUE
ITR=0
150 DO 155 I=1, NP1
CALL FUNC(I,X,Z,N, NP1,E)
155 CONTINUE
ITR=ITR+1
IF(ITR.GE.ITMAX)GO TO 145
IF(IPRINT)158,162,158
158 WRITE(N0,008)ITR
008 FORMAT(/,2X,17HITERATION NUMBER ,I3)
DO 160 J=1, NP1
160 WRITE(N0,006) (J,I,X(J,I), I=1,N)
WRITE(N0,009) (I,Z(I), I=1, NP1)
009 FORMAT(/,3(2X,2HF(,I2,4H) = ,E16.8))

162 ZHI = AMAX1(Z(1),Z(2),Z(3),Z(4),Z(5))
ZLO = AMIN1(Z(1),Z(2),Z(3),Z(4),Z(5))
DO 165 I=1, NP1
IF(ZHI.EQ.Z(I))GO TO 170
165 CONTINUE

170 K=I
EN=N
DO 180 J=1,N
SUM=0.
DO 175 I=1, NP1
IF(K.EQ.I)GO TO 175
SUM=SUM+X(I,J)
175 CONTINUE
180 XCEN(K,J)=SUM/EN
I=K
CALL FUNC(I,X,Z,N, NP1,E)
ZCEN=Z(I)
SUM=0.
DO 185 I=1, NP1
IF(K.EQ.I)GO TO 185
SUM=SUM+(Z(I)-ZCEN)*(Z(I)-ZCEN)/EN
185 CONTINUE
EJ=SQRT(SUM)
IF (EJ.LT.ACC)GO TO 998
IF (ZHI.LT.0.01) GO TO 700
DO 190 J=1,N
XREF(K,J)=XCEN(K,J)+ALFA*(XCEN(K,J)-X(K,J))
190 CONTINUE
I=K
CALL FUNC(I,X,Z,N, NP1,E)
ZREF=Z(I)
DO 200 I=1, NP1
IF(ZLO.EQ.Z(I))GO TO 205
200 CONTINUE

```

```

205 L=I
   IF(ZREF.LE.Z(L))GO TO 240
   DO 207 I=1,HP1
   IF(ZREF.LT.Z(I))GO TO 208
207 CONTINUE
   GO TO 215
208 DO 210 J=1,N
210 X(K,J)=XREF(K,J)
   GO TO 150
215 DO 220 J=1,N
220 XCON(K,J)=XCEN(K,J)+BETA*(X(K,J)-XCEN(K,J))
   I=K
   CALL FUNC(I,X,Z,N,HP1,E)
   ZCON=Z(I)
   IF(ZCON.LT.Z(K))GO TO 230
   DO 225 J=1,N
   DO 225 I=1,HP1
225 X(I,J)=(X(I,J)+X(L,I))/2.
   GO TO 150
230 DO 235 J=1,N
235 X(K,J)=XCON(K,J)
   GO TO 150
240 DO 245 J=1,N
245 XEX(K,J)=XCEN(K,J)+GAM*(XREF(K,J)-XCEN(K,J))
   I=K
   CALL FUNC(I,X,Z,N,HP1,E)
   ZEX=Z(I)
   IF(ZEX.LT.Z(L))GO TO 255
   DO 250 J=1,N
250 X(K,J)=XREF(K,J)
   GO TO 150
255 DO 260 J=1,N
260 X(K,J)=XEX(K,J)
   GO TO 150
950 FORMAT(///,10X,38HLEAST SQUARE ERROR CRITERIA SATISFIED.)
700 WRITE(NO,950)
   GO TO 998

145 WRITE(NO,011)ITHAX
011 FORMAT(///,10X,20HDID NOT CONVERGE IN ,I5,11HITERATIONS.)
998 WRITE(NO,012)ZLO
012 FORMAT(//,2X,21HOPTIMUM VALUE OF F = ,E16.8)
   WRITE(NO,013)
013 FORMAT(//,2X,27HOPTIMUM VALUE OF VARIABLES.)
   DO 300 I=1,N
300 WRITE(NO,014) I,X(HP1,I)
014 FORMAT(/,2X,2HX(,I2,4H) = ,1PE16.8)
   END

```

SUBROUTINE TO SPECIFY OBJECTIVE  
FUNCTION FOR MINIMISATION.

```

SUBROUTINE FUNC (I,X,Z,H,NP1,E)

DIMENSION X(5,5),Z(5),E(12),Q(12)
X1=X(I,1)
X2=X(I,2)
X3=X(I,3)
X4=X(I,4)
K=0
S = 0.0
T1=40.
T2=T1+273.

R1=((10.**5.18)*EXP(-6542.5/T2))*60.
R2=((10.**6.31)*EXP(-9562.15/T2))*60.
R3=((10.**4.26)*EXP(-7045.8/T2))*60.
R4=((10.**7.15)*EXP(-9562.15/T2))*60.
U0=6.90732
F0=9.18673
U=U0
F=F0
C1=X1*R1
C2=X2*R2
C3=X3*R3
C4=X4*R4

CALL ZERO(T)
20 A=-C1*U+F-C3*F*((F-2.*U)+(2.*U0-F0))
B=C2*((F-2.*U)+(2.*U0-F0))+C4*((U-F)-(U0-F0))
D1=A+B
D2=-C1*U+F+C2*(2.*(U0-U)-(F0-F))

CALL PRNTE(10.,60.,L1,L2)
IF(L2.EQ.1) GO TO 50
30 K=K+1
Q(K)=F
WRITE(NO,70) K,Q(K)
70 FORMAT(/,2X,2HQ(,I3,4H) = ,E16.8)
50 CONTINUE
IF (L1.EQ.2) GO TO 80
CALL INTI(T,1.0,4)

CALL INTX(F,D1)
CALL INTX(U,D2)
GO TO 20

80 DO 90 J=1,7
S=S+(Q(J)-E(J))**2
90 CONTINUE
WRITE(NO,60) S
60 FORMAT(/,2X,14H S VALUE IS = ,E16.8)
Z(I)=S
RETURN
END
FINISH

```

```

1  REM          "SOLUTION OF PLUG - FLOW MODELS"
2  REM
3  REM          "PROGRAM FOR U TO F MOLAR RATIO OF 1 TO 1.33"
4  REM
5  REM          "SYMBOLS GENERALLY AS DESCRIBED IN TEXT"
6  REM          "OTHER SYMBOLS ARE, R1-RADIUS, T3-STEAM"
7  REM          "TEMPERATURE, R2-DENSITY, H1-HEAT OF REACTION"
8  REM
9  REM          "UNITS OF USE, C.G.S., CONCENTRATION-MOL. /CM3"
10 REM
11 REM          "COMPUTER-HONEYWELL 316, LANGUAGE-BASIC"
12 REM
13 V0=91.13
14 K=14/104
15 R1=.3175
16 T3=393
18 H1=-6000
20 R2=.2E-01
22 S=22.844
24 T0=307
26 F0=.644E-02
28 U0=.4832E-02
29 U1=0
30 T2=T0
32 U=U0
34 F=F0
35 PRINT
36 PRINT
40 PRINT TAB(5);"X";TAB(20);"F";TAB(35);"U";TAB(50);"T"
41 REM
42 REM
43 REM          "INITIALISATION SECTION"
44 REM
45 CALL (1,X)
46 REM
47 REM
48 REM          "TEMPERATURE KINETICS RELAY SECTION"
49 REM
50 IF X>910 THEN 52
51 GOTO 54
52 V0=14.58
53 R1=.79374
54 IF T2<308 THEN 60
55 GOTO 90
60 Q1=.8534
65 Q2=1.00341
70 Q3=.10341
75 Q4=1.0144
80 Q5=0
85 Q6=0
87 GOTO 329
90 IF T2>323 THEN IF T2<343 GOTO 100
95 GOTO 140
100 Q1=.903
105 Q2=1.0034
110 Q3=1.00341
115 Q4=1.0144
120 Q5=0
125 Q6=0
130 GOTO 329

```

```

140 IF T2>323 THEN IF T2<342 GOTO 150
145 GOTO 190
150 Q1=1.0068
155 Q2=1.0068
160 Q3=4.0068
165 Q4=1.0289
170 Q5=0
175 Q6=0
180 GOTO 329
190 IF T2>343 THEN IF T2<383 GOTO 200
195 GOTO 240
200 Q1=1.0136
205 Q2=1.0136
210 Q3=5.0136
215 Q4=5.0578
220 Q5=0
225 Q6=0
230 GOTO 329
240 IF T2>383 THEN IF T2<405 GOTO 250
245 GOTO 290
250 Q1=1
255 Q2=1
260 Q3=5
265 Q4=1
270 Q5=.8333
275 Q6=.2
280 GOTO 500
290 IF T2>405 THEN 300
295 GOTO 500
300 Q1=1
305 Q2=1
310 Q3=8
315 Q4=4
320 Q5=.8333
325 Q6=1.2
326 GOTO 500
327 REM "PLUG-FLOW MODELS"
328 REM "RATES TO DIMETHYLOUREA"
329 REM
335 K1=Q1*((1015.18)*EXP(-6542.5/T2))*1000
340 K2=Q2*((1016.31)*EXP(-9562.15/T2))
345 K3=Q3*((1014.26)*EXP(-7045.8/T2))*1000
350 K4=Q4*((1017.15)*EXP(-9562.15/T2))
355 K5=0
360 K6=0
365 U1=2*(U0-U)-(F0-F)
370 U2=(U-F)-(U0-F0)
375 U3=0
380 G1=K1*U*F
385 G2=K2*U1
390 G3=K3*F*U1
395 G4=K4*U2
400 G5=0
405 G6=0
406 REM
410 D1=(-G1+G2)/V0
415 D2=(-G1-G3+G2+G4)/V0
420 D3=0
425 R3=G1+G3-G2-G4
430 C3=((K*4.634*(T3-T2)/R112))-H1*R3
435 D4=C3/(R2*S*V0)
440 GOTO 675

```

```

445 REM
446 REM
447 REM          "PLUG-FLOW MODELS"
448 REM          "RATES TO TRIMETHYLOLUREA"
449 REM
450 REM
500 K1=Q1*((10+5.18)*EXP(-6542.5/T2))*1000
510 K2=Q2*((10+6.31)*EXP(-9562.15/T2))
520 K3=Q3*((10+4.26)*EXP(-7045.8/T2))*1000
530 K4=Q4*((10+7.15)*EXP(-9562.15/T2))
540 K5=Q5*(1.2/9)*K1
541 K6=Q6*(K1/9)
570 U2=3*(U0-U)+(F-F0)-2*U1
580 U3=2*(U-U0)+(F0-F)+U1
590 G1=K1*U*F
600 G2=K2*U1
610 G3=K3*F*U1
620 G4=K4*U2
630 G5=K5*F*U2
640 G6=K6*U3
645 D1=(-G1+G2)/V0
650 D2=(-G1-G3-G5+G2+G4+G6)/V0
655 D3=(-G2+G1-G3+G4)/V0
660 R3=G1-G2+G3-G4+G5-G6
665 C3=((K*4.364*(T3-T2)/R1+2))-H1*R3
670 D4=C3/(R2*S*V0)
671 REM
672 REM
673 REM          "PRINT INTERVAL & EXIT CONDITIONS"
674 REM
675 CALL (2,10,1170,L1,L2)
680 IF L1=2 THEN 900
685 IF L2=2 THEN 700
690 GOTO 725
700 PRINT
710 PRINT X,TAB(15);F;TAB(30);U;TAB(45);T2
715 PRINT
720 PRINT
722 REM
723 REM
724 REM
725 REM          "INTEGRATION SECTION"
726 IF X>910 GOTO 728
727 GOTO 750
728 CALL (3,X,1,4)
729 GOTO 800
750 CALL (3,X,5,4)
800 CALL (4,F,D2)
810 CALL (4,U,D1)
820 CALL (4,U1,D3)
830 CALL (4,T2,D4)
850 GOTO 46
900 STOP

```

```

1  REM          "SOLUTION OF PLUG - FLOW MODELS"
2  REM
3  REM          "PROGRAM FOR U TO F MOLAR RATIO OF 1 TO 2.2"
4  REM
5  REM          "SYMBOLS GENERALLY AS DESCRIBED IN TEXT"
6  REM          "OTHER SYMBOLS ARE, R1-RADIUS, T3-STEAM"
7  REM          "TEMPERATURE, R2-DENSITY, H1-HEAT OF REACTION"
8  REM
9  REM          "UNITS OF USE, C.G.S., CONCENTRATION-MOL. /CM3"
10 REM
11 REM          "COMPUTER-HONEYWELL 316, LANGUAGE-BASIC"
12 REM
13 V0=45.57
14 K=14/1014
15 R1=.3175
16 T3=413
18 H1=-6000
20 R2=.2E-01
22 S=22.844
24 T0=298
26 F0=.8084E-02
28 U0=.36745E-02
29 U1=0
30 T2=T0
32 U=U0
34 F=F0
35 PRINT
36 PRINT
40 PRINT TAB(5);"X";TAB(20);"F";TAB(35);"U";TAB(50);"T"
41 REM
42 REM
43 REM          "INITIALISATION SECTION"
44 REM
45 CALL (1,X)
46 REM
47 REM
48 REM          "TEMPERATURE KINETICS RELAY SECTION"
49 REM
50 IF X>910 THEN 52
51 GOTO 54
52 V0=7.29
53 R1=.79374
54 IF T2<323 THEN 60
55 GOTO 90
60 Q1=1
65 Q2=1
70 Q3=1
75 Q4=1
80 Q5=.8333
85 Q6=1.2
87 GOTO 500
90 IF T2>323 THEN IF T2<343 GOTO 100
95 GOTO 140
100 Q1=.6
105 Q2=5
110 Q3=5
115 Q4=10
120 Q5=16.6667
125 Q6=24
130 GOTO 500

```

```

140 IF T2>343 THEN IF T2<363 GOTO 150
145 GOTO 190
150 Q1=5
155 Q2=5
160 Q3=40
165 Q4=40
170 Q5=.83E-02
175 Q6=.12E-01
180 GOTO 500
190 IF T2>363 THEN IF T2<383 GOTO 200
195 GOTO 240
200 Q1=1
205 Q2=1
210 Q3=80
215 Q4=30
220 Q5=16.6667
225 Q6=12
230 GOTO 500
240 IF T2>383 THEN IF T2<405 GOTO 250
245 GOTO 290
250 Q1=1.2
255 Q2=1
260 Q3=150
265 Q4=40
270 Q5=50
275 Q6=12
280 GOTO 500
290 IF T2>405 THEN 300
295 GOTO 500
300 Q1=.7
305 Q2=1
310 Q3=8
315 Q4=4
320 Q5=1.0833
325 Q6=1.56
326 GOTO 500
327 REM "PLUG-FLOW MODELS"
328 REM "RATES TO DIMETHYLOUREA"
329 REM
335 K1=Q1*((10+.18)*EXP(-6542.5/T2))*1000
340 K2=Q2*((10+.31)*EXP(-9562.15/T2))
345 K3=Q3*((10+.26)*EXP(-7045.8/T2))*1000
350 K4=Q4*((10+.15)*EXP(-9562.15/T2))
355 K5=0
360 K6=0
365 U1=2*(U0-U)-(F0-F)
370 U2=(U-F)-(U0-F0)
375 U3=0
380 G1=K1*U*F
385 G2=K2*U1
390 G3=K3*F*U1
395 G4=K4*U2
400 G5=0
405 G6=0
406 REM
410 D1=(-G1+G2)/V0
415 D2=(-G1-G3+G2+G4)/V0
420 D3=0
425 R3=G1+G3-G2-G4
430 C3=((K*4.634*(T3-T2)/R1+2))-H1*R3
435 D4=C3/(R2*S*V0)
440 GOTO 675

```

```

445 REM
446 REM
447 REM          "PLUG-FLOW MODELS"
448 REM          "RATES TO TRIMETHYLOLUREA"
449 REM
450 REM
500 K1=Q1*((10+5.18)*EXP(-6542.5/T2))*1000
510 K2=Q2*((10+6.31)*EXP(-9562.15/T2))
520 K3=Q3*((10+4.26)*EXP(-7045.8/T2))*1000
530 K4=Q4*((10+7.15)*EXP(-9562.15/T2))
540 K5=Q5*(1.2/9)*K1
541 K6=Q6*(K1/9)
570 U2=3*(U0-U)+(F-F0)-2*U1
580 U3=2*(U-U0)+(F0-F)+U1
590 G1=K1*U*F
600 G2=K2*U1
610 G3=K3*F*U1
620 G4=K4*U2
630 G5=K5*F*U2
640 G6=K6*U3
645 D1=(-G1+G2)/V0
650 D2=(-G1-G3-G5+G2+G4+G6)/V0
655 D3=(-G2+G1-G3+G4)/V0
660 R3=G1-G2+G3-G4+G5-G6
665 C3=((K*4.364*(T3-T2)/R1+2))-H1*R3
670 D4=C3/(R2*S*V0)
671 REM
672 REM
673 REM          "PRINT INTERVAL & EXIT CONDITIONS"
674 REM
675 CALL (2,10,1170,L1,L2)
680 IF L1=2 THEN 900
685 IF L2=2 THEN 700
690 GOTO 725
700 PRINT
710 PRINT X,TAB(15);F;TAB(30);U;TAB(45);T2
715 PRINT
720 PRINT
722 REM
723 REM
724 REM
725 REM          "INTEGRATION SECTION"
726 IF X>910 GOTO 728
727 GOTO 750
728 CALL (3,X,1,4)
729 GOTO 800
750 CALL (3,X,5,4)
800 CALL (4,F,D2)
810 CALL (4,U,D1)
820 CALL (4,U1,D3)
830 CALL (4,T2,D4)
850 GOTO 46
900 STOP

```

SOLUTION OF COMPLEX MODELS

PROGRAM FOR U:F MOLAR RATIO OF 1:1.33

COMMON/CONC/U0,F0,UFEQ,H1,S1,T0,R2  
 DIMENSION A(10),B(10),C(10),F(10),U(10),T(10)  
 DIMENSION D(10),E(10),G(10)  
 DIMENSION UF(10),HP(10),AF(10),UP(10)  
 DIMENSION V(6),Q(10),Y(10),Z(10)  
 DIMENSION P(10,20),R(10,20),S(10,20)

PHYSICAL DATA

V0=01.13  
 R1=0.3175  
 T3=393.  
 S1=22.844  
 H1=-6000.  
 EL=914.4  
 DP=1.43/(10.\*\*5.)  
 DQ=1.14/(10.\*\*5.)  
 DS=0.97/(10.\*\*5.)  
 DR=31.84/(10.\*\*4.)  
 U0=0.00482  
 F0=0.00644  
 UF10=0.0  
 UFEQ=0.00563  
 T0=307.  
 R2=.2E-01  
 H=0.2  
 HCS=0.0005027  
 ROU=0.4196

CALCULATED DATA

VFT=V0\*118.11  
 VELF=VFT\*\*(1./3.)  
 HTCF=VELF\*0.7495\*0.0001355  
 PHI=ROU/R1  
 W=EL/(2.\*V0\*(R1\*\*2.))  
 E1=DP\*U  
 E2=DQ\*U  
 E3=DR\*U  
 E4=DS\*W

INITIAL CONDITIONS

DO 100 I=1,6  
 U(I)=U0  
 F(I)=F0  
 UF(I)=UF10  
 Q(I)=1.  
 Z(I)=1.  
 HP(I)=0.0  
 100 CONTINUE  
 DO 110 I=1,5  
 T(I)=T0  
 Y(I)=1.  
 110 CONTINUE  
 T(6)=315.  
 Y(6)=T(6)/T0

VELOCITY PROFILE CALCULATION

```

DO 120 I=1,6
A7=(I-1)*H
V(I)=(1.-(A7**2.))
120 CONTINUE

```

INITIALISE CONTROLLING VARIABLES

```

1 NNN=1
  N1=11
  M1=6
  J=0
  N=1

```

INITIALISATION SECTION AND CONVERGENCE AID

```

CALL ZERO(X)
105 IF(X.GT.0.78) GO TO 106
    GO TO 109
106 EL=243.84
    V0=14.58
    K1=0.79375
    ROU=0.91821
    VFT=V0*118.11
    VELF=VFT*(1./3.)
    HTCf=VELF*0.8579*0.0001355
    HCS=0.0004186
    W=EL/(2.*V0*(R1**2.))
    E1=DP*W
    E2=DQ*W
    E3=DR*W
    E4=DS*W
    PHI=ROU/R1
109 IF(J.EQ.17)GO TO 10
    IF(J-4)10,20,30
    30 IF(J-8)10,40,50
    50 IF(J-12)10,60,70
    70 IF(J-16)10,80,10
    GO TO 10
    20 T(6)=340.
    Y(6)=T(6)/T0
    GO TO 10
    40 T(6)=393.
    Y(6)=T(6)/T0
    GO TO 10
    60 T(6)=393.
    Y(6)=T(6)/T0
    GO TO 10
    80 T(6)=393.
    Y(6)=T(6)/T0

```

POLYMERISATION RATE SECTION

```

10 DO 130 I=1,6
  T1=T(I)
  IF(T1.LT.303)CALL RATE1(T1,I,U(I),F(I),UF(I),A(I),B(I),C(I),AF(I),
1V0,EL)
  IF(T1.GT.303.AND.T1.LT.325)CALL RATE2(T1,I,U(I),F(I),UF(I),A(I),B
1I),C(I),AF(I),V0,EL)
  IF(T1.GT.325.AND.T1.LT.345)CALL RATE3(T1,I,U(I),F(I),UF(I),A(I),B
1I),C(I),AF(I),V0,EL)
  IF(T1.GT.345.AND.T1.LT.365)CALL RATE4(T1,I,U(I),F(I),UF(I),A(I),B
1I),C(I),AF(I),V0,EL)
  IF(T1.GT.365.AND.T1.LT.405)CALL RATE5(T1,I,U(I),F(I),UF(I),A(I),B
1I),C(I),AF(I),V0,EL)
  IF(T1.GT.405)CALL RATE6(T1,I,U(I),F(I),UF(I),A(I),B(I),C(I),AF(I),
1V0,EL)
130 CONTINUE

```

DIFFERENTIAL EQUATIONS

CENTRE LINE

```

B1=(Q(2)-Q(1))/(H**2.)
D(1)=((4.*B1*E1)/V(1))-(A(1)/V(1))
B2=(Z(2)-Z(1))/(H**2.)
E(1)=((4.*B2*E2)/V(1))-(B(1)/V(1))
B3=(Y(2)-Y(1))/(H**2.)
G(1)=((4.*B3*E3)/V(1))-(C(1)/V(1))
HPQ=(HP(2)-HP(1))/(H**2.)
WP(1)=((4.*HPQ*E4)/V(1))-(AF(1)/V(1))

```

INTERNAL GRID

```

DO 140 I=2,5
  B4=(Q(I+1)-(2.*Q(I))+Q(I-1))/(H**2.)
  B5=(Q(I+1)-Q(I-1))/(2.*(H**2.)*(I-1))
  D(I)=((E1/V(I))*(B4+B5))-(A(I)/V(I))
  B6=(Z(I+1)-(2.*Z(I))+Z(I-1))/(H**2.)
  B7=(Z(I+1)-Z(I-1))/(2.*(H**2.)*(I-1))
  E(I)=((E2/V(I))*(B6+B7))-(B(I)/V(I))
  B8=(Y(I+1)-(2.*Y(I))+Y(I-1))/(H**2.)
  B9=(Y(I+1)-Y(I-1))/(2.*(H**2.)*(I-1))
  G(I)=((E3/V(I))*(B8+B9))-(C(I)/V(I))
  HPS=(HP(I+1)-HP(I-1))/(2.*(H**2.)*(I-1))
  HPR=(HP(I+1)-(2.*HP(I))+HP(I-1))/(H**2.)
  WP(I)=((E4/V(I))*(HPR+HPS))-(AF(I)/V(I))
140 CONTINUE

```

PRINT, END VALUE, AND EXIT CONDITIONS

CALL PRNTE(0.1,1.0,L1,L2)  
IF(L1.EQ.2) GO TO 1000  
IF(L2.EQ.2) GO TO 1000

STEP LENGTH AND INTEGRATION TECHNIQUE

656 IF(X.GT.0.73) GO TO 658  
GO TO 659  
658 CALL INTI(X,0.0005,4)  
GO TO 222  
659 CALL INTI(X,0.002,4)

INTEGRATION SECTION

222 DO 150 I=1,5  
CALL INTX(Q(I),D(I))  
CALL INTX(Z(I),E(I))  
CALL INTX(Y(I),G(I))  
CALL INTX(HP(I),WP(I))  
150 CONTINUE

CHANGE OF TEMP. BOUNDARY CONDITION

IF(NNN.NE.1) GO TO 703  
IF(Y(5).LT.Y(6)) GO TO 725  
NNN=NNN+1  
703  $Y(6) = (HTCF * Y(5) + PHI * HCS * (T(6) / T_0)) / (HTCF + PHI * HCS)$

TUBE WALL EQUATIONS

725  $Q(6) = 0.000059 / F_0$   
 $Z(6) = 0.00054 / U_0$   
HP(6)=1  
DO 151 I=1,5  
IF(Q(I).LT.Q(6)) Q(I)=Q(6)  
IF(Z(I).LT.Z(6)) Z(I)=Z(6)  
151 CONTINUE

CHANGE TO DIMENSIONAL FORM

DO 160 I=1,6  
T(I)=Y(I)\*T\_0  
F(I)=Q(I)\*F\_0  
U(I)=Z(I)\*U\_0  
UF(I)=HP(I)\*UFER  
160 CONTINUE  
J=J+1  
GO TO 105

STORAGE OF RESULTS

1000 DO 170 I=1,6  
P(I,N)=Q(I)  
R(I,N)=Z(I)  
S(I,N)=Y(I)  
170 CONTINUE

INTERMEDIATE PRINT-OUT

```

N=N+1
KN1=N-1
WRITE(2,500)KN1,X
500 FORMAT(/,5X,14HSEGMENT NO. = ,I3,/,5X,15HD,LESS LENGTH = ,F10.4)
DO 180 I=1,6
WRITE(2,505)Y(I),T(I)
505 FORMAT(/,5X,14HDLESS TEMP. = ,E16.8,15X,7HTEMP = ,E16.8)
180 CONTINUE
IF(KN1.EQ.11) GO TO 4200
GO TO 656

```

FINAL RESULTS PRINT-OUT SECTION

```

4200 WRITE(2,5)
5 FORMAT(1H1,///,40X,35HFORMALDEHYDE CONCENTRATION RESULTS.)
WRITE(2,6)
6 FORMAT(/,2X,11HRADIAL GRID)
WRITE(2,7)(I,I=1,6)
7 FORMAT(/,15X,6(10X,15))
WRITE(2,8)
8 FORMAT(/,2X,10HAXIAL GRID)
DO 666 J=1,M1
WRITE(2,9)J,(P(I,J),I=1,M1)
9 FORMAT(/,5X,15,6(5X,E12.4))
666 CONTINUE
WRITE(2,12)
12 FORMAT(1H1,///,40X,27HUREA CONCENTRATION RESULTS.)
WRITE(2,6)
WRITE(2,7)(I,I=1,6)
WRITE(2,8)
DO 777 J=1,M1
WRITE(2,9)J,(R(I,J),I=1,M1)
777 CONTINUE
WRITE(2,14)
14 FORMAT(1H1,///,40X,28HTEMPERATURE PROFILE RESULTS.)
WRITE(2,6)
WRITE(2,7)(I,I=1,6)
WRITE(2,8)
DO 888 J=1,M1
WRITE(2,9)J,(S(I,J),I=1,M1)
888 CONTINUE
END

```

```

SUBROUTINE RATE1(T1,I,U,F,UF,A,B,C,AF,VO,EL)
COMMON/CONC/U0,F0,UFEQ,H1,S1,T0,R2
FNA(T1)=((10.**5.18)*EXP(-6542.5/T1))*1000.
FNB(T1)=((10.**6.31)*EXP(-9562.15/T1))
FNC(T1)=((10.**4.26)*EXP(-7045.3/T1))*1000.
FND(T1)=((10.**7.15)*EXP(-9562.15/T1))
FNE(T1)=0.0
FNF(T1)=0.0
Q1=0.85341
Q2=1.00341
Q3=0.10341
Q4=1.0144
Q5=0.0
Q6=0.0
UF=2.*(U0-U)-(F0-F)
UF2=(U-F)-(U0-F0)
UF3=0.0
G1=Q1*FNA(T1)*F*U
G2=Q2*FNB(T1)*UF
G3=Q3*FNC(T1)*F*UF
G4=Q4*FND(T1)*UF2
G5=Q5*FNE(T1)*F*UF2
G6=Q6*FNF(T1)*UF3
O1=G1-G2+G3-G4+G5-G6
O2=G1-G2
O3=0.0
W1=EL/(2.*VO)
A=(O1*U1)/F0
B=(O2*U1)/U0
AF=0.0
C=(O1*U1*H1)/(S1*T0*R2)
RETURN
END

```

```

SUBROUTINE RATE2(T1,I,U,F,UF,A,B,C,AF,VO,EL)
COMMON/CONC/U0,F0,UFEQ,H1,S1,T0,R2
FNA(T1)=((10.**5.18)*EXP(-6542.5/T1))*1000.
FNB(T1)=((10.**6.31)*EXP(-9562.15/T1))
FNC(T1)=((10.**4.26)*EXP(-7045.8/T1))*1000.
FND(T1)=((10.**7.15)*EXP(-9562.15/T1))
FNE(T1)=0.0
FNF(T1)=0.0
Q1=0.9030
Q2=1.0034
Q3=1.0034
Q4=1.0144
Q5=0.0
Q6=0.0
UF=2.*(U0-U)-(F0-F)
UF2=(U-F)-(U0-F0)
UF3=0.0
G1=Q1*FNA(T1)*F*U
G2=Q2*FNB(T1)*UF
G3=Q3*FNC(T1)*F*UF
G4=Q4*FND(T1)*UF2
G5=Q5*FNE(T1)*F*UF2
G6=Q6*FNF(T1)*UF3
O1=G1-G2+G3-G4+G5-G6
O2=G1-G2
O3=0.0
W1=EL/(2.*VO)
A=(O1*U1)/F0
B=(O2*U1)/U0
AF=0.0
C=(O1*U1*H1)/(S1*T0*R2)
RETURN
END

```

```

SUBROUTINE RATE3(T1, I, U, F, UF, A, B, C, AF, V0, EL)
COMMON/CONC/U0, F0, UFE0, H1, S1, T0, R2
FNA(T1) = ((10.**5.18)*EXP(-6542.5/T1))*1000.
FNB(T1) = ((10.**6.31)*EXP(-9562.15/T1))
FNC(T1) = ((10.**4.26)*EXP(-7045.3/T1))*1000.
FND(T1) = ((10.**7.15)*EXP(-9562.15/T1))
FNE(T1) = 0.0
FNF(T1) = 0.0
Q1 = 1.0068
Q2 = 1.0068
Q3 = 4.0068
Q4 = 1.0280
Q5 = 0.0
Q6 = 0.0
UF = 2.*(U0-U) - (F0-F)
UF2 = (U-F) - (U0-F0)
UF3 = 0.0
G1 = Q1*FNA(T1)*F*U
G2 = Q2*FNB(T1)*UF
G3 = Q3*FNC(T1)*F*UF
G4 = Q4*FND(T1)*UF2
G5 = Q5*FNE(T1)*F*UF2
G6 = Q6*FNF(T1)*UF3
O1 = G1 - G2 + G3 - G4 + G5 - G6
O2 = G1 - G2
O3 = 0.0
W1 = EL/(2.*V0)
A = (O1*U1)/F0
B = (O2*U1)/U0
AF = 0.0
C = (O1*U1*H1)/(S1*T0 + P2)
RETURN
END

```

```

SUBROUTINE RATE4(T1, I, U, F, UF, A, B, C, AF, V0, EL)
COMMON/CONC/U0, F0, UFE0, H1, S1, T0, R2
FNA(T1) = ((10.**5.18)*EXP(-6542.5/T1))*1000.
FNB(T1) = ((10.**6.31)*EXP(-9562.15/T1))
FNC(T1) = ((10.**4.26)*EXP(-7045.3/T1))*1000.
FND(T1) = ((10.**7.15)*EXP(-9562.15/T1))
FNE(T1) = 0.0
FNF(T1) = 0.0
Q1 = 1.0136
Q2 = 1.0136
Q3 = 5.0136
Q4 = 5.0578
Q5 = 0.0
Q6 = 0.0
UF = 2.*(U0-U) - (F0-F)
UF2 = (U-F) - (U0-F0)
UF3 = 0.0
G1 = Q1*FNA(T1)*F*U
G2 = Q2*FNB(T1)*UF
G3 = Q3*FNC(T1)*F*UF
G4 = Q4*FND(T1)*UF2
G5 = Q5*FNE(T1)*F*UF2
G6 = Q6*FNF(T1)*UF3
O1 = G1 - G2 + G3 - G4 + G5 - G6
O2 = G1 - G2
O3 = 0.0
W1 = EL/(2.*V0)
A = (O1*U1)/F0
B = (O2*U1)/U0
AF = 0.0
C = (O1*U1*H1)/(S1*T0 + R2)
RETURN
END

```

```

SUBROUTINE RATE5(T1,I,U,F,UF,A,B,C,AF,V0,EL)
COMMON/CONC/U0,F0,UFEQ,H1,S1,T0,R2
FNA(T1)=((10.**5.18)*EXP(-6542.5/T1))*1000,
FNB(T1)=((10.**6.31)*EXP(-9562.15/T1))
FNC(T1)=((10.**4.26)*EXP(-7045.8/T1))*1000,
FND(T1)=((10.**7.15)*EXP(-9562.15/T1))
FNE(T1)=(1.2/9.)*((10.**5.18)*EXP(-6542.5/T1))*1000.
FNF(T1)=(1./9.)*((10.**5.18)*EXP(-6542.5/T1))*1000.
Q1=1.0
Q2=1.0
Q3=5.0
Q4=1.0
Q5=0.8333
Q6=1.2
UF2=3.*(U0-U)+(F-F0)-2.*UF
UF3=2.*(U-U0)+(F0-F)+UF
G1=Q1*FNA(T1)*F*U
G2=Q2*FNB(T1)*UF
G3=Q3*FNC(T1)*F*UF
G4=Q4*FND(T1)*UF2
G5=Q5*FNE(T1)*F*UF2
G6=Q6*FNF(T1)*UF3
O1=G1-G2+G3-G4+G5-G6
O2=G1-G2
O3=-G1+G2+G3-G4
W1=EL/(2.*V0)
A=(O1*W1)/F0
B=(O2*W1)/U0
AF=(O3*W1)/UFEQ
C=(O1*W1*H1)/(S1*T0*R2)
RETURN
END

```

```

SUBROUTINE RATE6(T1,I,U,F,UF,A,B,C,AF,V0,EL)
COMMON/CONC/U0,F0,UFEQ,H1,S1,T0,R2
FNA(T1)=((10.**5.18)*EXP(-6542.5/T1))*1000,
FNB(T1)=((10.**6.31)*EXP(-9562.15/T1))
FNC(T1)=((10.**4.26)*EXP(-7045.8/T1))*1000,
FND(T1)=((10.**7.15)*EXP(-9562.15/T1))
FNE(T1)=(1.2/9.)*((10.**5.18)*EXP(-6542.5/T1))*1000.
FNF(T1)=(1./9.)*((10.**5.18)*EXP(-6542.5/T1))*1000.
Q1=1.0
Q2=1.0
Q3=8.0
Q4=4.0
Q5=0.8333
Q6=1.2
UF2=3.*(U0-U)+(F-F0)-2.*UF
UF3=2.*(U-U0)+(F0-F)+UF
G1=Q1*FNA(T1)*F*U
G2=Q2*FNB(T1)*UF
G3=Q3*FNC(T1)*F*UF
G4=Q4*FND(T1)*UF2
G5=Q5*FNE(T1)*F*UF2
G6=Q6*FNF(T1)*UF3
O1=G1-G2+G3-G4+G5-G6
O2=G1-G2
O3=-G1+G2+G3-G4
W1=EL/(2.*V0)
A=(O1*W1)/F0
B=(O2*W1)/U0
AF=(O3*W1)/UFEQ
C=(O1*W1*H1)/(S1*T0*R2)
RETURN
END
FINISH

```

SOLUTION OF COMPLEX MODELS

PROGRAM FOR U:F MOLAR RATIO OF 1:2.2

```
COMMON/CONC/U0,F0,UFEQ,H1,S1,T0,R2
DIMENSION A(10),B(10),C(10),F(10),U(10),T(10)
DIMENSION D(10),E(10),G(10)
DIMENSION UF(10),HP(10),AF(10),UP(10)
DIMENSION V(6),Q(10),Y(10),Z(10)
DIMENSION P(10,20),R(10,20),S(10,20)
```

PHYSICAL DATA

```
V0=45.57
R1=0.3175
T3=433.
S1=22.844
H1=-6000.
EL=914.4
DP=1.43/(10.**5.)
DQ=1.14/(10.**5.)
DS=0.97/(10.**5.)
DR=31.84/(10.**4.)
F0=0.003084
U0=0.003674
UF10=0.0
UFEQ=0.003175
T0=308.
R2=.2E-01
H=0.2
HCS=0.0005027
ROU=0.4196
```

CALCULATED DATA

```
VFT=V0*118.11
VELF=VFT**(1./3.)
HTCF=VELF*0.7495*0.0001355
PHI=ROU/R1
W=EL/(2.*V0*(R1**2.))
E1=DP*W
E2=DQ*W
E3=DR*W
E4=DS*W
```

INITIAL CONDITIONS

```
DO 100 I=1,6
U(I)=U0
F(I)=F0
UF(I)=UF10
Q(I)=1.
Z(I)=1.
HP(I)=0.0
100 CONTINUE
DO 110 I=1,5
T(I)=T0
Y(I)=1.
110 CONTINUE
T(6)=315.
Y(6)=T(6)/T0
```

VELOCITY PROFILE CALCULATION

DO 120 I=1,6  
 A7=(I-1)\*H  
 V(I)=(1.-(A7\*\*2.))

120 CONTINUE

INITIALISE CONTROLLING VARIABLES

NNN=1  
 N1=11  
 M1=6  
 J=0  
 N=1

INITIALISATION SECTION AND CONVERGENCE AID

CALL ZERO(X)  
 105 IF(X.GT.0.73) GO TO 106  
 GO TO 109  
 106 EL=243.84  
 V0=7.29  
 R1=0.79375  
 ROU=0.91821  
 VFT=V0\*113.11  
 VELF=VFT\*(1./3.)  
 HTCF=VELF\*0.8579\*0.0001355  
 HCS=0.0004136  
 W=EL/(2.\*V0\*(R1\*\*2.))  
 E1=DP\*U  
 E2=DQ\*W  
 E3=DR\*U  
 E4=DS\*W  
 PHI=ROU/R1  
 109 IF(J.EQ.17)GO TO 10  
 IF(J-4)10,20,30  
 30 IF(J-8)10,40,50  
 50 IF(J-12)10,60,70  
 70 IF(J-16)10,80,10  
 GO TO 10  
 20 T(6)=360.  
 Y(6)=T(6)/T0  
 GO TO 10  
 40 T(6)=393.  
 Y(6)=T(6)/T0  
 GO TO 10  
 60 T(6)=413.  
 Y(6)=T(6)/T0  
 GO TO 10  
 80 T(6)=433.  
 Y(6)=T(6)/T0

POLYMERISATION RATE SECTION

```

10 DO 130 I=1,6
  T1=T(I)
  IF(T1.LT.323)CALL RATE1(T1,I,U(I),F(I),UF(I),A(I),B(I),C(I),AF(I),
  1V0,EL)
  IF(T1.GT.323.AND.T1.LT.343)CALL RATE2(T1,I,U(I),F(I),UF(I),A(I),B(
  1I),C(I),AF(I),V0,EL)
  IF(T1.GT.343.AND.T1.LT.363)CALL RATE3(T1,I,U(I),F(I),UF(I),A(I),B(
  1I),C(I),AF(I),V0,EL)
  IF(T1.GT.363.AND.T1.LT.383)CALL RATE4(T1,I,U(I),F(I),UF(I),A(I),B(
  1I),C(I),AF(I),V0,EL)
  IF(T1.GT.383.AND.T1.LT.405)CALL RATE5(T1,I,U(I),F(I),UF(I),A(I),B(
  1I),C(I),AF(I),V0,EL)
  IF(T1.GT.405)CALL RATE6(T1,I,U(I),F(I),UF(I),A(I),B(I),C(I),AF(I),
  1V0,EL)
130 CONTINUE

```

DIFFERENTIAL EQUATIONS

CENTRE LINE

```

B1=(Q(2)-Q(1))/(H**2.)
D(1)=((4.*B1+E1)/V(1))-(A(1)/V(1))
B2=(Z(2)-Z(1))/(H**2.)
E(1)=((4.*B2+E2)/V(1))-(B(1)/V(1))
B3=(Y(2)-Y(1))/(H**2.)
G(1)=((4.*B3+E3)/V(1))-(C(1)/V(1))
HPQ=(HP(2)-HP(1))/(H**2.)
WP(1)=((4.*HPQ+E4)/V(1))-(AF(1)/V(1))

```

INTERNAL GRID

```

DO 140 I=2,5
  B4=(Q(I+1)-(2.*Q(I))+Q(I-1))/(H**2.)
  B5=(Q(I+1)-Q(I-1))/(2.*(H**2.)*(I-1))
  D(I)=((E1/V(I))*(B4+B5))-(A(I)/V(I))
  B6=(Z(I+1)-(2.*Z(I))+Z(I-1))/(H**2.)
  B7=(Z(I+1)-Z(I-1))/(2.*(H**2.)*(I-1))
  E(I)=((E2/V(I))*(B6+B7))-(B(I)/V(I))
  B8=(Y(I+1)-(2.*Y(I))+Y(I-1))/(H**2.)
  B9=(Y(I+1)-Y(I-1))/(2.*(H**2.)*(I-1))
  G(I)=((E3/V(I))*(B8+B9))-(C(I)/V(I))
  HPS=(HP(I+1)-HP(I-1))/(2.*(H**2.)*(I-1))
  HPR=(HP(I+1)-(2.*HP(I))+HP(I-1))/(H**2.)
  WP(I)=((E4/V(I))*(HPR+HPS))-(AF(I)/V(I))
140 CONTINUE

```

PRINT, END VALUE, AND EXIT CONDITIONS

CALL PRNTE(0.1,1.0,L1,L2)  
IF(L1.EQ.2) GO TO 1000  
IF(L2.EQ.2)GO TO 1000

STEP LENGTH AND INTIGRATION TECHNIQUE

656 IF(X.GT.0.78) GO TO 658  
GO TO 659  
658 CALL INTI(X,0.0005,4)  
GO TO 222  
659 CALL INTI(X,0.002,4)

INTIGRATION SECTION

222 DO 150 I=1,5  
CALL INTX(Q(I),D(I))  
CALL INTX(Z(I),E(I))  
CALL INTX(Y(I),G(I))  
CALL INTX(HP(I),WP(I))  
150 CONTINUE

CHANGE OF TEMP. BOUNDARY CONDITION

IF(NNN.NE.1) GO TO 703  
IF(Y(5).LT.Y(6))GO TO 725  
NNN=NNN+1  
703  $Y(6) = (HTCF * Y(5) + PHI * HCS * (T(6) / T0)) / (HTCF + PHI * HCS)$

TUBE WALL EQUATIONS

725  $Q(6) = 0.0003577 / F0$   
 $Z(6) = 0.0002 / U0$   
HP(6)=1  
DO 151 I=1,5  
IF(Q(I).LT.Q(6)) Q(I)=Q(6)  
IF(Z(I).LT.Z(6)) Z(I)=Z(6)  
151 CONTINUE

CHANGE TO DIMENSIONAL FORM

DO 160 I=1,6  
T(I)=Y(I)\*T0  
F(I)=Q(I)\*F0  
U(I)=Z(I)\*U0  
UF(I)=HP(I)\*UF0  
160 CONTINUE  
J=J+1  
GO TO 105

STORAGE OF RESULTS

1000 DO 170 I=1,6  
P(I,N)=Q(I)  
R(I,N)=Z(I)  
S(I,N)=Y(I)  
170 CONTINUE

INTERMEDIATE PRINT-OUT

```

N=N+1
KN1=N-1
WRITE(2,500)KN1,X
500 FORMAT(/,5X,14HSEQUENT NO. = ,I3,/,5X,15HD,LESS LENGTH = ,F10.4)
DO 180 I=1,6
WRITE(2,505)Y(I),T(I)
505 FORMAT(/,5X,14HDESS: TEMP. = ,E16.8,15X,7HTEMP = ,E16.8)
180 CONTINUE
IF(KN1.EQ.11) GO TO 4200
GO TO 656

```

FINAL RESULTS PRINT-OUT SECTION

```

4200 WRITE(2,5)
5 FORMAT(1H1,///,40X,35HFORMALDEHYDE CONCENTRATION RESULTS.)
WRITE(2,6)
6 FORMAT(/,2X,11HRADIAL GRID)
WRITE(2,7)(I,I=1,6)
7 FORMAT(/,15X,6(10X,15))
WRITE(2,8)
8 FORMAT(/,2X,10HAXIAL GRID)
DO 660 J=1,N1
WRITE(2,9)J,(P(I,J),I=1,M1)
9 FORMAT(/,5X,15,6(5X,E12.4))
660 CONTINUE
WRITE(2,12)
12 FORMAT(1H1,///,40X,7HUREA CONCENTRATION RESULTS.)
WRITE(2,6)
WRITE(2,7)(I,I=1,6)
WRITE(2,8)
DO 777 J=1,N1
WRITE(2,9)J,(R(I,J),I=1,M1)
777 CONTINUE
WRITE(2,14)
14 FORMAT(1H1,///,40X,28HTEMPERATURE PROFILE RESULTS.)
WRITE(2,6)
WRITE(2,7)(I,I=1,6)
WRITE(2,8)
DO 888 J=1,N1
WRITE(2,9)J,(S(I,J),I=1,M1)
888 CONTINUE
END

```

```

SUBROUTINE RATE1(T1,I,U,F,UF,A,B,C,AF,V0,EL)
COMMON/CONC/U0,F0,UFEQ,H1,S1,T0,R2
FNA(T1)=((10.**5.18)*EXP(-6542.5/T1))*1000.
FNB(T1)=((10.**6.31)*EXP(-9562.15/T1))
FNC(T1)=((10.**4.26)*EXP(-7045.8/T1))*1000.
FND(T1)=((10.**7.15)*EXP(-9562.15/T1))
FNE(T1)=(1.2/9.)*((10.**5.18)*EXP(-6542.5/T1))*1000.
FNF(T1)=(1./9.)*((10.**5.18)*EXP(-6542.5/T1))*1000.
Q1=1.0
Q2=1.0
Q3=1.0
Q4=1.0
Q5=0.6333
Q6=1.2
UF2=3.*(U0-U)+(F-F0)-2.*UF
UF3=2.*(U-U0)+(F0-F)+UF
G1=Q1*FNA(T1)*F*U
G2=Q2*FNB(T1)*UF
G3=Q3*FNC(T1)*F*UF
G4=Q4*FND(T1)*UF2
G5=Q5*FNE(T1)*F*UF2
G6=Q6*FNF(T1)*UF3
O1=G1-G2+G3-G4+G5-G6
O2=G1-G2
O3=G2-G1-G4+G3
W1=EL/(2.*V0)
A=(O1*U1)/F0
B=(O2*U1)/U0
AF=(O3*W1)/UFEQ
C=(O1*W1*H1)/(S1*T0*R2)
RETURN
END

```

```

SUBROUTINE RATE2(T1,I,U,F,UF,A,B,C,AF,V0,EL)
COMMON/CONC/U0,F0,UFEQ,H1,S1,T0,R2
FNA(T1)=((10.**5.18)*EXP(-6542.5/T1))*1000.
FNB(T1)=((10.**6.31)*EXP(-9562.15/T1))
FNC(T1)=((10.**4.26)*EXP(-7045.8/T1))*1000.
FND(T1)=((10.**7.15)*EXP(-9562.15/T1))
FNE(T1)=(1.2/9.)*((10.**5.18)*EXP(-6542.5/T1))*1000.
FNF(T1)=(1./9.)*((10.**5.18)*EXP(-6542.5/T1))*1000.
Q1=0.6
Q2=5.0
Q3=5.0
Q4=10.0
Q5=16.6667
Q6=24.
UF2=3.*(U0-U)+(F-F0)-2.*UF
UF3=2.*(U-U0)+(F0-F)+UF
G1=Q1*FNA(T1)*F*U
G2=Q2*FNB(T1)*UF
G3=Q3*FNC(T1)*F*UF
G4=Q4*FND(T1)*UF2
G5=Q5*FNE(T1)*F*UF2
G6=Q6*FNF(T1)*UF3
O1=G1-G2+G3-G4+G5-G6
O2=G1-G2
O3=G2-G1-G4+G3
W1=EL/(2.*V0)
A=(O1*U1)/F0
B=(O2*U1)/U0
AF=(O3*W1)/UFEQ
C=(O1*U1*H1)/(S1*T0*R2)
RETURN
END

```

```

SUBROUTINE RATE3(T1,I,U,F,UF,A,B,C,AF,VO,EL)
COMMON/CONC/U0,F0,UFEQ,H1,S1,T0,R2
FNA(T1)=((10.**5.18)*EXP(-6542.5/T1))*1000.
FNB(T1)=((10.**6.31)*EXP(-9562.15/T1))
FNC(T1)=((10.**4.26)*EXP(-7045.8/T1))*1000.
FND(T1)=((10.**7.15)*EXP(-9562.15/T1))
FNE(T1)=(1.2/9.)*((10.**5.18)*EXP(-6542.5/T1))*1000.
FNF(T1)=(1./9.)*((10.**5.18)*EXP(-6542.5/T1))*1000.
Q1=5.
Q2=5.
Q3=40.
Q4=40.
Q5=0.0083
Q6=0.012
UF2=3.*(U0-U)+(F-F0)-2.*UF
UF3=2.*(U-U0)+(F0-F)+UF
G1=Q1*FNA(T1)*F*U
G2=Q2*FNB(T1)*UF
G3=Q3*FNC(T1)*F*UF
G4=Q4*FND(T1)*UF2
G5=Q5*FNE(T1)*F*UF2
G6=Q6*FNF(T1)*UF3
O1=G1-G2+G3-G4+G5-G6
O2=G1-G2
O3=G2-G1-G4+G3
W1=EL/(2.*VO)
A=(O1*U1)/F0
B=(O2*U1)/U0
AF=(O3*U1)/UFEQ
C=(O1*U1*H1)/(S1*T0+R2)
RETURN
END

```

```

SUBROUTINE RATE4(T1,I,U,F,UF,A,B,C,AF,VO,EL)
COMMON/CONC/U0,F0,UFEQ,H1,S1,T0,R2
FNA(T1)=((10.**5.18)*EXP(-6542.5/T1))*1000.
FNB(T1)=((10.**6.31)*EXP(-9562.15/T1))
FNC(T1)=((10.**4.26)*EXP(-7045.8/T1))*1000.
FND(T1)=((10.**7.15)*EXP(-9562.15/T1))
FNE(T1)=(1.2/9.)*((10.**5.18)*EXP(-6542.5/T1))*1000.
FNF(T1)=(1./9.)*((10.**5.18)*EXP(-6542.5/T1))*1000.
Q1=1.0
Q2=1.
Q3=80.
Q4=30.
Q5=16.6667
Q6=12.
UF2=3.*(U0-U)+(F-F0)-2.*UF
UF3=2.*(U-U0)+(F0-F)+UF
G1=Q1*FNA(T1)*F*U
G2=Q2*FNB(T1)*UF
G3=Q3*FNC(T1)*F*UF
G4=Q4*FND(T1)*UF2
G5=Q5*FNE(T1)*F*UF2
G6=Q6*FNF(T1)*UF3
O1=G1-G2+G3-G4+G5-G6
O2=G1-G2
O3=G2-G1-G4+G3
W1=EL/(2.*VO)
A=(O1*U1)/F0
B=(O2*U1)/U0
C=(O1*U1*H1)/(S1*T0+R2)
AF=(O3*U1)/UFEQ
RETURN
END

```

```

SUBROUTINE RATE5(T1,I,U,F,UF,A,B,C,AF,V0,EL)
COMMON/CONC/U0,F0,UFEQ,H1,S1,T0,R2
FNA(T1)=((10.**5.18)*EXP(-6542.5/T1))*1000.
FNB(T1)=((10.**6.31)*EXP(-9562.15/T1))
FNC(T1)=((10.**4.26)*EXP(-7045.8/T1))*1000.
FND(T1)=((10.**7.15)*EXP(-9562.15/T1))
FNE(T1)=(1.2/9.)*((10.**5.13)*EXP(-6542.5/T1))*1000.
FNF(T1)=(1./9.)*((10.**5.18)*EXP(-6542.5/T1))*1000.
Q1=1.2
Q2=1.0
Q3=150.
Q4=40.
Q5=50.
Q6=12.
UF2=3.*(U0-U)+(F-F0)-2.*UF
UF3=2.*(U-U0)+(F0-F)+UF
G1=Q1*FNA(T1)*F*U
G2=Q2*FNB(T1)*UF
G3=Q3*FNC(T1)*F*UF
G4=Q4*FND(T1)*UF2
G5=Q5*FNE(T1)*F*UF2
G6=Q6*FNF(T1)*UF3
O1=G1-G2+G3-G4+G5-G6
O2=G1-G2
O3=-G1+O2+G3-G4
W1=EL/(2.*V0)
A=(O1*W1)/F0
B=(O2*W1)/U0
AF=(O3*W1)/UFEQ
C=(O1*W1*H1)/(S1*T0*R2)
RETURN
END

```

```

SUBROUTINE RATE6(T1,I,U,F,UF,A,B,C,AF,V0,EL)
COMMON/CONC/U0,F0,UFEQ,H1,S1,T0,R2
FNA(T1)=((10.**5.18)*EXP(-6542.5/T1))*1000.
FNB(T1)=((10.**6.31)*EXP(-9562.15/T1))
FNC(T1)=((10.**4.26)*EXP(-7045.8/T1))*1000.
FND(T1)=((10.**7.15)*EXP(-9562.15/T1))
FNE(T1)=(1.2/9.)*((10.**5.13)*EXP(-6542.5/T1))*1000.
FNF(T1)=(1./9.)*((10.**5.18)*EXP(-6542.5/T1))*1000.
Q1=0.7
Q2=1.0
Q3=8.0
Q4=4.0
Q5=1.0833
Q6=1.56
UF2=3.*(U0-U)+(F-F0)-2.*UF
UF3=2.*(U-U0)+(F0-F)+UF
G1=Q1*FNA(T1)*F*U
G2=Q2*FNB(T1)*UF
G3=Q3*FNC(T1)*F*UF
G4=Q4*FND(T1)*UF2
G5=Q5*FNE(T1)*F*UF2
G6=Q6*FNF(T1)*UF3
O1=G1-G2+G3-G4+G5-G6
O2=G1-G2
O3=-G1+O2+G3-G4
W1=EL/(2.*V0)
A=(O1*W1)/F0
B=(O2*W1)/U0
AF=(O3*W1)/UFEQ
C=(O1*W1*H1)/(S1*T0*R2)
RETURN
END
FINISH

```

## APPENDIX 8

### CALCULATIONS AND CALIBRATION CHARTS

Examples of calculations required to evaluate residence times and pump delivery rates are given below. Calibration charts for the urea and formalin pumps follow.

i. CALCULATION OF UREA SOLUTION AND FORMALIN WEIGHTS FOR A GIVEN MOLAR RATIO

Assume      Formalin Strength            = 36% w/w  
                 Urea Solution Strength = 50% w/w  
                 U:F Molar Ratio            = 1:2.2

Then

$$\frac{U/60}{F/30} = \frac{1}{2.2}$$

Or

$$\frac{2F}{U} = 2.2$$

For 1g mol of formaldehyde i.e. 30g, the urea required is given by

$$U = \frac{2 \times 30}{2.2} = 27.27g$$

Since the urea solution is 50% w/w this is equivalent to

$$U = 27.27 \times 2 = 54.54g \qquad \text{A.8.1.}$$

30g of formaldehyde at 100% is equivalent to

$$F = \frac{30}{36} \cdot 100 = 83.5g \quad \text{A.8.2.}$$

Total weight is therefore given by addition of A.8.1. to A.8.2., thus:

$$54.54 + 83.5 = 138.04g$$

therefore for a charge of w g at U:F molar ratio of 1:2.2.

Weight of 50% w/w Urea Solution

$$= \frac{54.54 w}{138.04} g$$

Weight of 36% w/w Formalin

$$= \frac{83.5 w}{138.04} g$$

#### ii. CALCULATION OF RESIDENCE TIMES

A sample of the calculations giving the residence times corresponding to each of the sampling valves in the reactor, is presented below.

Assuming the 53.50s residence time for the reaction length of reactor, two residence times have to be accounted for. This is because the diameter of the reactor tube changes from  $\frac{1}{4}$ " i.d. to  $\frac{5}{8}$ " i.d. 30ft from the reactor inlet (Chapter 5).

Let RT1 = residence time in 30ft of  $\frac{1}{4}$ " i.d. tube

RT2 = residence time in 8ft of  $\frac{5}{8}$ " i.d. tube

Then

$$RT1 + RT2 = 53.50 s \quad \text{A.8.3.}$$

And

$$\frac{RT_1}{RT_2} = \frac{V_1}{V_2} = \frac{30 \cdot \frac{\pi}{4} D_1^2}{8 \cdot \frac{\pi}{4} D_2^2} = 0.6 \quad \text{A.8.4.}$$

Solving A.8.3. and A.8.4. simultaneously:

$$RT_1 = 20.04 \text{ s}$$

$$RT_2 = 33.46 \text{ s}$$

Since the 30ft of  $\frac{1}{4}$ " i.d. tube is divided into three 10ft lengths, then the residence times corresponding to each of the sampling valves are:

<u>SAMPLING VALVE</u>	<u>RESIDENCE TIME s</u>
1	6.68
2	13.36
3	20.04
4	53.50

Similar calculations can be made for the 26.75 s residence time (Chapter 5),

### iii. CALCULATION OF VOLUMETRIC FLOW RATES

To calculate the individual volumetric flow rates for the urea solution and formalin, the residence times calculated in (ii) above have to be corrected for actual lengths of tube, thus:

$$RT_1 = 20.04 \frac{41,408}{30} = 27.66 \text{ s}$$

$$RT_2 = 33.44 \frac{8,433}{8.0} = 35.25 \text{ s}$$

Hence the total residence time is 62.91 s, and the total volumetric flow rate is given by

$$\text{VFR} = \frac{28.316}{12^3} \frac{V}{\text{ERT}} \cdot 1000 \text{ cm}^3/\text{s}$$

where

V = the total volume of reactor in cubic inches

ERT = the equivalent residence time, s

Hence for the above example

$$\text{VFR} = \frac{28.316}{12^3} \cdot \frac{55.411}{62.91} \cdot 1000 = 14.43 \text{ cm}^3/\text{s}$$

The total volumetric flow rate calculated above is used to evaluate the individual delivery rates of the formalin and urea pumps, thus:

Assuming a 50% w/w urea solution and a 36% w/w formalin:

$$\text{Density of the above composition} = 1.114 \text{ g/cm}^3$$

Therefore

$$\text{The mass flow rate} = 14.43 \times 1.114 = 16.075 \text{ g/cm}^3$$

Using the calculations discussed in part (i) of this appendix,

Mass flow rate of urea solution

$$= 16.075 \frac{54.54}{138.04} = 6.35 \text{ g/s}$$

Mass flow rate of formalin

$$= 16.075 \frac{83.5}{138.04} = 9.724 \text{ g/s}$$

Density of 50% w/w urea solution = 1.14 g/cm<sup>3</sup>

Density of 36% w/w formalin = 1.107 g/cm<sup>3</sup>

therefore

Volumetric flow rate for urea solution

$$= \frac{6.315}{1.14} = 5.67 \text{ cm}^3/\text{s}$$

and

Volumetric flow rate for formalin

$$= \frac{9.724}{1.107} = 8.76 \text{ cm}^3/\text{s}$$

The pump settings for these throughputs can be read off the calibration graphs of this appendix.

iv. CALIBRATION CHARTS FOR UREA PUMP

Fig. A.8.1. shows the calibration graph for the urea pump. Fig. A.8.2. is an enlarged section of Fig. A.8.1. at the lower pump settings which were predominantly used.

v. CALIBRATION CHART FOR FORMALIN PUMP

Fig. A.8.3. shows the calibration graph for the formalin pump. Fig. A.8.4. is an enlarged section of Fig. A.8.3. at the lower pump settings which were predominantly used.

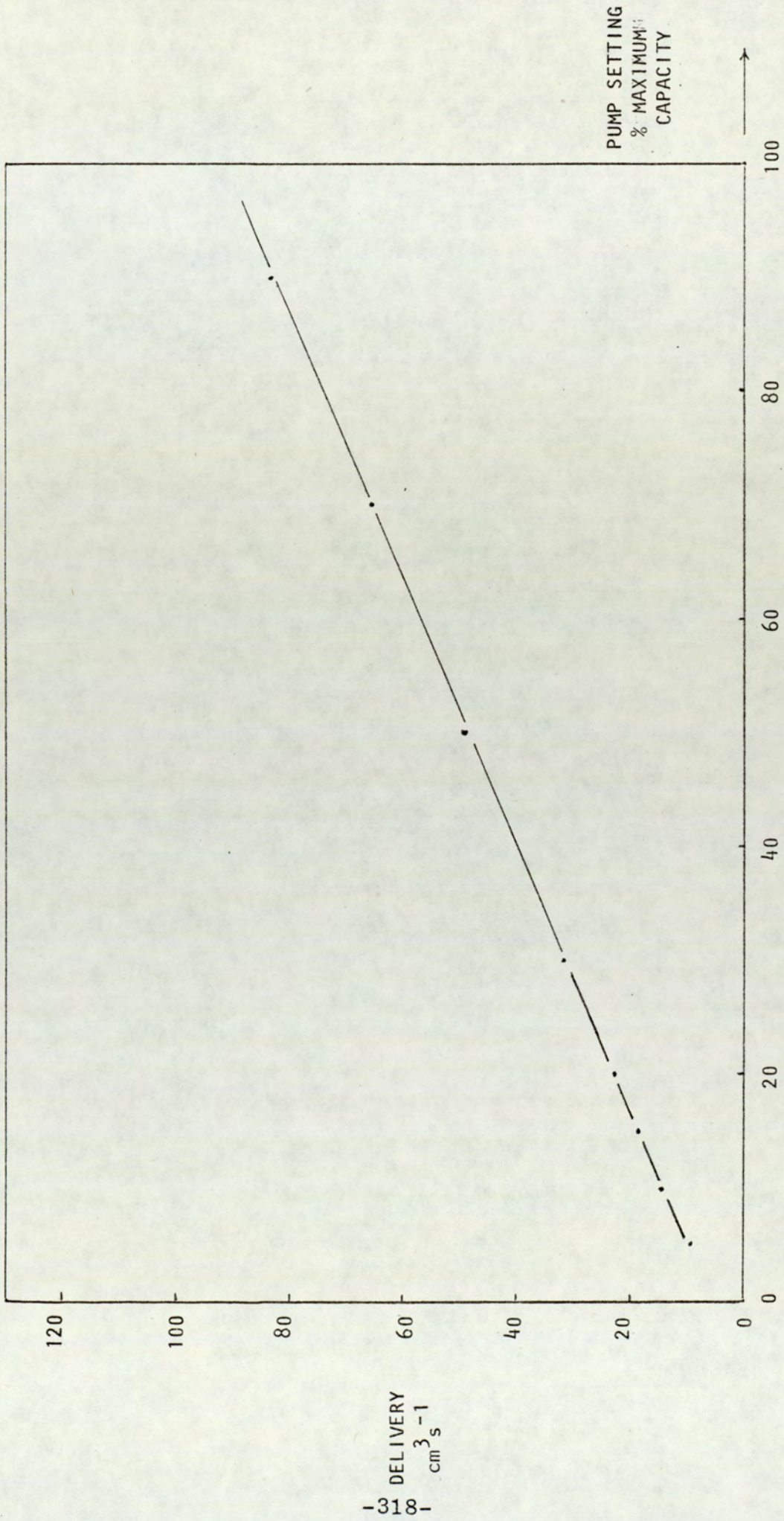


FIG. A.8.1.1.

UREA PUMP CALIBRATION CURVE

DELIVERY  
 $\text{cm}^3 \text{s}^{-1}$

PUMP SETTING  
 % MAXIMUM  
 CAPACITY

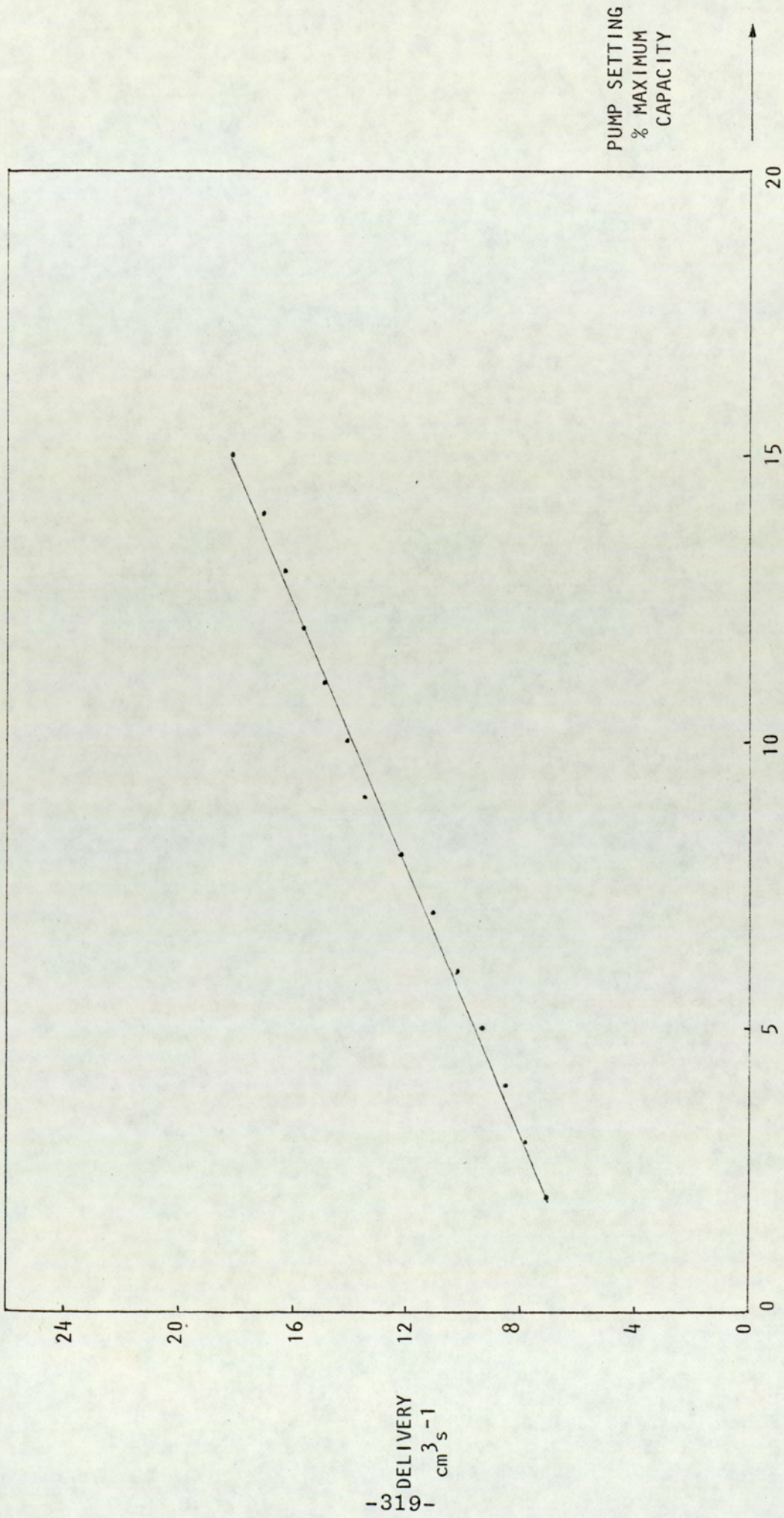


FIG. A.8.2.

UREA PUMP CALIBRATION CURVE FOR LOW SETTINGS

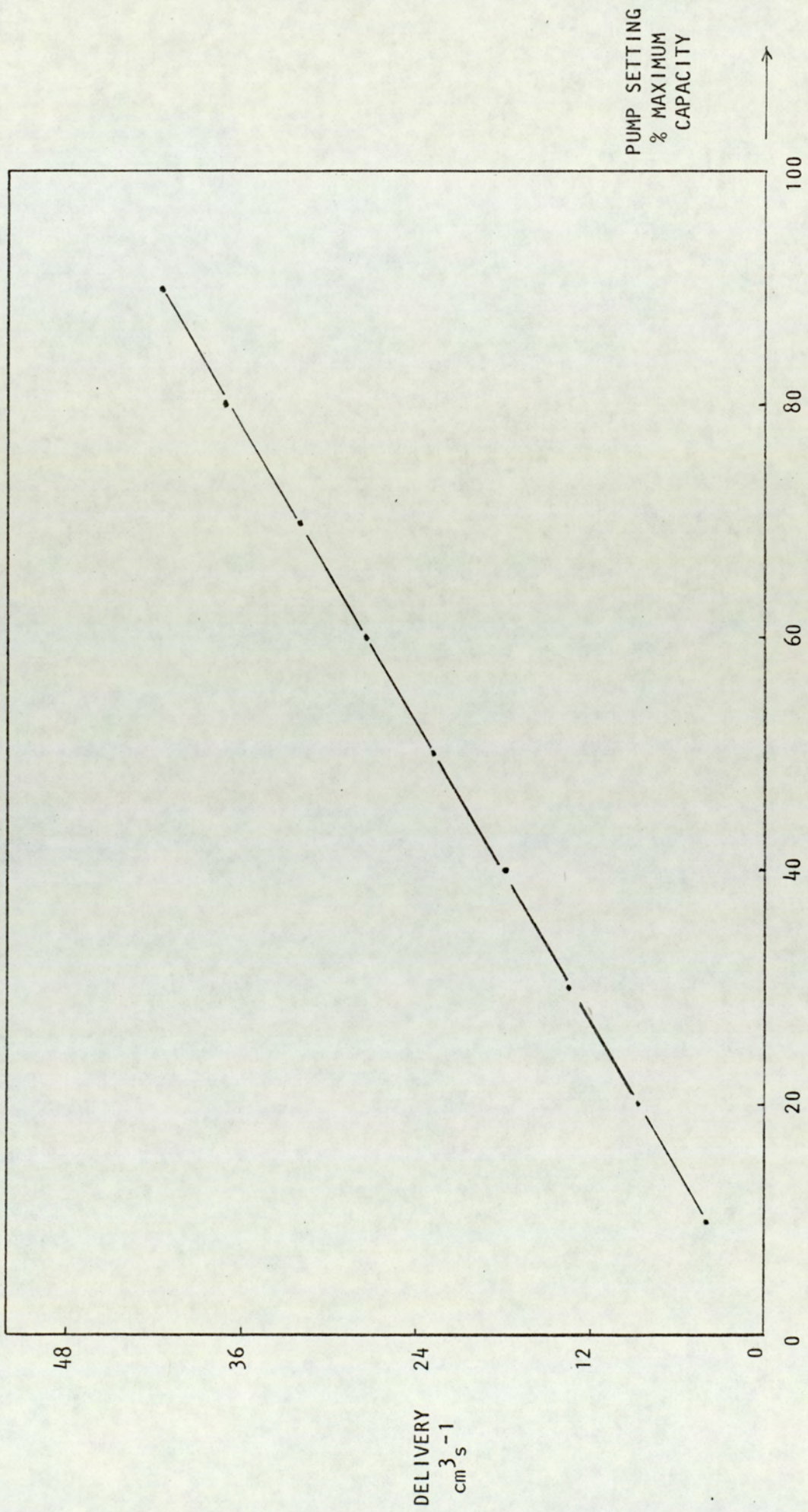


FIG. A.8.3.  
FORMALIN PUMP CALIBRATION CURVE

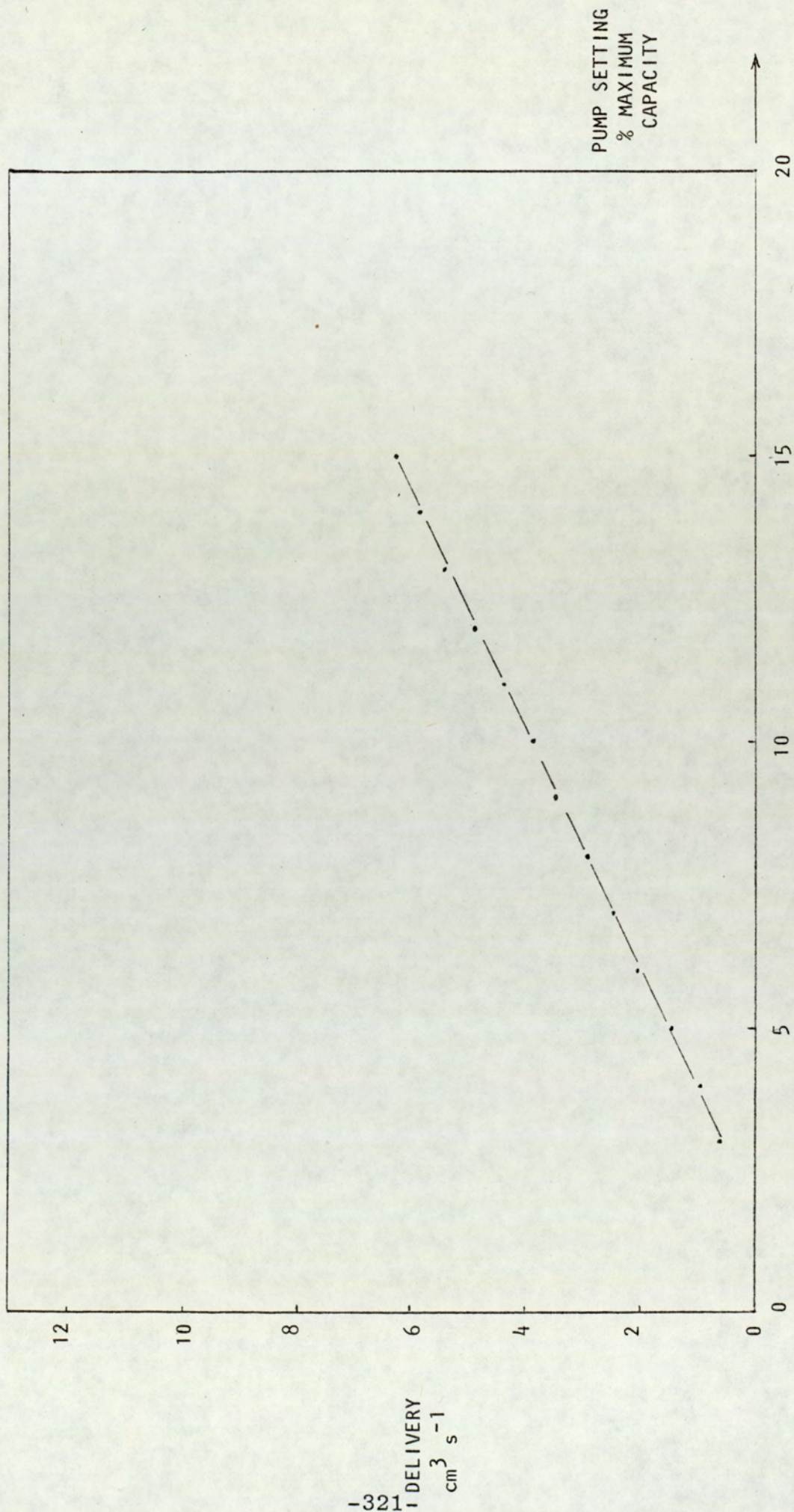


FIG. A.8.4.

FORMALIN PUMP CALIBRATION CURVE FOR LOW SETTINGS

1-321 DELIVERY  
cm<sup>3</sup> s<sup>-1</sup>

PUMP SETTING  
% MAXIMUM  
CAPACITY

## APPENDIX 9

### QUANTITATIVE ANALYSIS

#### 1. ANALYTICAL REAGENTS

The chemical reagents used in the quantitative analytical methods described later in this appendix were prepared as follows:-

##### i. 0.1N IODINE SOLUTION

20.00g of potassium iodide<sup>1</sup>\* was dissolved in 20 to 30 cm<sup>3</sup> of distilled water. To this solution was added 12.70g of iodine and the mixture thoroughly agitated until the iodine dissolved. The above solution was made up to 1000 cm<sup>3</sup> in a volumetric flask.

##### ii. 0.1N SODIUM THIOSULPHATE

An approximate 0.1N solution of sodium thiosulphate was prepared by dissolving 25g of the crystallised chemical in 1000 cm<sup>3</sup> of distilled water. 1 cm<sup>3</sup> of chloroform was added to the above solution to give better stability during storage(129).

<sup>1</sup> Footnote\* : Chemicals are of the specifications given in Appendix 6.

iii. 2M SODIUM SULPHITE SOLUTION

504.0g sodium sulphite was dissolved in a quantity of distilled water by thorough agitation. The solution was then made up to 1000 cm<sup>3</sup> with further addition of distilled water.

iv. THYMOLPHTHALEIN INDICATOR (0.1% IN ALCOHOL)

0.4g of solid thymolphthalein was dissolved in 600 cm<sup>3</sup> of alcohol and the solution made up to 1000 cm<sup>3</sup> with distilled water.

The following reagents, also used in the analytical technique, were prepared using standard methods(129).

These were:

- v. Sodium hydroxide solution, 10% w/v
- vi. Sodium hydroxide solution, 1 Normal
- vii. Sulphuric acid, 10% v/v
- viii. Sulphuric acid, 1 Normal

2. ANALYTICAL TECHNIQUES

The quantitative methods used for analysis of the resins prepared in the reactor were as follows:

i. STANDARDISATION OF NORMAL SODIUM HYDROXIDE (NaOH)

25 cm<sup>3</sup> aliquots of BDH standard IN HCl were pipetted into a conical flask. Three drops of thymolphthalein

indicator were added and the contents of the flask titrated with the NaOH solution until a light blue colour was obtained. This was the end-point.

Calculation:

$$\text{Normality of NaOH} = N_{\text{NaOH}} = \frac{25}{t}$$

where  $t$  = volume of NaOH used to neutralise the 1N HCl,  $\text{cm}^3$ ,

ii. STANDARDISATION OF NORMAL SULPHURIC ACID ( $\text{H}_2\text{SO}_4$ )

25  $\text{cm}^3$  aliquots of the  $\text{H}_2\text{SO}_4$  were pipetted into a conical flask. Three drops of thymolphthalein indicator were added and the contents of the flask titrated with the caustic which was normalised above, until a light blue colour was obtained. This was the end-point.

Calculation:

$$25 \times N_{\text{H}_2\text{SO}_4} = t \times N_{\text{NaOH}}$$

$$N_{\text{H}_2\text{SO}_4} = \frac{t \cdot N_{\text{NaOH}}}{25}$$

where  $t$  = volume of caustic used to neutralise the  $\text{H}_2\text{SO}_4$ ,  $\text{cm}^3$ ,

iii. STANDARDISATION OF 0.1N SODIUM THIOSULPHATE  
( $\text{Na}_2\text{S}_2\text{O}_3$ )

3.5670g of potassium iodate were dissolved in distilled water and made up to 1000  $\text{cm}^3$  in a volumetric flask. This gave an exactly 1 N potassium iodate solution. If

the above weight was slightly different the exact normality was calculated ( $N_{\text{KIO}_3}$ ),

25 cm<sup>3</sup> of the above solutions were treated with excess of pure potassium iodide (1g of the solid or 10 cm<sup>3</sup> of a 10% w/w solution). 6 cm<sup>3</sup> of normalised H<sub>2</sub>SO<sub>4</sub> were added. The iodine liberated was titrated with the Na<sub>2</sub>S<sub>2</sub>O<sub>3</sub> solution while constantly agitating: when the colour of the liquid became pale yellow, 0.2-0.5g of iodine starch indicator were added. The titration was continued until the end-point, i.e. where the colour changed from blue to colourless. Titrations were repeated until two consecutive ones agreed to within ± 0.1 cm<sup>3</sup>.

Calculation:

$$N_{\text{Na}_2\text{S}_2\text{O}_3} = \frac{25 \times N_{\text{KIO}_3}}{t_1}$$

where

t<sub>1</sub> = volume of Na<sub>2</sub>S<sub>2</sub>O<sub>3</sub> solution used to neutralise the potassium iodate solution, cm<sup>3</sup>.

#### iv. BLANK DETERMINATION FOR IODIMETRIC ANALYSIS

50 cm<sup>3</sup> of 0.1 N iodine solution were pipetted into an iodine flask containing 50 cm<sup>3</sup> of distilled water. To this solution was added a volume of 30 cm<sup>3</sup> of 10% w/v sodium hydroxide solution. The contents of the flask were thoroughly mixed and allowed to stand in the dark for 30 minutes.

45 cm<sup>3</sup> of 10% H<sub>2</sub>SO<sub>4</sub> were added to the flask and the liberated iodine was titrated against 0.1 N sodium thiosulphate using 0.2-0.5 g of iodine starch indicator. (The colour change at the end-point is blue to colourless).

The volume of the sodium thiosulphate consumed by the liberated iodine in the flask was noted. This was used as the blank value in subsequent analysis.

#### v. NEUTRALISATION OF SODIUM SULPHITE SOLUTION

About three drops of thymolphthalein indicator were added to 250 cm<sup>3</sup> of 2 Molar sodium sulphite solution. The solution was then titrated with normalised NaOH until a blue colour was obtained. This was the end-point for a neutral sodium sulphite solution.

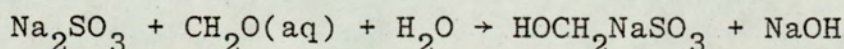
It should be noted that the neutral sodium sulphite is such with respect to the thymolphthalein indicator which operates at a pH of between 9.3 and 10.5. Normally it requires about 3 drops (0.2 cm<sup>3</sup>) of normal caustic to neutralise approximately 250 cm<sup>3</sup> of the sulphite. If any appreciable amount of caustic is required as has been noted when using some grades of sodium sulphite a blank determination should be carried out each time the sodium sulphite is used in any determination.

The procedure for doing a blank corresponds to that of "standardisation of formalin" (vi) except that the sample is omitted.

vi. STANDARDISATION OF FORMALIN

Approximately 1g of sample was accurately weighed and transferred into a 250 cm<sup>3</sup> conical flask which contained approximately 50 cm<sup>3</sup> of distilled water. About 1 cm<sup>3</sup> of thymolphthalein indicator was added and the contents just neutralised from colourless to blue using normalised sodium hydroxide solution.

50 cm<sup>3</sup> of neutralised sodium sulphite solution were then added to the above solution and the flask contents agitated and titrated with normalised sulphuric acid until all the blue colour disappeared. This was the end-point. The per cent w/w of formaldehyde is calculated from:



$$30\text{g}.\text{CH}_2\text{O} \equiv 1000 \text{ cm}^3 \text{ IN NaOH} \equiv 1000 \text{ cm}^3 \text{ IN H}_2\text{SO}_4$$

$$\% \text{CH}_2\text{O w/w} = \frac{0.03 \text{ t.n}}{w} \times 100$$

w = weight of sample, g

t = volume of H<sub>2</sub>SO<sub>4</sub> required to neutralise the liberated alkali, cm<sup>3</sup>

n = exact normality of the above sulphuric acid

vii. DETERMINATION OF FREE FORMALDEHYDE

THE ACIDIMETRIC SULPHITE METHOD

With reference to Chapter 5, where the technique for the collection of samples from the reactor has been described, the acidimetric sulphite method for determination of free formaldehyde was conducted as follows:-

A standard test tube (height 15 cm, radius 2.5 cm), including a stopper, was weighed accurately. Approximately  $30 \text{ cm}^3$  of distilled water were placed in the tube which was then reweighed.

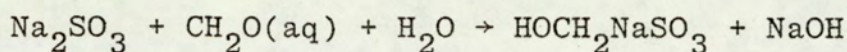
Approximately 5g of sample were introduced into the test tube from a reactor sampling valve as described in Chapter 5. External water was wiped off the outside and the tube weighed, inclusive of sample, water and stopper, accurately. Appropriate subtraction gave the weights of the reactor sample and the solution.

Depending on the quantity of free formaldehyde expected, between 4 and 6 g of the above solution were weighed by difference from a weighing bottle and decanted into a  $500 \text{ cm}^3$  conical flask containing approximately  $200 \text{ cm}^3$  of distilled water. The weight of the sample was chosen such that a reasonable titrate volume was used.

The solution was agitated to disperse the sample, then carefully neutralised with normal NaOH to thymolphthalein. At the end point the colour changed from colourless to blue.

$10 \text{ cm}^3$  of Normal  $\text{H}_2\text{SO}_4$  were added from a burette followed by  $25 \text{ cm}^3$  of neutralised sodium sulphite solution. The solution was allowed to stand for exactly 1 minute. The excess  $\text{H}_2\text{SO}_4$  was then back titrated with the Normal NaOH using thymolphthalein indicator. The end-point was given by a change of colour from colourless to blue.

Calculations:



$$30\text{g CH}_2\text{O} \equiv 1000 \text{ cm}^3 \text{ Normal NaOH}$$

$$\% \text{ Free CH}_2\text{O w/w} = \frac{(10 N_{\text{H}_2\text{SO}_4} - t N_{\text{NaOH}})0.03}{w_1} \frac{w_2}{w_3} \cdot 100$$

where

w1 = weight of sample used in analysis, g

w2 = weight of solution in the test tube, g

w3 = weight of sample from the reactor, g

$N_{\text{H}_2\text{SO}_4}$  = exact normality of  $\text{H}_2\text{SO}_4$

$N_{\text{NaOH}}$  = exact normality of NaOH

t = volume of the NaOH used to neutralise the  
 $\text{H}_2\text{SO}_4$ ,  $\text{cm}^3$

viii. DETERMINATION OF COMBINED (FREE AND METHYLOL)  
FORMALDEHYDE

THE IODIMETRIC METHYLOL ANALYSIS

From the contents of the test tube described in (vii) above, 1g of sample was weighed by difference using a weighing bottle. The sample was quantitatively transferred into an iodine (Mexican) flask containing  $50 \text{ cm}^3$  of distilled water. The contents were thoroughly agitated to disperse the sample.

$50 \text{ cm}^3$  of 0.1N iodine solution were pipetted into the flask followed by  $30 \text{ cm}^3$  of 10% NaOH. The contents were thoroughly mixed then allowed to stand in the dark

for 30 minutes. 45 cm<sup>3</sup> of 10% H<sub>2</sub>SO<sub>4</sub> were then added and the liberated iodine was titrated against 0.1N sodium thiosulphate solution. When a pale yellow colour was obtained 0.2-0.5g of iodine starch indicator was added and the titration continued until the end-point. The colour change at the end-point was from blue to colourless.

Calculation: (For reaction see (129))

$$30\text{g CH}_2\text{O} \equiv 1000 \text{ cm}^3 \text{ Normal Na}_2\text{S}_2\text{O}_3$$

$$3\text{g} \equiv 1000 \text{ cm}^3 \text{ 0.1N Na}_2\text{S}_2\text{O}_3$$

$$0.003\text{g} \equiv 1 \text{ cm}^3 \text{ 0.1N Na}_2\text{S}_2\text{O}_3$$

Since Na<sub>2</sub>S<sub>2</sub>O<sub>3</sub> is dibasic

$$0.0015\text{g} \equiv 1\text{cm}^3 \text{ 0.1N Na}_2\text{S}_2\text{O}_3$$

Therefore % (Free and Methylol) CH<sub>2</sub>O w/w

$$= \frac{0.0015 \text{ N(T2-T1)}}{0.1 \text{ w1}} \cdot \frac{\text{w2}}{\text{w3}} \cdot 100$$

where

w1 = weight of sample used in analysis, g

w2 = weight of solution in test-tube, g

w3 = weight of sample from the reactor, g

N = exact normality of Na<sub>2</sub>S<sub>2</sub>O<sub>3</sub>

T2 = volume of the Na<sub>2</sub>S<sub>2</sub>O<sub>3</sub> solution consumed by the iodine in blank, cm<sup>3</sup>.

T1 = volume of the Na<sub>2</sub>S<sub>2</sub>O<sub>3</sub> solution consumed by the iodine in sample solution, cm<sup>3</sup>

## BIBLIOGRAPHY

1. ELLIS, C., - "THE CHEMISTRY OF SYNTHETIC RESINS".  
Reinhold Pub.Corp., New York (1935).
2. DIETZE, M., Chemiefasern, March (1967),
3. ELLWOOD, P., Chem.Eng. 74, Nov. (1967).
4. POLLAK, F., B. Patents, 171,094 (1920); 181,014  
(1921); 193,420 (1922); 201,906 (1922); 238,904  
(1924); 248,729 (1925).
5. GOLDSCHMIDT, H. and NEUSS, O., B. Patents, 187,605  
(1921); 202,651 (1922); 208,761 (1922).
6. ELLIS, C., U.S. Patents, 1,482,357 (1922); 1,482,358  
(1922); 1,536,881 (1922); 1,536,882 (1922).
7. BRITISH CYANIDES CO. LTD., B. Patents, 248,477  
(1924); 258,950 (1925); 266,028 (1925).
8. I.G. FARBENINDUSTRIE, A.G., B. Patents, 258,289  
(1925); 288,346 (1926).
9. MESKIN, A.S., Internal Report No. C.10535. BIP LTD.,  
Chemical Division, Oldbury.
10. BIRD, R.B., STEWART, W.E., LIGHTFOOT, E.N., -  
"TRANSPORT PHENOMENA", Wiley, New York, (1960).
11. FRANKS, R.G.E., - "MODELLING AND SIMULATION IN  
CHEMICAL ENGINEERING", Wiley, New York (1972).
12. HIMMELBLAU, D.M., BISCHOFF, K.B., - "PROCESS ANALYSIS  
AND SIMULATION : DETERMINISTIC SYSTEMS", Wiley,  
New York (1970).
13. SMITH, C.L., PIKE, R.W., MURRILL, P.W., - "FORMULATION  
AND OPTIMISATION OF MATHEMATICAL MODELS",

International Textbook Co., (1970).

14. BROTZ, W., - "FUNDAMENTALS OF CHEMICAL REACTION ENGINEERING", Addison-Wesley, Reading, Mass. (1965).
15. WALAS, S.M., - "REACTION KINETICS FOR CHEMICAL ENGINEERS", McGraw-Hill, New York (1959).
16. CHAPPELEAR, D.C., SIMON, R.H.M., - "ADVANCES IN CHEMISTRY SERIES". No.91, American Chemical Society, Washington D.C. (1969).
17. HUI, A.W., HAMIELEC, A.E., J. Applied Polymer Sci., Vol.16, 749 (1972).
18. DENBIGH, K.G., Trans. Faraday Soc., Vol.43, 648 (1947).
19. EDGAR, T.D., HASAN, S., ANTHONY, R.G., Chem.Eng.Sci., Vol.25, 1463 (1970).
20. HUI, A.W., HAMIELEC, A.E., Ind.Eng.Chem.P.D.D., Vol.8, 105 (1969).
21. TERENCEZI, J.F., COSWAY, H.F., Ind.Eng.Chem.Fund., Vol.8, 199 (1969).
22. DENBIGH, K.G., J.Applied Chem., Vol.1,227 (1951).
23. KNORR, R.S., O'DRISCOLL, K.F., J.Applied Polymer Sci., Vol.14, 2683 (1970).
24. DUERKSEN, J.H., HAMIELEC, A.E., HODGINS, J.W., A.I.Ch.E. J., Vol.13, 1081 (1967).
25. POEHLEIN, G.W., Symposium on Polymerisation Reaction Engineering, Laval University, Quebec City, Canada, June 5-7 (1972).
26. DUERKSEN, J.H., HAMIELEC, A.E., J. Polymer Sci., Vol.25, 155 (1968).
27. LYNN, S., HUFF, J.E., A.I.Ch.E. J., Vol.17, 475 (1971).

28. MERRILL, L.S., Jr., HAMRIN, C.E., Jr., A.I.Ch.E. J.,  
Vol.16, 194 (1970).
29. WALLIS, J.P.A., Ph.D. Thesis, University of Calgary,  
Calgary, Alberta, Canada.
30. CINTRON-CORDERO, R., MOSTELLO, R.A., BIESENBERGER, J.A.,  
Can.J.Chem.Eng. Vol.46, 434 (1968).
31. BIESENBERGER, J.A., SACKS, M., DUVDEVANI, I.,  
Symposium on Polymer Reactor Engineering, Laval  
University, Quebec City, Canada. June 5-7 (1972).
32. EDWARDS, W.M., SALETAN, D.I., Ind.Eng.Chem. Vol.59  
(3), 37 (1967).
33. BOSWORTH, R.C.L., Phil.Mag. Vol.40, 314 (1949).
34. JOHNSON, M.M., Ind.Eng.Chem.Fundam., Vol.9, 681  
(1970).
35. NOVOSAD, Z., ULBRECHT, J., Chem.Eng.Sci. Vol.21,  
405 (1966).
36. ULRICHSON, D.L., SCHMITZ, R.A., Ind.Eng.Chem.Fundam.  
Vol.4,2 (1965).
37. CLELAND, F.A., WILHELM, R.H., A.I.Ch.E. J.  
Vol.2,489 (1956).
38. HSU, C., A.I.Ch.E. J. VOL.11,938 (1965).
39. LAUWERIER, H.A., Applied Sci.Res., Section 4,  
Vol.8,366 (1959).
40. WISSLER, E.H., SCHLECHTER, R.S., Applied Sci.Res.,  
Section A, Vol.10, 198 (1961).
41. VIGNES, J.P., TRAMBOUZE, P.J., Chem.Eng.Sci.,  
Vol.17,73 (1962).
42. HOVORKA, R.B., KENDALL, H.R., Chem.Eng.Progr.,  
Vol.56,(8), 58 (1960).

43. WAN, C.G., ZIEGLER, E.N., Chem.Eng.Sci. Vol.25,723  
(1970).
44. WAN, C.G., ZIEGLER, E.N., Ind.Eng.Chem.Fundam. Vol.12,  
(1),63(1973).
45. GIANETTO, A., BERBOTTO, G., Ing.Chim.Ital. Vol.1, (3),  
6 (1965).
46. GIANETTO, A., BERBOTTO, G., Ing.Chim.Ital. Vol.1, (3),  
79 (1965).
47. GIANETTO, A., BERBOTTO, G., Ing.Chim.Ital. Vol.1, (3),  
111 (1965).
48. FARREL, M.A., LEONARD, E.F., A.I.Ch.E.J. Vol.9, (2),  
190 (1963).
49. FELDER, R.M., HILL, F.B., Chem.Eng.Sci. Vol.24,  
385 (1969).
50. CATCHPOLE, J.P., FULFORD, G., Ind. and Eng. Chem.  
Vol.58, 3, (1966).
51. HOLMAN, J.P.,-"HEAT TRANSFER", McGraw-Hill, New York,  
(1963).
52. SELLARS, J.R., TRIBUS, M., KLEIN, J.S., Trans. A.S.M.E.,  
Vol.78, P.441, (1956).
53. HODGMAN, C.E., Ed., - "HANDBOOK OF PHYSICS AND  
CHEMISTRY" 38th Edition, Chemical Rubber Publishing  
Co., Cleveland, Ohio (1956).
54. PERRY, J.H., Ed.,-"CHEMICAL ENGINEERS' HANDBOOK".  
Third Edition, McGraw Hill Book Co., Inc. (1950).
55. INTERNATIONAL CRITICAL TABLES, VOL.5, P.69.
56. ARNOLD, J.H., J.Am.chem.Soc., Vol.52, 3937, (1930).
57. KRAMERS, H., WESTERTERP, K.R.,-"CHEMICAL REACTOR  
DESIGN AND OPERATION", Chapman and Hall Ltd.,  
London (1963).

58. KERN, D.Q.,-"PROCESS HEAT TRANSFER", McGraw Hill Book Co. Inc, (1960).
59. LAPIDUS, L.,-"DIGITAL COMPUTATION FOR CHEMICAL ENGINEERS", McGraw Hill Book Co. Inc. (1962).
60. WILKE, C.R., CHANG, P., A.I.Ch.E.J., Vol.1, 264-270, (1955).
61. TOLLENS, B., BER., VOL.17, 659 (1884).
62. EINHORN, A., HAMBERGER, A., Chem.Ber. Vol.41, 24-28 (1968).
63. JOHN, H., U.S. Patent, 1,355,834 (1920).
64. POLLAK, F., B. Patent, 171,094 (1920).
65. WALTER, G., Trans. Faraday Soc., Vol.32,377-395 (1936).
66. ELLIS, C., U.S. Patent, 1,536,882 (1922).
67. HENKEL AND CIE, G.N.B.H., B. Patent, 455,008 (1935).
68. DIXON, A.E., J.Chem.Soc., Vol.113, 238-239 (1918).
69. SMYTHE, L.E., J.Phys. Coll.Chem., Vol.51, 369 (1947).
70. SMYTHE, L.E., J.Am.Chem.Soc., Vol.73,2735 (1951).
71. CROWE, G.A., LYNCH, C.L., J.Am.Chem.Soc., Vol.70, 3796 (1948).
72. CROWE, G.A., LYNCH, C.L., Idem, Vol.71, 3791 (1949).
73. CROWE, G.A., LYNCH, C.L., Idem, Vol.72, 3622 (1950).
74. BETTELHEIM, L., CEDWALL, J., Svensk Kemisk Tidskrift, Vol.60,208 (1948).
75. DE JONG, J.I., DE JONGE, J., Rec,Trav.Chem., Vol.71., 643-660 (1952).
76. DE JONG, J.I., DE JONGE, J., Idem, Vol.71, 661-667 (1952).
77. DE JONG, J.I., DE JONGE, J., Idem, Vol.71, 890-898 (1952).

78. DE JONG, J.I., DE JONGE, J., EDEN, H., Idem, Vol.72, 88-90 (1953).
79. DE JONG, J.I., DE JONGE, J., Idem, Vol.72, 139-156 (1953).
80. DE JONG, J.I., DE JONGE, J., Idem, Vol.72, 169-172 (1953).
81. DE JONG, J.I., DE JONGE, J., Idem, Vol.72, 202-206 (1953).
82. DE JONG, J.I., DE JONGE, J., Idem, Vol.72, 1027-1036 (1953).
83. LANDQVIST, N., Acta.Chem.Scand., Vol.9, 1127-1142 (1955).
84. LANDQVIST, N., Idem, Vol.9, 1459-1465 (1955).
85. LANDQVIST, N., Idem, Vol.9, 1466-1470 (1955).
86. LANDQVIST, N., Idem, Vol.9, 1471-1476 (1955).
87. LANDQVIST, N., Idem, Vol.9, 1477-1483 (1955).
88. LANDQVIST, N., Idem, Vol.11, 776-779 (1957).
89. LANDQVIST, N., Idem, Vol.11, 780-785 (1957).
90. LANDQVIST, N., Idem, Vol.11, 786-791 (1957).
91. LANDQVIST, N., Idem, Vol.11, 792-803 (1957).
92. ITO, Y., Kogyo Kagaku Zasshi, Vol.64, 382-785, 385, 389 (1961).
93. ILICETO, A., Ann.Chim.(Rome), Vol.43, 625 (1953).
94. ZIGEUNER, G., Monatsh., Vol.82, 175 (1951).
95. ZIGEUNER, G., Idem, Vol.83, 1099 (1952).
96. ZIGEUNER, G., PITTER, R., Idem, Vol.86, 57 (1955).
97. DE JONG, J.I., DE JONGE, J., Rec.Trav.Chim., Vol. 72, 207 (1953).
98. DE JONG, J.I., DE JONGE, J., Idem, Vol.72, 213 (1953).

99. VALE, C.P., TAYLOR, W.G.K.,-"AMINOPLASTICS", Iliffe, London (1946).
100. KIENLE, R.H., Ind.Eng.Chem., Vol.22, 590 (1930).
101. HODGINS, T.D., HOVEY, A.G., Ind.Eng.Chem., Vol.31, 673 (1939).
102. KADOWAKI, H., Bull.Chem.Soc. Japan, Vol.11,248 (1936).
103. BROOKES, A.,-"UREA RESINS, INCLUDING MELAMINE RESINS", Plast.Inst.Monograph. No.2. Plastics, Vol.14, 6 (1942).
104. REDFRAN, C.A., Brit. Plastics, Vol,14, 6 (1942).
105. MARVEL, E.S., et al., J.Am.Chem.Soc., Vol.68, 1681 (1946).
106. THURSTON, J.T., Unpublished Paper given at the Gibson Island Conference on Polymeric Materials. (1941).
107. B.I.P. LTD., Chemicals Division, Oldbury, West Midlands, Private Communication.
108. GAY, B., PAYNE, S., Computer Journal, Vol.16, 2, 118-121 (1973).
109. SATO, K., Bull.Chem.Soc. Japan, Vol.40, 724-731 (1960).
110. GORBUNOV, Y.N., YASHINA, V.Z., Plast.Massy., No.4 (1960).
111. SMART, C., Final Year Practical Project, University of Aston in Birmingham (1974).
112. FERNANDO, B.P.B., M.Sc. Thesis, University of Aston in Birmingham (1976).
113. KUSTER, J.L., MIZE, J.H.,-"OPTIMISATION TECHNIQUES WITH FORTRAN", McGraw Book Co. (1973).

114. NELDER, J.A., MEAD, R., Computer Journal, Vol.7, 308-313 (1964).
115. SCHON, S.A., J.Chem.Phys., Vol.26, 72-76 (1929).
116. WALKER, J.F.,-"FORMALDEHYDE", Reinhold Pub.Co., New York (1944).
117. NEILSON, H., EBERS, E.S., J.Chem.Phys., Vol.5,823 (1937).
118. HIBBEN, J.H., J.Am.Chem.Soc., Vol.53, 2418-9 (1931).
119. KRISHNAMURTI, P., Indian. J.Phys., Vol.6, 309 (1931).
120. DAVIS, W.A., J.Soc.Chem.Ind., Vol.16, 502 (1897).
121. LUTTKE, H., Fishers Jahresbericht, 512 (1893).
122. NATTA, G.G., BACCAREDA, M., Givron.Chim.Ind.Applicata, Vol.15,273 (1933).
123. SMYTHE, L.E., Am.Chem.Soc., Vol.95,574 (1953).
124. LEE, W.Y., Ana.Chem., Vol.4. No.77, 1284-1285 (1922).
125. LADLUM, P.R., Analyst, 98, 107-115 (1973).
126. LADLUM, P.R., Idem, 116-121 (1973).
127. ALDERSLEY et al., Brit. Polym.Journal, Vol.1, 101-109, (1969).
128. HOPE, P., STARK, B.P., Idem, Vol.5, 363-378 (1973).
129. VOGEL, A.I.,-"A TEXTBOOK OF PRACTICAL ORGANIC CHEMISTRY INCLUDING QUANTITATIVE ORGANIC ANALYSIS", 3rd Edition, Longmans (1956).
130. JENSEN, V.G., JEFFREYS, G.V.,-"MATHEMATICAL METHODS IN CHEMICAL ENGINEERING", Academic Press, New York (1965).
131. FROBERG, C.E.,-"INTRODUCTION TO NUMERICAL ANALYSIS", Addison Wesley Pub. Co. (1970).
132. SELBY, M.S., - "STANDARD MATHEMATICAL TABLES",

pp.85-86, The Chemical Rubber Co., Cleveland,  
Ohio (1976).

133. DENBIGH, K.G., - "THE PRINCIPLES OF CHEMICAL  
EQUILIBRIUM", Cambridge University Press (1955).